Shifts in the microbiome during anti-tuberculosis therapy in an animal model

C Wepener



orcid.org/ 0000-0002-1384-6641

Dissertation submitted in fulfilment of the requirements for the degree *Magister Scientiae* in Pharmaceutical Sciences at the North-West University

Supervisor:	Prof A F Grobler
Co-Supervisor:	Dr J J Bezuidenhout
Ass-Supervisor:	Mr B C Mann

Graduation: August 2021

Preface and declaration

This dissertation is written in article format. Findings are presented in two separate chapters; of which Chapter 3 consist of a manuscript submitted for publication. Additional findings, that were not included in the manuscript, can be found at the end of the chapter. The manuscript was compiled by Mr B C Mann (PhD candidate) and reviewed by the rest of the authors before submission. Within the manuscript, experimental work and writing of findings regarding the sputum microbiome were conducted by Mr B C Mann and the representing gastro-intestinal microbiome by me. The manuscript is presented in both this dissertation and Mr Mann's thesis.

The study was carried out in accordance with the NWU code of conduct for researchers with ethics number NWU-00584-19-A5. The animal study, which included animal handling, treatment and organ harvesting, was previously conducted by Ms D van der Merwe. Caecum samples were stored for the present study.

All experimental work leading to amplicon sequencing was done by me with assistance from Mr B C Mann (assistant-supervisor). Amplicon sequencing of the gastro-intestinal microbiome DNA in Chapter 3 was done by the Agricultural Research Council (ARC) Biotechnology Platform, Onderstepoort, South Africa. Raw sequence data was analysed and interpreted by myself with assistance from my supervisors.

Preparation, amplicon sequencing and bioinformatics analysis of DNA samples presented in Chapter 4 were done by PHENOMIN-ICS, Strasbourg, France. Raw data and an operational taxonomic unit (OTU) output were sent back to me where the data was statistically analyzed by me with assistance from my supervisors. The OTU table received from PHENOMIN-ICS was converted with assistance from Dr J J Bezuidenhout prior to microbial and statistical analysis.

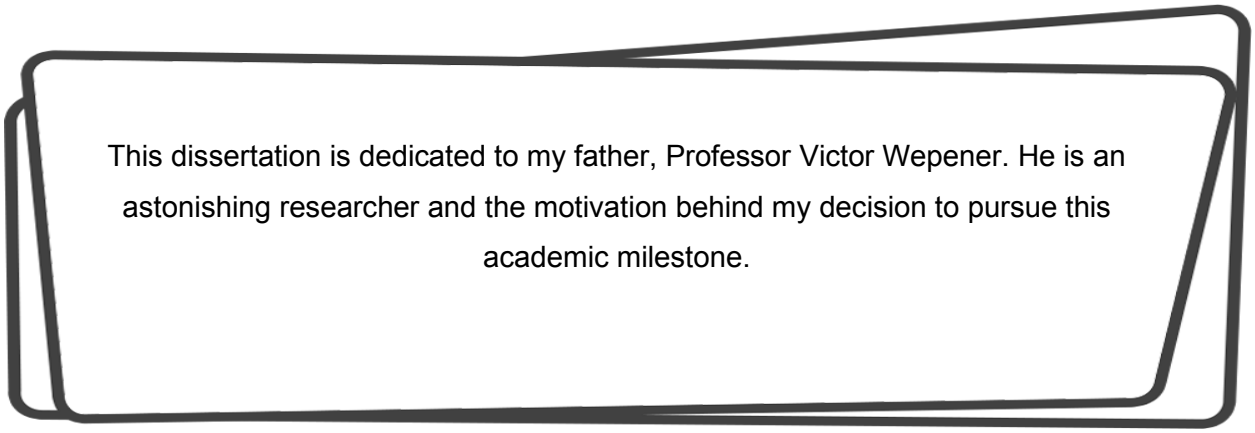
I, Cara Wepener, hereby declare that the dissertation titled "Shifts in the microbiome during anti-tuberculosis therapy in an animal model" is my own work and that all resources used were acknowledged and referenced after each chapter. I declare that this research has not been submitted before for examination at any other university.

Cara Wepener **Date:**

17-03-2021



Dedication


This dissertation is dedicated to my father, Professor Victor Wepener. He is an astonishing researcher and the motivation behind my decision to pursue this academic milestone.

Acknowledgements

I would like to express my thanks and appreciation to the following. The completion of the dissertation would not have been possible without you:

Firstly, to my Heavenly Father for making this opportunity part of His plan for me and giving me the strength and motivation to successfully complete this degree.

Thank you to my parents, Victor and Leanda Wepener, for always believing in me and my ability to pursue the degree; and my brother, Victor, for always showing interest in my progress towards completion.

I would like to thank my fiancé, Taetse Vorster, for all his motivational words, love and support from day one. You are my rock and I appreciate every little thing you have done for me these past few years.

To my supervisor, Prof Anne Grobler, for incorporating her expertise of the Pharmaceutical field into this study and for overseeing this project as main supervisor.

Thank you to Dr Jaco Bezuidenhout, my co-supervisor, for his input with regards to statistical analysis and the writing of this dissertation.

To Brendon, my assistant supervisor, who assisted me every step of the way; for always being available to discuss results, give advice and for reviewing every piece of work before it was submitted for review to the other supervisors.

This work is based on the research supported in part by the National Research Foundation of South Africa (Grant Number: 117255). I hereby acknowledge and thank the NRF for the financial support throughout the study period. Opinions, findings and conclusions are those of the authors and are not necessarily contributed to the NRF.

Thank you to Dr Guillaume Pavlovic and Loïc Linder at PHENOMIN for taking on the project as collaborators.

Lastly, I would like to thank my colleagues and fellow students Charl, Brunhildé, Nico, Shingai and Bisrat, at the PCDDP for showing interest in the process of the project and for always being there to discuss challenges and celebrate victories.

Abstract

Tuberculosis (TB) is a worldwide pandemic caused by the bacterial agent *Mycobacterium tuberculosis* (*Mtb*). The first-line treatment of the disease is invasive and consists of a combination of four antimicrobials to be administered for a period of at least six months. Antimicrobial administration is known to affect the diversity and structure of the gastro-intestinal microbiome by rapidly decreasing bacterial taxa present. Recently, the effect of TB and TB treatment on the gastro-intestinal microbiome has gained attention, since it is suggested that the microbiome plays a role in host immunity. In this study, the impact of different TB treatments on the gastro-intestinal microbiome of Kramnik mice was evaluated. To achieve this, an effective method for DNA extraction of the gastro-intestinal microbiome is necessary to successfully identify all bacteria present. To effectively extract DNA from the representative gastro-intestinal microbiome, commercially available kits namely QIAamp DNA microbiome kit (Qiagen, Germany) and the GenElute™ Stool DNA isolation kit (Sigma, USA) were compared to the NWU lysis method with and without purification steps. Based on these results, DNA from the gastro-intestinal environment was extracted using a similar commercial kit to determine microbiome composition from samples treated with TB therapies. TB therapies included standard TB therapy, Pheroid®-based TB therapy, and the Pheroid® formulation excluding active pharmaceutical ingredients (APIs). All DNA from the microbiome were analyzed with 16S amplicon sequencing using the Illumina Miseq platform. DNA data was analyzed using bioinformatics and community profiling was achieved by using MicrobiomeAnalyst. The various extraction methods did not indicate any significant differences in microbiome composition or structure of the gastro-intestinal environment. Therefore, extraction methods with similar lysis steps are suggested to be an effective approach for successful DNA isolation from the gastro-intestinal microbiome. However, inter-individual differences were observed between mice under the same environmental conditions. Exposure to all selected therapies had a significant impact on the microbiome diversity compared to *Mtb* infected mice, by decreasing the overall diversity of the microbiome. Members of the phylum Bacteroidota were significantly decreased and Firmicutes significantly increased. The effect of Pheroid®-based TB therapy on the microbiome did not differ significantly from standard TB therapy. However, the presence of members of the family Saccharimonadaceae was significantly more abundant in the microbiome of mice recovering from Pheroid®-based TB therapy, which is positively correlated with the immune response. Mice treated with the Pheroid® carriers (formulation excluding APIs) had a significantly higher abundance of *Lactobacillus* in their microbiome, which is associated with lipid metabolism. Mice treated with the latter did not indicate a significant reduction of *Mtb* in the lungs, but survived longer than the infected animals. It is suggested that the Pheroid® formulation has a possible immune support function. The proliferation

of commensal bacteria *Parasutterella* was observed in the microbiome of mice recovering from the Pheroid® carriers, indicating normalization of the microbiome after exposure. Therefore, the use of Pheroid® as an alternative for TB drug delivery does not necessarily improve the state of the microbiome during treatment, but might have the potential to stabilize the gastro-intestinal environment after treatment has ceased.

Key words: microbiome, gastro-intestinal, caecum, dysbiosis, tuberculosis, Pheroid®-based treatment, treatment outcome, 16S rRNA

TABLE OF CONTENTS

PREFACE AND DECLARATION ..... **I**

DEDICATION ..... **II**

ACKNOWLEDGEMENTS ..... **III**

ABSTRACT ..... **IV**

CHAPTER 1 GENERAL INTRODUCTION AND PROBLEM STATEMENT **1**

1.1 Background and problem statement **1**

1.1.1 Tuberculosis, TB therapy and the gastro-intestinal microbiome 1

1.1.2 Mouse gut microbiome translating to humans 2

1.1.3 Microbial quantification 3

1.1.4 Research questions 4

1.2 Aims of the study **4**

1.3 Study objectives **4**

1.4 Dissertation layout **4**

REFERENCES **6**

CHAPTER 2 LITERATURE REVIEW: TUBERCULOSIS AND THE GASTRO-INTESTINAL MICROBIOME **10**

2.1 Tuberculosis **10**

2.1.1 Mycobacterium tuberculosis 10

2.1.2 Prevalence of tuberculosis worldwide 12

2.1.3 Prevalence in South Africa 13

2.1.4 Co-infection of TB and HIV 14

2.1.5 Co-infection of TB and emerging viruses 15

2.2 Treatment of tuberculosis 15

2.2.1 Rifampicin 16

2.2.2 Isoniazid 17

2.2.3 Ethambutol 18

2.2.4 Pyrazinamide 18

2.3 Drug resistant tuberculosis 19

2.4 Alternative drug delivery systems for treatment of TB 20

2.4.1 Pheroid® technology as a tool for improved drug delivery 20

2.4.2 Nanoparticles as targeting ligands 21

2.4.2.1 Mycolic acids 22

2.4.3 Anti-mycobacterial actions of nanoparticles 22

2.4.3.1 Eicosapentaenoic acid 22

2.5 Kramnik mouse model for TB infection studies 23

2.6 The gastro-intestinal microbiome in health and disease 23

2.6.1 The microbiome and tuberculosis 25

2.6.2 Effect of tuberculosis on the microbiome 25

2.6.3 Microbiome dysbiosis due to antimicrobial therapy and its implications 27

2.7 Methodology for identification of microbial bacteria 32

2.7.1 Molecular techniques and technologies 32

2.7.2 Sequencing approaches 33

2.7.3 Methods used for microbiome studies 33

2.8 Role of the microbiome in treatment outcome 34

REFERENCES **35**

CHAPTER 3 EVALUATING AN EFFECTIVE APPROACH TO ISOLATE THE MICROBIAL COMMUNITY FROM MOUSE CAECUM FOR MICROBIOME ANALYSIS **54**

3.1 Manuscript **55**

3.2 Additional findings **76**

3.2.1 Background 76

3.2.2 Methods 77

3.2.3 Results 78

3.2.4 Discussion 82

3.2.5 Conclusion 85

REFERENCES **86**

CHAPTER 4 CHANGES OF MICROBIAL COMMUNITIES IN THE GUT DURING TREATMENT WITH PHEROID®- BASED TUBERCULOSIS THERAPY IN THE KRAMNIK MOUSE MODEL **90**

4.1 Introduction **90**

4.2 Materials and methods **92**

4.2.1 Study design 92

4.2.2 Sampling 94

4.2.3 DNA extraction 95

4.2.4 16S Sequencing 95

4.2.5 Data filtering and bioinformatics analysis 96

4.2.6 Microbial community analysis 96

4.2.6.1 Alpha diversity 96

4.2.6.2 Beta diversity 97

4.2.7 Statistical analysis 97

4.3 Results 98

4.3.1 Sequencing data 98

4.3.2 Diversity varies in each group over time 98

4.3.2.1 Rarefaction of samples 100

4.3.2.2 Longitudinal changes in alpha diversity 102

i. Phylum 102

ii. Family 104

iii. Genus 106

4.3.3 Overall community structure between groups 109

4.3.4 Relative abundance of bacteria in the caecum microbiome 120

4.3.4.1 Phylum 120

4.3.4.2 Family 123

4.3.4.3 Genus 127

4.4 Discussion 131

4.5 Conclusion 135

4.6 Data availability 135

4.7 Ethics statement 136

4.8 Funding 136

4.9 Acknowledgements 136

REFERENCES 137

CHAPTER 5 SUMMARY AND RECOMMENDATIONS 143

5.1 Introduction 143

5.2 Summary of study design, execution and results 144

5.2.1 Objective i 144

5.2.2 Objective ii 144

5.2.3 Objective iii 145

5.2.4 Objective iv 145

5.3 Study limitations and recommendations 146

5.4 Future prospects 146

REFERENCES 149

ANNEXURE A ETHICS APPROVAL 150

ANNEXURE B SUBMISSION GUIDELINES: MOLECULAR BIOLOGY REPORTS 151

ANNEXURE C SUPPLEMENTARY FIGURES ASSOCIATED WITH MANUSCRIPT (CHAPTER 3) 187

ANNEXURE D COLONY FORMING UNITS (CFUS) OF *MYCOBACTERIUM TUBERCULOSIS* (*MTB*) IN THE LUNGS OF C3HEB/FEJ MICE DURING AND AFTER TB THERAPIES (VAN DER MERWE, 2019) 189

LIST OF TABLES

Chapter 2

Table 2-1 Most recent studies indicating dysbiosis of gastro-intestinal microbial communities in murine models and clinical studies where TB therapy was administered. 29

Chapter 3

As presented in manuscript: "Comparative investigation of the suitability of DNA preparation methods for microbiome analysis of complex clinical samples"

Table 1 DNA Quality……63

LIST OF FIGURES

Chapter 2

Figure 2-1 Best estimates of TB incidence and mortality amongst patients co-infected with HIV and TB only in the past 10 years 14

Chapter 3

As presented in manuscript: "Comparative investigation of the suitability of DNA preparation methods for microbiome analysis of complex clinical samples"

Figure 1 Alpha-diversity, measured by Shannon, Chao1 and observed diversity indices for the selected clinical sputum sample (A) and the representative gut sample (B) ……..……..…65

Figure 2 Hierarchical clustering heat map based on the relative abundance of the most abundant genera classified to the genus level for the selected clinical sputum sample ……..…….66

Figure 3 Hierarchical clustering heat map based on the relative abundance of the most abundant genera classified to the genus level from the representative gut sample ……..……..….....67

Figure 3-1 Relative percentage abundance of phyla present in the gastro-intestinal microbiome of *Mtb* infected C3HeB/FeJ mice..... 79

Figure 3-2 Percentage of relative abundant Families present in the caecum microbiome of C3HeB/FeJ mice that are infected with *Mtb*..... 80

Figure 3-3 Taxonomic composition on genus level of C3HeB/FeJ microbiome. Relative percentage abundance is presented in the figure. 81

Figure 3-4 PCoA based on the Bray-Curtis index grouped according to subjects. Samples located closer to one another indicate similarity. 82

Figure 4-1 Copy of the original illustrated design of the study executed by van der Merwe (2019). 93

Figure 4-2 Schematic representation of the study design following the original design presented in Figure 4-1 above 94

Figure 4-3 Alpha diversity box plots of caecum microbiome diversities during infection (IC) and treatments with Pheroid® carrier control (PCC), Pheroid® based TB treatment (PT) and standard TB treatment (ST) tested with Kruskal-Wallis 99

Figure 4-4 Rarefaction analysis between the sequence sample size and the number of OTUs in each sample (species richness) 101

Figure 4-5 Changes in alpha diversity on phylum level using (A) Chao1, (B) Observed and (C) Shannon indices..... 103

Figure 4-6 Alpha diversity changes measured using (A) Chao1, (B) Observed and (C) Shannon indices on family level of classification 105

Figure 4-7 Levels of diversity of genera in samples measured over time using (A) Chao1 and (B) Observed indices along with measurements of diversity and evenness using the (C) Shannon index..... 108

Figure 4-8 Hierarchical clustering of samples based on genera abundancies using Bray-Curtis distancing 110

Figure 4-9 PCoA of beta diversity measures between all groups to indicate differences between the infected reference group and various treatment groups. 112

Figure 4-10 PCoA based on the Bray-Curtis Index for samples from the infected reference and various treatment groups (Standard and Pheroid®- based TB therapies and the Pheroid® carrier control) plotted individually on phylum level of classification 113

Figure 4-11 Differences in beta diversity measured with PCoA between all groups of interest. On family level of classification, there were significant differences overall ($p = 0.001$)..... 114

Figure 4-12 PCoA based on the Bray-Curtis Index for samples from the infected reference group and various treatment groups plotted individually on family level of classification..... 115

Figure 4-13 PCoA based on the Bray-Curtis Index for samples from the infected references and various treatment groups on genus level of classification. . 116

Figure 4-14 PCoA based on the Bray-Curtis Index for samples from the infected references and various groups treated with various therapies/compounds on genus level 117

Figure 4-15 PCoA of beta diversity measures between experimental groups at (A) week one, (B) week two and (C) week eight of infection. 119

Figure 4-16 Microorganisms present in the caecum microbiome of each group (infected reference, Pheroid® carrier control, standard TB therapy and Pheroid®-based TB therapy) over time. 122

Figure 4-17 Microorganisms present in the caecum microbiome at the family level of classification 125

Figure 4-18 LEfSe analysis between samples derived from the infected reference and Pheroid® carrier control, showing the differentially abundant families (A) during treatment with the carrier control and (B) during the recovery from exposure after treatment ceased 126

Figure 4-19 Relative abundance of microorganisms present in the caecum of each sample on the genus level of classification 129

Figure 4-20 LEfSe comparisons illustrating genera that are significantly different between the infected references and Pheroid® carrier controls during (A) treatment with the carrier control (Weeks 1-12) and (B) during the microbiome recovery phases after exposure with the carrier control is ceased (Weeks 16 & 20). 130

Figure 4-21 Analysis with LEfSe comparing genera that are significantly different between samples recovering from TB therapies 131

LIST OF ABBREVIATIONS

A

AAALAC	American Association for Accreditation of Laboratory Animal Care
ANOSIM	non-parametric analysis of similarities
ANOVA	one-way analysis of variance
API	active pharmaceutical ingredient
AUC	area under the curve

B

Balb/c	albino laboratory-bred strain of the house mouse
BCG	Bacille Calmette–Guérin
BGI	Beijing Genomics Institute

C

C3HeB/FeJ	strain of mice in the Kramnik mouse model.
C57BL/6	laboratory muse strain commonly known as Black 6 mice
CFU	colony forming unit
CLA	conjugated linoleic acid
C_{max}	maximum concentration
COPD	chronic obstructive pulmonary disease

D

DHA	docosahexaenoic acid
DMSO	dimethyl sulphoxide
DSI	Department of Science and Innovation

E

EDTA	ethylenediaminetetraacetic acid
EMB	ethambutol
EPA	eicosapentaenoic acid

F

FDC	fixed dose combination
FMT	faecal microbiome transplantation
FROGS	Find, Rapidly, OTUs (operational taxonomic units) with Galaxy Solution

G

GC	guanine/cytosine
GIT	gastro-intestinal tract
GM	germfree

H

HC	healthy controls
HIV	human immunodeficiency virus
HR	isoniazid-rifampicin
HRZ	isoniazid-rifampicin-pyrazinamide
HRZE	isoniazid-rifampicin-pyrazinamide-ethambutol

I

IMPC	International Mouse Phenotyping Consortium
INH	isoniazid
IVC	individually ventilated cages

K

KatG	catalyse peroxidase

L

LDA	linear discriminant analysis
LEfSe	linear discriminant analysis effect size
LMT	lysis micro tube
LTBI	latent tuberculosis (TB) infection

M

MA	mycolic acid
MDP	Marker Data Profiling
MDR-TB	multi drug-resistant tuberculosis (TB)
Mtb	*Mycobacterium tuberculosis*
MTBC	*Mycobacterium tuberculosis* complex
N	
NADH	nicotinamide adenine dinucleotide
NCBI	National Centre for Biotechnology Information
NGS	next generation sequencing
NP	nanoparticle
NOD	non-obese diabetic
NRF	National Research Foundation
NTB	patients newly diagnosed with tuberculosis (TB)
O	
ONT	Oxford nanopore technologies
OTU	operational taxonomic unit
P	
P450 3A4	important metabolizing hepatic and intestinal enzyme
PacBio	Pacific Biosciences
PBS	phosphate buffered saline
PCDDP	Preclinical Drug Development Platform
PCoA	principal coordinate analysis
PCR	polymerase chain reaction
PUFA	polysaturated fatty acid
PZA	pyrazinamide
Q	

QC	quality control
QIIME	Quantitive Insights Into Microbial Ecology
qPCR	real time polymerase chain reaction (PCR)
R	
RIF	rifampicin
rRNA	ribosomal RNA
RTB	patients re-infected with tuberculosis (TB)
S	
SANAS	South African National Accreditation Service
SARS-CoV-2	severe acute respiratory coronavirus 2
SCFA	short-chain fatty acid
SLBZS	sheng-ling-bai-zhu-san
SMEDS	self-micro emulsifying delivery system
SMRT	single molecule real-time
SNEDS	self-nano emulsifying delivery system
SRA	Sequence Read Archive
T	
TB	tuberculosis
TNF- α	tumour necrosis factor alpha
TSS	total sum scaling
U	
USEARCH	ultra-fast sequence analysis
W	
WHO	World Health Organization
X	
XDR-TB	extensively drug-resistant tuberculosis (TB)

Chapter 1 General introduction and problem statement

1.1 Background and problem statement

1.1.1 Tuberculosis, TB therapy and the gastro-intestinal microbiome

Tuberculosis (TB) was declared a worldwide health emergency by the World Health Organization (WHO) in April 1993 (WHO, 1994). Since then, total TB related deaths decreased from 3 million in 1993 to approximately 1.2 million in 2019 (WHO, 1994; WHO, 2020). Over the decades tremendous progress has been made, with around 60 million individuals being treated and cured of the disease since 2000 (WHO, 2020). The tubercle agent, namely *Mycobacterium tuberculosis* (*Mtb*), which causes the disease, was first isolated by Robert Koch in 1882 (Blevins & Bronze, 2010). Initial treatment of the disease dates back to 1950, when patients were treated with the antimicrobial streptomycin and para-amino salt derived from salicylic acid (Medical Research Council, 1950).

The gastro-intestinal microbiome habitats a wide variety of micro-organisms responsible for metabolism and host immunity (Cahenzli *et al*., 2013). When a change in the microbiome, known as dysbiosis, occurs, it impacts the immune response negatively and may lead to pathogens colonizing within the host. The development of inflammation is in turn also affected by the composition of the gastro-intestinal microbiome (Dudek-Wicher *et al*., 2018; Tarashi *et al*., 2018) The administration of combinations of antibiotics is increasing as a method used in disease studies to deplete the gastro-intestinal microbiome in murine mouse models. Subsequently the effect of the microbiome organisms in the gut on disease progression has been and is still being studied (Tirelle *et al*., 2020). First-line TB drugs comprise of a cocktail of broad and narrow spectrum antibiotics. Furthermore, when resistance to first-line drugs develops, second-line TB drugs are administered, that comprise of many more antibiotics. Several studies in humans and animals have indicated that TB-therapy induces a bacterial dysbiosis in the gut and examined the consequences of the changes in the bacterial diversities (Luo *et al*., 2017; Namasivayam *et al*., 2017; Wipperman *et al.* 2017; Maji *et al*., 2018; Khan *et al.,* 2019). This raises concern, since there is a proposed interaction between the gastro-intestinal microbiome and TB disease (Namasivayam *et al*., 2018). Furthermore, the human gastro-intestinal microbiome consists of microorganisms that carry a large number of antibiotic resistant genes, which can easily be transferred to possibly proliferated pathogens within the gut (O'Toole & Gautam, 2018).

Alternative drug delivery systems, based on nanoparticles (NPs) as carriers, for TB treatment have shown potential treatment outcome in light of increased bioavailability, decreased degradation, and enhanced solubility and pharmacokinetic profiles (Aminu *et al*., 2020). An example of such is the use of Pheroid® technology to aid in the delivery of active pharmaceutical ingredients (APIs). Pheroid® formulations are based on colloidal emulsions that deliver pharmaceutical compounds to sites of absorption (Grobler, 2013). Pheroid® consists of an oil, water and gas phase, which is known as the standard Pheroid® form. Pro-Pheroid® excludes the water phase, resulting in an oily substance. Once in contact with water, nano- and microparticles form, packing APIs in vesicles to be delivered to absorption sites in the gastro-intestinal tract in the case of oral administration (Grobler, 2013).

The impact of TB therapy delivered by carriers such as NPs in the Pheroid® delivery system on the microbiome has yet to be determined. Since administration of current drugs are known to cause microbial dysbiosis in the gut, it is of interest to determine whether alternative delivery of the same drugs cause less disturbance of the microbiome; and whether the Pheroid® may have a protective effect on the microbiome.

1.1.2 Mouse gut microbiome translating to humans

Several animal models have been used to examine TB disease, its progression and drug susceptibility (Singh & Gupta, 2018). Animals used for these types of studies include mice, rabbits, guinea pigs, non-human primates and other vertebrates such as zebrafish. Mice are however considered the preferential animal model to study TB, due to available immunological data, variety of genetically modified strains and ease of housing mice in a laboratory setting (Fonseca *et al*., 2017). Different mouse strains specifically used in TB research is the C57BL/6 strain, Balb/c and C3HeB/FeJ (Kramnik mouse model) (Zhan *et al*., 2017). However, the Kramnik mouse model is considered to mimic the human disease to better, since necrotic lesions in granulomas are formed as result of *Mtb* infection (Lanoix *et al*., 2015).

Mouse models are frequently used to examine microbiota-host interactions related to various diseases (Nguyen *et al*., 2015). However, several differences between mouse and human anatomy, physiology, dietary patterns and metabolism should be considered (Hugenholtz & de Vos, 2018). A major limitation of comparing the mouse and human microbiome is the low percentage of bacterial genes that are identical. In addition, the differences in the compositions of microbial communities between different mouse strains are significant, and several environmental factors influence the composition of the microbiome (Hugenholtz & de Vos, 2018). Although, despite limitations, the use of a mouse model is most suitable for microbiome

studies, taken into account the amount of research and knowledge there is of the model's gastroenterology, immunology and genetics compared to other models (Nguyen *et al*., 2015). Additionally, these models are easily available in an experimental set-up and are cost effective (Dharmadhikari & Nardell, 2008).

Dysbiosis of the gastro-intestinal microbiome as result of TB therapies has mainly been examined in variants of C57BL/6 mice, which is a frequently used to model TB infections *in vivo* (Namasivayam *et al*., 2017; Khan *et al.,* 2019). Interestingly, companion studies on the long-term effect of anti-TB therapy on the microbiome showed similar results in the mouse and humans (Namasivayam *et al*., 2017; Wipperman *et al*., 2017). In this study the Kramnik mouse model is introduced to examine the effect of TB therapies on the gastro-intestinal microbiome.

1.1.3 Microbial quantification

In the past, culturing methods were utilized to quantify diversity of the gastro-intestinal microbiome. However, the majority of microorganisms are unculturable, or require unknown growth conditions to be cultured in a laboratory environment (Fraher *et al*., 2012). Identification of bacteria present in the microbiome has evolved and genetic characterization has been used to eliminate the limitations of culturing methods. Techniques based on 16S ribosomal RNA (rRNA) sequencing are the most commonly used (Rajendhran & Gunasekaran, 2011). In addition, the correct DNA extraction method is required to accurately reflect the microbial community in the gastro-intestinal tract, hence extracting all DNA from the bacterial species in the community. The extracted DNA is used to generate a profile for the gastro-intestinal microbiome (Lim *et al.*, 2018). To obtain this DNA, commercial extraction kits are available, however, the lysis method (e.g. mechanical, chemical, heat, and enzymatic) and DNA isolation method (e.g. spin-column based and magnetic beads) in these commercial kits differ. The lysis step is crucial in obtaining not only Gram-negative (easy to lyse because of its thin cell wall), but also Gram-positive bacteria, which has a thick cell wall. DNA extraction kits are constantly advancing, and it is important to these newly developed kits to consider lysis and DNA binding as part of the protocol (Lim *et al.*, 2018). Commercial extraction methods for gastro-intestinal microbial DNA are mainly based on bead beating cell lysis and DNA binding on spin columns (Wagner Makenzie *et al*., 2015; Wu *et al*., 2019). However, commercial kits consist of many consumables and reagents and can be quite costly depending on sample sizes. Therefore, additional ways for DNA extraction have been developed and explored (Peng *et al*., 2013). An example of an alternative method for downstream microbial quantification is the NWU cell lysis method, primarily developed for molecular diagnostic purposes.

1.1.4 Research questions

Based on literature and gaps identified, the following research questions were addressed: (i) Does the NWU cell lysis method extract microbial DNA efficiently for downstream microbiome analysis? (ii) Does the Pheroid®-formulation have similar outcomes in dysbiosis of the Kramnik mouse gastro-intestinal microbiome when compared to a standard regimen during TB treatment? (iii) Does the Pheroid®-based treatment have an impact on potential treatment outcomes when comparing changes in the microbiome?

1.2 Aims of the study

The study aimed to examine the changes in the gastro-intestinal microbiome from caecum samples during Pheroid®-based TB therapy in the Kramnik (C3HeB/FeJ) mouse model; and to evaluate the potential role of Pheroid®-based TB therapy for improved treatment outcome.

1.3 Study objectives

Specific objectives that were set out to be accomplished to achieve the aims of the study were (i) to evaluate the NWU cell lysis method as preferential tool for downstream gut microbiome analysis; (ii) to evaluate changes in the gastro-intestinal microbiome of C3HeB/FeJ mice infected with the H37Rv *Mtb* strain during courses of both standard and Pheroid®-based TB therapies with 16S amplicon sequencing; (iii) to compare the changes during treatment with already available colony forming units (CFUs) data; and finally (iv) to determine whether the microbiome plays a role in improved treatment outcome.

1.4 Dissertation layout

This dissertation was submitted in fulfilment with the requirements of a *Magister Scientiae* in Pharmaceutical Sciences at the North-West University, Potchefstroom Campus, South Africa. The study was designed according to results obtained in a previous study done at the DSI/NWU Preclinical Drug Development Platform (PCDDP). Financial support was given by the National Research Foundation of South Africa (NRF) (UID: 117255) and the North-West University (NWU); and the study was financially supported by the Department of Science and Innovation (DSI) – forming part of the International Mouse Phenotyping Consortium (IMPC) project. Study design, data collection and interpretation of results are those of the author and are not attributed to the funders. The study was approved by the AnimCARE ethics committee of the NWU, Annexure A (NWU-00584-19-A5).

Each chapter was written to address specific objectives. The present chapter (chapter one) introduces the rationale of the study with its specific aims and objectives. Chapter two addressed a review of literature relevant to the study is based; chapter three addressed the first objective that forms part of a manuscript submitted to the journal Molecular Biology Reports. Chapter four addressed the aims and objectives ii to iv of the study regarding TB therapies and the gastro-intestinal microbiome. Chapter five provides the summary and recommendations of the study. Each chapter includes references related to literature in the specific chapter.

References

Aminu, N., Bello, I., Umar, N.M., Tanko, N., Aminu, A. & Audu, M.M. 2020. The influence of nanoparticulate drug delivery systems in drug therapy. *Journal of Drug Delivery Science and Technology*, 60:101961. doi:10.1016/j.jddst.2020.101961

Blevins, S.M. & Bronze, M.S. 2010. Robert Koch and the 'golden age' of bacteriology. *International Journal of Infectious Diseases*, *14*(9):e744-e751. doi:10.1016/j.ijid.2009.12.003

Cahenzli, J., Köller, Y., Wyss, M., Geuking, M.B. & McCoy, K.D. 2013. Intestinal microbial diversity during early-life colonization shapes long-term IgE levels. *Cell Host & Microbe*, 14:559-570. doi:10.1016/j.chom.2013.10.004

Dharmadhikari, A.S. and Nardell, E.A. 2008. What animal models teach humans about tuberculosis. *American journal of respiratory cell and molecular biology*, *39*(5):503-508. doi:10.1165/rcmb.2008-0154TR

Dudek-Wicher, R.K., Junka, A. & Bartoszewicz, M. 2018. The influence of antibiotics and dietary components on gut microbiota. *Przeglad Gastroenterologiczny*, 13(2):85-92. doi:10.5114/pg.2018.76005

Fonseca, K.L., Rodrigues, P.N., Olsson, I.A.S. & Saraiva, M. 2017. Experimental study of tuberculosis: from animal models to complex cell systems and organoids. *PLoS pathogens*, *13*(8):e1006421. doi:10.1371/journal.ppat.1006421

Fraher, M.H., O'toole, P.W. & Quigley, E.M. 2012. Techniques used to characterize the gut microbiota: a guide for the clinician. *Nature Reviews Gastroenterology & Hepatology*, 9(6):312. doi:10.1038/nrgastro.2012.44

Grobler, A.F. 2013. Nano & micro-delivery systems: the Pheroid® story. NWU: Potchefstroom Campus (Inaugural lecture).

Hugenholtz, F. & de Vos, W.M. 2018. Mouse models for human intestinal microbiota research: a critical evaluation. *Cellular and Molecular Life Sciences*, 75(1):149-160. doi:10.1007/s00018-017-2693-8

Khan, N., Mendonca, L., Dhariwal, A., Fontes, G., Menzies, D., Xia, J., Divangahi, M. & King, I.L. 2019. Intestinal dysbiosis compromises alveolar macrophage immunity to *Mycobacterium tuberculosis*. *Mucosal Immunology*, 12(3)772-783. doi:10.1038/s41385-019-0147-3

Lanoix, J.P., Lenaerts, A.J. & Nuermberger, E.L. 2015. Heterogeneous disease progression and treatment response in a C3HeB/FeJ mouse model of tuberculosis. *Disease Models & Mechanisms*, 8(6):603-610. doi:10.1242/dmm.019513

Lim, M.Y., Song, E.-J., Kim, S.H., Lee, J. & Nam, Y.-D. 2018. Comparison of DNA extraction methods for human gut microbial community profiling. *Systematic and Applied Microbiology*, 41(2):151-157. doi:10.1016/j.syapm.2017.11.008

Luo, M., Liu, Y., Wu, P., Luo, D-X., Sun, Q., Zheng, H., Hu, R., Pandol, S.J., Li, Q-F., Han, Y-P. & Zeng, Y. 2017. Alteration of gut microbiota in patients with pulmonary tuberculosis. *Frontiers in Physiology*, 8:822. doi:10.3389/fphys.2017.00822

Maji, A., Misra, R., Dhakan, D.B., Gupta, V., Mahato, N.K., Saxena, R., Mittal, P., Thukral, N., Sharma, E., Singh, A., Virmani, R., Gaur, M., Singh, H., Hasija, Y., Arora, G., Agrawal, A., Chaudhry, A., Khurana J.P., Sharma, V.K., Lal, R. & Singh, Y. 2018. Gut microbiome contributes to impairment of immunity in pulmonary tuberculosis patients by alteration of butyrate and propionate producers. *Environmental Microbiology*, 20(1):402-419. doi:10.1111/1462-2920.14015

Medical Research Council. 1950. Treatment of pulmonary tuberculosis with streptomycin and para-aminosalicylic acid. *British Medical Journal*, 2:1073-1085.

Namasivayam, S., Maiga, M., Yuan, W., Yuan, V., Costa, D.L., Mittereder, L.R., Wipperman, M.F., Glickman, M.S., Dzutsev, A., Trinchieri, G. & Sher, A. 2017. Longitudinal profiling reveals a persistent intestinal dysbiosis triggered by conventional anti-tuberculosis therapy. *Microbiome*, 5(1). doi:10.1186/s40168-017-0286-2

Namasivayam, S., Sher, A., Glickman, M.S. & Wipperman, M.F. 2018. The microbiome and tuberculosis: Early evidence for cross talk. *MBio*, 9(5):e01420-18. doi:10.1128/mBio.01420-18

Nguyen, T.L.A., Vieira-Silva, S., Liston, A. & Raes, J. 2015. How informative is the mouse for human gut microbiota research? *Disease models & mechanisms*, *8*(1):1-16. doi:10.1242/dmm.017400

O'Toole, R.F. & Gautam, S.S. 2018. The host microbiome and impact of tuberculosis chemotherapy. *Tuberculosis*, 113:26-29. doi:10.1016/j.tube.2018.08.015

Peng, X., Yu, K.Q., Deng, G.H., Jiang, Y.X., Wang, Y., Zhang, G.X. & Zhou, H.W. 2013. Comparison of direct boiling method with commercial kits for extracting fecal microbiome DNA

by Illumina sequencing of 16S rRNA tags. *Journal of Microbiological Methods*, *95*(3):455-462. doi:10.1016/j.mimet.2013.07.015

Rajendhran, J. & Gunasekaran, P. 2011. Microbial phylogeny and diversity: small subunit ribosomal RNA sequence analysis and beyond. *Microbiological Research*, 166(2):99-110. doi:10.1016/j.micres.2010.02.003

Singh, A. K., & Gupta, U. D. 2018. Animal models of tuberculosis: Lesson learnt. *The Indian Journal of Medical Research*, 147(5):456–463. doi:10.4103/ijmr.IJMR_554_18

Tarashi, S., Ahmadi Badi, S., Moshiri, A., Nasehi, M., Fateh, A., Vaziri, F. & Siadat, S.D. 2018. The human microbiota in pulmonary tuberculosis: Not so innocent bystanders. *Tuberculosis*, 113:215-221. doi:10.1016/j.tube.2018.10.010

Tirelle, P., Breton, J., Riou, G., Déchelotte, P., Coëffier, M. & Ribet, D. 2020. Comparison of different modes of antibiotic delivery on gut microbiota depletion efficiency and body composition in mouse. *BMC Microbiology*, 20:340. doi:10.1186/s12866-020-02018-9

Wagner Mackenzie, B., Waite, D.W. & Taylor, M.W. 2015. Evaluating variation in human gut microbiota profiles due to DNA extraction method and inter-subject differences. *Frontiers in Microbiology*, 6:130. doi:10.3389/fmicb.2015.00130

WHO: Word health organization. 1994. TB: a global emergency, WHO report on the global epidemic (WHO/TB/94.177). https://apps.who.int/iris/bitstream/handle/10665/58749/WHO_TB_94.177.pdf?sequence=1&isAllowed=y Date of access: 30 Nov. 2020.

WHO: World Health Organization. 2020. Global tuberculosis report 2020. https://www.who.int/publications/i/item/9789240013131 Date of access: 30 Nov. 2020.

Wipperman, M.F., Fitzgerald, D.W., Juste, M.A.J., Taur, Y., Namasivayam, S., Sher, A., Bean, J.M., Bucci, V. & Glickman, M.S. 2017. Antibiotic treatment for tuberculosis induces a profound dysbiosis of the microbiome that persists long after therapy is completed. *Scientific Reports*, 7(1):10767. doi:10.1038/s41598-017-10346-6

Wu, W.K., Chen, C.C., Panyod, S., Chen, R.A., Wu, M.S., Sheen, L.Y. & Chang, S.C. 2019. Optimization of fecal sample processing for microbiome study—The journey from bathroom to bench. *Journal of the Formosan Medical Association*, 118(2):545-555. doi:10.1016/j.jfma.2018.02.005

Zhan, L., Tang, J., Sun, M., & Qin, C. 2017. Animal models for tuberculosis in translational and precision medicine. *Frontiers in Microbiology*, 8:717. doi:10.3389/fmicb.2017.00717

Chapter 2 Literature review: Tuberculosis and the gastro-intestinal microbiome

2.1 Tuberculosis

2.1.1 Mycobacterium tuberculosis

Tuberculosis (TB) has plagued the human race for centuries; however, the causative agent, namely *Mycobacterium tuberculosis* (*Mtb*), was only discovered in 1882 by German microbiologist, Robert Koch (Daniel, 2006; Fogel, 2015). This agent is described as a pathogenic, slow-growing, obligate aerobic microorganism, and is classified as acid-fast by Ziehl-Neelsen staining (Trifiro *et al.*, 1990; Forrellad *et al.*, 2013; Koch & Mizrahi, 2018). Infection amongst people occurs by the spread of the microorganism through aerosol nuclei droplets that remain in the air for minutes to hours after expectoration from an active TB person (Cadmus *et al*., 2010; Namasivayam *et al*., 2018). The *Mycobacterium tuberculosis* complex (MTBC) comprises of several organisms of which *Mtb* forms part of. Members of the MTBC are known to cause TB disease associated with animals and/or humans. Other members of the MTBC include *Mycobacterium bovis*, *M. africanum*, *M. caprae*, *M. canettii*, *M. microti*, *M. pinnipedii*, *M. sunicattae*, *Oryx Bacillus*, *Dassie Bacillus* and most recently discovered *M. mungi* (Huard *et al*., 2006; Alexander *et al*., 2010). Of all these TB-causing organisms, *Mtb* and *M. africanum* are the main causative agents in the development of human TB disease. Apart from the various members of the MTBC, several lineages have been identified over years of research and is characterised by genetic differences in the organisms. Seven lineages that evolved from *Mtb* and *M. africanum* have been discovered and identified in different regions of the world (Senghore *et al*., 2020). Furthermore, a sister lineage (eighth lineage) of the MTBC has recently been discovered in multi-drug resistant patients in Tanzania (Ngabonziza *et al*., 2020).

When inhaled, *Mtb* travels to the alveoli of the human host; and is phagocytized by alveolar macrophages in the lungs where it then proceeds to grow slowly, replicating every 24 hours. The macrophages carry the *Mtb* from the lower respiratory tract to deeper tissues within the lung (Pagán & Ramakrishnan, 2015). Granuloma formation occurs as an innate immune response to *Mtb* infection and is a distinctive characteristic of the pathogenicity of *Mtb*.

The granuloma is a spherical structure of immune cells, walling off the bacteria from the extracellular environment. The feature was first described in 1679, 200 years prior to the discovery of *Mtb*, and was initially thought to be the cause of TB disease. For *Mtb*, the

surrounding immune cells provide a microenvironment to initiate latency (inactive state). (Sasindran & Torrelles, 2011; Ramakrishnan, 2012). The core of the granuloma comprises of infected macrophages and epithelioid cells, which subsequently provide *Mtb* with nutritional support for survival. Immune cells including neutrophils, B and T cells, natural killer cells, dendritic cells and fibroblasts also contribute to the formation of granulomas and activate inflammation mediators. Replication of *Mtb* in macrophages in the granuloma causes inflammation and subsequently causes necrosis by killing the host macrophages once activated. Progression of the necrotic lesions leads to the disruption of the granuloma and spread of free *Mtb* to other tissue/ areas of the lungs.

Out of all the members of the MTBC, the strain most widely used in TB research is the *Mtb* H37Rv strain, which has remained pathogenic since it was first isolated in 1905 (Camus *et al*., 2002). The whole genome of the strain was sequenced and consists of 4,411,529 base pairs containing roughly 4000 genes. It has a high guanine/ cytosine (GC) content of 65.6% which is equally spread throughout the whole genome (Phillipp *et* al., 1996; Cole *et al*., 1998). An early study done by Cole *et al.* (1998) deciphered the complete genome of the *Mtb* H37Rv strain and found that *Mtb* produces a large array of lipophilic molecules. These molecules range from simple fatty acids to long-chain, complex molecules such as mycolic acids (MAs). *Mtb* shows a shift in metabolism when inside the host as opposed to the behaviour observed during *in vitro* studies, changing from carbohydrate metabolism to using fatty acids when growing within the host (Smith, 2003). This phenomenon is explained by the presence of as many as 250 enzymes, all involved in the metabolism of fatty acids (Cole *et al*., 1998).

Many genes encode and contribute to the virulence and pathogenicity of the MTBC. However, the *Mtb* genome does not encode classical virulence factors like toxins produced by other pathogenic bacteria (Smith, 2003). The ability of *Mtb* to protect itself from destruction against the first-line of defence and multiply within macrophages in the host is one of its most intriguing properties regarding its pathogenicity. This self-defence is achieved by rearranging host cell functions during the immune response to the microorganism entering the respiratory system. In this event, *Mtb* infection causes immune cells to react to the mycobacteria present in the lungs and subsequently leads to the formation of granulomas, shifting the microorganism to an inactive state (latent/dormant). In this state, the bacteria can wait for an immune response shift or any other adverse event and subsequently emerge to cause active TB. The ability to avoid elimination in the host is what makes *Mtb* such a successful intracellular pathogen and the role of the granuloma raises challenges in prevention and treatment of TB (Parrish *et al.*, 1998; Tufariello *et al.*, 2003; Ramakrishnan, 2012).

In previous studies it has been observed that a change in the lipid metabolism of *Mtb* occurs between its dormancy (latent TB infection) and reactivation (active TB) phases (Raghunandanan *et al*., 2019). These changes result in a depletion of MAs – the main components in the cell wall of *Mtb* - in the dormancy phase and a reversed phenomenon in the reactivation phase. This allows *Mtb* to maintain cell energetics. When *Mtb* shifts to its reactivation phase, growth in the human host is associated with lung damage due to the widespread lesions that may lead to death due to insufficient oxygen levels. In addition to this, other forms of *Mtb* infection such as tubercular meningitis and tuberculomas in the brain may also lead to death due to inflammation in and around the brain (Smith, 2003; Cardona 2015).

2.1.2 Prevalence of tuberculosis worldwide

According to the World Health Organization (WHO, 2019), TB is not only one of the top 10 causes of deaths worldwide, but it is also the leading cause of mortality by any single infectious agent since 2007. Approximately 10 million people are infected annually. This figure has remained relatively stable in recent years, with a mortality rate of up to 20%. Globally, the disease caused 1.7 million deaths in 2016 alone, where 22% of the deaths were in patients co-infected with the human immunodeficiency virus (HIV). Furthermore, approximately 5% of the 10.4 million individuals infected with the disease in 2016 were resistant to at least two of the first-line TB drugs (Koch & Mizrahi, 2018; Namasivayam *et al*., 2018). Mortality rates decreased a fraction in 2017, with an estimate of 1.6 million deaths. Approximately 18.75% of these was HIV-positive (WHO, 2018). In 2018, a further reduction in the mortality rate was recorded and approximately 1.45 million individuals were deceased: a 27% reduction from the year 2000. From these mortalities 1.2 million deaths were amongst HIV-negative individuals and 251 000 (17.3%) amongst HIV-positive, reducing the mortality rates with 27% and 60% respectively since 2002. Given the WHO's (2020) End TB strategy to reduce TB mortalities and incidences with 95% and 90% respectively by the year 2035, a steep decrease in both mortality rates and TB incidences is required. To date, a global decrease of 14% (target: 35%) and 9% (target: 20%) reductions in TB deaths and TB incidences, respectively, were reported between 2015 and 2019.

Through the years, the WHO monitored TB infection and the effects thereof worldwide. Thirty countries have been identified as high TB burden countries. In 2019, these 30 high TB burden countries accounted for nearly 90% of the estimated TB incidence worldwide (WHO, 2020) and eight out of the 30 accounted for two thirds of the global incidence. These countries included India (2 640 000 estimated incidence), Indonesia (845 000 estimated incidence), China (833 000 estimated incidence), the Philippines (599 000 estimated incidence), Pakistan

(570 000 estimated incidence), Nigeria (440 000 estimated incidence), Bangladesh (361 000 estimated incidence) and South Africa (360 000 estimated incidence).

Not only does the intensity of TB incidence and mortality differ in various parts of the world, but also the different strains of *Mtb* present. Numerous studies have indicated that the genomic differences in the MTBC vary worldwide. According to Mekonnen *et al.* (2019), the east-west pole of Africa is the focal point of different lineages of *Mtb.* Umpeleva *et al*. (2020) found that the Beijing genotype of *Mtb* was predominant in an enclosed area of Russia. In Thailand, two strains were found to be predominant amongst the people, namely the Indo-Oceanic lineage and East-Asian lineage (mainly Beijing strains). Even though the East-Asian lineage is known to be highly virulent, the Indo-Oceanic lineage resulted in a higher mortality (Smittipat *et al*., 2019).

2.1.3 Prevalence in South Africa

According to the latest Global TB report (WHO, 2020), South Africa is identified as one of the top high TB burden countries, accounting for an estimated 3.6% of global TB incidence in 2018. An estimated 360 000 cases of TB were recorded in South Africa in 2019, of which approximately 16.7% of total cases led to mortality. Furthermore, 58% of the total TB cases were amongst individuals co-infected with HIV and mortality amongst these co-infected individuals accounted for 62% of the total mortality caused by TB. Figure 2-1 indicates a reduction of TB incidences and mortalities in South Africa over the last decade. With a population increase of almost 8.5 million people in the country (WHO, 2011; WHO, 2020), a decrease is observed in total TB incidence, TB incidence in HIV-positive patients, total TB related mortalities, and mortalities amongst HIV-positive individuals. Despite the total decrease in TB incidence, cases have emerged in the year 2019, which is worrying considering the urge to end the TB pandemic. On the contrary, mortality rates associated with TB lowered. Positively, notifications of TB diagnosis between January and June 2020, reduced significantly in South Africa, compared to 13 other high burden countries able to submit data to the WHO (2020) in the reporting months.

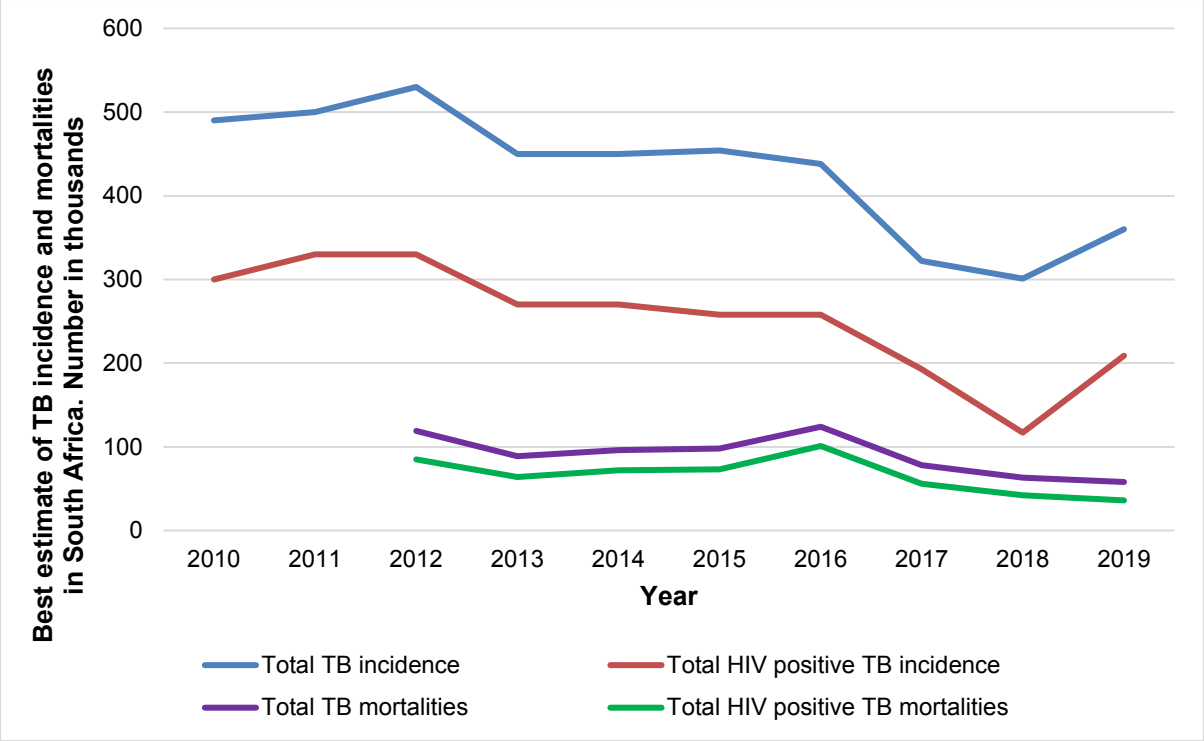


Figure 2-1 Best estimates of TB incidence and mortality amongst patients co-infected with HIV and TB only in the past 10 years. Numbers have decreased for all parameters, except total and HIV positive incidence in the last year. No data is available of HIV positive mortalities from 2009 until 2011. Data generated from WHO (2011-2020).

2.1.4 Co-infection of TB and HIV

Sub-Saharan Africa was identified as the region with the most HIV-associated TB incidence by the WHO, accounting for 70% of worldwide co-infection in 2000 (Maher *et al*., 2005). In recent years, co-infection in particularly South Africa, accounts for approximately 25% of worldwide co-infected incidence (WHO, 2020). This raises concern, since South Africa only accounts for 0.76% of the global population. HIV co-infection increases the rate of TB progression and may lead to an increase in transmission of the disease. Furthermore, it may lead to the amplification and dissemination of drug-resistant TB. TB reinfection is also often related to co-infection with HIV. The two diseases thus combined present very unique programmatic and treatment challenges (Khan *et al*., 2019b; Peters *et al*., 2019; Luo *et al*., 2017).

HIV infection is involved in the progression of latent TB infection (LTBI) to active TB infection (Singhvi *et al*., 2019). Granulomas caused by infections generally consist of the immunological $CD4^+$ T cells, $CD8^+$ T cells, macrophages, and to a lesser extent B cells. HIV infection causes a disruption of granulomas by infecting the $CD4^+$ T cells and subsequently lowers the cell

counts in HIV-positive individuals and compromises their immunity. This immunosuppression, accompanied by the disruption of granulomas, causes the reactivation of LTBI and susceptibility to newly acquired TB infection. TB infection additionally also has an effect on HIV viral load by stimulating its replication. The virus infects $CD4^+$ T cells that have been recruited by *Mtb* formed granulomas, resulting in a high viral load in the broncho-alveolar lavage (Jadhav *et al*., 2019). TB is the main cause of death amongst HIV-positive individuals; it is estimated that a 40% reduction of HIV-positive related TB deaths will occur when and if HIV-positive patients receive pre-TB-treatment to prevent infection (UNAIDS, 2019).

2.1.5 Co-infection of TB and emerging viruses

In December 2019, a cluster of pneumonia-related infections were observed in Wuhan, China relating to a novel viral infection namely the severe acute respiratory coronavirus 2 (SARS-CoV-2) (Rabi *et al*., 2020). Since then, extensive research has been done globally to develop a vaccine to stop the spread of the virus. It was previously found that mortality is higher in TB-influenza co-infections (Walaza *et al*., 2019). Cainelli *et al*. (2020) suggests that secondary lung damage due to TB may play a role in coronavirus infection outcomes. A preliminary study done by Pathak *et al*. (2020), indicated that infection with a coronavirus reactivates dormant TB in the lungs. However, it activates the altruistic stem cell defence mechanism, decreasing the viral load in the lungs. Although the results demonstrated the potential for developing vaccines, it predicts an increase in TB incidence (Pathak *et al*., 2020).

2.2 Treatment of tuberculosis

When diagnosed with TB, the treatment regimen requires the continuous administration of several antimicrobials for a very long period. Verrall *et al*. (2020) found that the early elimination of *Mtb* is associated with an innate immune response, by examining cytokine response to *Mtb* exposure in individuals that did not convert to active TB disease. These responses are similar to those activated during vaccinations. Revaccination of adolescents in South Africa with Bacille Calmette–Guérin (BCG) resulted in a decrease in *Mtb* infection in high burden settings (Nemes *et al*., 2018). Therefore, it is suggested that the innate immune system can be boosted through revaccination with BCG to help prevent *Mtb* infections and subsequently decrease TB transmission (Verrall *et al*., 2020). However, the prevention of the disease is limited and when active TB infection occurs, treatment measures should be put into place.

Active TB infection needs to be treated as soon as possible to both cure the patient and prevent the spread of the disease. Disease progression and spread can be prevented when

treatment is rapid and effective; hence the correct drug regimen is essential for positive treatment outcomes. Treatment of *Mtb* is difficult due to resistance factors inherent to the organism (intrinsic drug resistance). These factors include: the cell envelope's unique wax-like composition is hydrophobic, making it resistant to several antibiotics; secondly the organism comprises of enzymes (beta-lactamase) responsible for breakdown of beta-lactam antibiotics; and third the bacteria have efflux mechanisms that contributes to resistance of antibiotics in the classes tetracyclines and aminoglycosides (Kolyva & Karakousis, 2012).

Pulmonary TB is described as the disease when infection of *Mtb* affects the lungs. However, *Mtb* infection can occur in other parts of the human body, causing extrapulmonary TB. Nevertheless, the former and latter are both treated with similar drug regimens (WHO, 2017). Upon diagnosis with drug susceptible pulmonary TB, first-line treatment is given to the patient. A standard course consists of four antimicrobials namely rifampicin, isoniazid, pyrazinamide and ethambutol, administered for two months. After this initial intensive phase, the continuation phase follows, where rifampicin and isoniazid are administered for a remaining four months (Health, 2008; Health, 2014; Hiruy *et al*. 2015). Given the administration of multiple antibiotics for such a long period, fixed-dose combinations (FDCs) have been implemented as opposed to the administration of single drug formulations. FDCs are advantageous in the event of patient compliance, reducing the number of tablets to be consumed daily from as many as 16 tablets to three or four tablets. Subsequently it was suggested that the use of FDCs will reduce the presence of multi drug-resistant (MDR-) and extensively drug-resistant (XDR-) TB (Blomberg *et al*., 2001). Each first-line TB drug in the combination has its own mechanism of action when administered. Each individual drug interacts differently with *Mtb* in order to stop it from multiplying in the human host.

2.2.1 Rifampicin

Rifampicin (RIF) is a broad-spectrum antimicrobial targeting Gram-positive and some Gram-negative bacteria, including mycobacteria (Beauduy & Winston, 2018). It was discovered in 1963, making it the most frequently used first-line TB drug (TB Alliance, 2020a). The drug penetrates phagocytic cells in most tissues. Furthermore, it kills organisms that are not easily accessible to other drugs, such as organisms entrapped intracellularly, in abscesses and the lungs (Beauduy & Winston, 2018). However, the use of RIF alone is not effective in the treatment of many bacterial infections (CLSI, 2017) and it is therefore used in combination with other anti-mycobacterials for the treatment of TB.

The mode of action of RIF is bactericidal, causing bacteria to die as result of administration of the drug and is therefore very effective during the continuation phase of therapy (Pankey & Sabath, 2004; Health, 2008; CSLI, 2017; Wipperman *et al*., 2017). RIF acts by inhibiting RNA synthesis in the bacteria causing the infection (Carballeira, 2007). The drug inhibits RNA polymerase activity by blocking the beta-subunit of the enzyme. This results in closing of the RNA/DNA channel, blocking the growth of the RNA chain, and thus inhibiting protein synthesis (TB Alliance, 2020a).

The challenge occurs when treating TB patients co-infected with HIV, because of the pharmacokinetic feature of RIF that results in the induction of certain cytochrome P450s during metabolism in the liver (Seung *et al.,* 2015; TB Alliance, 2020a). Co-administration of RIF with the anti-retroviral drug Efavirenz reduce blood plasma concentrations of the latter, due to induced cytochrome P450 3A4 (Gong *et al*., 2019). RIF is not known to cause severe side effects, but common side effects include discoloured body secretions, accumulation of transaminase in the liver for a short period of time, hepatitis and gastro-intestinal discomfort (Seung *et al*., 2015). Chronic exposure to the drug may result in nausea, vomiting and unconsciousness (TB Alliance, 2020a). In certain instances, and when using the drug with pre-existing conditions, hepatotoxicity may worsen; however, this is a very rare occurrence.

2.2.2 Isoniazid

The mode of action of Isoniazid (INH), first discovered in 1952 is also bactericidal (Health, 2008; TB Alliance, 2020b). A combination of RIF and INH is very effective in treating *Mtb* infection and will cure as much as 95% of TB cases after 9 months of administration. The bactericidal activity of INH is rapid, killing actively growing bacteria within two weeks of treatment initiation. INH penetrates infected macrophages and is active against intra- and extracellular organisms. This drug is a pro-drug, meaning that it is activated in the presence of bacterial enzymes. In the case of INH, the presence of the mycobacterial catalase-peroxidase, KatG, activates the drug. INH is also suggested to be used for the treatment of LTBI, administering a fixed dose of 300 mg per day for a period of nine months (Beauduy & Winston, 2018; TB Alliance, 2020b).

INH's bactericidal activity is most effective in dividing cells, blocking MA synthesis in mycobacteria cell walls (Carballeira, 2007; Seung *et al*., 2015). This is achieved by the activated form of the drug forming a complex with acyl and beta-ketoacyl carrier proteins, causing an inhibition of the function of a NADH (nicotinamide adenine dinucleotide)-specific

enoyl acyl carrier protein reductase involved in synthesis of fatty acids (Beauduy & Winston, 2018; TB Alliance, 2020b).

INH is absorbed in the gastro-intestinal tract and metabolised in the liver, where small amounts of the drug and its metabolites are excreted in urine (Seung *et al*., 2015; Beauduy & Winston, 2018). General immunological reactions caused by INH include fever and rashes (Beauduy & Winston, 2018). Furthermore, INH causes hepatitis, especially amongst older individuals and in individuals that consume large amounts of alcohol. Another side effect of INH is peripheral neuropathy, which is dose-related and often seen in patients who is malnourished, diabetic and abuses alcohol. Less common side effects include gynecomastia (swelling of breast tissue in males), rash, psychosis and seizures (Seung *et al*., 2015; TB Alliance, 2020b).

2.2.3 Ethambutol

Ethambutol (EMB) was first discovered in 1961 and has a bacteriostatic mode of action, preventing the growth of bacteria by keeping it in the stationary phase (Pankey & Sabath, 2004; Health, 2008; TB Alliance, 2020c). EMB acts by inhibiting the enzyme activity of arabinosyl transferases in mycobacteria. This enzyme is responsible for polymerization of arabinoglycan, an essential structural component of the cell wall of mycobacteria. The presence of EMB therefore results in inhibition of lipid and cell-wall biosynthesis. The growth of *Mtb* and other mycobacterial strains that are susceptible to EMB, is inhibited at a dose of between one and five µg/mL *in vitro* (Beauduy & Winston, 2018; TB Alliance, 2020c).

The drug is well absorbed in the gastro-intestinal tract and is excreted in urine (20%) and faeces (50%). EMB is generally well tolerated, although a common side effect reported in patients is blindness that is normally reversable; however certain instances where the phenomenon is irreversible have been reported. Other side effects include hepatotoxicity, itching, arthritis/arthralgia, gastro-intestinal discomfort, headaches, mental confusion, dizziness, malaise, disorientations and possible hallucinations (Seung *et al*., 2015; Beauduy & Winston, 2018; TB Alliance, 2020c).

2.2.4 Pyrazinamide

Pyrazinamide (PZA) is a bactericidal drug that is used for the treatment of only TB. Though its bactericidal effect is less potent than that of RIF and INH, it has a potent sterilizing activity, targeting *Mtb* in their inactive phase (Kolyva & Karakousis, 2012). The drug remains inactive at a neutral pH but becomes active when the environment is slightly acidic, subsequently inhibiting the growth of tubercular bacilli by disrupting its membrane potential and interfering

with energy production. The latter is crucial for survival of *Mtb* in the acidic environment of the lungs (Health, 2008; Pham *et al*., 2015; Beauduy & Winston, 2018). PZA penetrates macrophages and acts on *Mtb* in the acidic environment of lysosomes. PZA is not sufficiently potent to cure TB by itself but acts as an additive in combination with RIF and INH to clear residual intracellular organisms and so to avoid relapse at a later stage. Furthermore, the addition of the drug to the TB treatment regimen shortens the therapeutic period from nine to six months (Beauduy & Winston, 2018; TB Alliance, 2020d).

Mycobacterial pyrazinamidase converts PZA to its active form, namely pyrazinoic acid, which then disrupts metabolism and transport functions of the cell membrane of *Mtb* (Beauduy & Winston, 2018). The drug is easily absorbed in the gastro-intestinal tract and distributed to many body tissues. PZA is metabolized in the liver and metabolites of the drug are excreted renally. The side effects of PZA include hepatotoxicity, arthritis/arthralgia, hyperuricemia and gastro-intestinal distress (nausea, vomiting and anorexia). Patients with severe liver damage or acute gout should be cautions when using PZA (Seung *et al*., 2015; Beauduy & Winston, 2018; TB Alliance, 2020d).

2.3 Drug resistant tuberculosis

The TB crisis is worsening due to the emergence of drug resistant *Mtb* strains. A *Mtb* strain is classified as MDR-TB when the strain is resistant to at least two of the first-line TB drugs, namely RIF and INH. Resistance occurs mainly due to mutations in genes encoding enzymes that are inhibited during treatment with first-line drugs (Beauduy & Winston, 2018). In 2018, half a million new RIF-resistant TB cases were reported, of which 78% were reported as MDR (WHO, 2019). Drug resistance occurs when treatment is used inadequately, mainly by the use of antimicrobials that are ineffective and termination of antimicrobial usage before the treatment course is complete. Spontaneous mutations, due to suboptimal treatment, in *Mtb* chromosomes can occur and subsequently cause the organism to be resistant to first-line TB drugs (Gygli *et al*., 2017). Furthermore, drug resistant pathogens can be transmitted from one individual to another in a community and as nosocomial infections. In the events of MDR-TB infection, the use of second-line treatment is required with increased treatment duration of 18-24 months (Seung *et al*., 2015). Second-line treatment includes administration of a combination of several antimicrobials. These drugs include injectables (kanamycin, amikacin, capreomycin & streptomycin), fluoroquinolones and other drugs administered orally i.e., aminoglycosides, cycloserine, ethionamide, amino alicyclic acid, clofazimine and linezolid amongst others. However, these drugs are not as effective and are more toxic when compared to the first-line TB drugs (Ramachandran & Swaminathan, 2015).

Progression to XDR-TB occurs when the *Mtb* strain is resistant to first-line and most of the second-line TB drugs (Health, 2008; Birhanu *et al.*, 2019). When *Mtb* develops resistance to first and second-line TB drugs, it becomes problematic because treatment will become nearly impossible due to the limitation of the gastro-intestinal, renal and/or neurological toxicities of newer drugs. The aforementioned contributes to the disease being “untreatable”, making it a serious public health threat (Carballeira, 2007).

The need for new *Mtb* targeting drugs and delivery systems is becoming ever more necessary to meet the long-term TB eradication goal set out by the WHO, due to the increase in MDR- and XDR-TB cases. A novel therapeutic approach to TB treatment includes the use of nanotechnology to fight against resistant pathogens including MDR- and XDR-TB (Ramachandran & Swaminathan, 2015; Costa-Gouveia *et al*., 2017; see section 2.4 below).

2.4 Alternative drug delivery systems for treatment of TB

According to WHO, the bioavailability of RIF in FDC treatments as opposed to single drug dose treatments is of concern (Blomberg *et al*., 2001). This suggests that other forms of drug delivery should be considered when treating TB with FDC drugs. Nanotechnology is an emerging field of research to develop drug delivery systems by identifying excipients that might aid as carriers for active pharmaceutical ingredients (APIs) specifically for bacterial infections (Jadhav *et al*., 2019). The use of nanoparticles (NPs) as carriers in a delivery system is emerging as a tool to enhance the bioavailability of drugs. Furthermore, incorporation in NPs provides protection against immediate degradation, thus extending the time during which the drug is present for absorption in the gastro-intestinal tract (GIT). It has been shown to control drug release at the absorption site; enhance solubility; and improve the pharmacokinetics profile (Aminu *et al*., 2020). Not only has NPs been identified as a promising mode of delivery, but other nanomedicine have also been researched as drug delivery systems. These include nanotubes, nanogels, liposomes and micelles for especially cancer treatment, amongst other diseases and infections (Liu *et al*., 2008; Mahmoodzadeh *et al*., 2019; Ashjari *et al*., 2020; Askari *et al*., 2020).

2.4.1 Pheroid® technology as a tool for improved drug delivery

Pheroid® technology might aid in the effective absorption and delivery of the standard antimicrobials (Grobler, 2013). Pheroid® technology is based on colloidal emulsion systems developed to entrap and deliver pharmaceutical compounds. Amongst others, Pheroid®-based studies have shown the use of the technology to have several unique advantages: for

instance, its biodegradable content is regarded as safe and may even show therapeutic effect (Grobler, 2013). Furthermore, the materials are cost-effective with simple manufacturing steps. In addition, the manufacturing of Pheroid® does not require harsh chemicals or contaminates water, thus making it environmentally friendly. Where Pheroid® consists of an oil, water and gas phase, pro-Pheroid® contains no water phase and physically looks like an oil. Upon interaction with a water phase, micro- and NPs form spontaneously and APIs that are present are packed into vesicles, microsponges and/or lipid aggregates. Despite the poor bioavailability of RIF in FDCs, it is also unstable in the presence of moisture. Pro-Pheroid® is thus an important form of delivery to accommodate for the nature of the drug when combined with the remaining first-line TB-drugs (Grobler, 2013).

Studies have shown that the use of Pheroid® resulted in an increase in bioavailability and stability of antimalarial compounds (Slabbert *et al*., 2011; Steyn *et al*., 2011). The use of Pheroid® in combination with TB treatment APIs has shown promising results *in vitro* and *in vivo* (Matthee, 2007; Nieuwoudt, 2009). Decrease in bacterial load at a lower concentration than free form drugs were observed in *in vitro* studies. Furthermore, effect of Pheroid®-based TB drugs on resistant strains has also been observed *in vitro* (Nieuwoudt, 2009). Increased concentrations of drugs were observed in blood plasma of animals and humans when delivered with Pheroid® (Nieuwoudt, 2009; Grobler, 2009). This delivery system may thus lead to improved treatment outcomes when combined with standard TB therapy in conjunction with additional compounds such as eicosapentaenoic acid (EPA) for its mycobactericidal mechanism of action (please see section 2.4.3.1 below) and mycolic acids (MA) as the targeting ligand for *Mtb* in the formulation (please see section 2.4.2.1 below).

2.4.2 Nanoparticles as targeting ligands

Numerous studies have examined the properties of NPs as drug carriers in targeting *Mtb* infected macrophages (Machelart *et al*., 2019; Upadhyay *et al*., 2019; Pi *et al*., 2020). Various NPs serving as carriers for TB drugs are continuously being evaluated to enhance treatment efficacy and simultaneously reduce dosage frequency and shorten duration of treatment (Pandey *et al*., 2003; Ahmad *et al*., 2006; Pandey *et al*., 2009; Grobler *et al*., 2016; Hakkimane *et al*., 2018; Pi *et al*., 2019). Furthermore, the use of drug carriers administered by various routes has also shown enhanced effects. For instance, in a recent study the administration NPs carrying TB-drugs indicated that RIF and INH can be successfully co-encapsulated by using crude soybean lecithin prepared liposomes to ensure macrophage-targeting actions when delivered by inhalation. (Nkanga *et al*., 2019). Additionally, Kisich *et al*. (2007) demonstrated the enhanced efficacy of the antimicrobial fluoroquinolone, moxifloxacin when

encapsulated in NPs *in vitro* and suggested that the drug accumulates in macrophages when administered intravenously.

2.4.2.1 Mycolic acids

MAs are long chain fatty acids that are high in molecular weight (Lee *et al*., 1997). Fatty acids form part of solid lipid NPs and are used as propitious drug carriers for delivery (Banyal *et al*., 2013). As one of the main components of *Mtb*'s cell wall, MA has been shown to contribute to the organism's pathogenicity (Ghazaei, 2018). Despite the pathogenetic properties of MA, it also has biological effects, such as induction of immune responses like the formation of foam cells and urging towards pro-inflammatory responses (Korf *et al*., 2005; Korf *et al*., 2006). According to Lemmer *et al.* (2015) MA derived from *Mycobacteria* can act as a targeting ligand in TB treatment. The incorporated MA carries NPs to *Mtb* infected macrophages, inducing phagocytic uptake of the drug (Lemmer *et al*., 2015).

2.4.3 Anti-mycobacterial actions of nanoparticles

The use of NPs with anti-mycobacterial activity further enhances the therapeutic effect of a drug. For instance, poly-β-cyclodextrins are successful drug carriers with inherent anti-mycobacterial properties by depleting cholesterol, which prevents *Mtb* uptake in macrophages (Machelart *et al*., 2019). As mentioned previously, fatty acids form part of solid lipid NPs that serve as carriers in drug delivery (Banyal *et al*, 2013). The use of carrier molecules with anti-mycobacterial effect is therefore of interest when developing new ways to fight against *Mtb* infection. *Mtb* displays mechanisms for the synthesis of fatty acids precursors of the MAs situated in the outer layer of pathogenic mycobacteria. These precursors can bind to cholesterol, the presence of which is considered to be one of the major virulence factors of mycobacteria (Carballeira, 2007; Lemmer *et al*., 2015). Chemical intervention in enzymes responsible for fatty acid synthesis is an attractive target in developing new anti-mycobacterial fatty acids (Carballeira, 2007).

2.4.3.1 Eicosapentaenoic acid

EPA is a long chain, omega-3 fatty acid found mainly in fish oils (Webster, 2019). In a study conducted *in vitro*, it has shown that EPA has anti-mycobacterial effects on various *Mycobacterium* strains in the minimum inhibitory concentration range (Saito *et al*., 1984). Recently, it was found that the supplementation of EPA and docosahexaenoic acid (DHA) in TB infected mice (C3HeB/FeJ mice) reduced the bacteria load, which is suggested to be

because of enhanced phagocytic activity of immune cells as response to the infection (Nienaber *et al*., 2020).

2.5 Kramnik mouse model for TB infection studies

The ideal animal models for TB infectious studies are those that best mimic human TB infection. The use of an appropriate model is of importance to enable valid scientific conclusions with regards to humans to be drawn. Various animal models have been implemented to examine TB disease *in vivo*, be it disease progression or drug susceptibility (Singh & Gupta, 2018). These animal models include larger mammals such as rabbits, guinea pigs and non-human primates, along with smaller mammals such as mice. Mouse models are considered the most practical animal model to study TB (Fonseca *et al*., 2017). Different mouse strains specifically used in TB research is the C57BL/6 strain, Balb/c and most recently C3HeB/FeJ (Kramnik mouse model) (Zhan *et al*., 2017).

Pulmonary TB in humans is characterized by various lesions that differ in cellular organization, composition, the degree of caseous necrosis and the extent of encapsulation (Canetti, 1955; Dartois, 2014). Of all the mouse models, the Kramnik model is thought to mimic human TB infection, since the mice develop well-defined hypoxic granulomas that display caseous necrotic lesions in the lungs with large quantities of bacteria present, both intracellularly and extracellularly after infection (Irwin *et al*., 2015). As discovered by the developers of the mouse model, three types of lesions form in the mice after *Mtb* infection. The first type of lesion is similar to those found in humans - solid necrotic caseous lesions. The second type of lesion is composed mainly of neutrophils and resemble granulocytic pneumonia (Irwin *et al*., 2015). The latter resembles polymorphonuclear alveolitis that can be seen in human TB (Canetti, 1955). A third type of lesion found in the Kramnik mouse model resembles similar lesions found in Bab/c mice post aerosol infection. However, cavitary lesions occur in Kramnik mice, which can be compared with human TB, since it contains bacteria resilient and/or resistant to immunological response and TB treatments.

2.6 The gastro-intestinal microbiome in health and disease

The gastro-intestinal microbiome can be seen as an additional organ in the human body (O'Hara & Shanahan, 2006). Microbiota and their metabolites within this "organ" play an essential role in the human physiology and have been shown to play a role in the state of immunity and metabolism of the healthy human as individual. A healthy microbiome is essential from early life to develop a normal immunoregulatory network for later in life (Cahenzli *et al*., 2013). Furthermore, the presence and also diversity of microbes in the gastro-

intestinal tract prevent colonisation of pathogens by competing for nutrients and binding sites and by the production of antimicrobial proteins.

The gastro-intestinal microbiome is suggested to play an important role in human health and disease through several mechanisms. Firstly, the microbiome increases the extraction of energy from food, it increases the absorption of nutrients and alters signalling of appetite. Secondly, the microbiome provides the human host with specific biochemical pathways and enzymes. Thirdly, the microbiome also serves as a physical barrier by protecting the host from pathogens through competition for nutrients and production of antimicrobial substances. Lastly, the microbiome forms part of the intestinal mucosa and the host's immune system (Wang *et al*., 2017).

An interaction between the gastro-intestinal microbiome and the brain, lungs and liver exists. This interaction is thought to regulate between the healthy and diseased states of individuals (Mayer, 2011; Enaud *et al*., 2020; Albillos *et al*., 2020). The gut-brain axis has been intensively studied, and research results indicate that the gastro-intestinal microbiome plays an essential role in behaviour, brain function, stress regulation, human development and mental diseases (Ross, 2019; Ezra-Nevo *et al*., 2020; Zhu *et al*., 2020). Furthermore, it is suggested that the microbiome can modulate endocrine, nervous and immune communication (Collins *et al.,* 2012). Metabolites produced such as short chain fatty acids also affect gut-brain signalling (Mohajeri *et al*., 2018). Recently it has been suggested that a healthy gastro-intestinal microbiota has an impact on depression and that the maintenance or restoration of a healthy gut is positively correlated with prevention and/or treatment of undiagnosed mental disorders (Liang *et al*., 2018).

A healthy gastro-intestinal microbiome is also linked to the liver and liver disease. A large volume of blood flows through the liver, carrying metabolites produced by the microbes of the microbiome. Microbial dysbiosis has been associated with the progression of chronic hepatitis, alcoholic liver disease, non-alcoholic fatty liver disease, cirrhosis and hepatocellular carcinoma (Jiang *et al*., 2019).

Recently, the gut and its interaction with the lungs and respiratory illnesses has also started gaining an increasing amount of attention. Dysbiosis of microbes in the gastro-intestinal microbiome along with the lung microbiome is associated with asthma, chronic obstructive pulmonary disease (COPD) and cystic fibrosis. The dysbiosis in both microbiomes either contributes to the severity of the condition or the condition causes the disruption of the microbial communities (Enaud *et al*., 2020; Hufnagl *et al*., 2020).

2.6.1 The microbiome and tuberculosis

Recent studies have indicated that the gut and lung microbiome are associated with TB infection and disease (Adami & Cervantes, 2015; Namasivayam *et al.*, 2018; Gupta *et al*., 2018). Namasivayam *et al*. (2018) pointed out that mechanisms within the microbiome may potentially influence the *Mtb* biology by

(i) influencing the susceptibility or response to therapy in the GIT;
(ii) affecting drug absorption in the GIT during TB treatment; and/or
(iii) producing metabolites that activate antimicrobial or immune activities and therefore directly influence *Mtb* growth.

When dysbiosis occurs among the normal microbiota, it has a negative impact on the immune responses and can lead to the colonization of pathogens. Furthermore, immune responses and inflammation development in turn are affected by the intestinal and respiratory microbiome (Dudek-Wicher *et al*., 2018; Tarashi *et al*., 2018). A change in the gastro-intestinal microbiome has an effect on the development of diseases, and because *Mtb* is regarded as one of the most important pathogens that rapidly colonize when a change in microbial composition occurs, it is of importance to maintain a stable microbiome. Furthermore, when an individual is infected with *Mtb*, its progression and chronicity are hypothesized to contribute to more dysbiosis (Adami & Cervantes, 2015; Tarashi *et al*., 2018).

In recent times it has been suggested that *Mtb* infection and TB disease progression may be related to the microbial composition and function (Namasivayam *et al.*, 2018). The healthy gastro-intestinal microbiome consists of thousands of organisms, including bacteria, fungi, archaea, viruses and protozoans. The different genera of microorganisms present in the microbiome stretches far. Members of the bacterial phyla Firmicutes and Bacteroidetes feature in the highest abundance; Actinobacteria, Proteobacteria and Verrucomicrobia members are also quite abundant, but to a lesser extent. Finally, small abundance of Fusobacteria and the archaea Euryarchaeota are present in the microbiome. These organisms generally remain constant in the intestines of individuals (Becattini *et al*., 2016; Dudek-Wicher *et al*., 2018).

2.6.2 Effect of tuberculosis on the microbiome

Several studies have been conducted relating to the gastro-intestinal microbiome, however, many of which have been in mouse models (Becattini, 2016). Even though some genera abundance differs between the mouse and human microbiome, the mouse model is a valuable

tool in studying and predetermining the impact on the human microbiome. The results of a murine study performed in parallel with a clinical trial have for instance shown that TB therapy induced dysbiosis of the microbiome, which persisted for a long time after treatment (Namasivayam *et al.,* 2017 & Wipperman *et al*., 2017). The relevance of comparisons of murine studies with human studies is enhanced by the reconstitution of germfree (GM) mice with other species' including human microbial communities.

A study done by Namasivayam *et al*. (2017) indicated that only minor changes appear in the gastro-intestinal microbiota in a variant of C57BL/6 mice when infected with TB. It was indicated that there was a slight decrease in diversity 12 weeks into the experiment, where a differential abundance in members of Firmicutes, Bacteroidetes and Tenericutes was noticed when compared to non-infected samples. However, Winglee *et al*. (2014) followed the progression of *Mtb* infection from pre-infection until death and the effect thereof on the gastro-intestinal microbiome in Balb/c mice. It was observed that a rapid loss in diversity occurs in mice infected with two separate *Mtb* strains (CDC1551 & H37Rv) in respective study groups. An initial loss in diversity was shown as early as six days post-infection. Microbiome recovery occurred during infection; however, it resulted in a different composition of microbes. The drastic decrease in members of *Clostridiales* and *Bacteroidales* are suggested to have interplay between the microbiome and the host immune system (Winglee *et al*., 2014). Wipperman *et al*. (2017) observed the effect of *Mtb* infection on the microbiome of patients in Haiti. Even though the effect of active TB infection on the human microbiome was not studied, it was observed that patients with LTBI and uninfected individuals did not show any microbiomic differences. In a later study, Maji *et al.* (2018) observed the shifts in the microbiome with TB infected patients at day zero of treatment. An abundance increase in microorganisms involved in butyrate and propionate metabolism (*Faecalibacterium*, *Coprococcus*, *Phascolarctobacterium* and *Psuedobutyrivibrio*) and *Bacteroides* were observed, with a decrease in in *Bifidobacterium* and *Prevotella*. This phenomenon may be explained due to diet limitations where *Prevotella spp*. is better equipped at consuming carbohydrates, which is derived from plants; the absence of fibre may allow *Bacteroides* to colonise in the gastro-intestinal environment, resulting in a decline in abundance of *Prevotella* (Koropatkin, 2012). The loss in appetite amongst TB patients may suggest the selection of *Bacteroides,* which is capable of using host mucus glycans more efficiently (Maji *et al*., 2019; Koropatkin, 2012). Hu *et al*. (2019) observed differences in increased abundancies between TB patients and healthy controls in China. It was found that there was a significant increase of 23 species in healthy controls of which nine were short-chain fatty acid (SCFA) producers (five butyrate producers; two lactose and acetate producers; two acetate and propionate producers). Furthermore, five SCFA fermentation associated metabolic pathways were

decreased in TB patients, explaining the decreased abundancy of SCFA producers in TB patients. Two species were significantly increased among TB patients, namely an unclassified *Coprobacillus* and *Clostridium bolteae*. A similar increase in *C. bolteae* have been observed in patients with autism and type two diabetes, which has subsequently been connected with abnormalities in the immune system (Hu *et al*., 2019).

The presence of *Mtb* in stool is not surprising since the GIT is exposed to pathogens invading the respiratory tract. However, the presence of the infectious agent in stool of members of the same household was also observed (Maji, 2019). This may suggest that members of the same household are LTBI and does not develop active TB infection. An increase in pathogens in a dysbiotic gastro-intestinal microbiome is also observed, with an increase in *Shigella sonnei*, *Escherichia coli*, *Streptococcus vestibularis* and *Streptococcus pneumonia* (Maji, 2019).

2.6.3 Microbiome dysbiosis due to antimicrobial therapy and its implications

When infected with a bacterial infectious agent, a course of antimicrobials is typically administered to treat the disease. The main effect of the antimicrobial is to target the infectious agent and cure the individual of the disease. However, it can be expected that the use of antimicrobials will also affect the general microbiome when consumed. Several studies have been conducted to examine the effect of certain antimicrobials on the microbiome. For instance, penicillin, cephalosporins, carbapenems and fluoroquinolones cause a decrease in bacteria such as *Enterobacteriacaea*, lactobacilli, bifidobacteria, *Escherichia coli*, *Bacteroides* and clostridia in the gastro-intestinal microbiome (Bhalodi *et al*., 2019). Gastro-intestinal dysbiosis as a result of antimicrobial therapy reflects in multiple conditions in new-borns and premature infants. Conditions include allergies, asthma, obesity, neurodevelopmental outcomes and eczema (Kelly *et al*., 2020). Furthermore, antimicrobial induced dysbiosis of the gastro-intestinal microbiome has also proven to impair the immune response against influenza virus and increase susceptibility to *E-coli*-pneumonia. Interestingly, fibre rich diets increased survival rate in mice, confirming the importance of diet in recovery of disease (Ichinohe *et a*l., 2011; Tsay *et al.,* 2011; Trompette *et al*, 2018).

Dysbiosis of the gastro-intestinal microbiome depends on the class, duration and dose of antimicrobials (Iizumi, 2017). Certain classes of antimicrobials cause a rapid effect on the microbiome, such as the fluroquinolones and β-lactams, which significantly decrease the microbial composition of the gut microbiome over a short period of time (seven-day treatment). A decrease in certain bacterial species that are susceptible to administered antimicrobials provides space for resistant strains to overgrow and dominate the niche (Panda *et al*., 2014). In the long term, antimicrobial clindamycin has shown a negative impact on the intestinal

microbiome by reduced resistance to colonization by pathogens (Jernberg *et al*., 2010). The treatment of infections with cefoperazone alters the microbial community within the GIT, causing a decrease in colonization susceptibility to *Clostridium difficile* – the cause of inflammation in the GIT (Theriot, 2013). Luo *et al.* (2017) observed an increase of *Escherichia coli* and other pathogens in the phyla Proteobacteria in patients re-infected with TB. It is hypothesised that the use of novel delivery systems may decrease gastro-intestinal dysbiosis by avoiding direct contact with the microbial communities within the environment and subsequently a decrease in the emergence of antimicrobial resistant microbes (Kelly *et al*., 2020).

Given *Mtb*'s intrinsic resistance to a large array of antibiotics, treatment is very specific. Treatment consists of a combination of anti-mycobacterials of which RIF is a broad-spectrum antimicrobial belonging to the non-β-lactam class Annamycin, targeting infections of Gram-positive and Gram-negative bacteria (CLSI, 2017; see section 2.2.1). Gastro-intestinal microbiome changes induced by RIF, in combination with PZA are closely related to changes in the microbiome induced by an antimicrobial cocktail containing vancomycin, ampicillin, neomycin and metronidazole (VANM) (Namasivayam *et al*., 2017). This suggests that alterations in the microbiome is largely due to treatment with RIF and PZA However, the effect of the remaining anti-mycobacterials targeting *Mycobacteria spp*. in the treatment of TB is not clear. Table 2-1 summarizes the changes in the microbiome observed in recent studies as results of different TB treatment regimes in murine mouse models and in clinical settings.

Table 2-1 Most recent studies indicating dysbiosis of gastro-intestinal microbial communities in murine models and clinical studies where TB therapy was administered.

Drug Regime	Drug administration and sample collection of subjects	Sample type	Dysbiosis	Effects of dysbiosis	Resource
Murine model					
HRZ+HR	Oral gavage in a C57BL/6 mouse model. Samples were collected from one week post infection (four weeks infected), during four months of treatment and three months after treatment was terminated in weekly intervals.	Stool	Significant decrease in diversity (mainly class *Clostridia* in phyla Firmicutes) of microbiome within a short time period with persistent, fluctuating shifts in its composition throughout the remainder of treatment. Dysbiosis occurred mainly because of antimicrobial treatment and not infection of *Mtb.* The main driver for dysbiosis was RIF.	Long term effect – Dysbiosis maintained for months after TB-therapy was complete. RIF altered the microbiome to the same extend as other broad-spectrum antimicrobials compared to INH and PZA.	Namasivayam *et al*. (2017)
RIF	Pre-treatment and treatment during *Mtb* infection through drinking water in a C57BL/6 mouse model. RIF was solubilized in DMSO (dimethyl sulphoxide) prior to adding it in the water. Mice were pre-treated for two months and stopped two days before infection with *Mtb*.	Stool	RIF pre-treatment resulted in significant changes of operational taxonomic units (OTUs) in both alpha and beta diversity. An increase in Bacteroidetes and Verrucomicrobia (family level *Bacteroides* and *Verrucomicrobiaceae*) was observed with a decrease in Firmicutes (family level *Lachnospiraceae*). Significant changes at genus-level were also observed.	Changes in the gastro-intestinal microbiome did not affect the T-cell response to *Mtb* infection. Although there was a drastic dysbiosis, no effect on the immune response against *Mtb* infection was observed.	Khan *et al.* (2019a)
INH&PZA			Pre-treatment with INH & PZA resulted in only moderate changes of alpha and beta diversity OTUs. An increase of the phyla Bacteroidetes (family level *Clostridiaceae*) was observed. Faecal transplant largely restored gut microbiota when observing changes in Clostridium XIV bacteria.	Host resistance to *Mtb* infection was compromised through pre-treatment. *Mtb*-specific T cell responses were not affected. Macrophage bactericidal activity (innate immune response) in the lungs was defected due to INH & PZA dependent dysbiosis of the gastro-intestinal microbiome.	

Table 2-1 (continued)

Human studies					
HRZE+HR	Treatment of TB patients from Haiti. Samples of non-infected, LTBI, TB patients undergoing treatment and cured TB patients were collected.	Stool	Patients were on average 3.4 months (halfway) into treatment. Little effect on diversity of the microbiome was observed; however, there was a depletion of bacteria with immunological functions (*Lactobacillus, Coprococus, Ruminococcus* of the phyla Firmicutes and *Bifidobacterium* of the phyla Actinobacteria) in treated patients. Changes in biochemical pathways further confirmed that treatment disturbs the functional and taxonomic structure in the microbiome.	Long term effect of microbiome dysbiosis lasting at least 1.2 years.	Wipperman *et al.* (2017)
HRZE+HR	Treatment of TB patients from China. Samples were collected from patients newly (NTB) diagnosed (one week into HRZE treatment), Re-infected (RTB) patients and healthy controls (HC) were collected.	Stool	Six RTB patients, where MDR *Mtb* infection was suggested to cause an increase in gastro-intestinal microbiota. A greater difference in microbial communities was observed between RTB and HC than new cases and HC. Phylum Bacteroidetes decreased in NTB and RTB patients compared to controls; Firmicutes decreased in RTB and Proteobacteria (phylum of many pathogens) increased two-fold in NTB and four-fold in RTB. *Prevotella, Lachnospira* and *Roseburia* (SCFA producers) were decreased in NTB and *Prevotella* and *Lachnospira* in RTB.	A positive correlation of microbiota composition and CD4+ lymphocytes were observed in patients with TB. CD4+ T cells were associated with the response to infections in adaptive immunity. *Pretovella* (from oral origin) and *Lachnospira* (from gut origin) were positively correlated with the CD4+ T cell count in patients newly diagnosed with TB and a reversed phenomenon with patients re-infected with TB.	Luo *et al*. (2017)

Table 2-1 (continued)

HRZE	Treatment of TB patients in India. Samples were collected before treatment, after treatment for a week and after treatment for a month.	Stool	Changes in phylogenetic and functional level of the gastro-intestinal microbiome were observed in TB subjects before and during treatment as compared to household controls. An increased Firmicutes to Bacteroidetes ratio was observed. *Mtb* identified in stool samples were reduced over the period of treatment of the TB patients.	Ratio increase affected SCFA, gastro-intestinal-derived metabolites, viz. acetate, propionate and butyrate. Butyrate and propionate metabolism increased in TB patients, implicating the role of the gastro-intestinal microbiome in TB pathophysiology.	Maji *et al*. (2018).

HRZ= isoniazid-rifampicin-pyrazinamide; HR= isoniazid-rifampicin; RIF= rifampicin; INH= isoniazid; PZA= pyrazinamide; HRZE= isoniazid-rifampicin-pyrazinamide-ethambutol; DMSO= dimethyl sulphoxide; OTU= operational taxonomic unit

2.7 Methodology for identification of microbial bacteria

For many years, traditional culturing methods were used to determine bacteria present in health and disease in clinical settings. These techniques include the isolation and culturing of bacteria in appropriate media to determine phenotypic characteristics and subsequently identifying bacteria, not only to species level, but in some cases to the specific strain (Gupta *et al*., 2019). However, the use of molecular techniques has emerged in microbiome studies.

2.7.1 Molecular techniques and technologies

Sequencing of bacterial genomes for identification have been used for over two decades and improved with the years. During the first revolution of DNA sequencing in the early 1990s, whole-genome shotgun sequencing was initiated. By using this approach, the whole bacterial genome is randomly segmented and sequenced by Sanger sequencing. These sequences are then assembled into a larger sequence using computer technologies. For this approach, colony culturing, picking and plasmid preparation are required to identify a single organism (Loman & Pallen, 2015).

In the mid-2000s, the second revolution of DNA sequencing occurred. During this time high throughput sequencing, also known as next generation sequencing (NGS) was introduced to the world, where short reads of various bacterial genomes within an environment are produced within one sample (Loman & Pallen, 2015). Short-read sequencing methods generate sequences of up to 600 base pairs (Amarasinghe *et al*., 2020). Several sequencers are available for the aforementioned. Roche's 454 pyrosequencing platform was the first instrument available for NGS and is based on pyrosequencing on beads (van Dijk *et al*., 2014). Thereafter, several NGS technologies have been introduced, including MiSeq, HiSeq, NovaSeq and NextSeq from Illumina (Caporaso *et al*., 2012; van Dijk *et al*., 2014; Senabouth *et al*., 2020); SOLiD from then Applied Bioscience, now Life Technologies (van Dijk *et al*., 2014; Cao *et al*., 2017); MGISEQ and BGISEQ from the Beijing Genomics Institute (BGI) (Fang *et al*., 2018; Senabouth *et al*., 2020); and Ion Torrent from Thermo Fisher (Rose *et al*., 2017). Despite generating short-reads, NGS is highly accurate and has a low error percentage (Loman & Pallen, 2015). A limitation in NGS and Sanger sequencing is the production of amplicons prior to synthesizing sequences. This is obtained with the use of an *in vitro* technique called polymerase chain reaction (PCR). During this process, copies of a desired gene within the organism are produced by cycling through various temperatures (Garibyan & Avashia, 2013).

Single molecule, long read sequencing was introduced during the third sequencing revolution (Loman & Pallen, 2015). Long read sequencing methods are used to retrieve long reads of genome sequences of most organisms, ranging from 10,000 to 100,000 base pairs per read. This approach was developed to eliminate the limiting step of PCR in first- and second-generation sequencing. Hereby in this approach single DNA molecules are sequenced directly, thus avoiding bias associated with amplification (Cao *et al*., 2017). However, this technology produces low accuracy reads. The most used technologies currently are single molecule real-time (SMRT) from Pacific Biosciences and nanopore sequencing from Oxford Nanopore Technologies (Loman & Pallen, 2015; Johnson & Raza, 2018; Amarasinghe *et al*., 2020).

2.7.2 Sequencing approaches

Two of the approaches for NGS sequencing most compared are shotgun sequencing (sequencing of random segments of an entire genome) and 16S barcode sequencing (sequencing all 16S ribosomal RNA [rRNA] gene amplicons present). All bacteria carry the 16S rRNA gene and this fact is used for designing gene specific primers to identify bacteria present in a clinical or environmental sample (Cao *et al*., 2017). In a study where sequencing of environmental samples was compared, 16S amplicon sequencing delivered more promising results, detecting double the number of phyla present in samples recovered during shotgun sequencing. Furthermore, approximately 30% fewer taxon abundancies were observed at family level in samples identified with shotgun sequencing (Tessler *et al*., 2017).

2.7.3 Methods used for microbiome studies

With Sanger sequencing, that forms part of the first sequencing technologies, only small proportions of amplicons are sequenced, resulting in a lower abundance of microbial community than expected. Therefore, 16S rRNA sequencing has been included in NGS platforms to identify more members of a microbial community at a low cost as compared to Sanger sequencing (Cao *et al*., 2017). To date, 16S rRNA sequencing is the most commonly used technique to identify members of microbiomes associated with the gastro-intestinal tract (Khan *et al*., 2019a; Maji *et al*., 2018; Mas-Lloret *et al*., 2020) in murine models and clinical studies, lungs (Xiong *et al*., 2020;) and sputum (Haldar *et al*., 2020) amongst other sites. Furthermore, 16S rRNA sequencing has been performed to cover microbial communities in/on sites of healthy humans as part of the Human Microbiome Project. These sites include amongst others, the gut, skin, oral cavity and airways (Faust & Raes, 2012). A large advantage when using 16S rRNA gene sequencing is the bioinformatic pipelines and tools freely available for data analysis. Quantitive Insights Into

Microbial Ecology (QIIME) (Caporaso *et al*., 2010), mothur (Schloss *et al*., 2009) and ultra-fast sequence analysis (USEARCH) (Edgar, 2010) are commonly used for 16S rRNA gene analysis (Cao *et al*., 2017). Furthermore, the Illumina platform is the most widely used NGS system. Illumina also accommodates most protocols for library preparation. Producing sequencing reads of up to 300 base pairs, Illumina has the highest throughput of all NGS platforms at a relatively low cost (van Dijk *et al*., 2014). Therefore, the use of 16S rRNA gene sequencing on the Illumina platform for NGS is a sufficient and affordable approach for microbiome studies.

2.8 Role of the microbiome in treatment outcome

A healthy gastro-intestinal microbiome remains relatively stable in the absence of antimicrobial exposure (Moya & Ferrer, 2016). As previously mentioned, the short- and/or long-term use of antimicrobials can cause severe dysbiosis of the human gastro-intestinal microbiome. Furthermore, the administration of TB treatment reduces the abundance of microbes in the GIT that are associated with immune responses of the host (Luo *et al*., 2017). As previously described (see section 2.6), there has been substantial evidence that the gastro-intestinal environment functions as an additional organ in prevention or treatment of various diseases associated with the lungs, brain, liver and *vice versa*. Studies done indicated that performing faecal microbiome transplantation (FMT) restores the microbial community of the gastro-intestinal environment and subsequently improves the condition of a disease, mainly *Clostridium difficile* infection (He *et al*., 2017; Borody *et al*., 2019; Park *et al*., 2019). Evidence is emerging that the microbiome plays a role in cancer treatment outcomes by significantly increasing the effect of chemotherapy (Heshiki *et al*., 2020).

Luo *et al*. (2017) evaluated the link between the gastro-intestinal microbiome during TB infection and its clinical relevance and suggested that homeostasis of the gastro-intestinal microbiome may benefit in host recovery and prevention of reinfection with *Mtb*. However, the role of the microbiome in the outcomes of TB treatment has not yet been established. With the use of available molecular techniques for microbiome studies, it is thus important to continue to evaluate the microbiome's response to TB infection and treatment, and to simultaneously evaluate the impact of new approaches for drug delivery, such as Pheroid® technology, on the microbiome and its potential role in treatment outcomes.

References

Adami, A.J. & Cervantes, J.L. 2015. The microbiome at the pulmonary alveolar niche and its role in *Mycobacterium tuberculosis* infection. *Tuberculosis (Edinb)*, 95(6):651-658. doi:10.1016/j.tube.2015.07.004

Ahmad, Z., Pandey, R., Sharma, S. & Khuller, G.K. 2006. Alginate nanoparticles as antituberculosis drug carriers: formulation development, pharmacokinetics and therapeutic potential. *Alginate Nanoparticle-based Antitubercular Drug Delivery*, 48:171-176. doi:10.1007/978-0-387-39571-5_174

Albillos, A., de Gottardi, A. & Rescigno, M. 2020. The gut-liver axis in liver disease: Pathophysiological basis for therapy. *Journal of Hepatology*, 72(3):558-577. doi:10.1016/j.jhep.2019.10.003

Alexander, K.A., Laver, P.N., Michel, A.L., Williams, M., van Helden, P.D., Warren, R.M. & Gey van Pittius, N.C. 2010. Novel *Mycobacterium tuberculosis* complex pathogen, *M. mungi*. *Emerging Infectious Diseases*, 16(8):1296-1299. doi:10.3201/eid1608.100314

Amarasinghe, S.L., Su, S., Dong, X., Zappia, L., Ritchie, M.E. & Gouil, Q. 2020. Opportunities and challenges in long-read sequencing data analysis. *Genome Biology*, 21(1):129. doi:10.1186/s13059-020-1935-5

Aminu, N., Bello, I., Umar, N.M., Tanko, N., Aminu, A. & Audu, M.M. 2020. The influence of nanoparticulate drug delivery systems in drug therapy. *Journal of Drug Delivery Science and Technology*, 60:101961. doi:10.1016/j.jddst.2020.101961

Ashjari, M., Panahandeh, F., Niazi, Z. & Abolhasani, M.M. 2020. Synthesis of PLGA–mPEG star-like block copolymer to form micelle loaded magnetite as a nanocarrier for hydrophobic anticancer drug. *Journal of Drug Delivery Science and Technology*, 56:101563. doi:10.1016/j.jddst.2020.101563

Askari, A., Tajvar, S., Nikkhah, M., Mohammadi, S. & Hosseinkhani, S. 2020. Synthesis, characterization and in vitro toxicity evaluation of doxorubicin-loaded magnetoliposomes on MCF-7 breast cancer cell line. *Journal of Drug Delivery Science and Technology*, 55:101447. doi:10.1016/j.jddst.2019.101447

Banyal, S., Malik, P., Tuli, H.S. & Mukherjee, T.K. 2013. Advances in nanotechnology for diagnosis and treatment of tuberculosis. *Current Opinion in Pulmonary Medicine*, 19(3):289-297. doi:10.1097/MCP.0b013e32835eff08

Beauduy, C.E. & Winston, L.G. 2018. Antimycobacterial drugs. In: Kaztung, B.G. eds. *Basic and clinical Pharmacology, fourteenth edition*. USA: McGraw-Hill Education. pp. 842-852.

Becattini, S., Taur, Y. & Pamer, E.G. 2016. Antibiotic-induced changes in the intestinal microbiota and disease. *Trends Molecular Medicine*, 22(6):458-478. doi:10.1016/j.molmed.2016.04.003

Bhalodi, A.A., van Engelen, T.S.R., Virk, H.S. & Wiersinga, W.J. 2019. Impact of antimicrobial therapy on the gut microbiome. *Journal of Antimicrobial Chemotherapy*, 74(1):i6-i15. doi:10.1093/jac/dky530

Birhanu, A.G., Yimer, S.A., Kalayou, S., Riaz, T., Zegeye, E.D., Holm-Hansen, C., Norheim, G., Aseffa, A., Abebe, M. & Tonjum, T. 2019. Ample glycosylation in membrane and cell envelope proteins may explain the phenotypic diversity and virulence in the *Mycobacterium tuberculosis* complex. *Scientific Reports*, 9:2927. doi:10.1038/s41598-019-39654-9

Blomberg, B., Spinaci, S., Fourie, B. and Laing, R. 2001. The rationale for recommending fixed-dose combination tablets for treatment of tuberculosis. *Bulletin of the World Health Organization*, 79:61-68. doi:10.1590/S0042-96862001000100012

Borody, T.J., Eslick, G.D. & Clancy, R.L. 2019. Fecal microbiota transplantation as a new therapy: from Clostridioides difficile infection to inflammatory bowel disease, irritable bowel syndrome, and colon cancer. *Current Opinion in Pharmacology*, 49:43-51. doi:10.1016/j.coph.2019.04.017

Cadmus, S.I., Okoje, V.N., Taiwo, B.O. & van Soolingen, D. 2010. Exposure of dentists to *Mycobacterium tuberculosis*, Ibadan, Nigeria. *Emerging Infectious Diseases*, 16(9):1479-1481. doi:10.3201/eid1609.100447

Cahenzli, J., Köller, Y., Wyss, M., Geuking, M.B. & McCoy, K.D. 2013. Intestinal microbial diversity during early-life colonization shapes long-term IgE levels. *Cell Host & Microbe*, 14:559-570. doi:10.1016/j.chom.2013.10.004

Cainelli, F., Dzudzor, B., Lanzafame, M., Goushchi, A., Chhem, S. & Vento, S. 2020. HIV and SARS-Coronavirus-2 Epidemics: Possible Interactions and Need for Studies, Especially in Africa. *Frontiers in Medicine*, 7:216. doi:10.3389/fmed.2020.00216

Camus, J.C., Pryor, M.J., Medigue, C. & Cole, S.T. 2002. Re-annotation of the genome sequence of *Mycobacterium tuberculosis* H37Rv. *Microbiology*, 148(10):2967-2973. doi:10.1099/00221287-148-10-2967

Canetti, G. 1955. The tubercle bacillus in the pulmonary lesion of man: histobacteriology and its bearing on the therapy of pulmonary tuberculosis: Springer Publishing Company.

Cao, Y., Fanning, S., Proos, S., Jordan, K. & Srikumar, S. 2017. A review on the applications of next generation sequencing technologies as applied to food-related microbiome studies. *Frontiers in Microbiology*, 8:1829. doi:10.3389/fmicb.2017.01829

Caporaso, J.G., Kuczynski, J., Stombaugh, J., Bittinger, K., Bushman, F.D., Costello, E.K., Fierer, N., Pena, A.G., Goodrich, J.K., Gordon, J.I., Huttley, G.A., Kelley, S.T., Knights, D., Koenig, J.E., Ley, R.E., Lozupone, C.A., McDonald, D., Muegge, B.D., Pirrung, M., Reeder, J., Sevinsky, J.R., Turnbaugh, P.J., Walters, W.A., Widmann, J., Yatsunenko, T., Zaneveld, J. & Knight, R. 2010. QIIME allows analysis of high-throughput community sequencing data. *Nature Methods*, 7(5):335-336. doi:10.1038/nmeth.f.303

Caporaso, J.G., Lauber, C.L., Walters, W.A., Berg-Lyons, D., Huntley, J., Fierer, N., Owens, S.M., Betley, J., Fraser, L., Bauer, M., Gormley, N., Gilbert, J.A., Smith, G. & Knight, R. 2012. Ultra-high-throughput microbial community analysis on the Illumina HiSeq and MiSeq platforms. *The ISME Journal*, 6(8):1621-1624. doi:10.1038/ismej.2012.8

Carballeira, N.M. 2007. New advances in fatty acids as antimalarial, antimycobacterial and antifungal agents. *Progress in Lipid Research*, 47(1):50-61. doi:10.1016/j.plipres.2007.10.002

Cardona, P-J. 2015. The key role of exudative lesions and their encapsulation: lessons learned from the pathology of human pulmonary tuberculosis. *Frontiers in Microbiology*, 6:612. doi:10.3389/fmicb.2015.00612

CLSI: Clinical and Laboratory Standards Institute. 2017. Performance standards for antimicrobial susceptibility testing. 27th ed. CLSI supplement M100.

Cole, S.T., Brosch, R., Parkhill, J., Garnier, T., Churcher, C., Harris, D., Gordon, S.V., Eigelmeier, K., Gas, S., Barry III, C.E., Tekaia, F., Badcock, K., Basham, D., Brown, D., Chillingworth, T.,

Connor, R., Davies, R., Devlin, K., Feltwell, T., Gentles, S., Hamlin, N., Holroyd, S., Hornsby, T., Jagels, K., Krogh, A., McLean, J., Moule, S., Murphy, L., Olivier, K., Osborne, J., Quail, M.A., Rajandream, M.-A., Rogers, J., Rutter, S., Seeger, K., Skelton, J., Squares, R., Squares, S., Sulston, J.E., Taylor, K., Whitehead, S. & Barrell, B.G. 1998. Deciphering the biology of *Mycobacterium tuberculosis* from the complete genome sequence. *Nature*, 393:537-544. doi:10.1038/31159

Collins, S.M., Surette, M. & Bercik, P. 2012. The interplay between the intestinal microbiota and the brain. *Nature Reviews Microbiology*, 10(11):735-742. doi:10.1038/nrmicro2876

Costa-Gouveia, J., Aínsa, J.A., Brodin, P. & Lucía, A. 2017. How can nanoparticles contribute to antituberculosis therapy? *Drug Discovery Today*, 22(3):600-607. doi:10.1016/j.drudis.2017.01.011

Daniel, T.M. 2006. The history of tuberculosis. *Respiratory Medicine*, 100(11):1862-1870. doi:10.1016/j.rmed.2006.08.006

Dartois, V. 2014. The path of anti-tuberculosis drugs: from blood to lesions to mycobacterial cells. *Nature Reviews Microbiology*, 12(3):159-167. doi:10.1038/nrmicro3200

Dudek-Wicher, R.K., Junka, A. & Bartoszewicz, M. 2018. The influence of antibiotics and dietary components on gut microbiota. *Przeglad Gastroenterologiczny*, 13(2):85-92. doi:10.5114/pg.2018.76005

Edgar, R.C. 2010. Search and clustering orders of magnitude faster than BLAST. *Bioinformatics*, 26(19):2460-2461. doi:10.1093/bioinformatics/btq461

Enaud, R., Prevel, R., Ciarlo, E., Beaufils, F., Wieërs, G., Guery, B. & Delhaes, L. 2020. The gut-lung axis in health and respiratory diseases: A place for inter-organ and inter-kingdom crosstalks. *Frontiers in Cellular and Infection Microbiology*, 10:9. doi:10.3389/fcimb.2020.00009

Ezra-Nevo, G., Henriques, S.F. & Ribeiro, C. 2020. The diet-microbiome tango: how nutrients lead the gut brain axis. *Current Opinion in Neurobiology*, 62:122-132. doi:10.1016/j.conb.2020.02.005

Fang, C., Zhong, H., Lin, Y., Chen, B., Han, M., Ren, H., Lu, H., Luber, J.M., Xia, M., Li, W., Stein, S., Xu, X., Zhang, W., Drmanac, R., Wang, J., Yang, H., Hammarstrom, L., Kostic, A.D., Kristiansen, K. & Li, J. 2018. Assessment of the cPAS-based BGISEQ-500 platform for metagenomic sequencing. *Gigascience*, 7(3):gix133. doi:10.1093/gigascience/gix133

Faust, K. & Raes, J. 2012. Microbial interactions: from networks to models. *Nature Reviews Microbiology*, 10(8):538-550. doi:10.1038/nrmicro2832

Fogel, N. 2015. Tuberculosis: a disease without boundaries. *Tuberculosis*, 95(5):527-531. doi:10.1016/j.tube.2015.05.017

Forrellad, M.A., Klepp, L.I., Gioffre, A., Sabio y Garcia, J., Morbidoni, H.R., de la Paz Santangelo, M., Cataldi, A.A. & Bigi, F. 2013. Virulence factors of the *Mycobacterium tuberculosis* complex. *Virulence*, 4(1):3-66. doi:10.4161/viru.22329

Garibyan, L. & Avashia, N. 2013. Research techniques made simple: polymerase chain reaction (PCR). *The Journal of investigative dermatology*, 133(3):e6. doi:10.1038/jid.2013.1

Ghazaei, C. 2018. Mycobacterium tuberculosis and lipids: Insights into molecular mechanisms from persistence to virulence. *Journal of Research in Medical Sciences*, 23:63. doi:10.4103/jrms.JRMS_904_17

Gong, Y., Haque, S., Chowdhury, P., Cory, T.J., Kodidela, S., Yallapu, M.M., Norwood, J.M. & Kumar, S. 2019. Pharmacokinetics and pharmacodynamics of cytochrome P450 inhibitors for HIV treatment. *Expert opinion on drug metabolism & toxicology*, 15(5):417-427. doi:10.1080/17425255.2019.1604685

Grobler, A., Perez Sierra, Z. & Viljoen, H.J. 2016. Modeling nanoparticle delivery of TB drugs to granulomas. *Journal of Theoretical Biology*, 388:85-95. doi:10.1016/j.jtbi.2015.10.004

Grobler, A.F. 2013. Nano & micro-delivery systems: the Pheroid® story. North-West University: Potchefstroom Campus (Inaugural lecture).

Gupta, N., Kumar, R & Agrawal, B. 2018. New players in immunity to tuberculosis: the host microbiome, lung epithelium, and innate immune cells. *Frontiers in Immunology*, 9:709. doi:10.3389/fimmu.2018.00709

Gupta, S., Mortensen, M.S., Schjørring, S., Trivedi, U., Vestergaard, G., Stokholm, J., Bisgaard, H., Krogfelt, K.A. & Sørensen, S.J. 2019. Amplicon sequencing provides more accurate microbiome information in healthy children compared to culturing. *Communications Biology*, 2:291. doi:10.1038/s42003-019-0540-1

Gygli, S.M., Borrell, S., Trauner, A. & Gagneux, S. 2017. Antimicrobial resistance in *Mycobacterium tuberculosis*: mechanistic and evolutionary perspectives. *FEMS microbiology reviews*, 41(3):54-373. doi:10.1093/femsre/fux011

Hakkimane, S.S., Shenoy, V.P., Gaonkar, S.L., Bairy, I. & Guru, B.R. 2018. Antimycobacterial susceptibility evaluation of rifampicin and isoniazid benz-hydrazone in biodegradable polymeric nanoparticles against Mycobacterium tuberculosis H37Rv strain. *International Journal of Nanomedicine*, 13:4303-4318. doi:10.2147/IJN.S163925

Haldar, K., George, L., Wang, Z., Mistry, V., Ramsheh, M.Y., Free, R.C., John, C., Reeve, N.F., Miller, B.E., Tal-Singer, R., Webb, A.J., Brookes, A.J., Tobin, M.D., Singh, D., Donaldson, G.C., Wedzicha, J.A., Brown, J.R., Barer, M.R. & Brightling, C.E. 2020. The sputum microbiome is distinct between COPD and health, independent of smoking history. *Respiratory Research*, 21:183. doi:10.1186/s12931-020-01448-3

He, Z., Cui, B.T., Zhang, T., Li, P., Long, C.Y., Ji, G.Z. & Zhang, F.M. 2017. Fecal microbiota transplantation cured epilepsy in a case with Crohn's disease: The first report. *World Journal of Gastroenterology*, 23(19):3565-3568. doi:10.3748/wjg.v23.i19.3565

Health: Department of Health KwaZulu Natal. 2008. Diagnosis and management of tuberculosis. http://www.kznhealth.gov.za/medicine/adulttb.pdf Date of access: 1 Apr. 2019.

Health: Department of Health South Africa. 2014. National tuberculosis management guidelines 2014. http://www.tbonline.info/media/uploads/documents/ntcp_adult_tb-guidelines-27.5.2014.pdf Date of access: 1 Apr. 2019

Heshiki, Y., Vazquez-Uribe, R., Li, J., Ni, Y., Quainoo, S., Imamovic, L., Li, J., Sorensen, M., Chow, B.K.C., Weiss, G.J., Xu, A., Sommer, M.O.A. & Panagiotou, G. 2020. Predictable modulation of cancer treatment outcomes by the gut microbiota. *Microbiome*, 8:28. doi:10.1186/s40168-020-00811-2

Hiruy, H., Rogers, Z., Mbowane, C., Adamson, J., Ngotho, L., Karim, F., Gumbo, T., Bishai, W. & Jeena, P. 2015. Subtherapeutic concentrations of first-line anti-TB drugs in South African children treated according to current guidelines: the PHATISA study. *Journal of Antimicrobial Chemotherapy*, 70(4):1115-1123. doi:10.1093/jac/dku478

Hu, Y., Feng, Y., Wu, J., Liu, F., Zhang, Z., Hao, Y., Liang, S., Li, B., Li, J., Lv, N., Xu, Y., Zhu, B. & Sun, Z. 2019. The gut microbiome signatures discriminate healthy from pulmonary tuberculosis patients. *Frontiers in Cellular and Infection Microbiology*, 9:90. doi:10.3389/fcimb.2019.00090

Huard, R.C., Fabre, M., de Haas, P., Lazzarini, L.C., van Soolingen, D., Cousins, D. & Ho, J.L. 2006. Novel genetic polymorphisms that further delineate the phylogeny of the *Mycobacterium tuberculosis* complex. *Journal of Bacteriology*, 188(12):4271-4287. doi:10.1128/JB.01783-05

Hufnagl, K., Pali-Schöll, I., Roth-Walter, F. & Jensen-Jarolim, E. 2020. Dysbiosis of the gut and lung microbiome has a role in asthma. *Seminars in Immunopathology*, 42(1):75-93. doi:10.1007/s00281-019-00775-y

Ichinohe, T., Pang, I.K., Kumamoto, Y., Peaper, D.R., Ho, J.H., Murray, T.S. & Iwasaki, A. 2011. Microbiota regulates immune defense against respiratory tract influenza A virus infection. *Proceedings of the National Academy of Sciences*, 108(13):5354-5359. doi:10.1073/pnas.1019378108

Iizumi, T., Battaglia, T., Ruiz, V. & Perez Perez, G.I. 2017. Gut microbiome and antibiotics. *Archives of Medical Research*, 48(8):727-734. doi:10.1016/j.arcmed.2017.11.004

Irwin, S.M., Driver, E., Lyon, E., Schrupp, C., Ryan, G., Gonzalez-Juarrero, M., Basaraba, R.J., Nuermberger, E.L. & Lenaerts, A.J. 2015. Multiple lesion types displaying vastly different microenvironments in C3HeB/FeJ mice following aerosol infection with M. tuberculosis. *Disease models & mechanisms*, 8(6):591-602. doi:10.1242/dmm.019570

Jadhav, M., Khan, T., Bhavsar, C., Momin, M. & Omri, A. 2019. Novel therapeutic approaches for targeting TB and HIV reservoirs prevailing in lungs. *Expert Opinion on Drug Delivery*, 16(7):687-699. doi:10.1080/17425247.2019.1621287

Jernberg, C., Lofmark, S., Edlund, C. & Jansson, J.K. 2010. Long-term impacts of antibiotic exposure on the human intestinal microbiota. *Microbiology*, 156(11):3216-3223. doi:10.1099/mic.0.040618-0

Jiang, J.-W., Chen, X.-H., Ren, Z. & Zheng, S.-S. 2019. Gut microbial dysbiosis associates hepatocellular carcinoma via the gut-liver axis. *Hepatobiliary & Pancreatic Diseases International*, 18(1):19-27. doi:10.1016/j.hbpd.2018.11.002

Johnson, E. & Raza, S. 2018. What is long read sequencing? phg foundation. https://www.phgfoundation.org/documents/long-read-sequencing-introduction.pdf Date of access: 20 Sept. 2020.

Kelly, S.A., Rodgers, A.M., O'Brien, S.C., Donnelly, R.F. & Gilmore, B.F. 2020. Gut Check Time: Antibiotic Delivery Strategies to Reduce Antimicrobial Resistance. *Trends in Biotechnology*, 38(4):447-462. doi:10.1016/j.tibtech.2019.10.008

Khan, N., Mendonca, L., Dhariwal, A., Fontes, G., Menzies, D., Xia, J., Divangahi, M. & King, I.L. 2019a. Intestinal dysbiosis compromises alveolar macrophage immunity to *Mycobacterium tuberculosis*. *Mucosal Immunology*, 12(3)772-783. doi:10.1038/s41385-019-0147-3

Khan, P.Y., Yates, T.A., Osman, M., Warren, R.M., van der Heijden, Y., Padayatchi, N., Nardell, E.A., Moore, D., Mathema, B., Gandhi, N., Eldholm, V., Dheda, K., Hesseling, A.C., Mizrahi, V., Rustomjee, R. & Pym, A. 2019b. Transmission of drug-resistant tuberculosis in HIV-endemic settings. *The Lancet Infectious Diseases*, 19(3):e77-e88. doi:10.1016/ S1473-3099(18)30537-1

Kisich, K.O., Gelperina, S., Higgins, M.P., Wilson, S., Shipulo, E., Oganesyan, E. & Heifets, L. 2007. Encapsulation of moxifloxacin within poly(butyl cyanoacrylate) nanoparticles enhances efficacy against intracellular Mycobacterium tuberculosis. *International Journal of Pharmaceutics*, 345(1-2):154-162. doi:10.1016/j.ijpharm.2007.05.062

Koch, A. & Mizrahi, V. 2018. *Mycobacterium tuberculosis*. *Trends Microbiology*, 26(6):555-556. doi:10.1016/j.tim.2018.02.012

Kolyva, A.S. & Karakousis, P.C. 2012. Old and new TB drugs: mechanisms of action and resistance. In: Cardona, D.P.-J., eds. *Understanding Tuberculosis–New Approaches to Fighting Against Drug Resistance*. Europe: InTech. pp. 209-32.

Korf, J., Stoltz, A., Verschoor, J., De Baetselier, P. & Grooten, J. 2005. The Mycobacterium tuberculosis cell wall component mycolic acid elicits pathogen-associated host innate immune responses. *European Journal of Immunology*, 35(3):890-900. doi:10.1002/eji.200425332

Korf, J.E., Pynaert, G., Tournoy, K., Boonefaes, T., Van Oosterhout, A., Ginneberge, D., Haegeman, A., Verschoor, J.A., De Baetselier, P. & Grooten, J. 2006. Macrophage reprogramming by mycolic acid promotes a tolerogenic response in experimental asthma. *American Journal of Respiratory and Critical Care Medicine*, 174(2):152-160. doi:10.1164/rccm.200507-1175OC

Koropatkin, N.M., Cameron, E.A. & Martens, E.C. 2012. How glycan metabolism shapes the human gut microbiota. *Nature Reviews Microbiology*, 10(5):323-35. doi:10.1038/nrmicro2746

Lee, R.E., Armour, J.W., Takayama, K., Brennan, P.J. & Besra, G.S. 1997. Mycolic acid biosynthesis: definition and targeting of the Claisen condensation step. *Biochimica et Biophysica Acta (BBA)-Lipids and Lipid Metabolism*, 1346(3):275-284. doi:10.1016/S0005-2760(97)00051-9

Lemmer, Y., Kalombo, L., Pietersen, R.D., Jones, A.T., Semete-Makokotlela, B., Van Wyngaardt, S., Ramalapa, B., Stoltz, A.C., Baker, B., Verschoor, J.A., Swai, H.S. & de Chastellier, C. 2015. Mycolic acids, a promising mycobacterial ligand for targeting of nanoencapsulated drugs in tuberculosis. *Journal of Controlled Release*, 211:94-104. doi:10.1016/j.jconrel.2015.06.005

Liang, S., Wu, X., Hu, X., Wang, T. & Jin, F. 2018. Recognizing depression from the microbiota-gut-brain axis. *International Journal of Molecular Sciences*, 19(6):1592. doi:10.3390/ijms19061592

Liu, Z., Chen, K., Davis, C., Sherlock, S., Cao, Q., Chen, X. & Dai, H. 2008. Drug delivery with carbon nanotubes for *in vivo* cancer treatment. *Cancer Research*, 68(16):6652-6660. doi:10.1158/0008-5472.CAN-08-1468

Loman, N.J. & Pallen, M.J. 2015. Twenty years of bacterial genome sequencing. *Nature Reviews Microbiology*, 13(12):787-794. doi:10.1038/nrmicro3565

Luo, M., Liu, Y., Wu, P., Luo, D-X., Sun, Q., Zheng, H., Hu, R., Pandol, S.J., Li, Q-F., Han, Y-P. & Zeng, Y. 2017. Alteration of gut microbiota in patients with pulmonary tuberculosis. *Frontiers in Physiology*, 8:822. doi:10.3389/fphys.2017.00822

Machelart, A., Salzano, G., Li, X., Demars, A., Debrie, A-S., Menendez-Miranda, M., Pancani, E., Jouny, S., Hoffmann, E., Deboosere, N., Belhauane, I., Rouanet, C., Simar, S., Talahari, S., Giannini, V., Villemagne, B., Flipo, M., Brosch, R., Nesslany, F., Deprez, B., Muraille, E., Locht, C., Baulard, A.R., Willand, N., Majlessi, L., Gref, R. & Brodin, P. 2019. Intrinsic antibacterial activity of nanoparticles made of β-cyclodextrins potentiates their effect as drug nanocarriers against tuberculosis. *ACS Nano*, 13(4):3992-4007. doi:10.1021/acsnano.8b07902

Maher, D., Harries, A. & Getahun, H. 2005. Tuberculosis and HIV interaction in sub-Saharan Africa: impact on patients and programmes; implications for policies. *Tropical Medicine and International Health*, 10(8):734-742. doi:10.1111/j.1365-3156.2005.01456.x

Mahmoodzadeh, F., Ghorbani, M. & Jannat, B. 2019. Glutathione and pH-responsive chitosan-based nanogel as an efficient nanoplatform for controlled delivery of doxorubicin. *Journal of Drug Delivery Science and Technology*, 54:101315. doi:10.1016/j.jddst.2019.101315

Maji, A., Misra, R., Dhakan, D.B., Gupta, V., Mahato, N.K., Saxena, R., Mittal, P., Thukral, N., Sharma, E., Singh, A., Virmani, R., Gaur, M., Singh, H., Hasija, Y., Arora, G., Agrawal, A., Chaudhry, A., Khurana J.P., Sharma, V.K., Lal, R. & Singh, Y. 2018. Gut microbiome contributes to impairment of immunity in pulmonary tuberculosis patients by alteration of butyrate and propionate producers. *Environmental Microbiology*, 20(1):402-419. doi:10.1111/1462-2920.14015

Mas-Lloret, J., Obon-Santacana, M., Ibanez-Sanz, G., Guino, E., Pato, M.L., Rodriguez-Moranta, F., Mata, A., Garcia-Rodriguez, A., Moreno, V. & Pimenoff, V.N. 2020. Gut microbiome diversity detected by high-coverage 16S and shotgun sequencing of paired stool and colon sample. *Scientific Data*, 7:92. doi:10.1038/s41597-020-0427-5

Matthee, L.I. 2007. A preclinical evaluation of the possible enhancement of the efficacy of antituberculosis drugs by Pheroid™ technology. NWU: Potchefstroom Campus. (Dissertation – MSc).

Mayer, E.A. 2011. Gut feelings: the emerging biology of gut–brain communication. *Nature Reviews Neuroscience*, 12(8):453-466. doi:10.1038/nrn3071

Mekonnen, D., Derbie, A., Abeje, A., Shumet, A., Kassahun, Y., Nibret, E., Munshea, A., Bobosha, K., Wassie, L., Biadglegne, F., Aseffa, A & Sack, U. 2019. Genomic diversity and transmission dynamics of *M. tuberculosis* in Africa: a systematic review and meta-analysis. *The International Journal of Tuberculosis and Lung Disease*, 23(12):1314-1326. doi:10.5588/ijtld.19.0127

Mohajeri, M.H., Brummer, R.J., Rastall, R.A., Weersma, R.K., Harmsen, H.J., Faas, M. & Eggersdorfer, M. 2018. The role of the microbiome for human health: from basic science to clinical applications. *European journal of nutrition*, 57(1):1-14. doi: 10.1007/s00394-018-1703-4

Moya, A. & Ferrer, M. 2016. Functional redundancy-induced stability of gut microbiota subjected to disturbance. *Trends in microbiology*, 24(5):402-413. doi: 10.1016/j.tim.2016.02.002

Namasivayam, S., Maiga, M., Yuan, W., Yuan, V., Costa, D.L., Mittereder, L.R., Wipperman, M.F., Glickman, M.S., Dzutsev, A., Trinchieri, G. & Sher, A. 2017. Longitudinal profiling reveals a

persistent intestinal dysbiosis triggered by conventional anti-tuberculosis therapy. *Microbiome*, 5:71. doi:10.1186/s40168-017-0286-2

Namasivayam, S., Sher, A., Glickman, M.S. & Wipperman, M.F. 2018. The microbiome and tuberculosis: Early evidence for cross talk. *MBio*, 9(5):e01420-18. doi:10.1128/mBio.01420-18

Nemes, E., Geldenhuys, H., Rozot, V., Rutkowski, K.T., Ratangee, F., Bilek, N., Mabwe, S., Makhethe, L.,Erasmus, M., Toefy, A., Mulenga, H., Hanekom, W.A., Self, S.G., Bekker, L.-G., Ryall, R., Gurunathan, S., DiazGranados, C.A., Andersen, P., Kroman, I., Evans, T., Ellis, R.D., Landry, B., Hokey, D.A., Hopkins, R., Ginsberg, A.M., Scriba, T.J & Hatherrill, M. 2018. Prevention of *M. tuberculosis* infection with H4:IC31 vaccine or BCG revaccination. *The New England Journal of Medicine*, 379:138-149. doi:10.1056/NEJMoa1714021

Ngabonziza, J.C.S., Loiseau, C., Marceau, M., Jouet, A., Menardo, F., Tzfadia, O., Antoine, R., Niyigena, E.B., Mulders, W., Fissette, K., Diels, M., Gaudin, C., Duthoy, S., Ssengooba, W., Andre, E., Kaswa, M.K., Habimana, Y.M., Brites, D., Affolabi, D., Mazarati, J.B., de Jong, B.C., Rigouts, L., Gagneux, S., Meehan, C.J. & Supply, P. 2020. A sister lineage of the *Mycobacterium tuberculosis* complex discovered in the African Great Lakes region. *Nature Communications*, 11:2917. doi:10.1038/s41467-020-16626-6

Nienaber, A., Baumgartner, J., Dolman, R.C., Ozturk, M., Zandberg, L., Hayford, F.E., Brombacher, F., Blaauw, R., Parihar, S.P., Smuts, C.M. & Malan, L. 2020. Omega-3 fatty acid and iron supplementation alone, but not in combination, lower inflammation and anemia of infection in *Mycobacterium tuberculosis*-infected mice. *Nutrients*, 12(9):2897. doi:10.3390/nu12092897

Nieuwoudt, L. 2009. The impact of Pheroid™ technology on the bioavailability and efficacy of anti-tuberculosis drugs in an animal model. NWU: Potchefstroom Campus. (Dissertation – MSc).

Nkanga, C.I., Noundou, X.S., Walker,R.B. & Krause, R.W.M. 2019. Co-encapsulation of rifampicin and isoniazid in crude soybean lecithin liposomes. *South African Journal of Chemistry*, 72:80-87. doi:10.17159/0379-4350/2019/v72a11

O'Hara, A.M. & Shanahan, F. 2006. The gut flora as a forgotten organ. *EMBO Reports*, 7(7):688-693. doi:10.1038/sj.embor.7400731

Pagán, A.J. & Ramakrishnan, L. 2015. Immunity and Immunopathology in the Tuberculous Granuloma. *Cold Spring Harbor Perspectives in Medicine*, 5(9):a018499. doi:10.1101/cshperspect.a018499

Panda, S., El khader, I., Casellas, F., Lopez Vivancos, J., Garcia Cors, M., Santiago, A., Cuenca, S., Guarner, F. & Manichanh, C. 2014. Short-term effect of antibiotics on human gut microbiota. *PLoS One*, 9(4):e95476. doi:10.1371/journal.pone.0095476

Pandey, R., Sharma, S. & Khuller, G.K. 2006. Chemotherapeutic efficacy of nanoparticle encapsulated antitubercular drugs. *Drug Delivery*, 13(4):287-294. doi:10.1080/10717540500398076

Pandey, R., Zahoor, A., Sharma, S. & Khuller, G.K. 2003. Nanoparticle encapsulated antitubercular drugs as a potential oral drug delivery system against murine tuberculosis. *Tuberculosis (Edinb)*, 83(6):373-378. doi:10.1016/j.tube.2003.07.001

Pankey, G.A., Sabath, L.D. 2004. Clinical relevance of bacteriostatic versus bactericidal mechanisms of action in the treatment of Gram-positive bacterial infections. *Clinical Infectious Diseases*, 38(6):864-870. doi:10.1086/381972

Park, H., Laffin, M.R., Jovel, J., Millan, B., Hyun, J.E., Hotte, N., Kao, D. & Madsen, K.L. 2019. The success of fecal microbial transplantation in Clostridium difficile infection correlates with bacteriophage relative abundance in the donor: a retrospective cohort study. *Gut Microbes*, 10(6):676-687. doi:10.1080/19490976.2019.1586037

Parrish, N.M., Dick, J.D. & Bishai, W.R. 1998. Mechanisms of latency in *Mycobacterium tuberculosis*. *Trends in Microbiology*, 6(3):107-112. doi: 10.1016/S0966-842X(98)01216-5

Pathak, L., Gayan, S., Pal, B., Talukdar, J., Bhuyan, S., Sandhya, S., Yeger, H., Baishya, D. & Das, B. 2020. Corona virus activates a stem cell mediated defence mechanism that accelerates activation of dormant tuberculosis: implications for the COVID-19 pandemic. (preprint) doi:10.1101/2020.05.06.077883

Peters, J.S., Andrews, J.R., Hatherill, M., Hermans, S., Martinez, L., Schurr, E., van der Heijden, Y., Wood, R., Rustomjee, R. & Kana, B.D. 2019. Advances in the understanding of *Mycobacterium tuberculosis* transmission in HIV-endemic settings. *The Lancet Infectious Diseases*, 19(3):e65-e76. doi:10.1016/S1473-3099(18)30477-8

Pham, D.D., Fattal, E. & Tsapis, N. 2015. Pulmonary drug delivery systems for tuberculosis treatment. *International journal of pharmaceutics*, 478(2):517-529. doi:10.1016/j.ijpharm.2014.12.009

Philipp, W.J., Poulet, S., Eiglmeier, K., Pascopella, L., Balasubramanian, V., Heym, B., Bergh, S., Bloom, B.R., Jacobs Jr, W.R. & Cole, S.T. 1996. An integrated map of the genome of the tubercle bacillus, *Mycobacterium tuberculosis* H37Rv, and comparison with *Mycobacterium leprae*. Proceedings of the National Academy of Sciences of the United States of America, 93(7):3132-3137. doi:10.1073/pnas.93.7.3132

Pi, J., Shen, L., Shen, H., Yang, E., Wang, W., Wang, R., Huang, D., Lee, B.S., Hu, C., Chen, C., Jin, H., Cai, J., Zeng, G. & Chen, Z.W. 2019. Mannosylated graphene oxide as macrophage-targeted delivery system for enhanced intracellular M.tuberculosis killing efficiency. *Material Science and Engineering C Matererials for Biological Applications*, 103:109777. doi:10.1016/j.msec.2019.109777

Pi, J., Shen, L., Yang, E., Shen, H., Huang, D., Wang, R., Hu, C., Jin, H., Cai, H., Cai, J., Zeng, G. & Chen, Z.W. 2020. Macrophage-targeted isoniazid–selenium nanoparticles promote antimicrobial immunity and synergize bactericidal destruction of tuberculosis bacilli. *Angewandte Chemie International Edition*, 59(8):3226-3234. doi:10.1002/anie.201912122

Rabi, F.A., Al Zoubi, M.S., Kasasbeh, G.A., Salameh, D.M. & Al-Nasser, A.D. 2020. SARS-CoV-2 and Coronavirus Disease 2019: What We Know So Far. *Pathogens*, 9(3):231. doi:10.3390/pathogens9030231

Raghunandanan, S., Jose, L., Gopinath, V. & Kumar, R.A. 2019. Comparative label-free lipidomic analysis of *Mycobacterium tuberculosis* during dormancy and reactivation. *Scientific Reports*, 9:3660. doi:10.1038/s41598-019-40051-5

Ramachandran, G. & Swaminathan, S. 2015. Safety and tolerability profile of second-line anti-tuberculosis medications. *Drug Safety*, 38(3):253-269. doi:10.1007/s40264-015-0267-y

Ramakrishnan, L. 2012. Revisiting the role of the granuloma in tuberculosis. *Nature Reviews Immunology*, 12(5):352-366. doi:10.1038/nri3211

Rose, G., Ranellou, K., Misra, R., Crump, C., Wooldridge, D., Parmar, S., Maddren, C., Gharbia, S. & Jalal, H. 2017. Complete genome sequences of BK polyomavirus strains from two patients

with urinary tract infection, sequenced using the ion torrent platform. *Genome Announcements*, 5(46):e01293-17. doi:10.1128/genomeA.01293-17

Ross, S.M. 2019. Gut-brain axis and stress regulation: effects of probiotics on neurocognition. *Holistic Nursing Practise*, 33(5):312-315. doi:10.1097/HNP.0000000000000346

Saito, H., Tomioka, H. & Yoneyama, T. 1984b. Growth of group IV mycobacteria on medium containing various saturated and unsaturated fatty acids. *Antimicrobial agents and chemotherapy*, 26(2):164-169. doi:10.1128/aac.26.2.164

Sasindran, S.J. & Torrelles, J.B. 2011. *Mycobacterium tuberculosis* infection and inflammation: what is beneficial for the host and for the bacterium? *Frontiers in Microbiology*, 2:2. doi:10.3389/fmicb.2011.00002

Schloss, P.D., Westcott, S.L., Ryabin, T., Hall, J.R., Hartmann, M., Hollister, E.B., Lesniewski, R.A., Oakley, B.B., Parks, D.H., Robinson, C.J., Sahl, J.W., Stres, B., Thallinger, G.G., Van Horn, D.J. & Weber, C.F. 2009. Introducing mothur: open-source, platform-independent, community-supported software for describing and comparing microbial communities. *Applied Environmental Microbiology*, 75(23):7537-7541. doi:10.1128/AEM.01541-09

Senabouth, A., Andersen, S., Shi, Q., Shi, L., Jiang, F., Zhang, W., Wing, K., Daniszewski, M., Lukowski, S.W., Hung, S.S.C., Nguyen, Q., Fink, L., Beckhouse, A., Pébay, A., Hewitt, A.W. & Powell, J.E. 2020. Comparative performance of the BGI and Illumina sequencing technology for single-cell RNA-sequencing. *NAR Genomics and Bioinformatics*, 2(2):lqaa034. doi:10.1093/nargab/lqaa034

Senghore, M., Diarra, B., Gehre, F., Otu, J., Worwui, A., Muhammad, A.K., Kwambana-Adams, B., Kay, G.L., Sanogo, M., Baya, B., Orsega, S., Doumbia, S., Diallo, S., de Jong, B.C., Pallen, M.J. & Antonio, M. 2020. Evolution of *Mycobacterium tuberculosis* complex lineages and their role in an emerging threat of multidrug resistant tuberculosis in Bamako, Mali. *Scienctific Reports*, 10:327. doi:10.1038/s41598-019-56001-0

Seung, K.J., Keshavjee, S. & Rich, M.L. 2015. Multidrug-resistant tuberculosis and extensively drug-resistant tuberculosis. *Cold Spring Harbor Perspectives in Medicine*, 5(9):a017863. doi:10.1101/cshperspect.a017863

Singhvi, N., Gupta, V., Gaur, M., Sharma, V., Puri, A., Singh, Y., Dubey, G.P. & Lal, R. 2019. Interplay of human gut microbiome in health and wellness. *Indian Journal of Microbiology*, 60:26-36. doi:10.1007/s12088-019-00825-x

Slabbert, C., Plessis, L.H. & Kotze, A.F. 2011. Evaluation of the physical properties and stability of two lipid drug delivery systems containing mefloquine. *International Journal of Pharmaceutics*, 409(1-2):209-215. doi:10.1016/j.ijpharm.2011.01.050

Smith, I. 2003. *Mycobacterium tuberculosis* pathogenesis and molecular determinants of virulence. *Clinical Microbiology reviews*, 16(3):463-496. doi:10.1128/CMR.16.3.463–496.2003

Smittipat, N., Miyahara, R., Juthayothin, T., Billamas, P., Dokladda, K., Imsanguan, W., Intralawan, D., Rukseree, K., Jaitrong, S., Chaiyasirinroje, B., Wongjai, J., Disratthakit, A., Chaiprasert, A., Nedsuwan, S., Mahasirimongkol, S., Toyo-Oka, L., Tokunaga, K., Yamada, N., Palittapongarnpim, P. & Yanai, H. 2019. Indo-Oceanic Mycobacterium tuberculosis strains from Thailand associated with higher mortality. *International Journal of Tuberculosis and Lung Disease*, 23(9):972-979. doi:10.5588/ijtld.18.0710

Steyn, J.D., Wiesner, L., du Plessis, L.H., Grobler, A.F., Smith, P.J., Chan, W.C., Haynes, R.K. & Kotze, A.F. 2011. Absorption of the novel artemisinin derivatives artemisone and artemiside: potential application of Pheroid™ technology. *International Journal of Pharmaceutics*, 414(1-2):260-266. doi:10.1016/j.ijpharm.2011.05.003

Tarashi, S., Ahmadi Badi, S., Moshiri, A., Nasehi, M., Fateh, A., Vaziri, F. & Siadat, S.D. 2018. The human microbiota in pulmonary tuberculosis: Not so innocent bystanders. *Tuberculosis*, 113:215-221. doi:10.1016/j.tube.2018.10.010

TB Alliance. 2020a. Compounds: Rifampin. https://www.tballiance.org/portfolio/compound/rifampin Date of access: 27 April 2020.

TB Alliance. 2020b. Compounds: Isoniazid. https://www.tballiance.org/portfolio/compound/isoniazid Date of access: 27 April 2020.

TB Alliance. 2020c. Compounds: Ethambutol. https://www.tballiance.org/portfolio/compound/ethambutol Date of access: 27 April 2020.

TB Alliance. 2020d. Compounds: Pyrazinamide. https://www.tballiance.org/portfolio/compound/pyrazinamide Date of access: 27 April 2020.

Tessler, M., Neumann, J.S., Afshinnekoo, E., Pineda, M., Hersch, R., Velho, L.F.M., Segovia, B.T., Lansac-Toha, F.A., Lemke, M., DeSalle, R., Mason, C.E. & Brugler, M.R. 2017. Large-scale differences in microbial biodiversity discovery between 16S amplicon and shotgun sequencing. *Scientific Reports*, 7:6589. doi:10.1038/s41598-017-06665-3

Theriot, C.M., Koenigsknecht, M.J., Carlson Jr, P.E., Hatton, G.E., Nelson, A.M., Li, B., Huffnagle, G.B., Li, J.Z. & Young, V.B. 2014. Antibiotic-induced shifts in the mouse gut microbiome and metabolome increase susceptibility to *Clostridium difficile* infection. *Nature Communications*, 5:3114. doi:10.1038/ncomms4114

Trifiro, S., Bourgault, A.M., Lebel, F. & Rene, P. 1990. Ghost mycobacteria on Gram stain. *Journal of Clinical Microbiology*, 28(1):146-147. doi:10.1128/JCM.28.1.146-147

Trompette, A., Gollwitzer, E.S., Pattaroni, C., Lopez-Mejia, I.C., Riva, E., Pernot, J., Ubags, N., Fajas, L., Nicod, L.P. & Marsland, B.J. 2018. Dietary fiber confers protection against flu by shaping ly6c− patrolling monocyte hematopoiesis and CD8+ T cell metabolism. *Immunity*, 48(5):992-1005.e1008. doi:10.1016/j.immuni.2018.04.022

Tsay, T.-B., Yang, M.-C., Chen, P.-H., Hsu, C.-M. & Chen, L.-W. 2011. Gut flora enhance bacterial clearance in lung through toll-like receptors 4. *Journal of Biomedical Science*, 18:68. doi:10.1186/1423-0127-18-68

Tufariello, J.M., Chan, J. & Flynn, J.L. 2003. Latent tuberculosis: mechanisms of host and bacillus that contribute to persistent infection. *The Lancet infectious diseases*, 3(9):578-590. doi:10.1016/S1473-3099(03)00741-2

Umpeleva, T., Belousova, K., Golubeva, L., Boteva, T., Morozova, I., Vyazovaya, A., Mokrousov, I., Eremeeva, N. & Vakhrusheva, D. 2020. Molecular characteristics of *Mycobacterium tuberculosis* in the "closed" Russian town with limited population migration. *Infection, Genetics and Evolution*, 79:104174. doi:10.1016/j.meegid.2020.104174

UNAIDS. 2019. Fact sheet: World AIDS day 1 December 2019. https://www.unaids.org/sites/default/files/media_asset/UNAIDS_FactSheet_en.pdf Date of access: 27 May 2020.

Upadhyay, T.K., Fatima, N., Sharma, A., Sharma, D. & Sharma, R. 2019. Nano-Rifabutin entrapment within glucan microparticles enhances protection against intracellular *Mycobacterium*

tuberculosis. *Artificial Cells, Nanomedicine and Biotechnology*, 47(1):427-435. doi:10.1080/21691401.2018.1559180

Van Dijk, E.L., Auger, H., Jaszczyszyn, Y. & Thermes, C. 2014. Ten years of next-generation sequencing technology. *Trends in Genetics*, 30(9):418-426. doi:10.1016/j.tig.2014.07.001

Verrall, A.J., Schneider, M., Alisjahbana, B., Apriana, L., van Laarhoven, A., Koeken, V.A.C.M., van Dorp, S., Diadani, E., Utama, F., Hannaway, R.F., Indrati, A., Netea, M.G., Sharples, K., Hill, P.C., Ussher, J.E. & van Crevel, R. 2020. Early clearance of *Mycobacterium tuberculosis* is associated with increased innate immune responses. *The Journal of Infectious Diseases*, 221(8):1342–1350. doi:10.1093/infdis/jiz147

Walaza, S., Tempia, S., Dawood, H., Variava, E., Wolter, N., Dreyer, A., Moyes, J., Von Mollendorf, C., McMorrow, M., Von Gottberg, A., Haffejee, S., Venter, M., Treurnicht, F.K., Hellferscee, O., Martinson, N.A., Ismail, N. & Cohen, C. 2019. The impact of influenza and tuberculosis interaction on mortality among individuals aged ≥15 years hospitalized with severe respiratory illness in South Africa, 2010–2016. *Open Forum Infectious Diseases*, 6(3):ofz020. doi:10.1093/ofid/ofz020

Wang, B., Yao, M., Lv, L., Ling, Z. & Li, L. 2017. The human microbiota in health and disease. *Engineerin*g, 3(1):71-82. doi: 10.1016/J.ENG.2017.01.008

Webster, M. 2019. Eicosampentaenoic acid. https://www.merriam-webster.com/dictionary/eicosapentaenoic%20acid Date of access: 4 April 2019.

WHO: World Health Organization. 2011. Global tuberculosis control 2011. https://apps.who.int/iris/bitstream/handle/10665/44728/9789241564380_eng.pdf?sequence=1&isAllowed=y Date of access: 20 Apr. 2020.

WHO: World Health Organization. 2012. Global tuberculosis report 2012. https://www.who.int/tb/publications/global_report/gtbr12_main.pdf Date of access: 20 Apr. 2020.

WHO: World Health Organization. 2013. Global tuberculosis report 2013. https://apps.who.int/iris/bitstream/handle/10665/91355/9789241564656_eng.pdf?sequence=1 Date of access: 20 Apr. 2020.

WHO: World Health Organization. 2014. Global tuberculosis report 2014. https://apps.who.int/iris/bitstream/handle/10665/137094/9789241564809_eng.pdf?sequence=1&isAllowed=y Date of access: 20 Apr. 2020.

WHO: World Health Organization. 2015. Global tuberculosis report 2015. https://apps.who.int/iris/bitstream/handle/10665/191102/9789241565059_eng.pdf?sequence=1&isAllowed=y Date of access: 20 Apr. 2020.

WHO: World Health Organization. 2016. Global tuberculosis report 2016. https://apps.who.int/iris/bitstream/handle/10665/250441/9789241565394-eng.pdf?sequence=1&isAllowed=y Date of access: 20 Apr. 2020.

WHO: World Health Organization. 2017. Global tuberculosis report 2017. https://www.who.int/tb/publications/global_report/gtbr2017_main_text.pdf Date of access: 20 Apr. 2020.

WHO: World Health Organization. 2017. Guidelines for treatment of drug-susceptible tuberculosis and patient care. http://apps.who.int/iris/bitstream/10665/255052/1/9789241550000-eng.pdf Date of access: 5 Apr. 2019.

WHO: World Health Organization. 2018. Global tuberculosis report 2018. https://www.who.int/tb/publications/global_report/en/ Date of access: 1 Apr. 2019.

WHO: World Health Organization. 2019. Global tuberculosis report 2019. https://apps.who.int/iris/bitstream/handle/10665/329368/9789241565714-eng.pdf?ua=1 Date of access: 16 April 2020.

WHO: World Health Organization. 2020. Global tuberculosis report 2020. https://www.who.int/publications/i/item/9789240013131 Date of access: 30 Nov. 2020.

Winglee, K., Eloe-Fadrosh, E., Gupta, S., Guo, H., Fraser, C. & Bishai, W. 2014. Aerosol *Mycobacterium tuberculosis* infection causes rapid loss of diversity in gut microbiota. *PLoS One*, 9(5):e97048. doi:10.1371/journal.pone.0097048

Wipperman, M.F., Fitzgerald, D.W., Juste, M.A.J., Taur, Y., Namasivayam, S., Sher, A., Bean, J.M., Bucci, V. & Glickman, M.S. 2017. Antibiotic treatment for tuberculosis induces a profound dysbiosis of the microbiome that persists long after therapy is completed. *Scientific Reports*, 7:10767. doi:10.1038/s41598-017-10346-6

Xiong, Y., Hu, S., Zhou, H., Zeng, H., He, X., Huang, D. & Li, X. 2020. High-throughput 16S rDNA sequencing of the pulmonary microbiome of rats with allergic asthma. *Genes & Diseases*, 7(2):272-282. doi:10.1016/j.gendis.2019.03.006

Zhu, F., Ju, Y., Wang, W., Wang, Q., Guo, R., Ma, Q., Sun, Q., Fan, Y., Xie, Y., Yang, Z., Jie, Z., Zhao, B., Xiao, L., Yang, L., Zhang, T., Feng, J., Guo, L., He, X., Chen, Y., Chen, C., Gao, C., Xu, X., Yang, H., Wang, J., Dang, Y., Madsen, L., Brix, S., Kristiansen, K., Jia, H. & Ma, X. 2020. Metagenome-wide association of gut microbiome features for schizophrenia. *Nature Communications*, 11:1612. doi:10.1038/s41467-020-15457-9

Chapter 3 Evaluating an effective approach to isolate the microbial community from mouse caecum for microbiome analysis

Findings in this chapter feature in both a full-length article that has been submitted to the journal Molecular Biology Reports and additional findings in the last section of the chapter; please see Additional findings below. The author guidelines for submission are available in Annexure B. In this manuscript, microbiome data represented by a gastro-intestinal component were analyzed along with the microbiome representing clinical sputum samples from a parallel study. Tables and figures are inserted as they will appear in the article. Supplementary figures associated with the manuscript are available in Annexure C. The chapter deals with the first objective of the study, namely the evaluation of the NWU lysis method as preferential tool for downstream gastro-intestinal microbiome analysis. A novel application of the method was compared to commercially available DNA isolation kits, to assess efficacy of the former in isolating microbial bacteria present in an impure lysate with short and long read next generation sequencing (NGS) techniques. Additional findings that did not form part of the article can be found following the manuscript. Figures presented in the additional findings are numbered according to the chapter's layout and do not follow the numbering of figures in the manuscript.

3.1 Manuscript

Comparative investigation of the suitability of DNA preparation methods for microbiome analysis of complex clinical samples

Mann, B.C.[1], Wepener, C.[1], Bezuidenhout, J.J.[2], Vermeulen, U.[3,4], & Grobler, A.F. [1,3,4]

Abstract

Efficient DNA preparation is essential for accurate and reproducible microbial data acquisition. In this study an in-house method (NWU lysis system), involving a lysis micro tube (LMT) was employed to determine its suitability for safe, rapid and accurate characterisation of the bacterial microbiome associated with clinical samples in comparison to two available commercial DNA extraction kits. During the experimental setup, it was confirmed that the LMT is suitable for downstream bacterial microbiome analyses with the incorporation of short read sequencing; but due to the fragmented nature of the DNA its suitability is highly dependent on the sequencing technology applied downstream. The study also served to demonstrate that shearing of DNA can have a significant impact on downstream microbiome analyses, based on the sequencing technology used; and that care must be taken especially if long read sequencing is to be employed.

Keywords

DNA preparation, Mechanical lysis, Bead beating, 16S rRNA gene sequencing, Microbiome

1

Introduction

Since the onset of next generations sequencing (NGS) the field of clinical genetics has been rapidly changing (Vrijenhoek *et al.*, 2015). The swift progression of NGS technology and its use in clinical laboratories has allowed for remarkable progress in the genetic diagnosis of both inherited disorders and infectious diseases, as well as the provision of methods for studying accompanying risk factors such as the microbiome (Di Reste *et al.*, 2018). Novel interactions between the human microbiome and health and disease are continuously emerging, and important host–microbiome interactions are increasingly used as targets for both diagnostics and personalised therapeutics (Behrouzi *et al.*, 2019). The majority of NGS platforms still carry high initial infrastructure costs, have extensive computing requirements and are not of a compact and portable nature. These limitations have resulted in the introduction of platforms such as the MinION developed by Oxford nanopore technologies (ONT), as well as rapidly reducing the cost associated with current technologies such as the Illumina Miseq (Besser *et al.*, 2018). Taking the rapid development, improvement and reduction in costs of various NGS platforms into account, many clinical laboratories and research entities are preparing and/or are already in the progress of adapting their diagnostic process to incorporate or focus mainly on NGS approaches Vrijenhoek *et al.*, 2015.

Sequencing of the 16S gene is a commonly employed method to evaluate the microbial community in clinical samples (Pollock *et al.,* 2018). Previous studies have emphasized that effective DNA preparation is crucial for the accurate characterisation of the complex bacterial populations often present in clinical samples, and that lysis efficiency is a major limitation, especially with samples containing hard to lyse bacteria (Lim *et al.*, 2018). Several methods are currently available for effective DNA preparation prior to 16S sequencing, in the form of various commercial kits. These approaches to cellular lysis of available commercial DNA preparation methods differ, and the lysis method may depend on heat, chemical, enzymatic, or mechanical lysis. Additionally, the specific DNA isolation techniques used also differ, such as spin column-based methods or the use of magnetic beads; while others have opted for

direct DNA amplification of crude lysates, forgoing conventional DNA purification (Videvall *et* al., 2017; Pollock *et al.*, 2018; Fiedorová *et al.*, 2019)

The NWU-TB test is a molecular-based sensitive and specific TB diagnostic tool. The NWU-TB system consists of three sequential steps: cell lysis in a LMT (Supplementary figure 2), using an automated lyser device (NWU lysis system: Supplementary figure 3) completely inactivating TB within 7 minutes, followed by multiplex-PCR within 25 min. The lysis step of the NWU-TB test is a highly efficient and cost effective process that is based on the use of heat, chemical and mechanical means to achieve cellular lysis. In addition to its lysis efficacy, the lysis process is also extremely safe, with lysis occurring within the confines of a lysis micro tube, offering the potential for this system to be used with decreased biosafety measures (Mutingwende *et al.*, 2015).

Authors of recent studies have emphasized that the inclusion of mechanical lysis in conjunction with other lysis methods is essential to minimize possible biases due to some microbial cells being more resistant to lysis than others (Lim *et al.*, 2018; Pollock *et al.,* 2018). The decision was thus made to evaluate DNA obtained by means of the NWU lysis method as preferential tool for downstream microbiome analyses on two sample types: a clinical sputum sample evaluated with long read sequencing technology (ONT MinION), representing a lower complexity sample and a more complex gut sample evaluated with short read sequencing technology (Illumina Miseq), focussing on 16S amplicon-based sequencing in comparison to DNA obtained with the use of various commercially available kits.

Materials and methods

Samples and DNA preparation

DNA obtained by means of the NWU lysis method (method H) was compared to DNA obtained by means of two available commercial kits on both the *caecum* contents from an available mouse study (representing a gut sample), and a previously collected less complex clinical sputum sample; thus representing two samples types of varying complexity. The two commercial kits selected for comparison included the QIAamp

DNA microbiome kit (Qiagen, Germany) and the GenElute™ Stool DNA Isolation Kit (Sigma, USA), and were labelled as method Q and S respectively. These kits were selected on the basis that both were bead-beating kits, and thus included both chemical and mechanical lysis to ensure that difficult to lyse bacteria are properly lysed during the DNA preparation process.

Sputum sample

For the evaluation of a low complexity clinical sample, a sputum sample of sufficient volume was collected from a concurrently running study. The sample was initially collected, snap frozen and stored at -80°C until processing. The selected sample was divided into 12 x 250 µl aliquots before further processing. Aliquots were extracted in triplicate using either method Q or S; while lysate was prepared with the NWU in-house cell lysis method (H) with and without additional purification (carried out with the spin column technology of method Q and labelled as HQ).

Extractions with method Q and S were done according to the manufacturers' instructions. Freeze–thaw cycles may compromise bacterial integrity, and the benzonase treatment used during the host DNA removal Protocol of method Q may lead to a loss of exposed bacterial DNA. The decision was thus made to omit the host DNA removal step from method Q considering the samples have been previously frozen. Preparation of the crude lysate using the NWU in-house cell lysis method was done according to previously described methods (Mutingwende *et al.*, 2015). For the NWU cell lysis method, lysis was carried out using the NWU lyser device: 250 µl of sample was mixed with 250 µl of a proprietary lysis buffer. The LMT was placed on the pre-set (95 °C and 3600 rpm) lyser device for 7 min. Bacterial cell lysis was concurrently achieved through chemical, thermal and mechanical means (Mutingwende *et al.*, 2015).

DNA concentration was assessed using the Qubit 4 Fluorometer (Thermofisher Scientific, USA) along with the Qubit BR assay kit (Thermofisher Scientific, USA), while quality was determined by nanodrop spectrophotometry on a Nanodrop One (Thermofisher Scientific, USA). The integrity of extracted genomic DNA was evaluated

by visualization of a 1.5% (w/v) agarose gel using GelRed® dye (Biotium, USA), after electrophoresis in the presence of a 1kb ladder as size reference standard.

Representative gut sample

The *caecum* content from a concurrently running mouse study was investigated as a complex sample. As part of the initial study the *caecums* were dissected, snap frozen and stored at -80 °C prior to further analysis. To generate sufficient sample volume, three *caecums* from C3HeB/FeJ mice were physically cut open and the content was added to phosphate buffered saline (PBS). The mixture was vortexed at high speed for 2 minutes to generate a homogenized sample; 250 µl of this mix was then used for DNA extraction and lysate preparation in triplicate. DNA was extracted and/or prepared, subjected to quality control and samples were labelled as described under section 2.1.1

Amplicon library and flow cell preparation

Two sequencing runs were carried out; one for the sputum sample and one for the gut sample. For the sputum sample a 16S rRNA sequencing library was constructed according to the 16S Barcoding Kit (SQK-RAB204) Protocol (Oxford Nanopore Technologies, Oxford, UK) for sequencing on the ONT MinION platform. Library construction for the gut sample was performed according to the 16S metagenomics sequencing library preparation protocol (Illumina, San Diego, CA, USA) for sequencing on the Illumina MiSeq platform.

Sputum sample

Sequencing of the sputum sample was carried out at the North-West University using the ONT 16S Barcoding Kit (SQK-RAB204) according to the ONT Protocol with the only difference being the use of an inhibitor tolerant high-fidelity polymerase. Polymerase chain reaction barcoding amplification was conducted on a C1000™ Thermal Cycler (Bio-Rad, US). A 50 µl reaction volume consisting of: 1 µl (10 µM) of 16S barcode primer (Oxford Nanopore Technologies, Oxford, UK), 25 µl of Invitrogen

Platinum SuperFi DNA Polymerase master mix (Thermo Fisher Scientific, USA), 10 µl of GC enhancer (Thermo Fisher Scientific, USA), 13 µl nuclease-free water (Sigma-Aldrich, USA) and 1 µl of template DNA (10 ng/µl) was prepared for each sample. In the case of the lysate produced by the NWU in-house cell lysis method, 1 µl of sample was added to the reaction mixture. PCR cycling conditions were set at 95 °C for 1 min followed by 25 cycles of denaturation at 95 °C for 20 s, annealing at 55 °C for 30 s, extension at 65 °C for 2 min and a final extension step of 65 °C for 5 min before holding at 4 °C. PCR products were cleaned using AMPure XP beads (Beckman Coulter, USA) and eluted in 10 µl of a buffer containing 10 mM Tris-HCl pH 8.0 and 50 mM NaCl. Following PCR, 1 µl of eluted sample was quantified using a Qubit fluorometer in order to pool the DNA barcoded libraries at an equal ratio. All barcoded libraries were pooled in the desired ratios to a total of 50-100 fmoles in 10 µl of 10 mM Tris-HCl pH 8.0 and/ 50 mM NaCl. Platform quality control (QC) was carried out using MinKNOW™ on 2 new R9.4.1 chemistry MinION™ flow cells before the flow cell was primed. In total 75 µl of sequencing mix consisting of the DNA library, sequencing buffer and library loading beads was prepared according to the ONT Protocol and added in a drop-wise fashion via the SpotOn sample port. The standard 48 h sequencing script was chosen with 1D live base calling.

Representative gut sample

The V3 and V4 regions of the 16S rRNA gene from the isolated microbiome were amplified on the C1000™ Thermal Cycler (Bio-Rad, US). A 25 µl reaction volume consisting of: 1 µl (5 µM) of forward primer, 1 µl (5 µM) of reverse primer, 12.5 µl of Invitrogen Platinum SuperFi DNA Polymerase master mix (Thermo Fisher Scientific, USA), 5 µl of GC enhancer (Thermo Fisher Scientific, USA), 4.5 µl nuclease-free water (Sigma-Aldrich, USA) and 1 µl of template DNA (20 ng/µl) was prepared for each sample. In the case of the lysate produced by the NWU in-house cell lysis method, 1 µl of sample was added to the reaction mixture. The following PCR conditions were used during amplification: initial denaturation at 98°C for 30 s, followed by 25 cycles of 98°C for 10 s, 55°C for 10 s and 72°C for 30 s and a final elongation step at 72°C for 300 s. After amplification, PCR products were purified using the Agencourt AMPure XP PCR Purification kit (Beckman Coulter, USA); and transported to the Agricultural

Research Council Biotechnology Platform (ARC-LNR), Pretoria, South Africa, for sequencing on the Illumina MiSeq platform according to the standard protocol.

Bioinformatics analysis

Fast 5 files generated from the sputum sample sequencing runs on the MinION™ were base called and de-multiplexed, followed by removal of adapter and primer sequences using ONT's Guppy™ sequencing software (version 3.2.4). The resultant fastq files were then filtered to remove reads with a Phred score below 7; and lengths below 1200 and above 1500bp, using NanoFilt (https://github.com/wdecoster/nanofilt) (De Coster *et al*., 2018). Taxonomy was assigned to sequences using the sintax command from Usearch (Edgar, 2018), with a sintax cut-off of 0.8. Sequences were classified using the RDP 16S training set v16 (RTS) database comprising 13,212 sequences belonging to 2,126 genera. Following classification, the output sintax files were processed with in-house R scripts to produce OTU tables and excel summary files. The OTU table along with a mapping file were then fed into the MicrobiomeAnalyst online software suite for further evaluation, which included alpha and beta diversity determination, rarefaction curve generation and clustering analyses (Dhariwa *et al*., 2017; Chong *et al*., 2020).

Fastq files produced by the Illumina MiSeq platform were processed and analysed using the mothur (version 1.42.3) shell program (Schloss *et al.,* 2009). The sequences were aligned with SILVA-based bacterial reference alignment (version July 2019). Chimeric reads were filtered out using the abundant sequences (dereplicate=t) as a reference with the VSEARCH command in the shell program. Host DNA sequences along with other undesirable sequences were removed with the remove.lineage command where the DNA of chloroplasts, mitochondria, archaea and eukaryotes were removed. Sequences that shared a minimum of 97% pairwise nucleotide identity were clustered into operational taxonomic units (OTUs). OTUs were classified up to species level using the 16S rRNA RDP reference (version 16) and the classify.otu command in the mothur shell program. The abundance file obtained using the make.shared command and the taxonomy file obtained using the classify.otu command was exported for further analyses (Schloss *et al.,* 2009).

Statistical analysis

To evaluate the influence of each extraction method on the DNA quantity/yield and quality (A260/A280 and A260/A230); ANOVA (one-way analysis of variance) was employed with Tukey's post-hoc test for multiple pairwise comparisons [15]. Statistical testing was carried out using Statistica (v13.1) (Statsoft, Inc, USA) and visualised in GraphPad Prism (v8) (GraphPad, Inc., USA). Statistical analyses and visualisation of microbiome data were done with the assistance of MicrobiomeAnalyst on default settings unless specified otherwise (Dhariwa *et al*., 2017; Chong *et al*., 2020). Data was normalised using total sum scaling (TSS). The alpha diversity of samples was measured by observed, Chao1 and Shannon diversity indexes (Corcoll *et al*., 2017). The observed and Chao1 indices act as measures of species richness. The observed species index measures the number of distinguishable taxa in every sample; whereas the Chao1 index is a qualitatively measure, which beside species richness also takes into account the ratio of singletons, and hence gives more weight to rare species. The Shannon diversity index on the other hand, is a measure of both richness and evenness of the microbes of the given sample; thus addressing the question of whether there is evenness and possible domination in the main genera/species found in the sample (Xia & Sun, 2017).

Beta-diversity calculations, which describes the diversity in a microbial community between different samples, were visualized using principal coordinate analysis plots (PCoA). Beta-diversity PCoA plots were based on Bray–Curtis distances, and compared using the nonparametric analysis of similarities (ANOSIM) test. Heat maps of the most abundant genera classified to the genus level were generated using complete hierarchical clustering by Euclidian distance (Dhariwa *et al*., 2017; Xia & Sun, 2017; Chong *et al*., 2020). These tests were performed at the feature level with only the higher abundance taxa (>0.1% of total).

Results

Yield and quality of prepared nucleic acids

The concentration and quality of the prepared nucleic acids were compared for the various methods used for both sample types as summarised in Table 1. Method H without the addition of a purification step yields a crude lysate and thus no quality assessments could be obtained.

Table 1: DNA Quality

Sample	Nanodrop Concentration (ng/µL)	A260/A280	A260/A230
	Sputum sample		
H	-	-	-
HQ	15,03 ± 0,13 [a]	1,95 ± 0,03 [a]	1,96 ± 0,38 [b]
Q	186,53 ± 5,89 [b]	1,87 ± 0 [b]	2,15 ± 016 [b]
S	20,2 ± 0,31 [a]	2,12 ± 0,03 [c]	0,13 ± 0,12 [a]
	Gut sample		
H	-	-	-
HQ	10.43 ± 2.74 [a]	1.77 ± 0.01 [b]	1.33 ± 0.27 [a,b]
Q	610.5 ± 111.49 [b]	2.06 ± 0.04 [a]	1.86 ± 0.41 [b]
S	79.87 ± 23.72 [a]	1.96 ± 0.05 [a]	0.67 ± 0.34 [a]

Values sharing a common letter belong to the same group according to one way ANOVA with Tukey's post-hoc test for multiple pairwise comparisons. These values do not differ significantly according to the test ($p > 0.05$). Values not sharing a common lower case letter indicate a statistically significant difference in comparison to a value belonging to other groups ($p < 0.05$).

Sputum sample

Initial nanodrop results (Table 1) indicate the nucleic acid concentration obtained with method Q was significantly higher ($p < 0.05$) when compare to HQ, and S. All methods with the exception of method S (2.1) had a A260/A280 absorbance ratio between 1.7-2.0, suggesting the preparation of pure nucleic acids. Both methods HQ and Q had A260/A230 ratios within the acceptable range, while method S had a significantly lower A260/A230 ratio. The integrity of the prepared DNA was assessed by agarose gel electrophoresis. Method S yielded high molecular weight intact DNA with minimal shearing, while method Q produced large amounts of high molecular weight DNA, but shearing was also evident. Method HQ on the other hand produced sheared low molecular weight DNA.

Representative gut sample

Upon examination of DNA obtained from the gut sample, a similar pattern in the average nucleic acid concentrations obtained can be seen (Table 1). Method Q again had a significantly higher nucleic acid concentration when compared to other methods. Again all had acceptable A260/A280 absorbance ratios between 1.7-2.0, while only method Q had A260/A230 ratios within the acceptable range. DNA integrity was assessed by agarose gel electrophoresis and revealed similar results to those obtained with the selected sputum sample.

NGS analyses of bacterial diversity and composition of samples from various DNA preparation methods

NGS analyses of bacterial diversity and composition from various DNA preparation methods were carried out on sequencing reads produced for both sample types.

Sputum sample

A single sequencing run on a MinION™ flow cell of R9.4 chemistry, produced 5 169 844 reads from 12 DNA barcodes. Platform quality control (QC) analysis preceding the sequencing run revealed a total of 1356 available pores, split into 4 groups. The mean read length was 1352 base pairs (bp), with an average Phred score of 10.01. The alpha diversity based on the number of observed species, Chao1 and Shannon diversity indices, was compared according to the DNA preparation method (Figure 1: A).

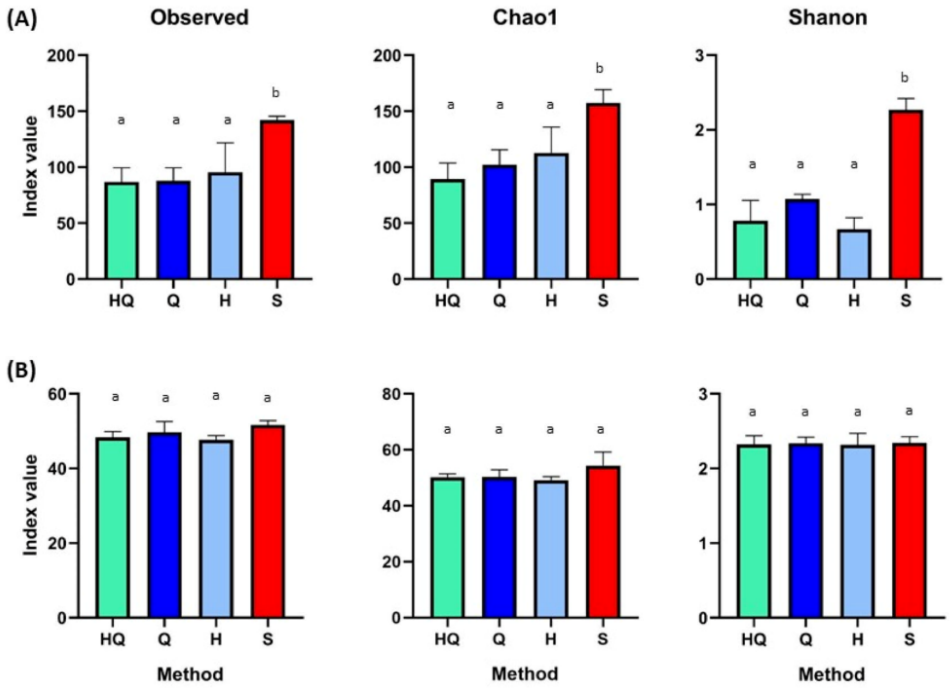


Figure 1: Alpha-diversity, measured by Shannon, Chao1 and observed diversity indices for the selected clinical sputum sample (A) and the representative gut sample (B). Error bars show the standard error of the mean (SEM). Methods sharing a common lower case letter belong to the same group according to one way ANOVA with Tukey's post-hoc test for multiple pairwise comparisons. These values do not differ significantly according to the test ($p > 0.05$). Values not sharing a common lower case letter indicate a statistically significant difference in comparison to a value belonging to other groups ($p < 0.05$).

As seen in Figure 1 A, there was no significant difference between methods HQ, Q and H, based on the Shannon, Chao1 and observed indices, while method S ranked significantly higher than any of the other methods for all three alpha diversity measures. Clustering analyses were performed by means of a hierarchical clustering heat map (Figure 2), which revealed three clusters: Cluster one, consisting of method H and HQ, and one cluster each for methods Q and S respectively. In samples extracted with method S, Gram-negative bacterial genera were more abundant, while samples extracted with method Q resulted in an increased abundance for Gram-positive bacterial genera.

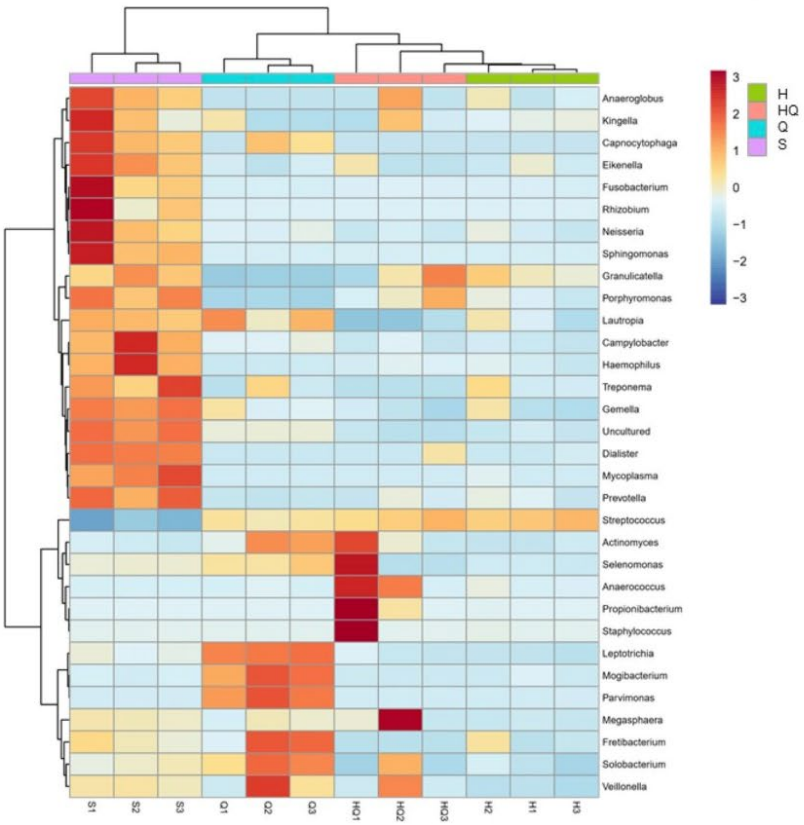


Figure 2: Hierarchical clustering heat map based on the relative abundance of the most abundant genera classified to the genus level for the selected clinical sputum sample. Individual cells in the heat map are colour-coded according to the row Z-scores

Principal coordinate analysis of beta-diversity yielded similar results, showing significant clustering according to the method. Methods H and HQ clustered together, while methods Q and S formed unique clusters (Supplementary figure 1(A)). Analyses of similarity confirmed significant variability among the preparation methods ([ANOSIM] R: 0.74691; p-value < 0.001).

Gut sample

The resulting run on the Illumina Miseq platform produced 4 582 278 reads for 12 samples, with an average quality of 32.58 and an average length of 453 bp. Again the alpha diversity based on the number of observed species, Chao1 and Shannon diversity indices, was compared according to the DNA preparation method (Figure 1:

B). For the representative gut sample, there was no significant difference between methods H, HQ, Q and S based on the Shannon, Chao1 and observed indices. Clustering analyses performed by means of a hierarchical clustering heat map, revealed random clustering among samples, also suggesting no statistically significant difference based on the various preparation methods (Figure 3).

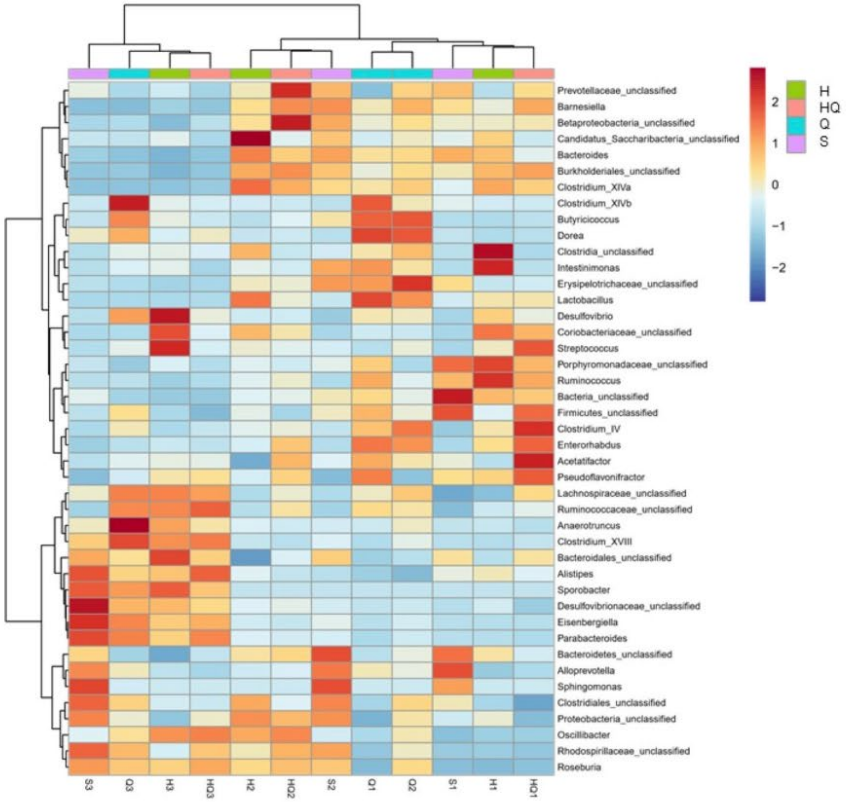


Figure 3: Hierarchical clustering heat map based on the relative abundance of the most abundant genera classified to the genus level from the representative gut sample. Individual cells in the heat map are colour-coded according to the row Z-scores.

This was again confirmed by principal coordinate analysis of beta-diversity (Supplementary figure 1(B)), which revealed no statistically significant difference between samples based on preparation method. Analyses of similarity confirmed no significant variability among the preparation methods ([ANOSIM] R: -0.11728; p-value < 0.759).

Discussion

The A260/A280 ratio is viewed as the primary measure of DNA purity, and DNA with a ratio between 1.70 and 2.00 is generally accepted as pure (Lucena-Aguilar *et al.*, 2016; Teng *et al.*, 2018). All methods evaluated produced relatively pure DNA when examining the A260/A280 absorbance ratio; although the A260/A230 ratio was generally lower for all methods evaluated, especially for method S. The expected value for the A260/A230 absorbance ratio is between 2.0 and 2.22. The low A260/A230 may be due to such factors as carbohydrate carryover, proteins, lipids, EDTA, phenol or salts such as guanidine HCL, a common substance found in various commercial DNA extraction kits (Lucena-Aguilar *et al.*, 2016). None the less, the A260/A230 ratio is viewed as a secondary measure of DNA quality, due to the instability of this value when certain elution buffers are used to elute the DNA (Lucena-Aguilar *et al.*, 2016). PCR amplicons were successfully obtained from all samples; thus the results indicate that all methods yielded nucleic acid of sufficient quality and quantity for sequencing of the 16S rRNA gene (Pollock *et al.*, 2018). Fragmentation of DNA was assessed by agarose gel electrophoresis. The DNA extracted with methods S and Q yielded high molecular weight DNA. Method H was originally designed to form part of a TB diagnostic system and as such the lysis procedure is incredibly robust primarily producing sheared single stranded DNA. The method was originally incorporated with real time qPCR, involving the amplification of short fragments of DNA; and the potential impact of shearing on larger PCR products has not been previously investigated (Kennedy *et al.*, 2009).

NGS analyses of bacterial diversity and composition were compared between different DNA preparation methods and with two sequencing approaches. Evaluations of a representative gut sample with the incorporation of short read sequencing on the Illumina Miseq platform indicated no statistically significant difference between either DNA preparation methods at the end of analyses of the microbiome. Analysis of the sputum sample with the incorporation of long read sequencing, on the other hand showed a statistically significant difference when compared to one of the commercial methods (S). When comparing methods H and HQ it is evident that purification of the DNA obtained with method H did not have any significant impact on the end results

and that the differences observed were the result of the level of integrity of the DNA and the sequencing method applied. The DNA obtained with methods H, HQ and Q was consistently sheared, which may not be a problem when sequencing short fragments; but for single molecule or long-read sequencing technologies, particularly those from Pacific Biosciences (PacBio) and ONT, this can be a major issue (Lim *et al.*, 2018). The MinION 16S workflow incorporates full length 16S amplicons of around 1500bp, and it would thus follow that a workflow incorporating larger amplicons will fail to capture the true diversity of a sample if there is a low amount of intact DNA, as illustrated by the current results.

A limitation of the present study was the use of only one representative sample for each evaluation. It was therefore not possible to determine whether the variation between the preparation methods was less than the inter-subject variation. According to previous studies the inter-subject variation generally tends to be greater than the technical variation. Hence, it is expected that analysis of additional samples would be in accordance with those of prior accounts (Lim *et al.*, 2018; Kennedy *et al.,* 2014). This study focussed on an evaluation of a new method, producing a crude lysate and its efficiency in comparison to already existing validated commercial DNA extraction methods (Wagner Mackenzie *et* al., 2015; Lim *et al.*, 2018). Various studies tend to use mock microbial samples of known composition to evaluate new methods, but these mock samples also have their limitations: They are often presented in a liquid or broth and as such lack the complexity of real biological samples such as sputum, in which the viscosity of the sample is a major stumbling block. Furthermore, mock microbial communities tend to have a lower degree of diversity when compared to actual clinical samples, which harbour a much more diverse bacterial population. Given the growing significance of the microbiome, new products and tools are consistently being developed to study the human microbiome and its various relations to health and disease (Mohajeri *et al.*, 2018). Despite the mentioned limitations, the current study provides useful information, describing the potential of a LMT to carry out downstream microbiome analyses with improved speed and safety.

Conclusion

To conclude, the NWU lysis system is a promising prospect for clinical microbiome studies due to its lysis efficiency. In addition to lysis efficiency the system also provides improved safety due to the fact that lysis of clinical specimens take place within a closed container. In its current form though the lysis method is only compatible with short read sequencing because of the sheared nature of the DNA produced and further optimisation will be required before the lysis step can be incorporated into a portable sequencing technology such as the ONT MinION. In addition, this study also highlights the importance of evaluating the integrity of DNA, as shearing may greatly impact the final composition of the microbiome depending on the sequencing technology employed.

References

Behrouzi A, Nafari AH, Siadat SD (2019) The significance of microbiome in personalized medicine. Clin Transl Med 13;8(1):16. doi: 10.1186/s40169-019-0232-y.

Besser J, Carleton HA, Gerner-Smidt P, Lindsey RL, Trees E (2018) Next-generation sequencing technologies and their application to the study and control of bacterial infections. Clin Microbiol Infect 24(4):335-341. doi: 10.1016/j.cmi.2017.10.013.
Lim MY, Song EJ, Kim SH, Lee J, Nam YD (2018) Comparison of DNA extraction methods for human gut microbial community profiling. Syst Appl Microbiol 41(2):151-157. doi: 10.1016/j.syapm.2017.11.008.

Chong J, Liu P, Zhou G, Xia J (2020) Using MicrobiomeAnalyst for comprehensive statistical, functional, and meta-analysis of microbiome data. Nat Protoc 15(3):799-821. doi: 10.1038/s41596-019-0264-1.

Corcoll N, Österlund T, Sinclair L, Eiler A, Kristiansson E, Backhaus T, Eriksson KM (2017) Comparison of four DNA extraction methods for comprehensive assessment of 16S rRNA bacterial diversity in marine biofilms using high-throughput sequencing. FEMS Microbiol Lett 1;364(14). doi: 10.1093/femsle/fnx139.

De Coster W, D'Hert S, Schultz DT, Cruts M, Van Broeckhoven C (2018) NanoPack: visualizing and processing long-read sequencing data. Bioinformatics 34(15):2666–2669. https://doi.org/10.1093/bioinformatics/bty149.

Dhariwal A, Chong J, Habib S, King IL, Agellon LB, Xia J (2017) MicrobiomeAnalyst: a web-based tool for comprehensive statistical, visual and meta-analysis of microbiome data. Nucleic Acids Res 3(45):180-188. doi: 10.1093/nar/gkx295.

Di Resta C, Galbiati S, Carrera P, Ferrari M (2018) Next-generation sequencing approach for the diagnosis of human diseases: open challenges and new opportunities. EJIFCC 29(1):4-14.

Edgar RC (2018) Accuracy of taxonomy prediction for 16S rRNA and fungal ITS sequences. PeerJ 6. https://doi.org/10.7717/peerj.4652

Fiedorová K, Radvanský M, Němcová E, Grombiříková H, Bosák J, Černochová M, Lexa M, Šmajs D, Freiberger T (2019) The Impact of DNA Extraction Methods on Stool Bacterial and Fungal Microbiota Community Recovery. Front Microbiol 17;10:821. doi: 10.3389/fmicb.2019.00821.

Kennedy NA, Walker AW, Berry SH, Duncan SH, Farquarson FM, Louis P, Thomson JM; UK IBD Genetics Consortium, Satsangi J, Flint HJ, Parkhill J, Lees CW, Hold GL (2014) The impact of different DNA extraction kits and laboratories upon the assessment of human gut microbiota composition by 16S rRNA gene sequencing. PLoS One 24;9(2):e88982. doi: 10.1371/journal.pone.0088982.

Lucena-Aguilar G, Sánchez-López AM, Barberán-Aceituno C, Carrillo-Ávila JA, López-Guerrero JA, Aguilar-Quesada R (2016) DNA Source Selection for Downstream Applications Based on DNA Quality Indicators Analysis. Biopreserv Biobank 14(4):264-70. doi: 10.1089/bio.2015.0064.

Mohajeri MH, Brummer RJM, Rastall RA, Weersma RK, Harmsen HJM, Faas M, Eggersdorfer M (2018) The role of the microbiome for human health: from basic science to clinical applications. Eur J Nutr 57:1-14. doi: 10.1007/s00394-018-1703-4.

Mutingwende I, Vermeulen U, Steyn F, Viljoen H, Grobler A (2015) Development and evaluation of a rapid multiplex-PCR based system for Mycobacterium tuberculosis diagnosis using sputum samples. J Microbiol Methods 116:37-43. doi: 10.1016/j.mimet.2015.06.007.

Pollock J, Glendinning L, Wisedchanwet T, Watson M (2018) The Madness of Microbiome: Attempting To Find Consensus "Best Practice" for 16S Microbiome Studies. Appl Environ Microbiol 84(7). https://doi.org/10.1128/AEM.02627-17.

Schloss PD, Westcott SL, Ryabin T, Hall JR, Hartmann M, Hollister EB, Lesniewski RA, Oakley BB, Parks DH, Robinson CJ, Sahl JW, Stres B, Thallinger GG, Van Horn DJ, Weber CF (2009) Introducing mothur: open-source, platform-independent, community-supported software for describing and comparing microbial communities. Appl Environ Microbiol 75(23):7537-41. doi: 10.1128/AEM.01541-09.

Teng F, Darveekaran Nair SS, Zhu P, Li S, Huang X, Li J, Xu J, Yang F (2018) Impact of DNA extraction method and targeted 16S-rRNA hypervariable region on oral microbiota profiling. Sci Rep *8*(1):16321. https://doi.org/10.1038/s41598-018-34294-x.

Videvall E, Strandh M, Engelbrecht A, Cloete S, Cornwallis CK (2017) Direct PCR Offers a Fast and Reliable Alternative to Conventional DNA Isolation Methods for Gut Microbiomes. *mSystems*. 2(6). https://doi.org/10.1128/mSystems.00132-17.

Vrijenhoek T, Kraaijeveld K, Elferink M, de Ligt J, Kranendonk E, Santen G, Nijman IJ, Butler D, Claes G, Costessi A, Dorlijn W, van Eyndhoven W, Halley DJ, van den Hout MC, van Hove S, Johansson LF, Jongbloed JD, Kamps R, Kockx CE, de Koning B, Kriek M, Lekanne Dit Deprez R, Lunstroo H, Mannens M, Mook OR, Nelen M, Ploem C, Rijnen M, Saris JJ, Sinke R, Sistermans E, van Slegtenhorst M, Sleutels F, van der Stoep N, van Tienhoven M, Vermaat M, Vogel M, Waisfisz Q, Marjan Weiss J, van den Wijngaard A, van Workum W, Ijntema H, van der Zwaag B, van IJcken WF, den Dunnen J, Veltman JA, Hennekam R, Cuppen E (2015) Next-generation sequencing-based genome diagnostics across clinical genetics centers: implementation choices and their effects. Eur J Hum Genet 23(9):1142-50. doi: 10.1038/ejhg.2014.279

18

Wagner Mackenzie B, Waite DW, Taylor MW (2015) Evaluating variation in human gut microbiota profiles due to DNA extraction method and inter-subject differences. Front Microbiol 18(6):130. doi: 10.3389/fmicb.2015.00130.

Xia Y, Sun J (2017) Hypothesis Testing and Statistical Analysis of Microbiome. Genes Dis 4(3):138-148. doi: 10.1016/j.gendis.2017.06.001.

Funding

This study was performed, and the manuscript compiled with the support of funding provided by the South African Department of Science and Innovation in conjunction with the International Mouse Phenotyping Consortium (IMPC) and HANKS TB Diagnostics (Pty) Ltd. The authors also acknowledge financial support from the National Research Foundation of South Africa (DST-NRF Innovation Master's Scholarship Grant No.117255). Opinions expressed, findings and concluding statements are those of the authors and are not necessarily attributed to the NRF.

Author information

Affiliation

[1]DSI/NWU Preclinical Drug Development Platform, Faculty of Health Sciences, North-West University, Potchefstroom, South Africa

Mann, B.C., Wepener, C.

[2]Unit for Environmental Science and Management: Microbiology, North-West University, Potchefstroom Campus, South Africa.

Bezuidenhout, J.J.

[3]HANKS TB Diagnostics, Hoffman Street, Potchefstroom, South Africa.

Vermeulen, U., & Grobler, A.F.

[4]Austell Pharmaceuticals, Sherborne Road, Parktown, South Africa.

Vermeulen, U., & Grobler, A.F.

Contributions

Mann, B.C: Conceptualization, Methodology, Software, Validation, Formal analysis, Investigation, Data Curation, Writing - Original Draft, Writing - Review & Editing, Visualization

Wepener, C: Software, Formal analysis, Investigation, Writing - Review & Editing, Visualization

Bezuidenhout, J.J: Conceptualization, Methodology, Software, Writing - Review & Editing, Resources, Supervision, Project administration

Vermeulen, U: Conceptualization, Methodology, Writing - Review & Editing, Resources

Grobler, A.F: Conceptualization, Methodology, Writing - Review & Editing, Resources, Supervision, Project administration, funding acquisition

Corresponding author

Correspondence to **Bezuidenhout, J.J.**

Ethics declarations

Conflicts of interest/Competing interests

HANKS TB Diagnostics have funded a portion of the project involving an evaluation of their method. Of the research team Prof A.F. Grobler is a former director at HANKS TB Diagnostics and a Mr U. Vermeulen the former COO. The remaining authors have no conflicts of interest to declare.

Ethical approval

This study was approved by the North-West University Health Research Ethics Committee (NWU-HREC) and the North-West University and the Animal Care, Health and Safety Research Ethics Committee (NWU-AnimCareREC), under ethics numbers NWU-00127-18-A1 and NWU-00584-19-A5 respectively. The protocol and consent for the acquisition and use of samples as well as the dissemination of results were performed according to the guidelines and regulations approved by these committees.

Availability of data and material

All data is publicly available from Genbank and the NCBI SRA under Bio projects PRJNA675726 (SRR13014341-SRR13014338) and PRJNA675484 (SRR1301004 - SRR13010037).

.

3.2 Additional findings

3.2.1 Background

The microbial composition of the gastro-intestinal microbiome in mice has been examined in various murine mouse models. However, the mouse microbiome and *Mycobacterium tuberculosis* (*Mtb*) infection has been examined in Balb/c and C57BL/6 mice in particular (Winglee *et al*., 2014; Dumas *et al*., 2018; Nadeem *et al*., 2020). The work described in the present chapter is the first such study on *Mtb* infected C3HeB/FeJ mice (Kramnik mouse model). Various factors influence the gastro-intestinal composition in different strains of mice, including genetic and environmental factors (Hildebrand *et al*., 2013). Hildebrand *et al*. (2013) found that there are two major enterotypes present in the microbiomes of common laboratory mouse strains. Different taxa dominate the microbial composition of the gastro-intestinal microbiota between various enterotypes. The authors further suggest that the formation of enterotypes is caused by or contributes to inflammation. The microbiome of some mouse strains is more similar to one another, though may completely differ from others (Laukens *et al*., 2016). It was also previously found that abundance of genera *Akkermansia*, *Alistipe*s, *Prevotella, Ruminococcus* and *Lactobacillus* differ significantly between commonly used strains namely C57BL/6, Balb/c and non-obese diabetic (NOD) mice (Hugenholtz & de Vos, 2018; Horne *et al*., 2019). Increased abundance of *Prevotella* in C57BL/6 mice is of particular interest, since it is associated with the human enterotype (Horne *et al*., 2019).

The use of different mouse models, for tuberculosis (TB) studies in particular, are suggested to have an impact on study results. It was previously found that *Mtb* infection in Balb/c mice alters the gastro-intestinal microbiome significantly; whereas no significant alterations in the gastro-intestinal microbiome in C57BL/6J-CD45a(Ly5a) mice were found following infection (Winglee *et al*., 2014; Namasivayam *et al*., 2017). Microbiome compositions of Balb/c mice, whether under normal conditions or infected with *Mtb*, predominantly consist of the phylum Firmicutes. However, the abundance of Bacteroidetes in the mouse model was much lower in the microbiome of uninfected mice. This is unexpected, because the microbiome normally constitutes both Firmicutes and Bacteroidetes in the highest abundance (Winglee *et al*., 2014; Huazano-García *et al*., 2017). Microbiome compositions of C57BL/6J mice consist of predominantly Firmicutes and Bacteroidetes, followed by members that belong to phylum Proteobacteria (Dumas *et al*., 2018).

Animal models are essential in safety and efficacy testing of newly developed drugs during pre-clinical studies. For instance, the biology of non-human primates resembles that of the human the best and are considered ideal for non-human safety testing of medicine. However, certain studies

have found that efficacy studies of new drugs in non-human primates did not add significant value to its pre-clinical evaluation (Ferreira *et al*., 2019). A major limitation that has recently received increasing attention, is the lack of a "natural" microbiome amongst laboratory mice frequently used for pre-clinical evaluation of several drugs. Rosshart *et al*. (2019) demonstrated that the microbiome composition of laboratory mice differs from that of wild-type mice. These differences resulted in insufficient results about the immune response to drugs pre-clinically, subsequently resulting in an opposite effect in clinical trials. It was further shown that wild-type mice portray immune responses closer to the human response. These findings accentuate the importance of the gastro-intestinal microbiome during pre-clinical testing of newly discovered drugs, whether it is for efficacy or safety testing.

In this study, the representative gastro-intestinal content was derived from a mouse model. Furthermore, caecum samples were utilized as supposed to faeces, which is more commonly used in gastro-intestinal microbiome studies in mice (Abdo *et al*., 2019; Song *et al*., 2019; Moretó *et al*., 2020). The use of the caecum content to evaluate the gastro-intestinal microbiome has been described recently (Jenior *et al*., 2018; Zhou *et al*., 2020; Vrbanac *et al*., 2020). The organ is a component of the intestine and hosts a high level of bacterial counts ranging from 10^{11} colony forming units per mL (CFU/mL), making it a promising component and representative of an "undisturbed" sample to study the gut microbial composition; and is suggested to portray microbes with active bacterial metabolism (Jenior *et al*., 2018; Stumpff *et al*., 2019). Additionally, the mouse caecum hosts a number of microbes responsible for short-chain fatty acid (SCFA) synthesis, a key feature in energy homeostasis of a healthy gastro-intestinal tract (Holota *et al*., 2019).

3.2.2 Methods

In addition to the result analyses presented above, relative abundances of microbiota present in caecum samples were illustrated using MicrobiomeAnalyst. Furthermore, principal coordinate analysis (PCoA), using Bray-Curtis distances, was used to calculate differences between selected mouse caecums. Filtering and normalization in MicrobiomeAnalyst were performed as described in the article (see section on statistical analysis on page 58 in article above).

3.2.3 Results

In addition to the results demonstrated in the article above, the composition of the same representative gastro-intestinal microbiome in *Mtb* infected C3Heb/FeJ mice was evaluated. Recent studies demonstrated the composition of the gastro-intestinal microbiome of different mouse strains infected with *Mtb*. Figure 3-1 illustrates the relative percentage abundance of phyla present in the microbiome of three different mice. Each caecum sample was extracted using a different extraction method (see section on sample and DNA preparation on page 53 in the article above). Nevertheless, similar abundance of genera remains present in the microbiome of each mouse. A more in-depth illustration of taxa present in the microbiome was evaluated on family (Figure 3-2) and genus (Figure 3-3) levels of classification. As seen in Figure 3-1, it is illustrated in Figure 3-2 and Figure 3-3 that the composition of all samples is similar to one another.

In Figure 3-1, percentage of relative abundance of phyla is illustrated. The gastro-intestinal microbiome of infected C3HeB/FeJ mice consists of a steady ratio of members belonging to Firmicutes and Bacteroidetes (Figure 3-1). In addition to this, a relatively high abundance of Proteobacteria was also present amongst all caecum samples. However, a small abundance of β-Proteobacteria was classified amongst these samples (Figure 3-2). Families that harbor the majority of the C3HeB/FeJ microbiome were Porphyromonadacea, Lachnospirceae, Ruminococcaceae, Prevotellaceae, Bacteroidaceae and Rikenellaceae. Remaining families that were present to a less extent is illustrated in Figure 3-2. In Figure 3-3, genera that were present in the gastro-intestinal microbiome are illustrated. Classified genera that were predominantly abundant in the microbiome were *Prevotella, Bacteroides, Alistipes* and *Oscillibacter* (Figure 3-3).

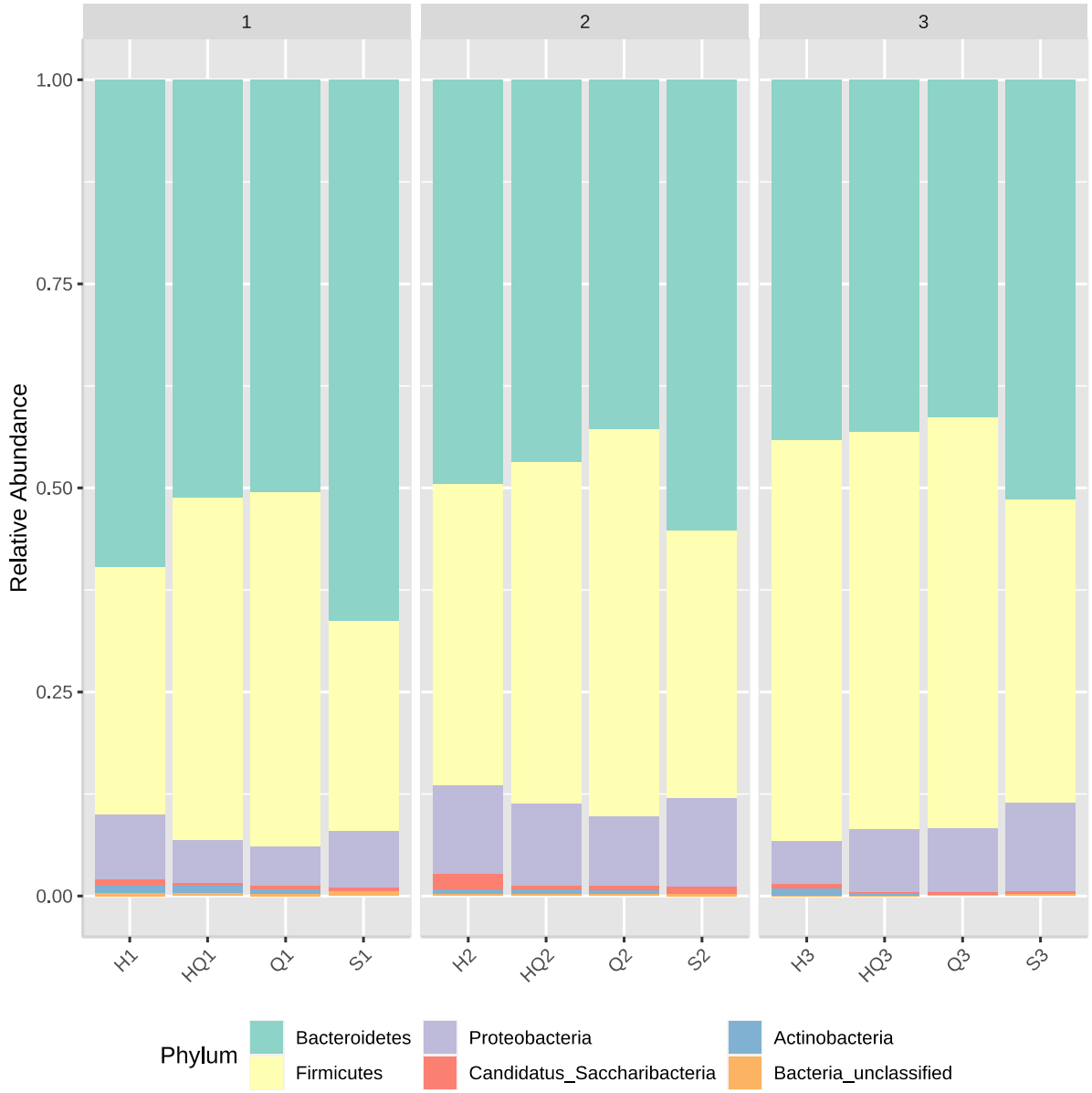


Figure 3-1 Relative percentage abundance of phyla present in the gastro-intestinal microbiome of *Mtb* infected C3HeB/FeJ mice. The microbiome primarily consists of the phyla Bacteroidetes (green) and Firmicutes (yellow), followed by Proteobacteria (purple). Members from the phyla Candidatus Saccharibacteria (red) and Actinobacteria (blue) were present in smaller amounts. Unclassified bacteria are presented in orange.

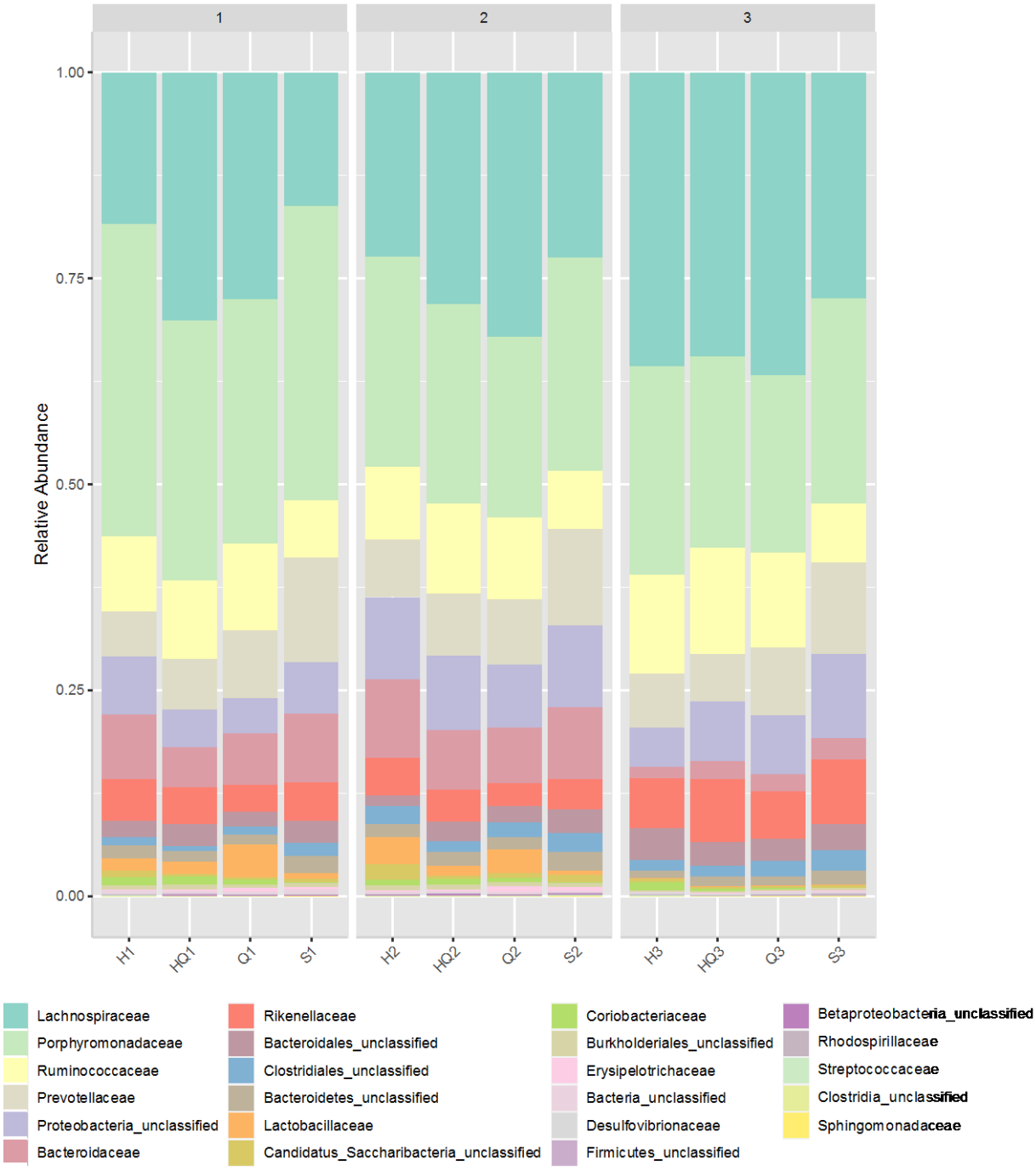


Figure 3-2 Percentage of relative abundant Families present in the caecum microbiome of C3HeB/FeJ mice that are infected with *Mtb*. Taxa present on family level are presented in the legend below the figure. Each colour represents a different family member.

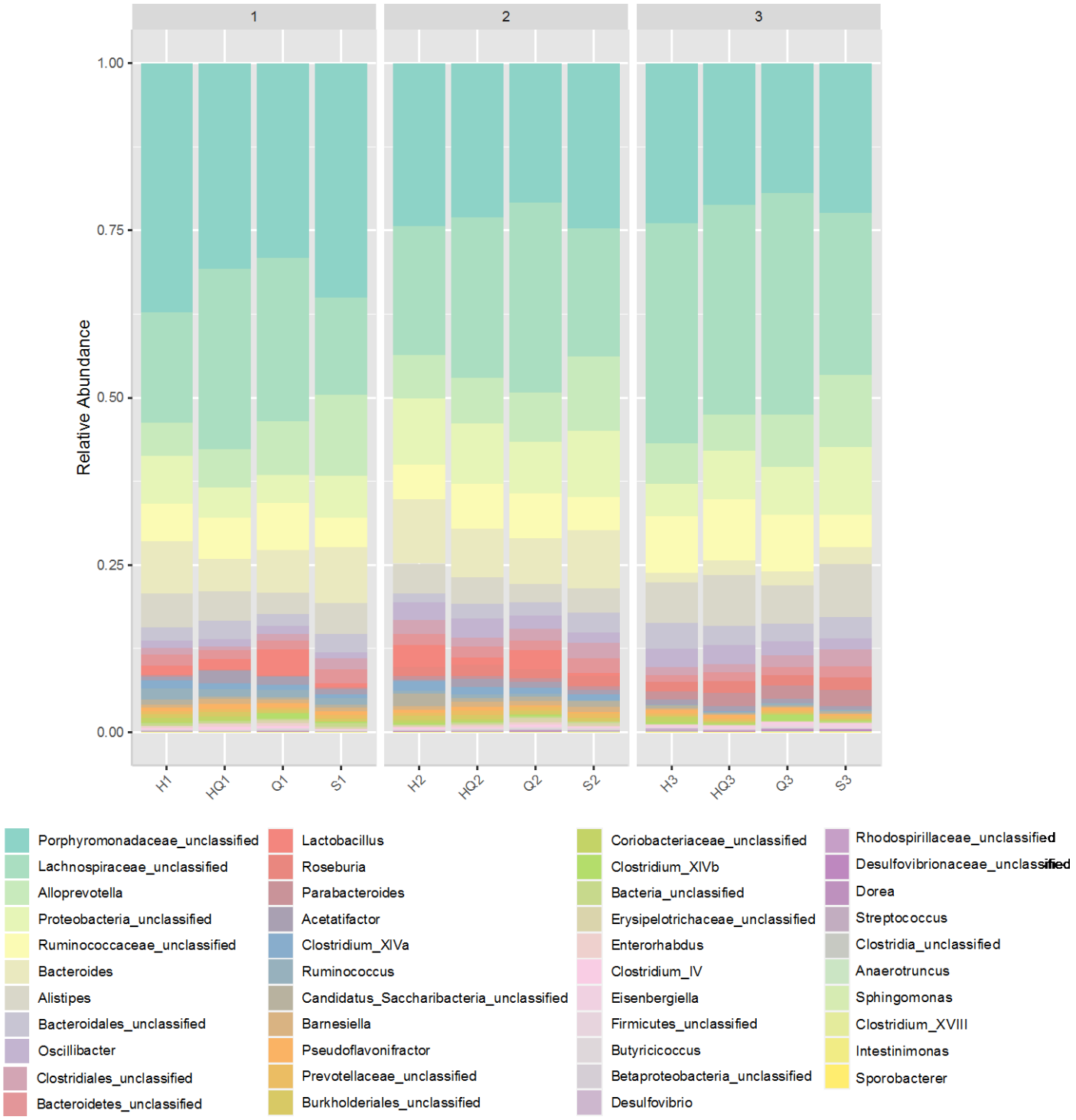


Figure 3-3 Taxonomic composition on genus level of C3HeB/FeJ microbiome. Relative percentage abundance is presented in the figure. Description of genera illustrated in the figure is presented in the legend, each colour representing a specific taxon.

It is evident in Figure 3-1, Figure 3-2 and Figure 3-3 that there were slight differences in microbial composition between the three mice. Upon analysis of beta diversity with principal coordinate analysis (PCoA), significant differences between individual mice were determined, regardless of the method used for DNA extraction (Figure 3-4). It is suggested that inter-individual variation needs to be taken into account between each mouse. The R-value (R=1) also indicated that there was significant dissimilarity between each mouse, therefore clustering samples derived from the same mouse is observed.

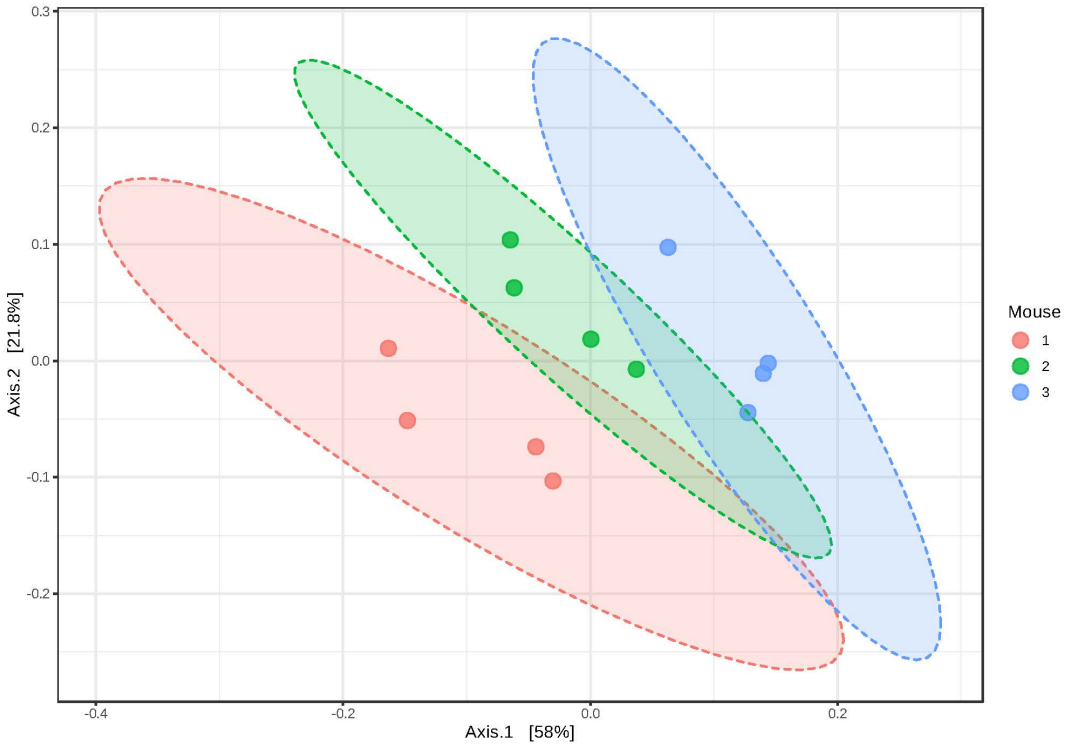


Figure 3-4 PCoA based on the Bray-Curtis index grouped according to subjects. Samples located closer to one another indicate similarity. Different mice had significant differences in similarity as tested by ANOSIM (R = 1; p = 0.002).

3.2.4 Discussion

With regards to other mouse models, Winglee *et al*. (2018) found that the *Mtb* infected gastro-intestinal microbiomes of female Balb/c mice predominately consist of members that belong to the phylum Firmicutes, in particular *Lactobacillus*. Furthermore, an almost complete depletion of Bacteroidetes was the result of an infected microbiome in Balb/c mice. The microbiome of C3HeB/FeJ mice, presented in the present study, is shown to be more similar to C57BL/6 mice (Dumas *et al*., 2018). Slightly younger C57BL/6 mice's infected microbiota harbors mainly Firmicutes and Bacteroidetes, followed by members of β-Proteobacteria (Dumas *et al*., 2018).

Also, as is the case with the microbiota of C57BL/6 mice, those of C3HeB/FeJ consist of β-Proteobacteria, though in very low abundance. *Bacteroides,* members that belong to the phylum Bacteroidetes, were found to decrease significantly in C57BL/6 mice due to *Mtb* infection (Khan *et al*., 2016). Higher levels of *Bacteroides* were, however, present in the microbiome of C3HeB/FeJ mice. In addition, *Lactobacillus* abundance in samples derived from C3HeB/FeJ mice differs from abundance in C57BL/6 mice, where abundance in the latter is higher than in the former (Khan *et al*., 2016).

At the time of writing, evaluation of the gastro-intestinal microbiome in C3HeB/FeJ mice has not been studied intensively and limited literature is available. It has only recently been suggested that there is a crosstalk between TB and the gastro-intestinal microbiome (Namasivayam *et al*., 2018), by evaluating microbiome changes in other mouse models (please refer to section 2.6.2 and 2.6.3). Arias *et al*. (2019) examined abundance of bacteria in the microbiome of this mouse model and found that the microbiota predominantly consists of Bacteroidetes and Firmicutes, followed by Proteobacteria. This was in animals that consume a normal diet. These results are similar to those found by Dumas *et al*. (2018) in C57BL/6 mice. Our results correspond to the findings of Arias *et al*. (2019) on the phylum level of classification. Results in the present study on family level also correlate with results found by Arias *et al*. (2019). Family Porphyromonadacea (members of the phylum Bacteroidetes) dominate the gastro-intestinal environment of C3HeB/FeJ mice, contributing to approximately 45 % of the bacteria of the microbiome. On the genus level of classification, our results indicate that *Clostridium* abundance are low in *Mtb* infected mice, as does Arias *et al*. (2019). Contrary to Arias *et al*. (2019) though, was the low abundance of *Barnsiella*, members of Bacteroidetes in infected mice.

Significant differences in the microbiome were observed amongst individual mice. These differences could not be contributed to the various extraction methods that were implemented to isolate microbial DNA (see results section on gut sample on page 62 in the article above). There are several factors that may have caused this phenomenon. Primary factors that influence the murine mouse microbiome composition in the gut include diet, species-independent enterotypes associated with inflammation, housing, genotypes and inter-individual variation (Tumbaugh *et al*., 2009; Hildebrand *et al*., 2013). Additionally, it is well known that age and gender influence the gut microbial community in humans, resulting in microbial variation in the gut (Mariat *et al*., 2009; Haro *et al*., 2016). As in humans, age and gender in mice should also be considered, as it is suggested that these factors have a critical impact on the microbial community (Kozik *et al*., 2017). Given that the mice were from the same species, genetics do not play a role in the dissimilarities of beta-diversity that was observed. All mice were female and aged between eight- and ten-weeks

prior to infection with *Mtb*. Small differences of age between mice might contribute to the inter-individual differences, though the duration of infection were the same and age of mice did not differ much. Furthermore, differences observed cannot be attributed to environmental factors, since the mice were kept under similar housing conditions and given the same diet, as per protocol (van der Merwe, 2019). In short, the mice were housed in a Bio-safety level III unit in enriched individually ventilated cages (IVC) on a rack isolator system. Temperature (21 ± 2 °C) and humidity (55 ± 10 %) were controlled; and 20 air changes per hour in maintained positive pressure were retained. A 12-hour day-night cycle was upheld firmly; and food and water were provided *ad libitum*. Sterile, dust-free corncob chips that contribute to reducing toxic gasses, were used as bedding to provide a safe environment for the animals. The different mice might have been housed in separate cages, resulting in a slightly different environment. However, it has been found that mice living in the same housing conditions do have similar gut microbial communities (Schmidt *et al*., 2019). The level of infection between each mouse was considered to be similar, since samples utilized were dissected at the same timepoint. *Mtb* colony forming units (CFUs) determined previously confirmed the similarity of infection at this timepoint (log 10 CFUs 6.40 ± 0.08) (van der Merwe, 2019; Annexure D). The small deviation of CFU counts from the mice at this specific timepoint of infection, indicated that infection between individual mice were not identical, but close. This deviation might contribute to the differences observed between each mouse. Comparison between uninfected mice of the same age and under the same environmental conditions are crucial to determine whether infection does have an effect in differences observed between individual mice (please refer to section 5.3 I). However, the differences in beta-diversity observed between mice can most probably be ascribed to inter-individual variation. According to Kostic *et al*. (2013), inter-individual variation is strain specific, where the extent of variation is dependent on the specific strain. Therefore, an observation of differences in the microbial composition of mice of the same strain is normal. The results of the study described here, do however illustrate that there is no difference in species diversity amongst the different mice, but differences correlate with the abundance of the diversity organisms. In addition to selecting an effective DNA extraction method for successful microbial downstream analysis, various factors that contribute to variation amongst microbial data should also be considered. This is important when compiling a study design to ensure consistency and reliable results in investigating the microbiome of all animal models.

3.2.5 Conclusion

In the present study, it was indicated that the gastro-intestinal microbiome of different mouse models used in TB studies differ in diversity and abundance. It was found that the gastro-intestinal microbiome of *Mtb* infected C3HeB/JeF mice (Kramnik mouse model) are more similar to that of C57BL/6 mice, rather than Balb/c mice. Furthermore, it was demonstrated that inter-individual variation does occur between the microbiome of infected mice, regardless of variables that were considered to be identical for all mice. Observably, inter-individual differences were not correlated with the diversity present within each sample, but with the distribution of bacterial abundance. Richness of specific taxa in the microbiome has been shown to have different immune responses to selected drugs in a pre-clinical study (Rosshart *et al*., 2019). Despite similar abundance of phyla in the microbiome, different taxa within the phylum differ in the microbiomes of particularly mouse and human. This is relevant to the distribution of bacterial species in the phylum Firmicutes, which correlates with immunity (Chung *et al.* 2012). These findings imply that microbial composition of selected animal models for pre-clinical testing are of utmost importance to take into account when compiling a study design.

References

Abdo, Z., LeCureux, J., LaVoy, A., Eklund, B., Ryan, E.P. & Dean, G.A. 2019. Impact of oral probiotic *Lactobacillus acidophilus* vaccine strains on the immune response and gut microbiome of mice. *PloS one*, 14(12):e0225842. doi:10.1371/journal.pone.0225842

Arias, L., Goig, G.A., Cardona, P., Torres-Puente, M., Díaz, J., Rosales, Y., Garcia Aguilera, E., Tapia, G., Comas, I., Vilaplana, C. & Cardona, P.J. 2019. Influence of gut microbiota on progression to tuberculosis generated by high fat diet-induced obesity in C3HeB/FeJ Mice. *Frontiers in Immunology*, 10:2464. doi:10.3389/fimmu.2019.02464

Chung, H., Pamp, S.J., Hill, J.A., Surana, N.K., Edelman, S.M., Troy, E.B., Reading, N.C., Villablanca, E.J., Wang, S., Mora, J.R. & Umesaki, Y. 2012. Gut immune maturation depends on colonization with a host-specific microbiota. *Cell*, 149(7):1578-1593. doi:10.1016/j.cell.2012.04.037

Dumas, A., Corral, D., Colom, A., Levillain, F., Peixoto, A., Hudrisier, D., Poquet, Y. & Neyrolles, O. 2018. The host microbiota contributes to early protection against lung colonization by *Mycobacterium tuberculosis*. *Frontiers in immunology*, *9*:2656. doi:10.3389/fimmu.2018.02656

Ferreira, G.S., Veening-Griffioen, D.H., Boon, W.P., Moors, E.H., Gispen-de Wied, C.C., Schellekens, H. & van Meer, P.J. 2019. A standardised framework to identify optimal animal models for efficacy assessment in drug development. *PloS one*, 14(6):e0218014. doi:10.1371/journal.pone.0218014

Haro, C., Rangel-Zuniga, O.A., Alcala-Diaz, J.F., Gomez-Delgado, F., Perez-Martinez, P., Delgado-Lista, J., Quintana-Navarro, G.M., Landa, B.B., Navas-Cortes, J.A., Tena-Sempere, M., Clemente, J.C., Lopez-Miranda, J., Perez-Jimenez, F. & Camargo, A. 2016. Intestinal microbiota is influenced by gender and body mass index. *PLoS One*, 11(5):e0154090. doi:10.1371/journal.pone.0154090

Hildebrand, F., Nguyen, T.L., Brinkman, B., Yunta, R.G., Cauwe, B., Vandenabeele, P., Liston, A. & Raes, J. 2013. Inflammation-associated enterotypes, host genotype, cage and inter-individual effects drive gut microbiota variation in common laboratory mice. *Genome Biology*, 14(1):R4. doi:10.1186/gb-2013-14-1-r4

Holota, Y., Dovbynchuk, T., Kaji, I., Vareniuk, I., Dzyubenko, N., Chervinska, T., Zakordonets, L., Stetska, V., Ostapchenko, L., Serhiychuk, T. & Tolstanova, G. 2019. The long-term

consequences of antibiotic therapy: Role of colonic short-chain fatty acids (SCFA) system and intestinal barrier integrity. *PloS one*, 14(8):p.e0220642. doi:10.1371/journal.pone.0220642

Horne, R., Pierre, J.S., Odeh, S., Surette, M. & Foster, J.A. 2019. Microbe and host interaction in gastrointestinal homeostasis. *Psychopharmacology*, 236(5):1623-1640. doi:10.1007/s00213-019-05218-y

Huazano-García, A., Shin, H. & López, M.G. 2017. Modulation of gut microbiota of overweight mice by agavins and their association with body weight loss. *Nutrients*, 9(9):821. doi:10.3390/nu9090821

Hugenholtz, F. & de Vos, W.M. 2018. Mouse models for human intestinal microbiota research: a critical evaluation. *Cellular and Molecular Life Sciences*, 75(1):149-160. doi:10.1007/s00018-017-2693-8

Jenior, M.L., Leslie, J.L., Young, V.B. & Schloss, P.D. 2018. *Clostridium difficile* alters the structure and metabolism of distinct cecal microbiomes during initial infection to promote sustained colonization. *Msphere*, 3(3):e00261-18. doi:10.1128/mSphere.00261-18

Khan, N., Vidyarthi, A., Nadeem, S., Negi, S., Nair, G. & Agrewala, J.N. 2016. Alteration in the gut microbiota provokes susceptibility to tuberculosis. *Frontiers in immunology*, 7:529. doi:10.3389/fimmu.2016.00529

Kostic, A.D., Howitt, M.R. & Garrett, W.S. 2013. Exploring host–microbiota interactions in animal models and humans. *Genes & Development*, *27*(7):701-718. doi:10.1101/gad.212522.112

Kozik, A.J., Nakatsu, C.H., Chun, H. & Jones-Hall, Y.L. 2017. Age, sex, and TNF associated differences in the gut microbiota of mice and their impact on acute TNBS colitis. *Experimental and Molecular Pathology*, 103(3):311-319. doi:10.1016/j.yexmp.2017.11.014

Laukens, D., Brinkman, B.M., Raes, J., De Vos, M. & Vandenabeele, P. 2016. Heterogeneity of the gut microbiome in mice: guidelines for optimizing experimental design. *FEMS Microbiology Reviews*, 40(1):117-132. doi:10.1093/femsre/fuv036

Mariat, D., Firmesse, O., Levenez, F., Guimarães, V.D., Sokol, H., Doré, J., Corthier, G. & Furet, J.P. 2009. The Firmicutes/Bacteroidetes ratio of the human microbiota changes with age. *BMC Microbiology*, 9(1). doi:10.1186/1471-2180-9-123

Moretó, M., Miró, L., Amat, C., Polo, J., Manichanh, C. & Pérez-Bosque, A. 2020. Dietary supplementation with spray-dried porcine plasma has prebiotic effects on gut microbiota in mice. *Scientific reports*, 10:2926. doi:10.1038/s41598-020-59756-z

Nadeem, S., Maurya, S.K., Das, D.K., Khan, N. & Agrewala, J.N. 2020. Gut dysbiosis thwarts the efficacy of vaccine against *Mycobacterium tuberculosis*. *Frontiers in Immunology*, 11:726. doi:10.3389/fimmu.2020.00726

Namasivayam, S., Maiga, M., Yuan, W., Thovarai, V., Costa, D.L., Mittereder, L.R., Wipperman, M.F., Glickman, M.S., Dzutsev, A., Trinchieri, G. & Sher, A. 2017. Longitudinal profiling reveals a persistent intestinal dysbiosis triggered by conventional anti-tuberculosis therapy. *Microbiome*, 5(1):1-17. doi:10.1186/s40168-017-0286-2

Namasivayam, S., Sher, A., Glickman, M.S. & Wipperman, M.F. 2018. The microbiome and tuberculosis: Early evidence for cross talk. *MBio*, 9(5):e01420-18. doi:10.1128/mBio.01420-18

Rosshart, S.P., Herz, J., Vassallo, B.G., Hunter, A., Wall, M.K., Badger, J.H., McCulloch, J.A., Anastasakis, D.G., Sarshad, A.A., Leonardi, I. & Collins, N. 2019. Laboratory mice born to wild mice have natural microbiota and model human immune responses. *Science*, 365(6452):aaw4361. doi:10.1126/science.aaw4361

Schmidt, E., Mykytczuk, N. & Schulte-Hostedde, A.I. 2019. Effects of the captive and wild environment on diversity of the gut microbiome of deer mice (*Peromyscus maniculatus*). *ISME Journal*, 13(5):1293-1305. doi:10.1038/s41396-019-0345-8

Song, M., Zeng, J., Jia, T., Gao, H., Zhang, R., Jiang, J., Li, G. & Su, T. 2019. Effects of sialylated lactulose on the mouse intestinal microbiome using Illumina high-throughput sequencing. *Applied Microbiology and Biotechnology*, 103:9067-9076. doi:10.1007/s00253-019-10169-7

Stumpff, F., Manneck, D. & Martens, H. 2019. Unravelling the secrets of the caecum. *European Journal of Physiology*, 471:925-926. doi:10.1007/s00424-019-02292-1

Turnbaugh, P.J., Ridaura, V.K., Faith, J.J., Rey, F.E., Knight, R. & Gordon, J.I. 2009. The effect of diet on the human gut microbiome: a metagenomic analysis in humanized gnotobiotic mice. *Science Translational Medicine*, 1(6):6ra14. doi:10.1126/scitranslmed.3000322

Van der Merwe, D. 2019. Determination of the therapeutic efficacy of a novel Pheroid® formulation in a rodent tuberculosis model. NWU: Potchefstroom Campus (Dissertation – MSc).

Vrbanac, A., Patras, K.A., Jarmusch, A.K., Mills, R.H., Shing, S.R., Quinn, R.A., Vargas, F., Gonzalez, D.J., Dorrestein, P.C., Knight, R. & Nizet, V. 2020. Evaluating Organism-Wide Changes in the Metabolome and Microbiome following a Single Dose of Antibiotic. *Msystems*, 5(5):e00340-20. doi:10.1128/mSystems.00340-20

Winglee, K., Eloe-Fadrosh, E., Gupta, S., Guo, H., Fraser, C. & Bishai, W., 2014. Aerosol *Mycobacterium tuberculosis* infection causes rapid loss of diversity in gut microbiota. *PloS one*, *9*(5):e97048. doi:10.1371/journal.pone.0097048

Zhou, J., Shu, R., Yu, C., Xiong, Z., Xiao, Q., Li, Z., Xie, X. & Fu, Z. 2020. Exposure to low concentration of trifluoromethanesulfonic acid induces the disorders of liver lipid metabolism and gut microbiota in mice. *Chemosphere*, 258:127255. doi:10.1016/j.chemosphere.2020.127255

Chapter 4 Changes of microbial communities in the gut during treatment with Pheroid®- based tuberculosis therapy in the Kramnik mouse model

4.1 Introduction

Tuberculosis (TB), caused by the bacterial agent *Mycobacterium tuberculosis* (*Mtb)*, is a worldwide pandemic, affecting approximately 10 million people per year (WHO, 2019). The drug regimen for treatment of susceptible TB is quite intensive, comprising a cocktail of first-line antibiotics administered for at least six months. Furthermore, drug-resistant TB requires a more demanding treatment regimen, sometimes continuing for up to two years. These treatments necessitate strict patient compliance to prevent relapse and treatment failure (WHO, 2019). First-line TB treatment includes the broad spectrum antibiotic rifampicin (RIF), together with narrow spectrum anti-mycobacterials isoniazid (INH), pyrazinamide (PZA), and ethambutol (EMB) (Beauduy & Winston, 2018). RIF targets Gram-positive and some Gram-negative bacteria, including mycobacteria, whereas the remaining anti-mycobacterials are known for their targeted effect primarily on Mycobacterial *species* (Beauduy & Winston, 2018). It was however, recently suggested that some of the narrow spectrum drugs in the regimen do not necessarily target only mycobacteria, but may also have an effect on other microbes (Namasivayam *et al*., 2017). Drug resistant TB is one of the major concerns when it comes to treatment. Acquired drug resistance to the first-line drugs used to treat *Mtb* infection develop by spontaneous mutations in in several identified genes (Johnson *et al.,* 2006; Kolyva & Karakousis, 2012). These genes include the loci *rpoB* for resistance to RIF; *katG*, *inhA*, *aphC*, *kasA* and *ndh* for resistance to INH; *pncA* for PZA resistance; and *embB* for resistance against EMB. Acquired resistance may be caused by suboptimal drug administration or poor patient compliance because of long treatment durations. To address the growing concern of TB drug resistance, more effective and quicker treatments are being explored.

Alternative delivery systems for antimicrobial administration to improve efficacy of treatment of infections at lower doses are emerging. Pheroid® vesicles, based on Pheroid® technology, are used as one such delivery system. Pheroid® mainly consists of three phases namely an oil, a water and a gas (nitrous oxide). Pro-Pheroid® consists only of the oil phase and is mainly composed of esters of unsaturated fatty acids. The latter is based on self-micro- and nano-emulsifying delivery systems (SMEDS & SNEDS), aiming to self-emulsify poorly soluble compounds that is administered orally. Once entering the gastro-intestinal environment, Pheroid®

vesicles form immediately. In addition to the self-emulsifying action of the pro-Pheroid®, adding nitrous oxide gas to the formulation also results in micro and nano vesicles with the entrapment of the desired active pharmaceutical ingredients (APIs) (Grobler, 2009; Grobler, 2013; van Zyl *et al*.,2016). Studies involving TB treatment APIs incorporated in Pheroid® formulations have previously been conducted and showed promising results *in vitro*, *in vivo* and in a clinical setting, as mentioned in section 2.4 in Chapter 2. In these previous studies, it was indicated that a reduced dose of antimicrobial APIs in Pheroid® resulted in an increase of bacterial clearance *in vitro*, compared to free drugs. Additionally, resistant strains were more susceptible to Pheroid®-based TB drugs than free drugs *in vitro.* Furthermore, TB treatment APIs entrapped in Pheroid® vesicles enhance bioavailability compared to standard Rifafour®-e275 treatment, in animal and human studies, by increasing the area under the curve (AUC) and maximum concentrations in blood plasma (C_{max}). Pheroid®-based TB therapy also appears to be more effective than the free drug *in vivo* (Grobler, 2009; Nieuwoudt, 2009).

The gastro-intestinal environment of mammals consists of millions of microbes, including bacteria, protozoans, fungi, archaea and protozoans. Amongst all the micro-organisms present, bacteria play an essential role in metabolism and immunity of an individual. As described in Chapter 2 (see section 2.6.3), the impact of TB therapy on the gastro-intestinal microbiome has previously been examined in both human and animal models (Namasivayam *et al*., 2017; Wipperman *et al*., 2017; Khan *et al*., 2019). In studies of the effects of TB therapy on the gastro-intestinal microbiome, a decrease in diversity within the microbiome were detected and species after did not recolonize or rebounded back to normal homeostatic structure after initiation of TB treatment. Such changes in microbiome composition are known as dysbiosis. Dysbiosis caused by antibiotics in TB infected cases results in perturbed immune responses in animals and humans (Dumas *et al*., 2018; Maji *et al*., 2018). Therefore, it is important to reduce dysbiosis of gastro-intestinal microbiota, possibly with alternative treatment approaches. The effect of an alternative treatment approach, such as Pheroid®-based TB therapies, on the gastro-intestinal microbiome has not been determined to date.

Several animal models have been used to study TB (Singh & Gupta, 2018). No animal model fully replicates the TB disease pathology as found in humans; however, mice have previously been used as model for TB immunology, drug and vaccination evaluation, and determination of relapse and latency of the disease. Additionally, mice are convenient models because it does not require much laboratory space and the costs are significantly lower. Mouse strains mainly used in TB studies are C57BL/6, Balb/c and C3HeB/FeJ (Zhan *et al*., 2017). The latter is considered humanized, due to its ability to develop hypoxic lesions in lungs after *Mtb* infection, a key feature

in human TB (Harper *et al*., 2012). TB, TB therapy and the gastro-intestinal microbiome has gained a lot of attention regarding health and the state of disease in humans (see section 2.6 in Chapter 2). Furthermore, the effect of TB treatment on the microbiome in the Kramnik model (C3HeB/FeJ) is of interest, since it is regarded as a humanized mouse model and has not been evaluated at the time of writing. In this chapter, a study aimed at studying the changes in structural microbial composition of Kramnik mouse caecum samples is described. The microbial composition was determined at various timepoints for different TB treatment regimens. Shifts in the microbial structure during standard and Pheroid®-based TB therapy was compared and analysed over time. The effect of the therapies on the recovering microbiome after treatment ceased was also evaluated in the present study. Additionally, shifts in microbial composition as a result of the administration of a carrier formulation, were simultaneously determined and compared to infected mice that did not receive any treatment (infected reference group). It was hypothesized that the different TB treatment regimens have different effects on the microbiome of this animal model; and that microbiome recovery was achieved after treatment with an alternative delivery approach.

4.2 Materials and methods

4.2.1 Study design

The infection with *Mtb*, the treatment of mice with different drug regimens, as well as the sample collection were executed in a previous study by van der Merwe (2019). Figure 4-1 illustrates a copy of the original study design. The study was carried out on eight to ten (8-10) week-old female Kramnik mice, also known as the C3HeB/FeJ mouse strain. Mice were provided by the internationally (American Association for Accreditation of Laboratory Animal Care [AAALAC], and locally accredited South African National Accreditation Service [SANAS]) Vivarium of the North-West University. The animals were infected with the H37Rv *Mycobacterium tuberculosis* strain, intranasally. A 1 mL aliquot of 6.8 x 10^7 CFU of the strain was diluted with phosphate buffered saline (PBS) 100-fold. Prior to infection, mice were anesthetized in a 1 L chamber with a 2.5 % isoflurane/O_2 exposure at a rate of 2 L/min. During the procedure, the mice were monitored for signs of distress. Each unconscious mouse was infected intranasally with an estimate of 3.4 x 10^4 CFU *Mtb* by gradually releasing the dilution into the nostrils with a sterile gauge feeding needle. As extracted from van der Merwe (2019), “The rate of release was adjusted so as to allow the mouse to inhale the inoculum, the formation of bubbles helps to aerosolise the inoculum and aids in the infection.” Thereafter, mice were treated with three different TB therapies for 12 weeks (van

der Merwe, 2019). After treatment, animals were monitored for a three-month period post treatment.

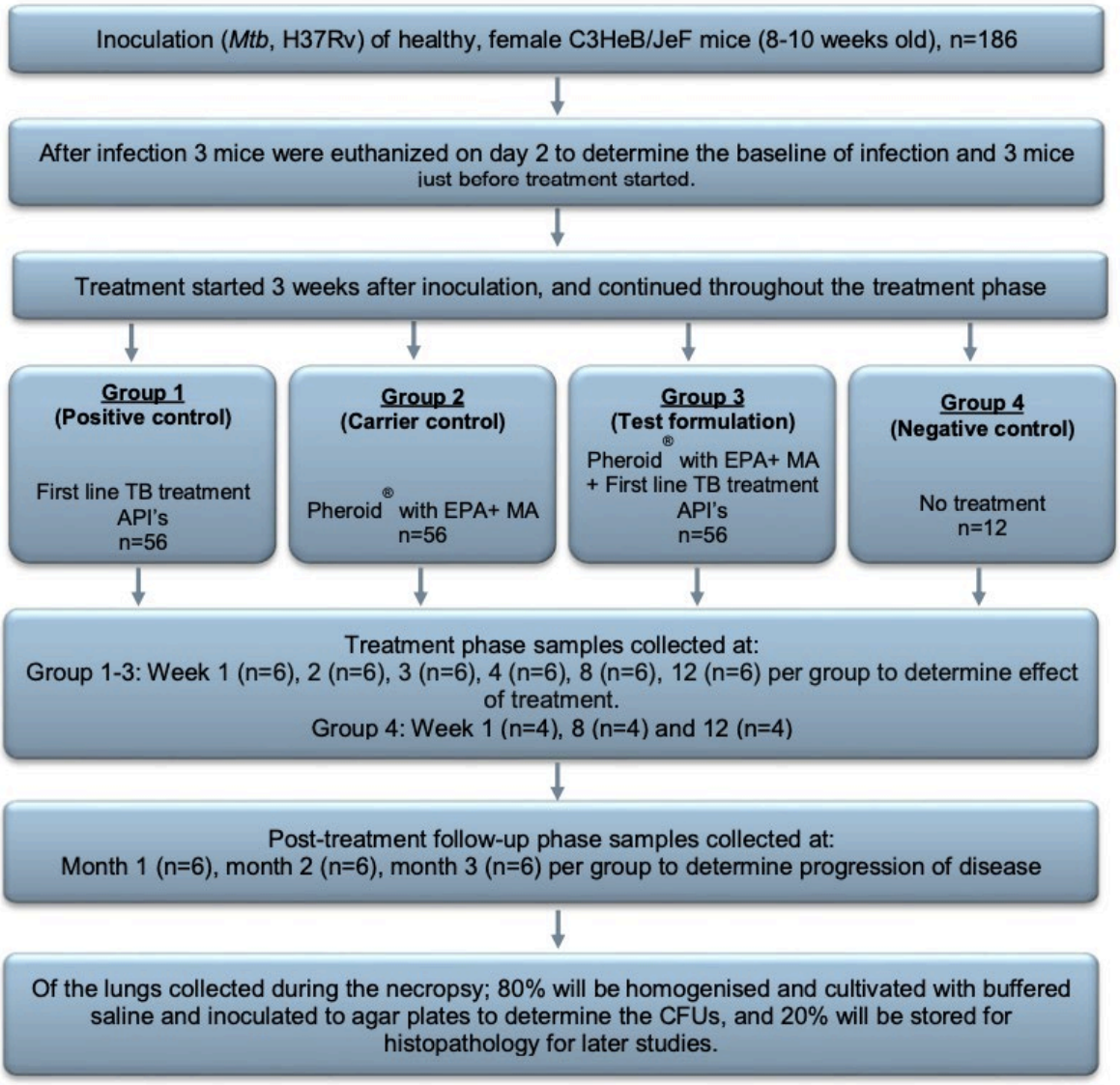


Figure 4-1 Copy of the original illustrated design of the study executed by van der Merwe (2019). Reprinted with the permission from the author.

On the basis of the original study design (Figure 4-1); a study design was compiled for the evaluation of the microbiome from samples derived from the original study (Figure 4-2). Groups 1-4 were renamed as follow:

Group 1 (positive control- Figure 4-1) was renamed to standard TB therapy;
Group 2 (carrier control- Figure 4-1) was renamed to Pheroid® carrier control;
Group 3 (test formulation- Figure 4-1) to Pheroid®-based TB therapy; and

Group 4 (negative control- Figure 4-1) to infected reference group (Figure 4-2).

The reference group comprised of caecum samples derived from infected, but not treated mice. The Pheroid® carrier control group were treated with a formulation of carrier compounds, excluding the APIs used for the conventional treatment of TB. Animals that underwent standard TB therapy were treated with standard Rifafour-e275®-based treatment; whereas animals that underwent Pheroid®-based TB therapy were treated with standard Rifafour®-e275 APIs incorporated in the carrier Pheroid®-formulation. The follow-up phase presented in the original study design (Figure 4-1) was renamed to the microbiome recovery phase, since no administration of any treatments were given during this time and the microbiome had time to normalize. Two biological replicates (*n*=2) from each timepoint were utilized for microbiome studies. DNA from selected caecum samples (see section 4.2.2 below), representing the gastro-intestinal microbiome, was isolated and the 16S ribosomal RNA (rRNA) was analyzed with amplicon sequencing. Sequence data were filtered, and bioinformatics analysis was performed to identify bacterial taxa in each sample; after which microbiome community analysis was performed (Figure 4-2).

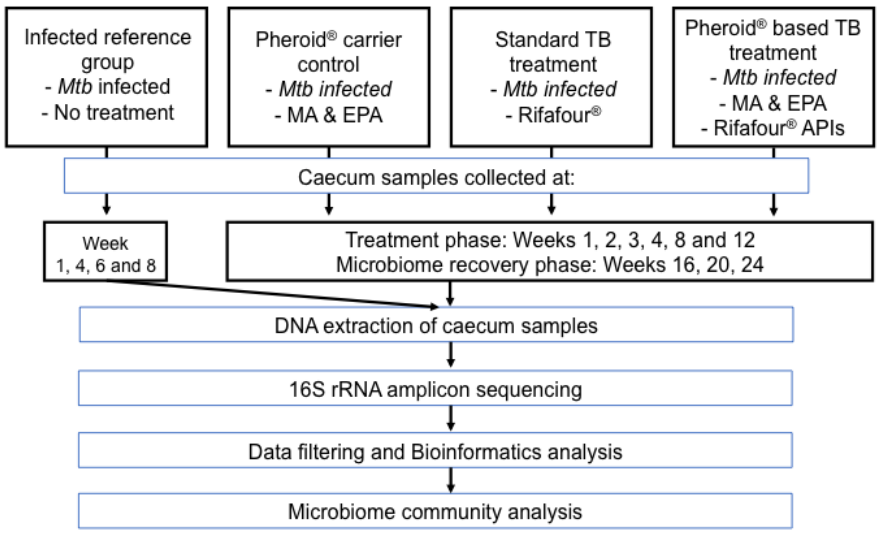


Figure 4-2 Schematic representation of the study design following the original design presented in Figure 4-1 above. Groups of mice undergoing treatment and without treatment were renamed before collection of caecum samples for microbial analysis, as well as the different timepoints for sample collections (Van der Merwe, 2019) as shown in this figure. Caecum samples were also obtained from Kramnik mice prior to the initiation of the presented study.

4.2.2 Sampling

Caecum samples were collected during the treatment phase as well as during the microbiome recovery (follow-up) phase after termination of treatment. Mice were euthanized weekly and

caecum samples were dissected, snap frozen and stored at -80 °C until further analysis. Figure 4-2 above illustrates the different treatments the mice were subjected to, and the various time periods at which samples were collected. A total of 60 caecum samples were harvested and examined to determine the shifts in the bacterial microbiome structure within the samples as a result of different regimens of TB therapy. Infected reference samples (n=6) were only collected at early stages (weeks 1, 4, 6 and 8) due to the low survival rate of the TB infected mice. Caecum samples from mice that underwent different treatments (n=54) were collected at week one, two, three, four, eight and 12; and during the microbiome recovery phase at weeks 16, 20 and 24. No samples were collected for week 24 in the Pheroid® carrier control group, due to mice becoming *moribund* at this time, and had to be euthanized per the study's protocol (van der Merwe, 2019).

4.2.3 DNA extraction

As determined in the study described in Chapter 3, microbiome DNA from the caecum as representative of the gastro-intestinal tract, can easily be extracted using commercial DNA extraction kits, provided that the kit consists of mechanical and chemical lysis steps. Therefore, caecum samples were digested with 20 µL Proteinase K (20 mg/mL) (Macherey-Nagel, Germany) and lysed in the supplied buffer from the extraction kit (ST1) at 56 °C for two hours. DNA extraction continued with further cell lysis in bead lysis tubes using the NucleoSpin® DNA Stool kit (Macherey-Nagel, Germany) according to the manufacturer's protocol. Due to supply difficulties, DNA from week one of the infected reference group (Figure 4-2) was extracted using an alternative extraction method. The alternative extraction method selected is similar to the one used for the rest of the samples and included chemical (lysis buffer) and mechanical (bead beating) lysis of cells; and binding of DNA using spin columns. Previous studies have demonstrated that the inclusion of a mechanical cell lysis step by bead beating yields sufficient amounts of DNA for microbiome profiling (Yuan *et al*., 2012; Lim *et* al., 2018; Ducarmon *et al*., 2020). The quality and quantity of the eluted DNA were determined with a NanoDrop One Spectrophotometer (Thermo Fisher Scientific, US) and stored at -20 °C for further analysis.

4.2.4 16S Sequencing

Extracted DNA samples were transported to a collaborator – PHENOMIN-ICS, Strasbourg, France - to be sequenced. A polymerase chain reaction (PCR) of isolated DNA was performed for each sample by amplifying the V3-V4 region of the 16S rRNA gene. Primer sequences used for amplification of the region were: forward primer 5'- TCGTCGGCAGCGTCAGATG TGTATAAGAGACAGCCTACGGGNGGCWGCAG -3' and reverse primer 5'- GTCTCGTGGG

CTCGGAGATGTGTATAAGAGACAGGACTACHVGGGTATCTAATCC-3', as described by Klindworth *et al*. (2013). Thereafter, amplified DNA was sequenced using the Illumina MiSeq platform at France Genomique.

4.2.5 Data filtering and bioinformatics analysis

Amplicon sequences generated by Illumina MiSeq were normalized and filtered using a Galaxy-supported pipeline, namely FROGS (Find, Rapidly, OTUs [operational taxonomic units] with Galaxy Solution) as described by Escudié *et al*. (2018). After normalization and filtration of data within FROGS, OTUs of relative abundance were generated (Escudié *et al*., 2018) and exported to the tab separated values (.tsv) format for statistical and advanced microbial community analysis.

4.2.6 Microbial community analysis

Using the FROGS bioinformatics pipeline, tables of relative abundance were generated, which were edited to the appropriate format for import into the web-based analyses server: MicrobiomeAnalyst (Chong, *et al*., 2020), where Marker Data Profiling (MDP) was performed for the data set. MicrobiomeAnalyst is a phyloseq R packaged program and was used for representation of microbial communities of the samples from the different treatment groups over time. The program was also used for community profiling and visual examination of the relative abundance bacteria present in the microbiome. No further data filtering and normalization were performed for MDP, unless specified otherwise in the result sections. Community profiling included an investigation of differences in alpha and beta diversity amongst samples from the various groups (Figure 4-2). Rarefaction curves were generated for each of the groups to examine species richness amongst samples over time. Additionally, hierarchical clustering using Bray-Curtis distancing of samples was performed in Primer 7 software (Clarke & Warwick, 1994). Prior to clustering analysis, abundance data were transformed to Log (X+1). Stacked bar graphs were generated to illustrate actual microbial abundance in various groups over time at the phylum, family and genus classification levels.

4.2.6.1 Alpha diversity

Alpha diversity using the Chao1, Observed and Shannon indices were determined for the infected reference and treatment groups. The results determined the changes in microbial composition in each group over time. Graphs illustrating alpha diversity were generated with GraphPad Prism

version 8. All graphs were generated to represent phyla, family and genus level of microbial communities. Due to the small sample size at each individual timepoint, selected treatment timepoints were combined for a statistical significance testing. In the treatment phase of the different therapies, weeks one and two were merged, as were weeks three and four, and weeks eight and 12. Weeks 16, 20 and 24 (for standard and Pheroid®-based TB therapy groups) of the microbiome recovery phase were combined. Significant differences were determined on family and genus levels.

4.2.6.2 Beta diversity

Beta diversity was measured for the infected reference and various treatment groups to determine the differences in microbial composition of the microbiome as a result of the various treatments. Differences in beta diversity between the treatment groups were determined by means of Principal Coordinate Analysis (PCoA) using Bray-Curtis distancing. Significance was regarded as $p \leq 0.05$. An R value closer to one, indicated dissimilarity between groups, whereas a value near zero indicated no significant differences between groups. Significant differences between individual groups were also performed to ascertain which treatment groups differed significantly from each other.

4.2.7 Statistical analysis

Prior to significance testing, normal distribution of data sets was tested with the D'Agostino & Pearson omnibus. Normality of alpha diversity indices was tested with the Shapiro-Wilk test. If data sets were normally distributed, statistically significant differences between samples from different treatment groups were measured with parametric one-way analysis of variance (ANOVA), using Tukey's multiple comparisons test. Contrarily, when data sets did not pass normality tests, statistical significance was tested with non-parametric Kruskal-Wallis tests, using Dunn's multiple comparisons test. Significance was regarded as $p \leq 0.05$. Normality and significance tests were conducted with GraphPad Prism version 8 (GraphPad Software Inc, USA). Significance is indicated in text and on associated figures.

Linear discriminant analysis (LEfSe) algorithm was used to determine differentially abundant phyla, families and genera between different groups (infected reference, Pheroid® carrier control, standard TB therapy, and Pheroid®-based TB therapy). For LEfSe tests, data were rarefied to minimum library size and total sum scaling was performed. Kruskal-Wallis rank sums tests were

used to determine differences. Features were regarded as significantly different with the linear discriminant analysis (LDA) effect size < 2.0 and p-value < 0.05.

4.3 Results

4.3.1 Sequencing data

Extracted DNA from caecum samples were of good quality and absorbance values at different wavelengths indicated that the quality of DNA was in the accepted range amongst all samples (Matlock, 2015). After 16S rRNA PCR of the extracted DNA; 16S sequencing; and data filtering through bioinformatics analysis, a total of 505 135 read counts were obtained from 60 extracted caecal microbiome DNA samples, averaging 8 862 counts per sample. The abundance table contained a total of 381 operational taxonomic units (OTUs) from the sequence reads. However, only 380 OTUs had reads above two counts and therefore these were the OTUs used for further microbial analysis.

4.3.2 Diversity varies in each group over time

To address the primary question, the effects of TB therapy administered by standard delivery and Pheroid® delivery on the microbiome of *Mtb* infected mice were compared. Additionally, the impact of the Pheroid® carrier control – the formulation excluding TB treatment APIs - on the gastro-intestinal microbiome was evaluated. Data from all timepoints within each group were pooled together to determine whether TB therapy had an effect on diversity. Standard and Pheroid®-based TB therapy had a significant impact on diversity in the gastro-intestinal microbiome of *Mtb* infected mice (Figure 4-3). The Pheroid® carrier control had a significant impact on the microbiome's alpha diversity of the infected mice on the family level of classification when measured with the Observed index. Differences between healthy, uninfected mice and the infected reference groups were not determined in the present study, since caecum samples from healthy mice were not collected in the previous study (Figure 4-1; van der Merwe, 2019).

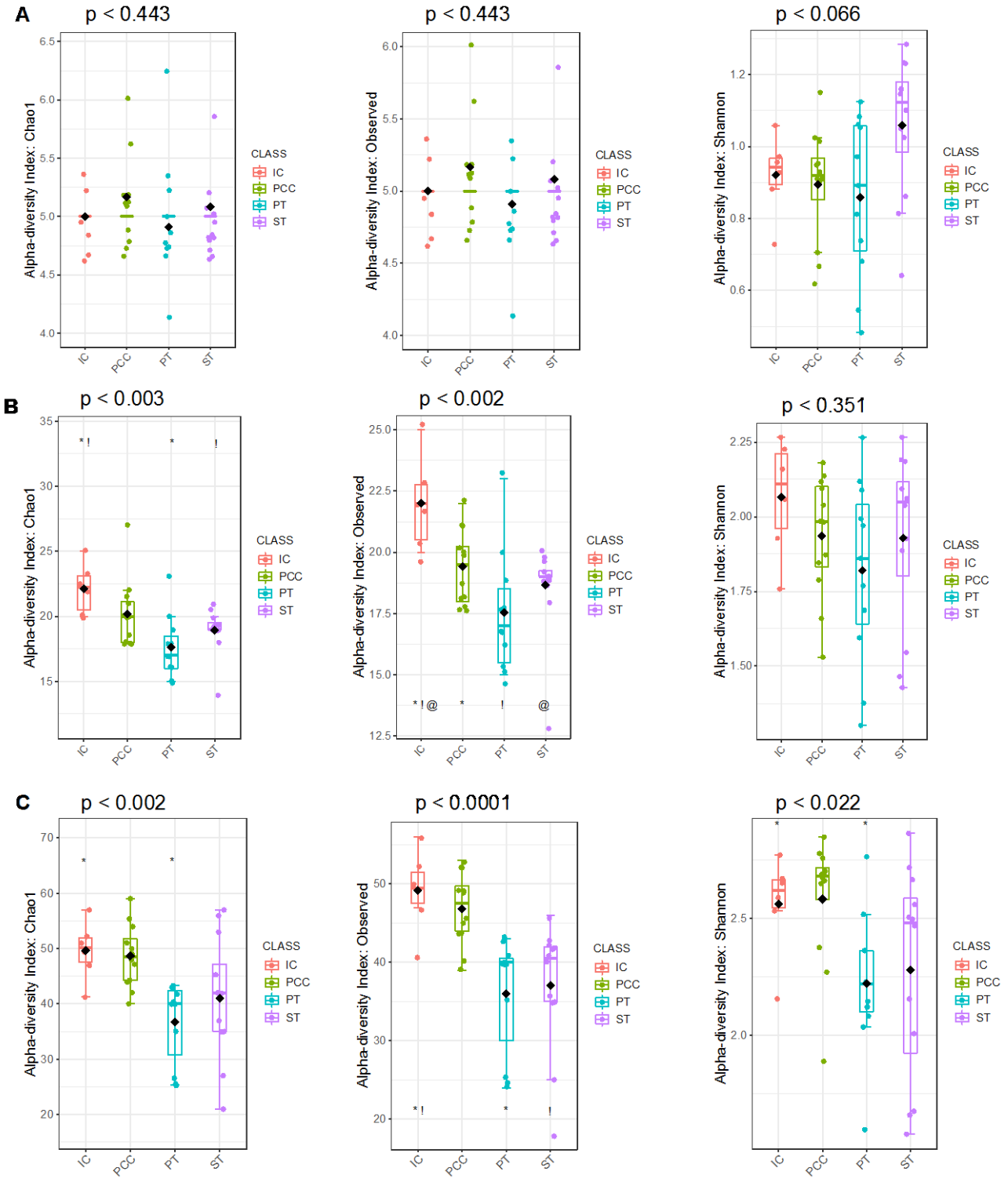


Figure 4-3 Alpha diversity box plots of caecum microbiome diversities during infection (IC) and treatments with Pheroid® carrier control (PCC), Pheroid® based TB treatment (PT) and standard TB treatment (ST) tested with Kruskal-Wallis. Alpha diversity is presented on (A) phylum, (B) family and (C) genus level of classification and were tested with Chao1, Observed and Shannon indices. Statistical significance between groups on each level is presented on the figure with various symbols (*, ! and @).

4.3.2.1 Rarefaction of samples

Since the two TB therapies had a significant effect on the microbiome, OTUs per timepoint were critically evaluated for trends in alpha diversity. Firstly, rarefaction plots demonstrated that sufficient sampling depth was achieved to capture within species richness of each sample (Figure 4-4). This is represented by the “plateau” effect of each sample, indicating that more sequences would not attribute to novel OTUs in each sample. Additionally, it can be observed with the rarefaction of samples that species richness varied amongst samples from the different groups. Changes between timepoints and between different treatment groups were further evaluated using alpha and beta diversity metrics (please refer to sections 4.3.2.2 and 4.3.3 below).

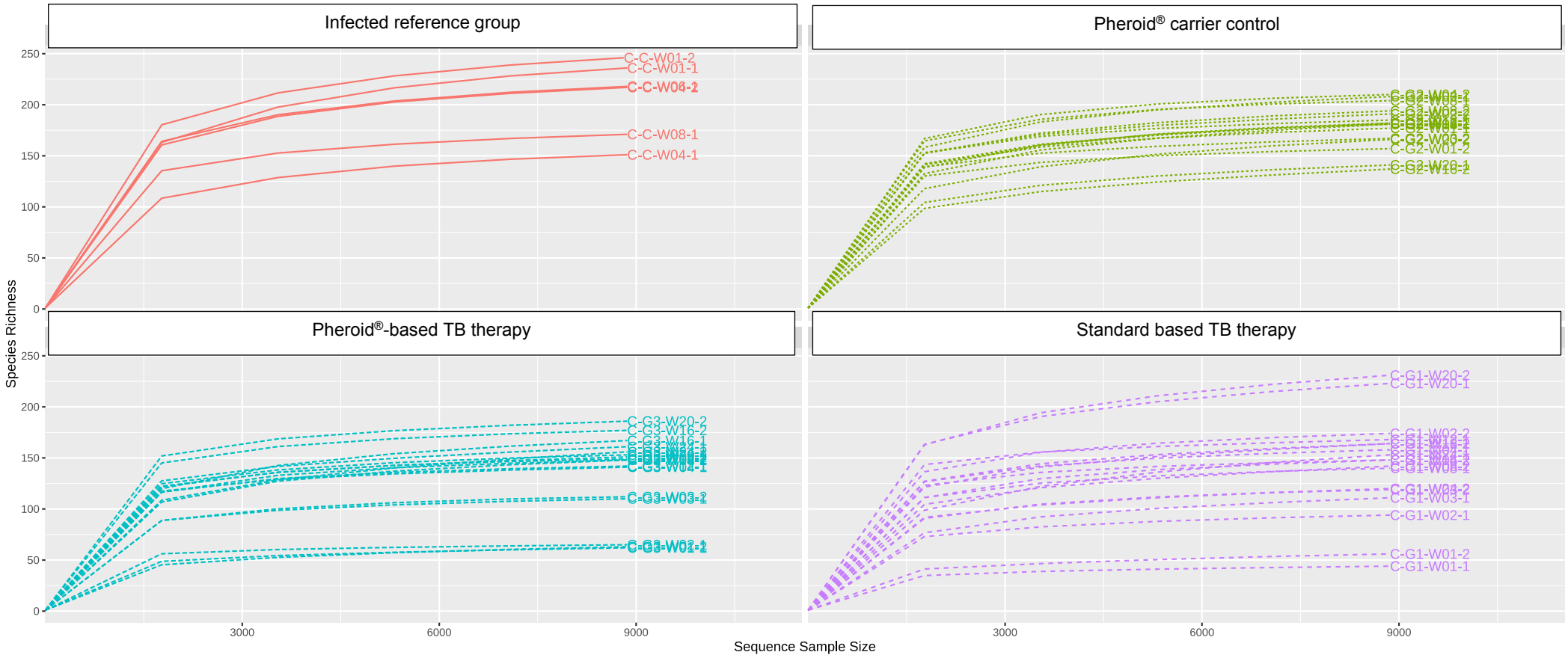


Figure 4-4 Rarefaction analysis between the sequence sample size and the number of OTUs in each sample (species richness). As the sequence sample size increased, the number of OTUs reaches saturation.

4.3.2.2 Longitudinal changes in alpha diversity

With fluctuations in OTUs observed temporally (Figure 4-4), alpha diversity measures were calculated to examine the changes in diversity in each sample from the treatment phases as well as during microbiome recovery phase. Species richness and evenness of phyla, families and genera within each group were measured over a period of time. Figure 4-5, Figure 4-6 and Figure 4-7 illustrate the measured changes in alpha diversity using Chao1, Observed and Shannon indices, respectively. No statistical analysis was performed for the infected reference group, due to small sample size. However, trends were examined for changes over time.

i. Phylum

There were no significant trends of changes observed over time in the infected reference, Pheroid® carrier control and standard TB therapy using both Chao1 and Observed species indices (Figure 4-5 A & B). However, the Pheroid® carrier control had an increase in alpha diversity during the third week, indicating that members from another phylum emerged at this point of treatment. There was a similar increase during the last week of treatment (Week 12) with a decrease again during microbiome recovery (Weeks 16, 20 & 24). A similar trend was noticed during the last week of treatment with standard TB therapy. An increase was also noticed over time between samples treated with Pheroid®-based TB therapy (Figure 4-5 A & B). There was an initial decrease in species richness at onset of treatment. Thereafter, diversity increased between weeks one and two and remained stable for four weeks. Another increase was observed during the last week of treatment (Week 12). The alpha diversity remained high throughout the microbiome recovery phases (Weeks 16, 20 & 24).

According to Figure 4-5 C, alpha diversity, measured with the Shannon index, between samples fluctuated in all groups. Samples from the infected reference group remained relatively stable throughout the timepoints. Standard TB therapy and the Pheroid® carrier control had similar occurrences where there was a decrease early on in treatment. An increase occurred between weeks three and four and a slight decrease was observed during microbiome recovery (weeks 16, 20 & 24). An intriguing trend that was observed was that between standard and Pheroid®-based TB therapies, where there was an increase in diversity later on in treatment for samples treated with the latter (Figure 4-5 C).

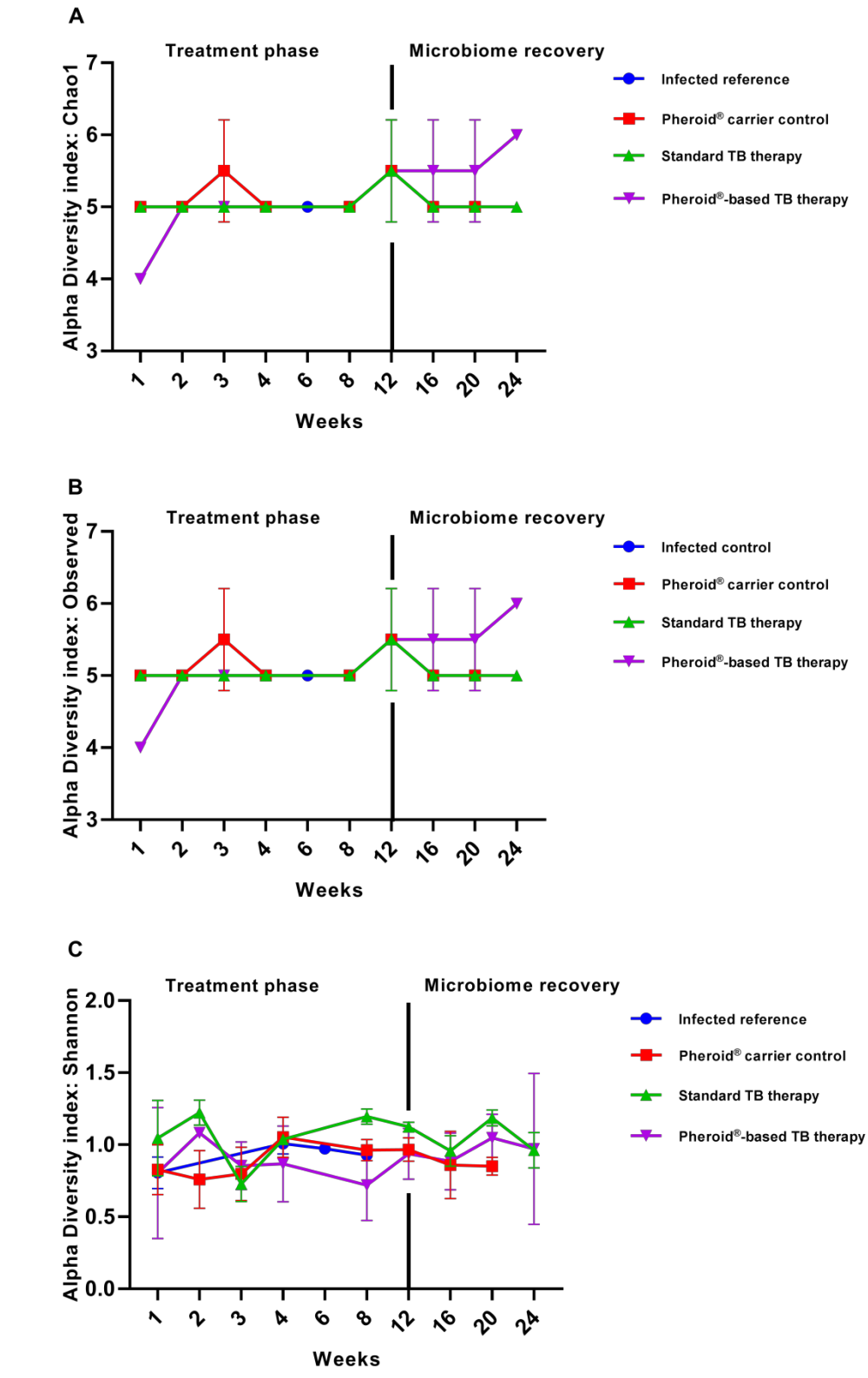


Figure 4-5 Changes in alpha diversity on phylum level using (A) Chao1, (B) Observed and (C) Shannon indices. Each group is represented by a different colour. Blue represents the infected reference group; red the Pheroid® carrier control; green the changes that occurred during standard TB treatment and purple those of the Pheroid®-based TB treatment group.

ii. Family

As opposed to the phylum level, more changes in alpha diversity were observed on the family level of classification. The results are illustrated in Figure 4-6. The infected reference group indicated little to no changes in diversity over time when measured with Chao1 and Observed species indices (Figure 4-6 A & B). However, although the diversity of the microbiome in the infected reference group did not differ significantly over the period of infection, the effect of infection on the microbiome is unknown since no healthy mice were evaluated. Nevertheless, diversity measures amongst the microbiome of the infected reference group were higher than in the treatment groups. According to the Shannon index, a slight increase in diversity was observed for the infected reference group (Figure 4-6 C). Even though an upward trend was noticed more so than on phylum level, diversity remained relatively stable from week to week on family level of classification (Figure 4-6 A & B).

A drastic decrease in diversity was the result of both TB therapies at onset of treatment. Furthermore, diversity was slightly reduced at onset of treatment with the carrier formulation. Generally, diversity increased over time in all treatment groups as the microbiome attempted to normalize after being exposed to foreign substances (Figure 4-6 A & B). According to the Chao1 and Observed indices, a significant increase of alpha diversity was observed during Pheroid®-based treatment and microbiome recovery (F_{Chao1} = 9.778, p_{Chao1}=0.001; $F_{Observed}$ = 0.7.682, $p_{Observed}$ = 0.003). According to the Shannon index, a more drastic fluctuation in diversity occurred when animals were treated with standard TB therapy than Pheroid®-based TB therapy (Figure 4-6 C). For standard TB therapy, diversity decreased during week three of treatment, and increased again at week four. Thereafter it remained relatively stable during the rest of the treatment phase. Nevertheless, diversity changes between timepoints were not significantly different ($p>0.05$).

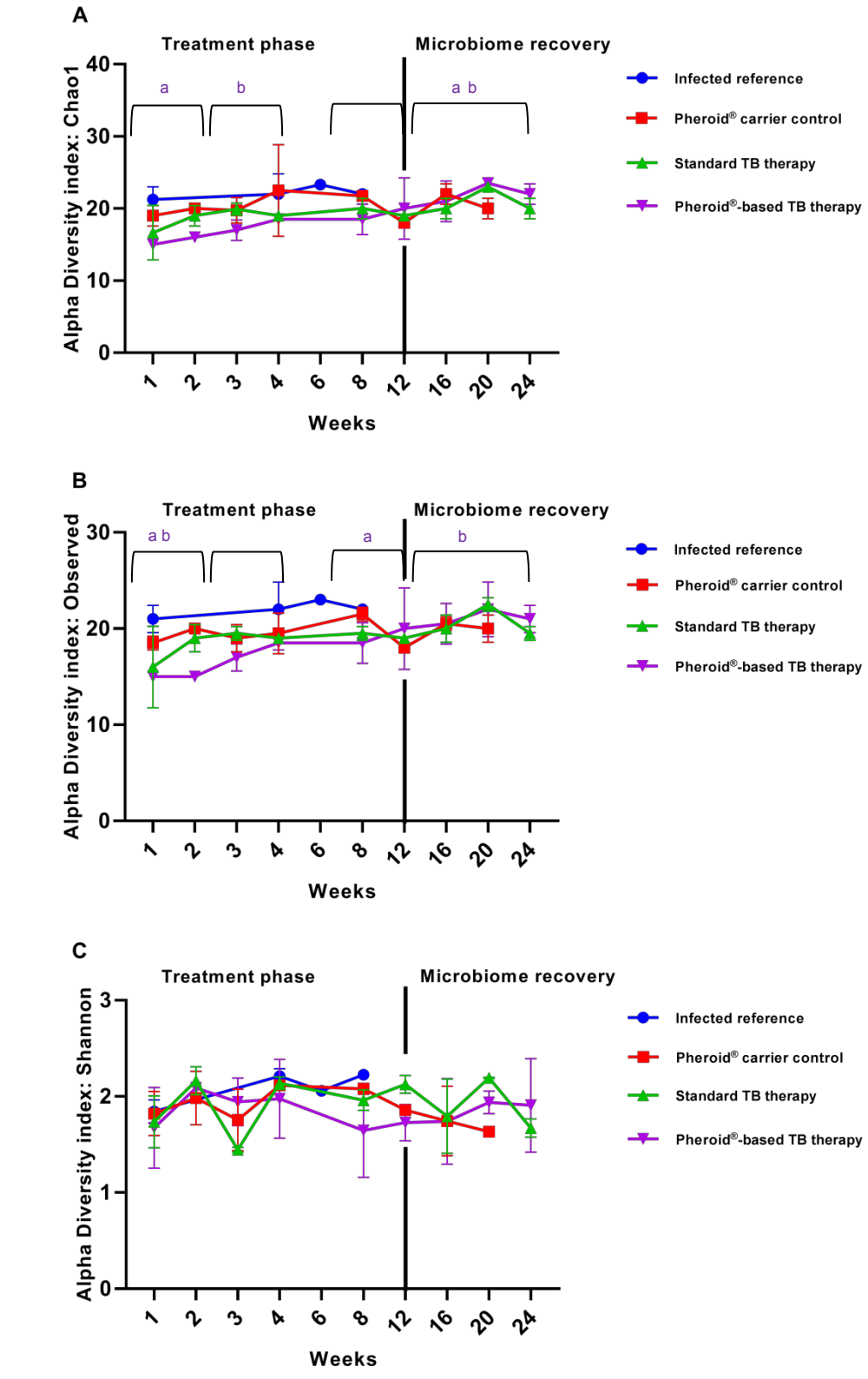


Figure 4-6 Alpha diversity changes measured using (A) Chao1, (B) Observed and (C) Shannon indices on family level of classification. Chao1 and Observed species indices measures species richness between samples, whereas the Shannon index measures distribution of diversity over time. Lowercase alphabetical letters indicate statistical significance between treatment phases and the microbiome recovery ($p \leq 0.05$).

iii. Genus

The genus level of classification indicated wider and more noticeable trends of fluctuations in alpha diversity over time. Figures representing the alpha diversity changes on genus level include linear regression lines to illustrate the general effect of treatments on the microbiome during the treatment and recovery respectively (Figure 4-7). According to Figure 4-7 A and Figure 4-7 B, the infected reference group did not indicate any significant trends of diversity changes over eight weeks in general. However, changes that might have occurred at the onset of infection is unknown. Overall, the infected reference group's alpha diversity remained high during infection. During exposure to the Pheroid® carrier control, alpha diversity remained relatively stable in general, with slight fluctuations at each timepoint (Figure 4-7). The total species richness decreased slightly compared to the infected references, though not significantly (Figure 4-3) A decrease in diversity was noticed during the microbiome recovery, though not significant ($p>0.05$). Similar trends in alpha diversity changes, according to the Chao1 and Observed index, were observed for both the infected reference group and the Pheroid® carrier control during treatment (Figure 4-7 A & B). There were no significant changes in diversity over eight weeks for both groups. However, a decrease in diversity was noted during the last week of exposure to the Pheroid® carrier control.

An initial reduction in microbial diversity was observed with both TB therapies at onset of treatment. Thereafter, both modes of TB therapies (standard and Pheroid®-based) indicated an increase in diversity over time when measured with Chao1 and Observed species indices (Figure 4-7 A & B). A more rapid increase in diversity was noticed the second week into standard TB therapy as supposed to the Pheroid®-based treatment. A slow increase in diversity was observed during the rest of the treatment phases (Figure 4-7 A & B). Standard TB therapy caused a statistically significant increase in diversity between treatment initiation (weeks 1 & 2) and the microbiome recovery, measured with Chao1 index ($p = 0.031$). As for Pheroid®- based TB therapy, diversity significantly increased from initiation up to the end of the treatment phase and further during microbiome recovery ($F_{Chao1}= 25.95$, $p_{Chao1}< 0.0001$; $F_{Observed} = 34.86$, $p_{Observed} < 0.0001$; Kruskal-Wallis $statistic_{Observed} = 11.55$, $p_{Observed}= 0.009$) (Figure 4-7 A & B). Trend lines indicate rebound of microbial diversity during both standard and Pheroid®-based TB therapies using the Chao1 and Observed indices (Figure 4-7 A & B). However, when measured with the Chao1 index, there was a significant increase in diversity during microbiome recovery for animals treated with Pheroid®-based therapy; as opposed to a relatively stationary phase during recovery from standard therapy (Figure 4-7 A). Interestingly, the Pheroid® carrier control and the Pheroid®-based TB therapy had a similar effect on diversity when measured with the Shannon index, generally decreasing the alpha

diversity during the course of treatment with the respective formulations (Figure 4-7 C). According to the Shannon index (Figure 4-7 C), the alpha diversity decreased once again during the microbiome recovery in samples treated with standard TB therapy. The reduction is probably due to disease progression, since the animals were not fully cured of TB, as shown by the presence of colony forming units (CFUs) in the lungs of the mice for all groups (van der Merwe, 2019; Annexure D). A decrease in microbiome diversity because of disease progression in animals is directly correlated with the human gastro-intestinal microbiome response to disease (see section 2.5.1 in Chapter 2). Furthermore, this may suggest that infection does in fact have an impact on the microbiome structure.

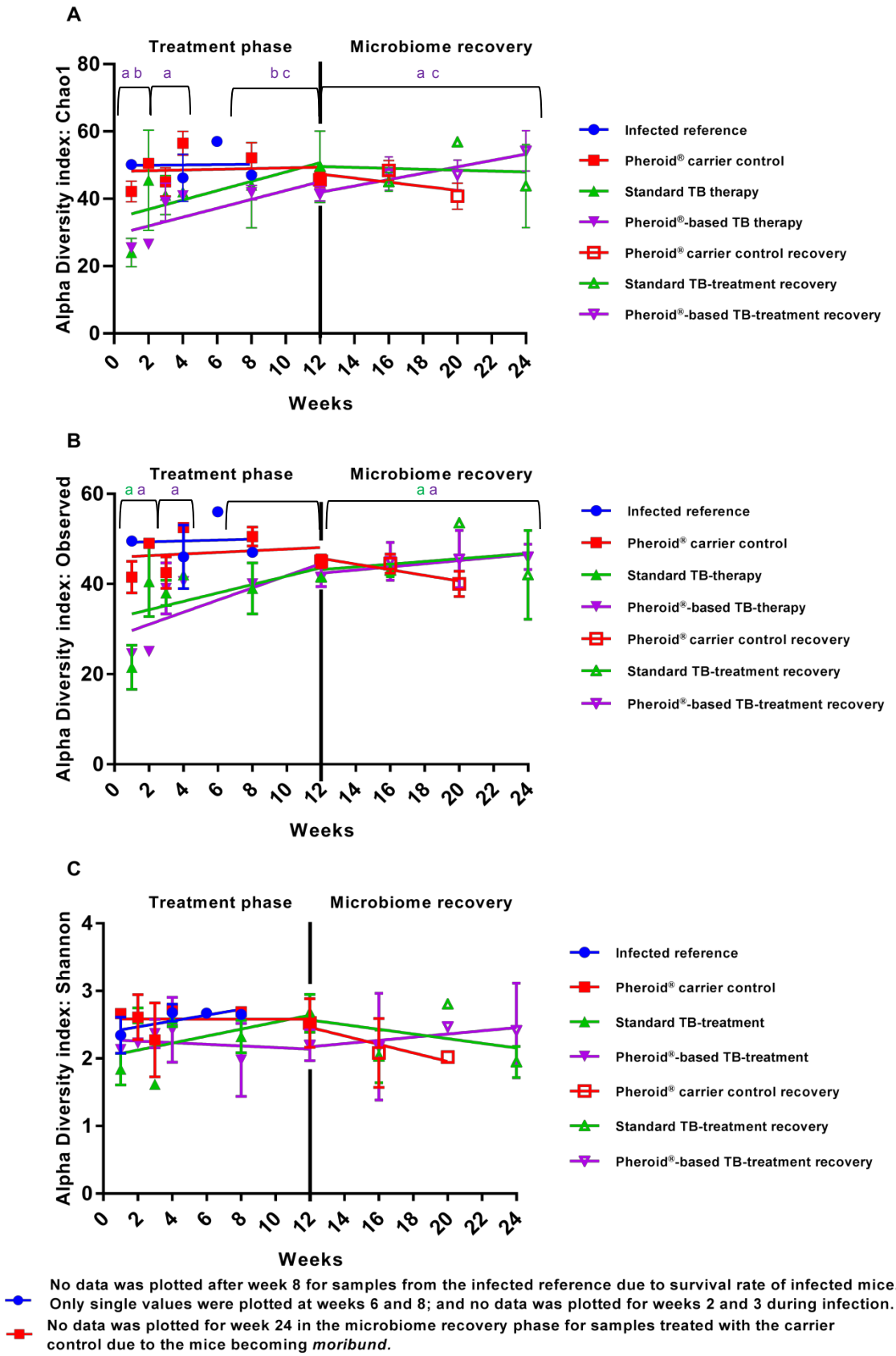


Figure 4-7 Levels of diversity of genera in samples measured over time using (A) Chao1 and (B) Observed indices along with measurements of diversity and evenness using the (C) Shannon index. Lowercase alphabetical letters indicate statistical significance between treatment phases and microbiome recovery ($p \leq 0.05$). Linear regression lines during treatment and microbiome recovery are represented respectively

4.3.3 Overall community structure between groups

Next, the overall composition and community structure of bacteria between groups were determined. It can be demonstrated that the hierarchical clustering of samples from the infected reference animals were similar in structure and composition by their clustering (Figure 4-8). Furthermore, decreased diversity during the first weeks of treatment with both TB therapies (standard and Pheroid®-based), were confirmed with clustering of samples from both these treatment groups during the first few weeks of infection. In addition, when taking overall similarity into account, all samples shared 50 % or more similarity with each other (Figure 4-8). The infected reference group along with the Pheroid® carrier control were more similar to one another compared to the treatment groups.

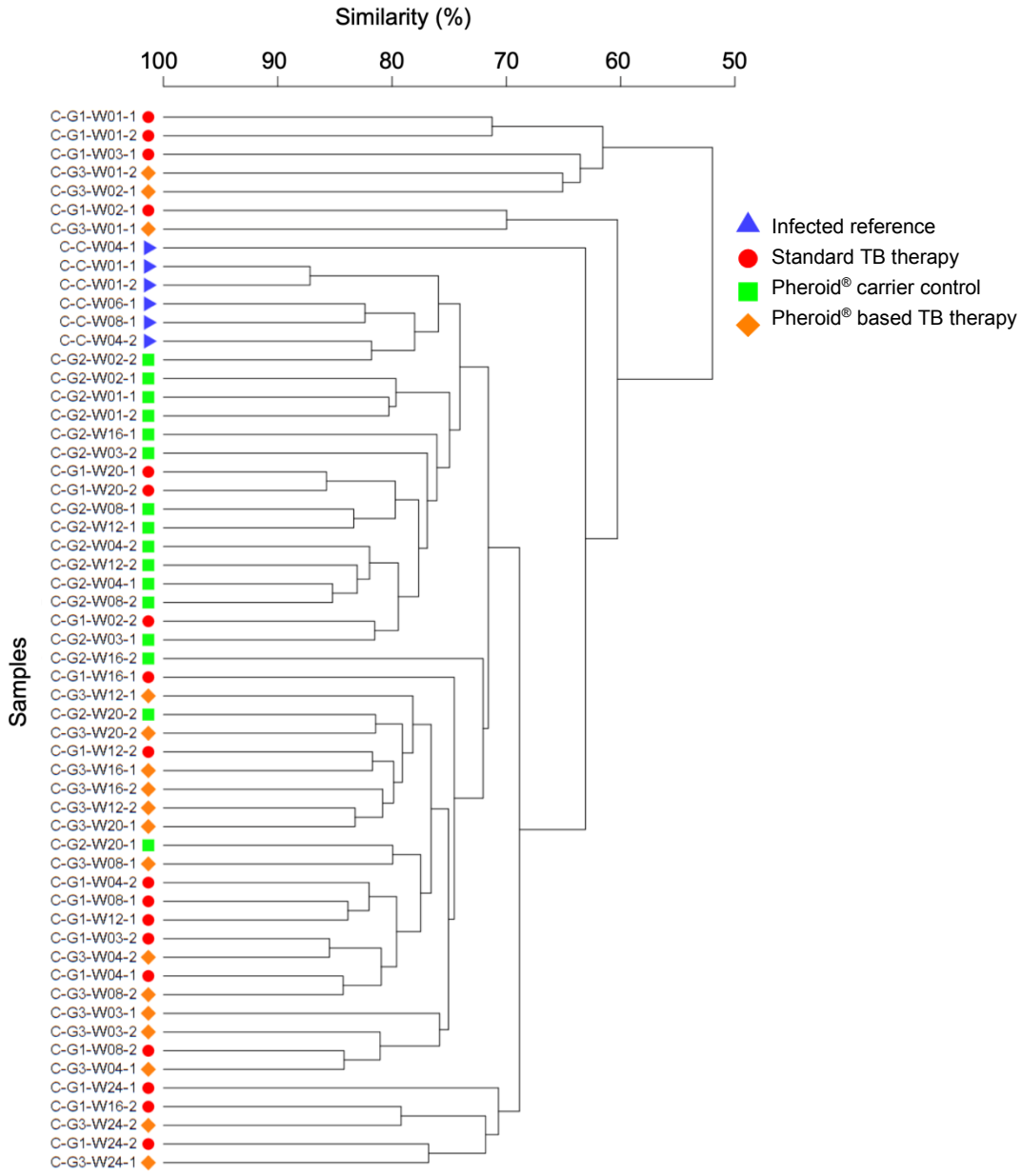


Figure 4-8 Hierarchical clustering of samples based on genera abundancies using Bray-Curtis distancing. The blue triangles represent the infected reference group; red circles represent standard TB therapy samples; green squares represent the Pheroid® carrier control samples; and orange squares represents samples derived from mice treated with Pheroid®-based TB therapy.

Principal coordinate analysis (PCoA) confirmed significant clustering of samples from various groups with beta diversity analyses. According to Figure 4-9, Figure 4-11 and Figure 4-13, there was significant clustering of samples from respective groups (infected reference group and various treatment groups). Statistically, there was an overall significant difference between the groups on phylum level of classification (R=0.132, p=0.002) (Figure 4-9). When comparing groups individually, significant differences were observed between the infected reference and standard TB therapy (standard treatment) (R=0.371, p=0.003), the Pheroid® carrier control (carrier control) (R=0.462, p=0.001) and Pheroid®-based TB therapy groups (Pheroid®-based treatment) (R=0.543, p=0.001) respectively (Figure 4-10).

As illustrated in

Figure 4-10, samples from the infected reference were clustered closer together, indicating that the samples are similar to one another. With regards to *Mtb* infection of the samples, this indicates that the mice had similar responses to the infection. Small differences in diversity can be expected, since the gastro-intestinal microbiome differs inter-individually (see section 0 in Chapter 3). Moreover, beta-diversity between samples treated with the Pheroid® carrier control had a similar clustering of samples closer together. This indicates that the changes in microbial diversity induced by treatment with the carrier control, did not change the composition over time as much as the two TB therapies; but rather had a similar response to the exposure at any given timepoint.

Similar to the results observed on phylum level, there was an overall statistical difference in diversity between the various groups on family level (R=0.138, p=0.001) (Figure 10). As on phylum level, differences exist between the infected reference group and standard TB therapy (R=0.386, p=0.004,), Pheroid® carrier control (R=0.286, p=0.012) and Pheroid®-based TB therapy (G3) (R=0.538, p=0.001), respectively (Figure 4-11).

Clustering of the infected reference and Pheroid® carrier control on family level (Figure 4-12) were similar to clustering observed on phylum level of classification (

Figure 4-10). This indicates that family members present in the microbiome proliferated or decreased similarly between individual mice in response to infection and treatment, as previously described. Family members in the carrier control did however not cluster as close together as on phylum level, whereas the infected reference clustered closer together at this level of classification (Figure 4-12 A-C). This indicates that the taxa within a specific phyla of the microbiome had a different response to the carrier control over time (Figure 4-12 B, D & F). Interestingly, effects of the Pheroid® carriers and the incorporation of APIs in the

formulation on the microbiome, resulted in similar clustering, compared to standard TB therapy (Figure 4-12 D & F).

Figure 4-13 illustrates differences in beta diversity between groups on genus level. As with the higher classification levels presented, a significant difference in beta diversity between groups was measured (R=0.162, p=0.001). Similar to phylum and family levels, differences occurred only between the infected reference group and the treatment groups (R=0.443, p=0.002; R=0.364, p=0.006; R=0.612, p=0.001) (Figure 4-14).

In Figure 4-14, the infected reference clustered together closely, indicating once again that the mice's response towards infection was similar when not treated for the infection. As at phylum and family level, this occurrence can also be observed at genus level of classification. However, the carrier control and the different TB treatment groups did indicate less similarity at genus level.

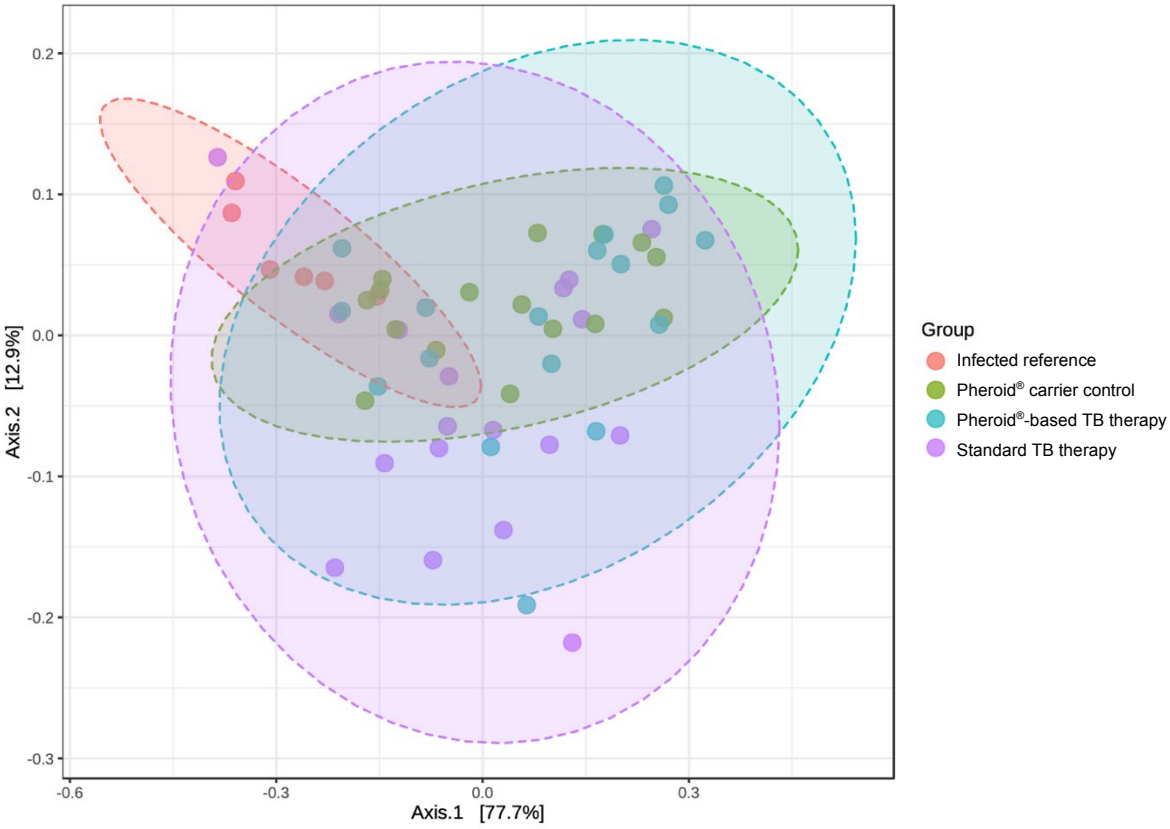


Figure 4-9 PCoA of beta diversity measures between all groups to indicate differences between the infected reference group and various treatment groups. Groups had significant differences in similarity tested with ANOSIM on phylum level (p = 0.002).

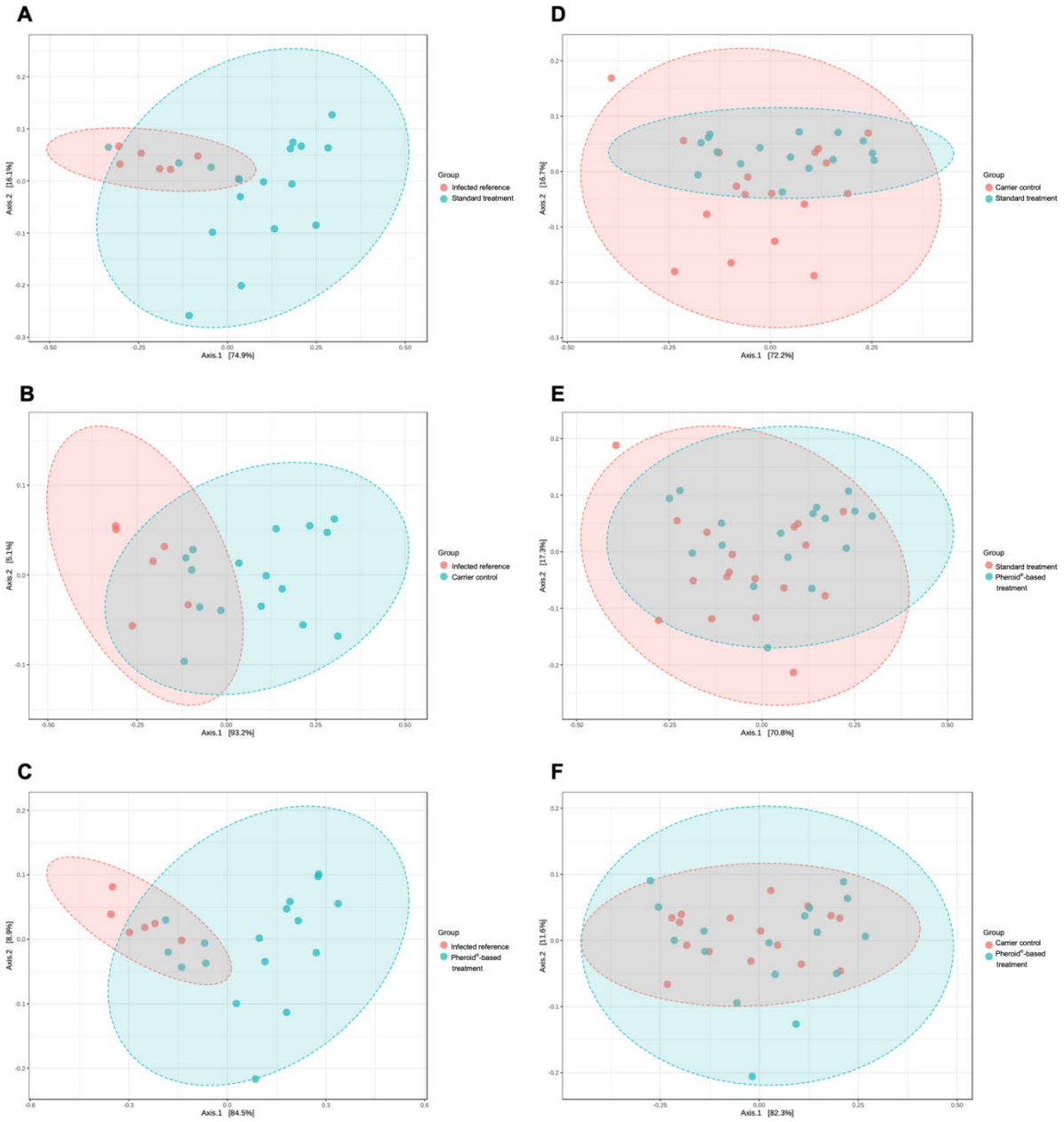


Figure 4-10 PCoA based on the Bray-Curtis Index for samples from the infected reference and various treatment groups (Standard and Pheroid®- based TB therapies and the Pheroid® carrier control) plotted individually on phylum level of classification. Data points clustering closer together indicate similarity. The infected reference group showed significant differences between (A) standard TB treatment (p=0.003); (B) the Pheroid® carrier control (p=0.001); and (C) Pheroid® based TB treatment (p=0.001). (D-F) The different treatment groups had no significant differences between each other.

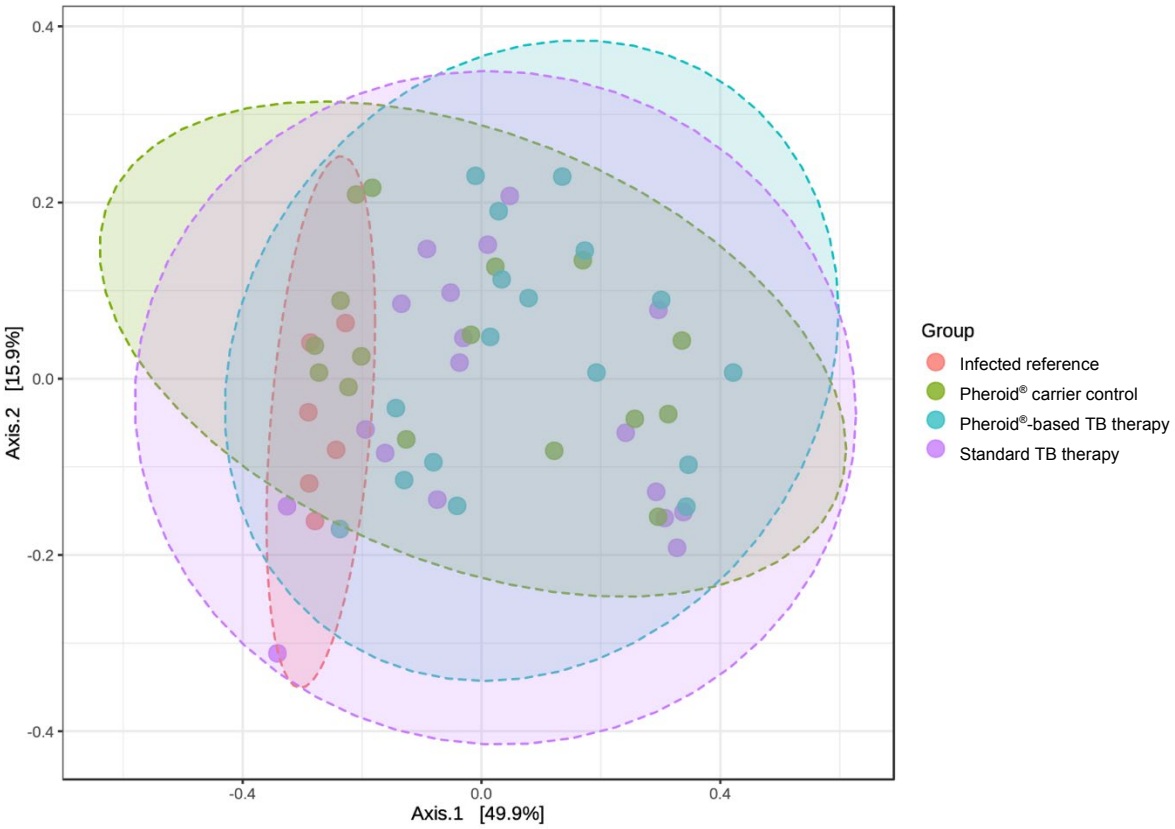


Figure 4-11 Differences in beta diversity measured with PCoA between all groups of interest. On family level of classification, there were significant differences overall (p = 0.001).

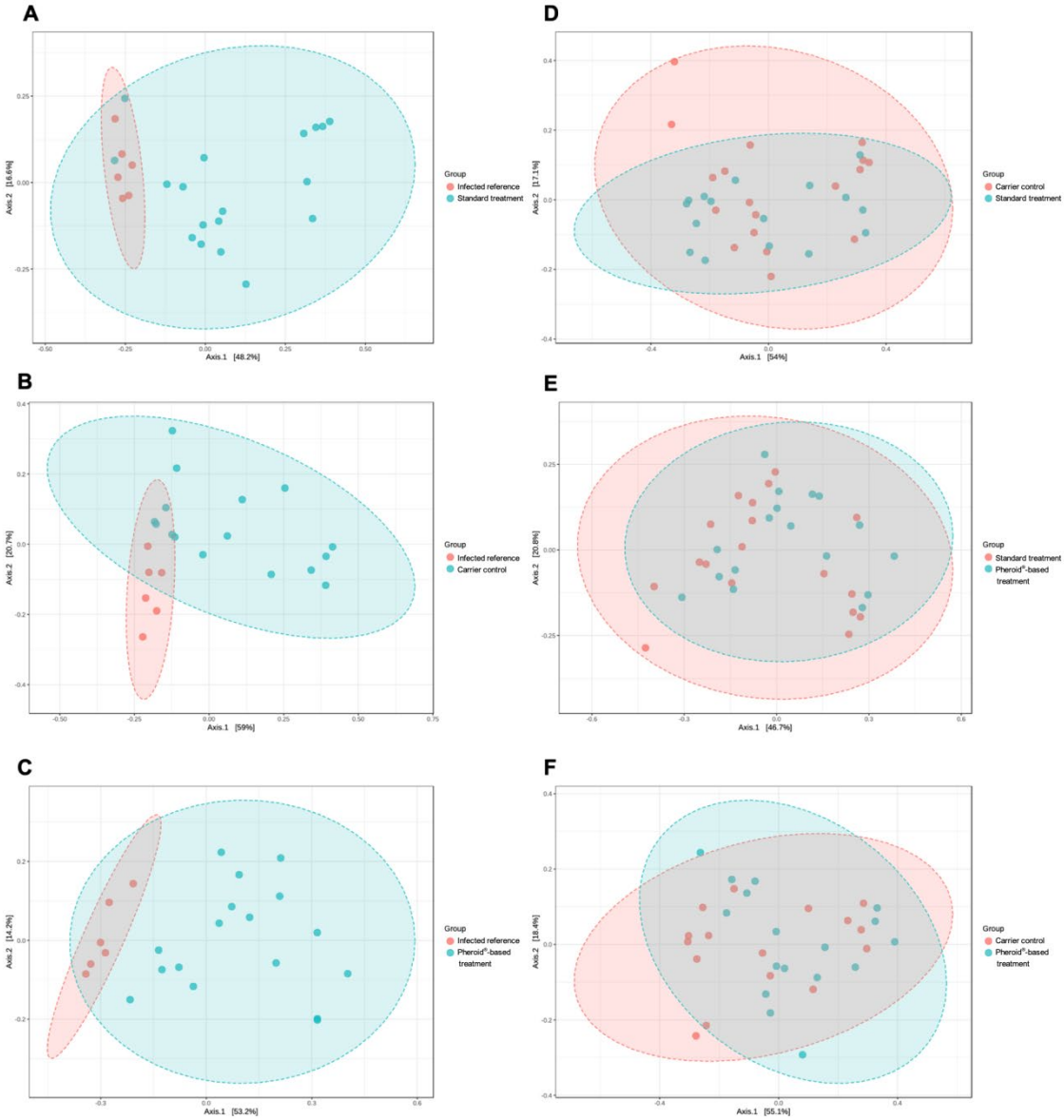


Figure 4-12 PCoA based on the Bray-Curtis Index for samples from the infected reference group and various treatment groups plotted individually on family level of classification. Data points clustered closer together indicates similarity. The infected reference showed significant differences between (A) standard TB treatment (p=0.003); (B) the Pheroid® carrier control (p=0.001); and (C) Pheroid® based TB treatment (p=0.001). (D-F) Groups had no significant differences between each other.

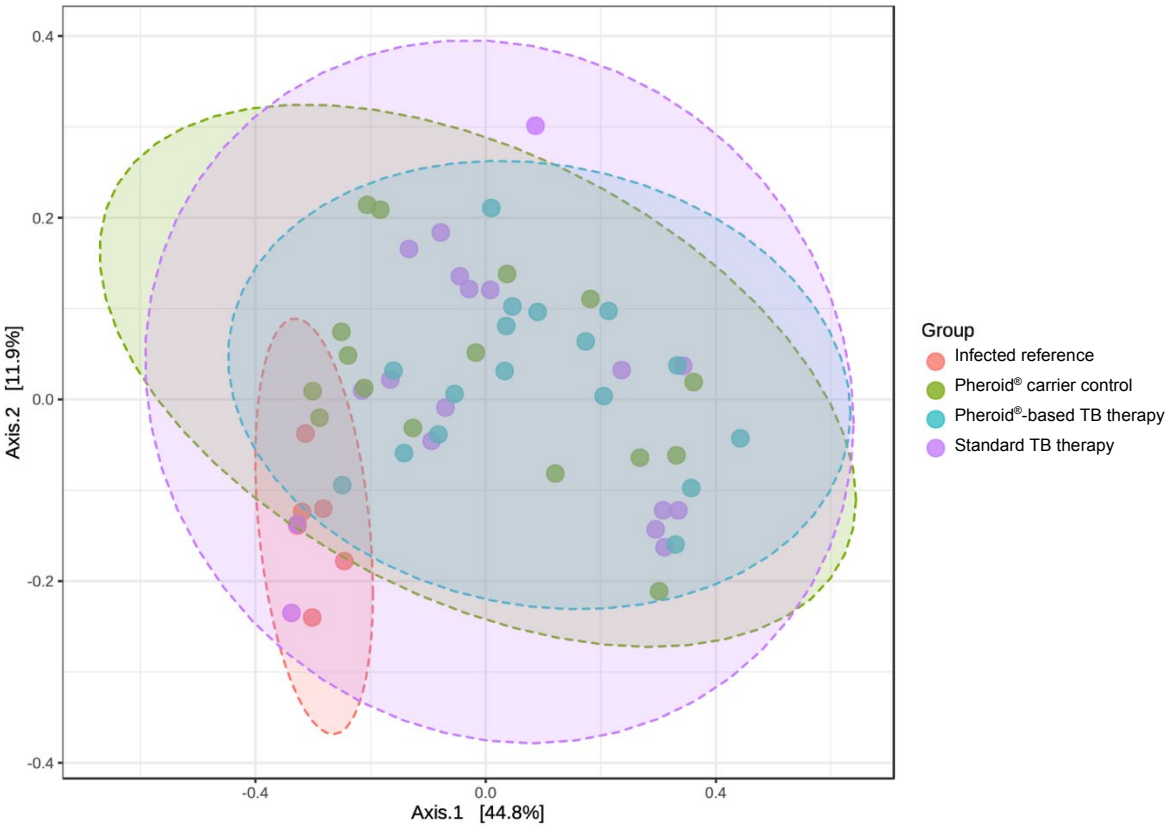


Figure 4-13 PCoA based on the Bray-Curtis Index for samples from the infected references and various treatment groups on genus level of classification. There was a significant difference between groups (p = 0.001).

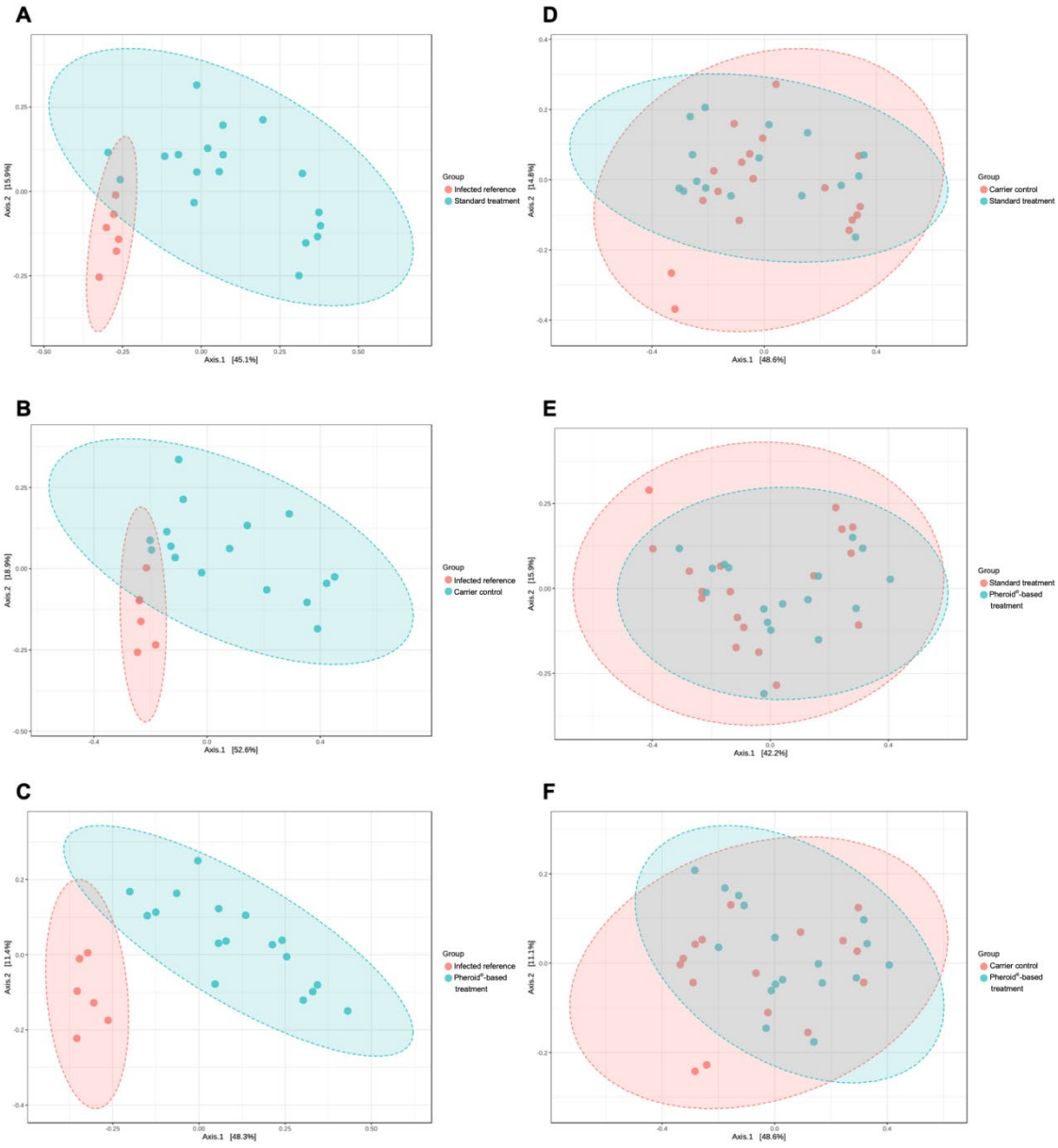


Figure 4-14 PCoA based on the Bray-Curtis Index for samples from the infected references and various groups treated with various therapies/compounds on genus level. Data points clustered closer together indicates similarity. The infected reference had significant differences between (A) standard TB treatment (p=0.003); (B) the Pheroid® carrier control (p=0.001); and (C) Pheroid® based TB-treatment (p=0.001). (D-F) There were no significant differences between various treatment groups.

It was previously determined in section 4.3.3 that there is a difference between the infected reference and various treatments when comparing the overall community structure of the respective groups. However, differences between each group at the various timepoint were not analysed when comparing the overall community structure. Beta diversity analysis between experimental groups at each timepoint were evaluated on genus level of classification (Figure 4-15). The beta diversity changes between the infected reference group and respective treatment groups were compared during weeks one, four and eight. There were no statistically significant differences between experimental groups at week one (Figure 4-15 A; p=0,06) and eight (Figure 4-15 C; p=0.06) of infection. At week four, a statistically significant difference between groups occurred (Figure 4-15 B; $p<0.05$). However, no statistical significance was observed when replicate samples at each timepoint were compared individually ($p>0.05$). Trends in Figure 4-15 does however indicate differences in alpha diversity between the treatment groups and the infected reference group. At week one of infection, beta diversity between the infected reference and the Pheroid® carrier control was more similar than later on in treatment. The small sample size per timepoint (n=2) limits conclusions to be made from the observations (please refer to section 5.2). A larger sample size per timepoint should therefore be considered in future studies.

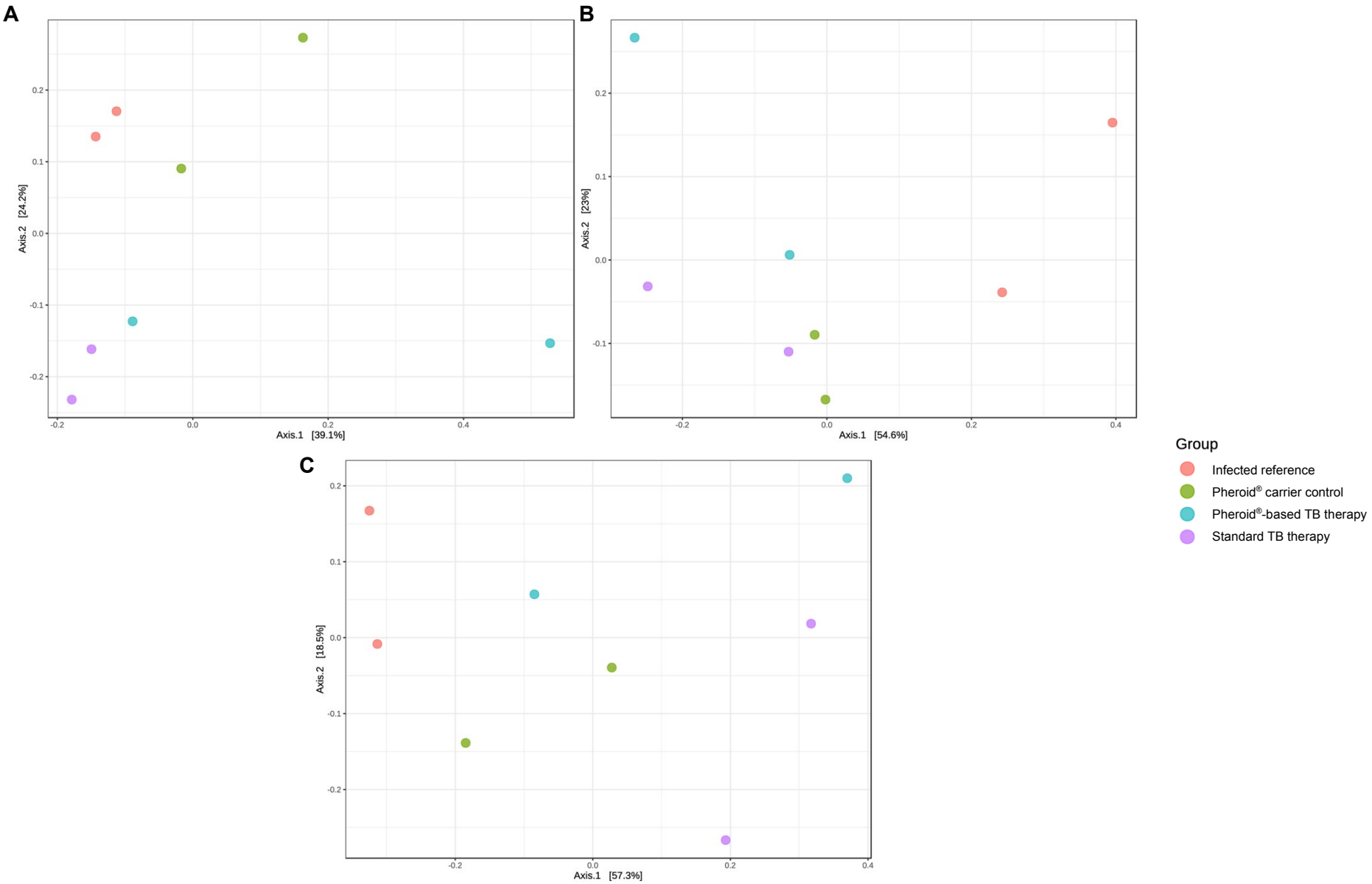


Figure 4-15 PCoA of beta diversity measures between experimental groups at (A) week one, (B) week two and (C) week eight of infection. Analysis at the specific timepoints were analysed to accommodate for differences between various treatments and the infected reference group. A statistically significant difference between groups were observed at week four (B) ($p<0.05$) of infection as tested with ANOSIM.

4.3.4 Relative abundance of bacteria in the caecum microbiome

Relative abundance of microbes present were analysed within each group over time to determine which of the members decreased or increased during the course of TB therapies with standard and Pheroid®-based deliveries. Microbial abundancies were determined according to OTUs assigned to specific sequences and are illustrated in Figure 4-16, Figure 4-17 and Figure 4-19.

4.3.4.1 Phylum

A total of six phyla were identified between all groups. These phyla included Firmicutes and Bacteroidota in the highest abundance, followed by Desulphobacterota and Actinobacteriota. Furthermore, Proteobacteria were present in all samples. A sixth phylum, namely the commensals Patescibacteria were present in the microbiome recovery phase of mice treated with Pheroid®-based TB therapy. Figure 4-16 illustrates the relative abundance of phyla present in all samples. It was observed that samples from the infected reference group all had a higher abundance of Bacteriodota than Firmicutes. In contrast, all groups that were exposed to either therapy or Pheroid® compounds (standard and Pheroid®-based TB therapies and the Pheroid® carrier control) had a higher abundance Firmicutes throughout the exposure period and during microbiome recovery.

The infected reference group, compared to the Pheroid® carrier controls, had a contrasting Firmicutes: Bacteroidota ratio, which remained relatively stable throughout infection, but fluctuated during exposure to the carrier control. A single sample at week four of infection from the infected reference group varied amongst the remaining samples within the group. It is possible that the sample did undergo contamination during collection or handling of the individual mouse. There were however no sufficient time or environment for such a contaminant to grow to detectable levels after collection. Interestingly, members of the phyla Proteobacteria emerged in this sample (Figure 4-16). In both the infected reference and Pheroid® carrier control, Desulfobacterota and Proteobacteria were present amongst all samples over time. However, Proteobacteria abundance remained relatively low throughout the exposure period with the carrier control. Actinobacteriota however increased over time of treatment and were noticeably high in abundance two months post treatment. Regardless of the trend observed in Figure 4-16, significant features were present among the untreated infected reference and the carrier control groups. During treatment with the carrier control (Weeks 1, 2, 3, 4, 8 & 12), the phylum Firmicutes was a significant feature ($p=0.001$). In contrast, Bacteroidota was significant to the untreated reference group throughout infection

(p=0.002). Furthermore, assuming the infected reference's abundancies remained stable for weeks following infection, similar trends were observed between the infected reference and carrier control groups during the microbiome recovery. A significantly high abundance of Firmicutes (p=0.011) remained present during recovery of the microbiome treated with the Pheroid®-based carrier control (Weeks 16 & 20).

Similar to exposure with the Pheroid® carrier control, treatment with both standard and Pheroid®-based TB therapies decreased the Bacteroidota: Firmicutes ratio, favouring the growth of members in the Firmicutes phylum. A significant feature of standard TB therapy on phylum level was the high abundance of Desulfobacteria, compared to Pheroid®-based treatment (p=0.036). During the microbiome recovery phases of the treatments, a significantly higher abundance of Patescibacteria were present in the caecum microbiome of mice treated with Pheroid®-based treatment (p=0.022). Higher abundance of Actinobacteriota was observed later in treatment with standard TB therapy. This high abundance of the phylum remained in the microbiome recovery phases. Furthermore, there was a decrease in abundance of members of Proteobacteria over time. Desulfobacterota had fluctuations in abundance throughout the standard treatment phase, however there was a noticeable decrease in the phylum during week three of treatment. An observable increase in Actinobacteriota at the end of the treatment phase (week 12) with Pheroid®-based therapy was noted, as opposed to earlier on with standard treatment. Lower abundance of Bacteroidota and higher abundance of Actinobacteriota were noticed in the microbiome recovery phases of the Pheroid®-based TB therapy compared to the standard treatment. Furthermore, as mentioned previously, abundance of Patescibacteria arose during microbiome recovery in samples of mice treated with Pheroid®-based TB therapy.

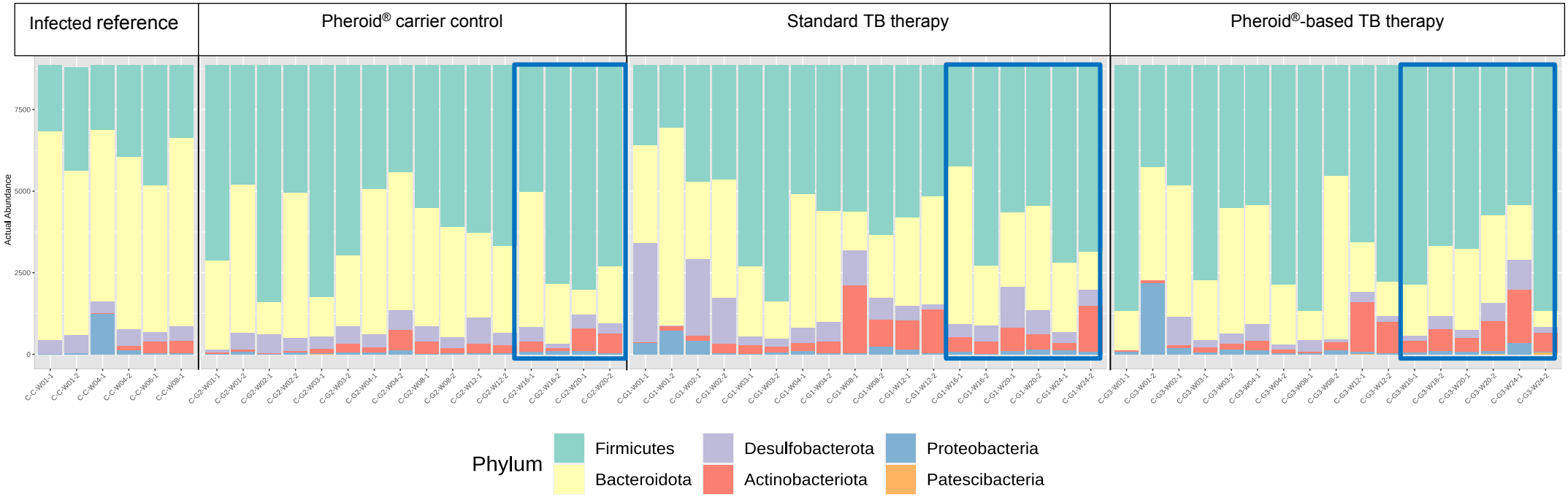


Figure 4-16 Microorganisms present in the caecum microbiome of each group (infected reference, Pheroid® carrier control, standard TB therapy and Pheroid®-based TB therapy) over time. Actual abundancies are presented on phylum level for each sample. The microbiome recovery phases of each treatment group are presented in blue boxes. No data is shown for week 24 (recovery phase) of the carrier control group due to mice becoming *moribund* during treatments.

4.3.4.2 Family

A more in depth look at the abundancies of the caecum microbiome were examined on family level of classification. A total of 30 families have been identified amongst the infected reference and various treatment groups (Figure 4-17). A significant trend of change was observed between the infected reference group and the Pheroid® carrier control group (Figure 4-17). In contrast, no striking difference in abundance was observed between standard and Pheroid®-based TB therapies over time.

A significantly higher abundance of members from Lactobacillaceae were present in the Pheroid® carrier control compared to infected mice (p=0.019) (Figure 4-18 A). However, abundance within the group varied over time. Higher abundance of Lactobacillaceae were present during early stages of treatment (Week 2 & 3) and during microbiome recovery (Weeks 16 & 20). As for the infected reference group, Lactobacillaceae abundance remained low throughout infection of untreated mice. Furthermore, Oscillospiraceae (p=0.049); Streptococcaceae (p=0.029); and Monoglobaceae (p=0.011) were significantly higher in abundance in samples derived from mice treated with the Pheroid® carrier control (Figure 4-18 A). Similar features were present during the microbiome recovery phases of samples from mice treated with the carrier control compared to the untreated mice. However, instead of the significant feature Oscillospiraceae during treatment, Sutterellaceae (p=0.019) were significantly abundant in samples recovering from treatment with the carrier control (Figure 4-18 B). As previously described (see section 4.3.2.1), a decrease in diversity was found in a single sample from the infected reference animals. These low diversities proliferated the growth of some underlying members belonging to the Enterobacteriaceae (phylum: Proteobacteria); Erysipelatoclostridiaceae (phylum: Firmicutes); Tannerellaceae (phylum: Bacteriodota); and members of the Eubacterium coprostanoligenes group (phylum: Firmicutes). Furthermore, a complete depletion of Anaerovoracaceae (phylum: Firmicutes); and decrease in Lachnospiraceae (phylum: Firmicutes) was observed in this sample compared to the remaining samples within the group (Figure 4-17). Decreased diversity may contribute to the emergence of potential pathogens, hence the increase of Enterobacteriaceae.

Similar to the changes in alpha diversity, Figure 4-17 also indicates that there is a diversity decrease in samples treated with Pheroid® carrier control, compared to untreated infected mice. During infection of the untreated mice, abundancies of Families Peptococcaecea ($p<0.001$); Christensenellaceae ($p<0.001$); Eubacterium coprostanoligenes group (p=0.036); Rikenellaceae (p=0.001); Prevotellacaea (p=0.001); and unknown families (p=0.007) were

significant features of the microbiomes (Figure 4-18 A). Unknown families' highest form of classification was from the order Clostridia. As for significantly abundant families during the recovery phase, the significant features remained similar to those of the treatment phase (Figure 4-18 B). Differences were that Ruminococcaceae ($p=0.033$) and Tannerellaceae ($p=0.019$) were significantly higher in samples derived from the untreated, infected reference group (Figure 4-18 B).

From the 30 families identified, only a few significant features are constant in samples derived from mice treated with standard TB therapy compared to Pheroid®-based TB therapy. The presence of Oscillospiracea and Desulfovivrionaceae were significant features during the treatment phase of standard TB therapy, where lower abundancies of members belonging to these families were present during Pheroid®-based treatment ($p=0.043$ & $p=0.036$, respectively). During microbiome recovery of the treatments, a significant feature for samples derived from mice treated with Pheroid®-based treatment, were members belonging to the family Saccharimonadaceae ($p=0.022$).

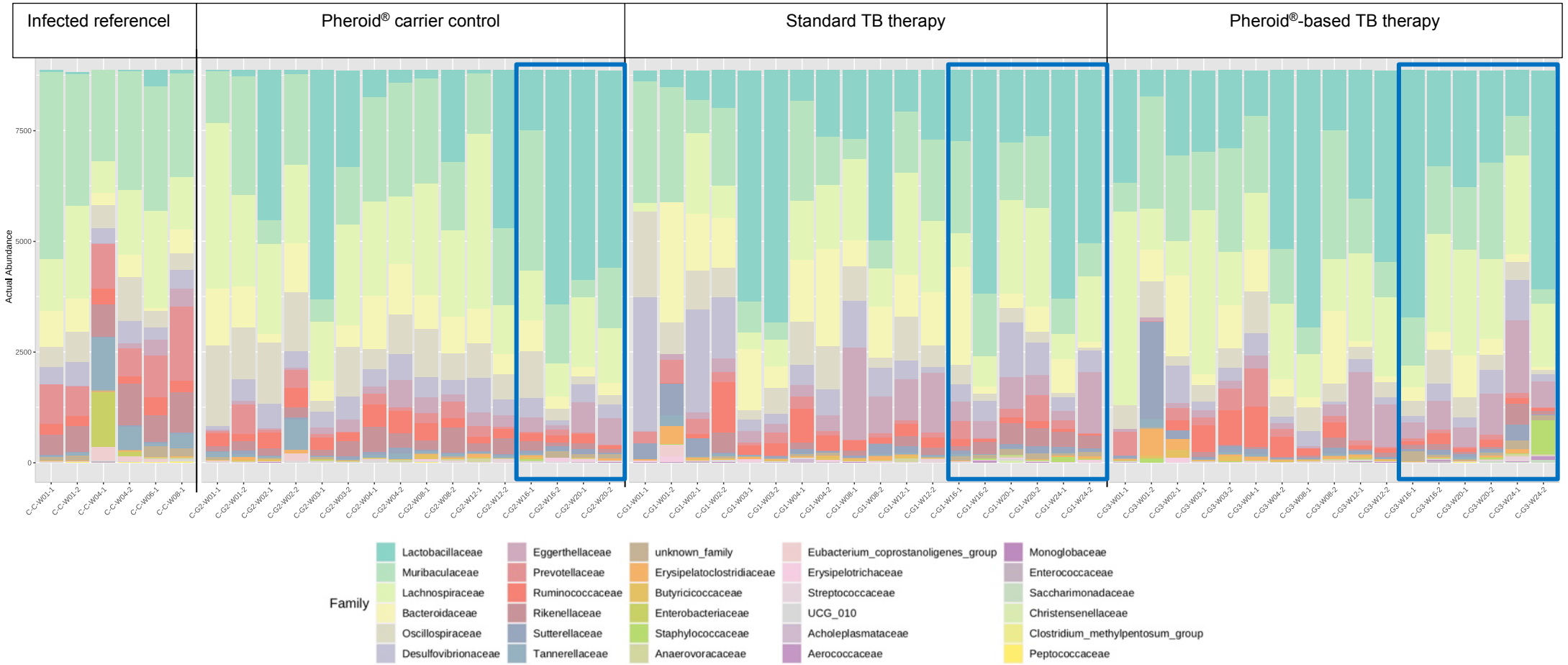


Figure 4-17 Microorganisms present in the caecum microbiome at the family level of classification. The microbiome recovery phase of each treatment is presented in a blue box. Actual abundance of each family is presented.

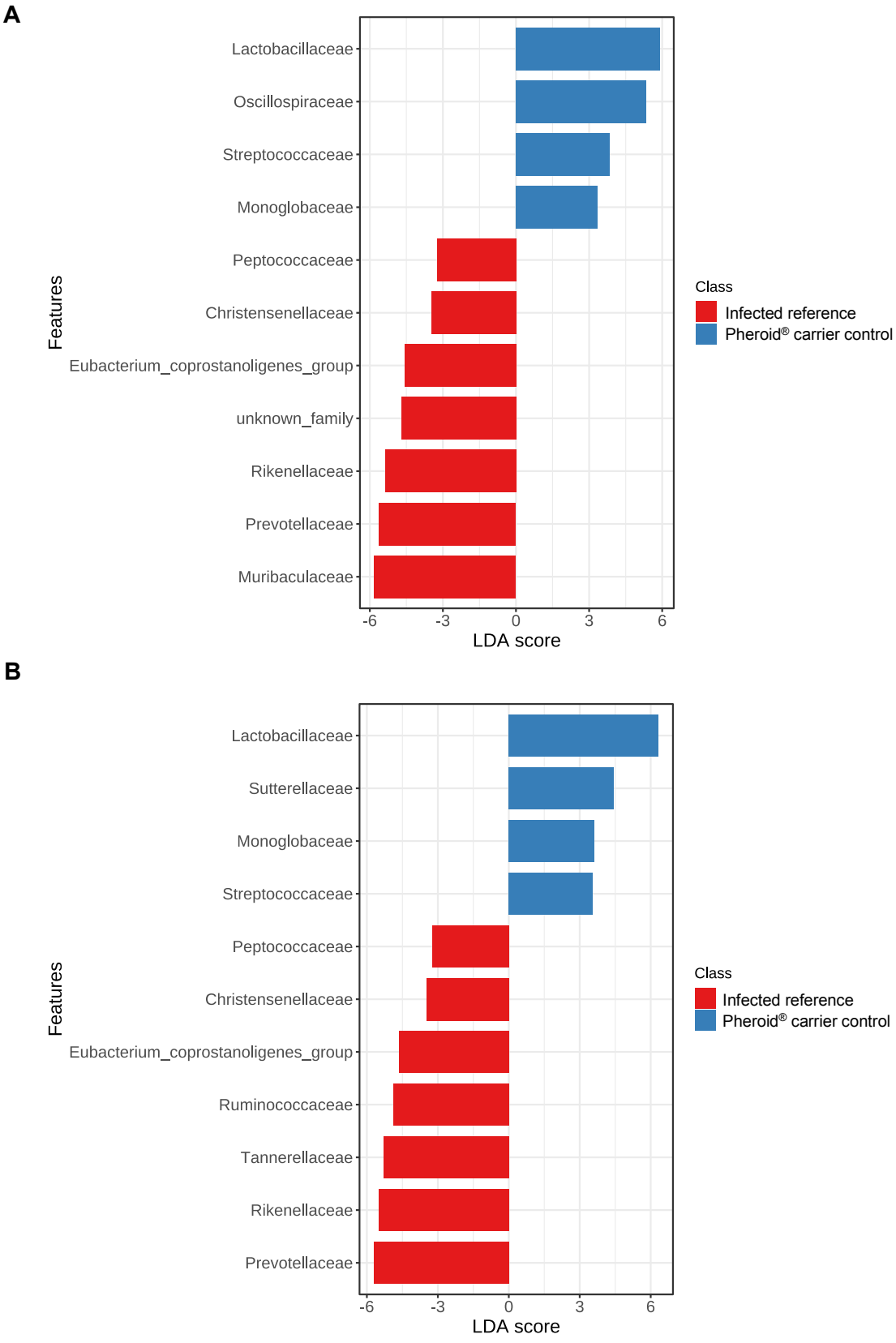


Figure 4-18 LEfSe analysis between samples derived from the infected reference and Pheroid® carrier control, showing the differentially abundant families (A) during treatment with the carrier control and (B) during the recovery from exposure after treatment ceased. Taxa significantly more in either the infected reference or carrier controls are represented with blue or red bars, respectively.

4.3.4.3 Genus

A total of 65 distinctive genera were identified from all groups (infected reference, Pheroid® carrier control, standard TB therapy & Pheroid®-based TB therapy). The different genera's abundancies varied between all groups and over time as a result of the different treatment regimens (Figure 4-19).

During treatment with the carrier control, significant features became obvious when comparing the treatment groups with the untreated infected group (Figure 4-20 A). A total of six significant features were present in samples derived from treated mice, whereas eight were significantly more abundant in infected references.

i. Significant features in the treatment phase of the carrier controls were the genera *Lactobacillus* (p=0.019), A2 (Lachnospiraceae bacterium) (p=0.001), *Colidextribacter* (p=0.015), Lachnospiraceae UCG 006 (p=0.001), *Streptococcus* (p=0.030), and *Monoglobus* (p=0.007).
ii. In contrast, higher abundancies of the family XIII AD3011 group (Anaerovoraceae) (p=0.008), *Christensenellaceae* R7 group (p<0.001), *Sellimonas* (p=0.040), ASF356 (Lachnospiraceae) (p=0.004), *Ruminococcus* (p=0.043), Eubacterium fissicatena group (p=0.013), *Alistipes* (p<0.001) and *Alloprevotella* (p=0.001) were present in the infected references that did not undergo any treatment. Furthermore, the sample that was an outlier from the clustered infected reference group (C-C-W4-1 in Figure 4-8, section 4.3.3) had high abundance of the *Escherichia/Shingella* taxa (phylum Proteobacteria).
iii. During recovery of the microbiome from the carrier control treatment, significant features remained similar to those during treatment. *Colidextribacter* and Lachnospiraceae UCG 006 did not have significantly different abundant features between the untreated, infected references and the microbiome recovery phase of the carrier control treated samples. However, significant features of *Parasutterella* arose during microbiome recovery (p=0.019) Figure 4-20 B). Furthermore, *Bilophila* (p=0.023) and *Parabacteroides* (p=0.019) were significant features between samples in the infected, untreated reference samples compared to recovering samples (Figure 4-20 B).

During the treatment phases of standard versus Pheroid®-based TB therapy, *Faecalitalea* (p=0.05) and *Colidextribacter* (p=0.036) were significant features in samples treated with standard treatment. More significant features were present during microbiome recovery phases of the respective treatments. A higher abundance of genera labelled A2

(Lachnospiraceae bacterium) and *Candidatus-Saccharimonas* (p=0.037 & p=0.022) were present in samples recovering from Pheroid®-based treatment. However, a larger diversity was significantly featured in samples recovering from standard treatment. These genera included NK4A214 group (Lachnospiraceae) (p=0.022), *Bilophila* (p=0.037), Rikenellaceae RC9 gut group (p=0.030) and *Alistipes* (p=0.037) (Figure 4-21).

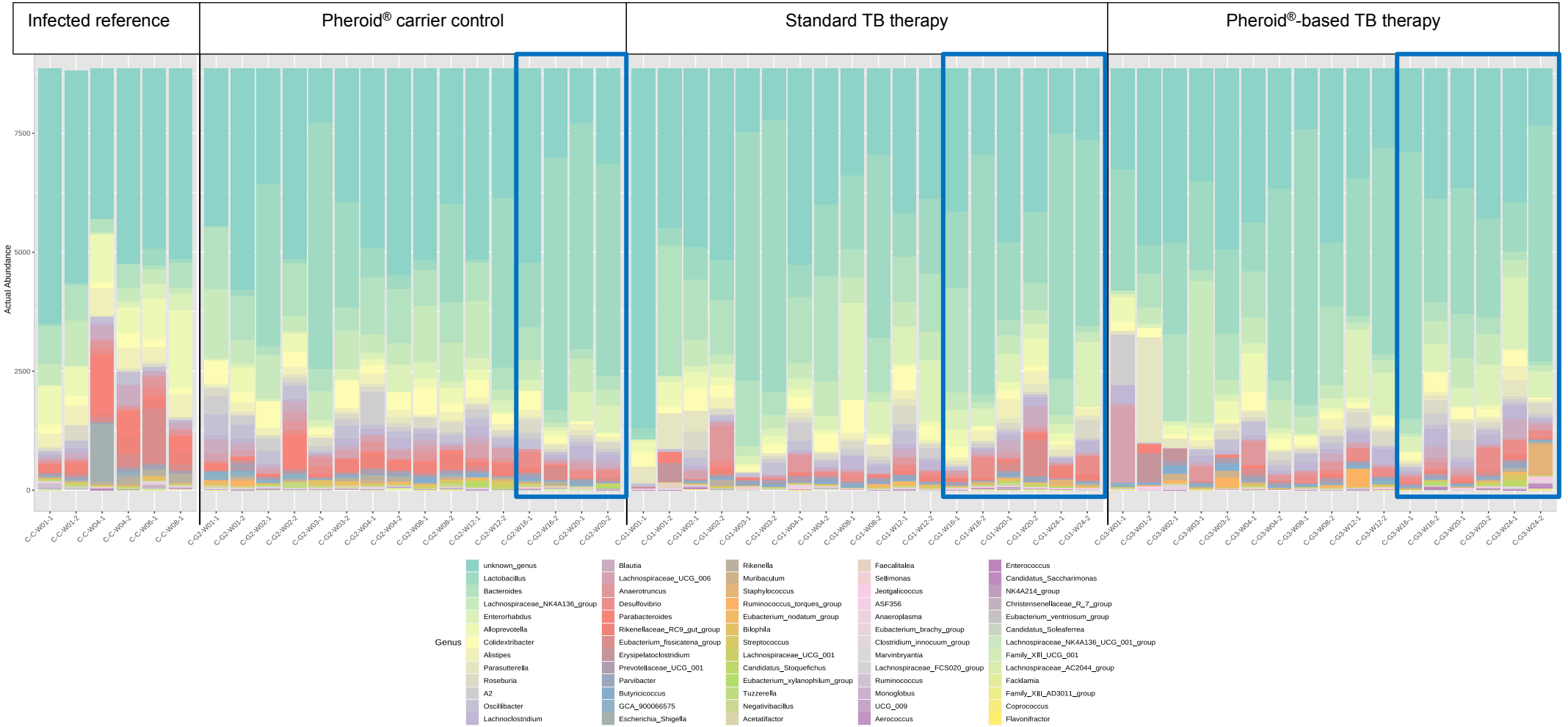


Figure 4-19 Relative abundance of microorganisms present in the caecum of each sample on the genus level of classification. The microbiome recovery phases of each treatment group are presented in blue boxes.

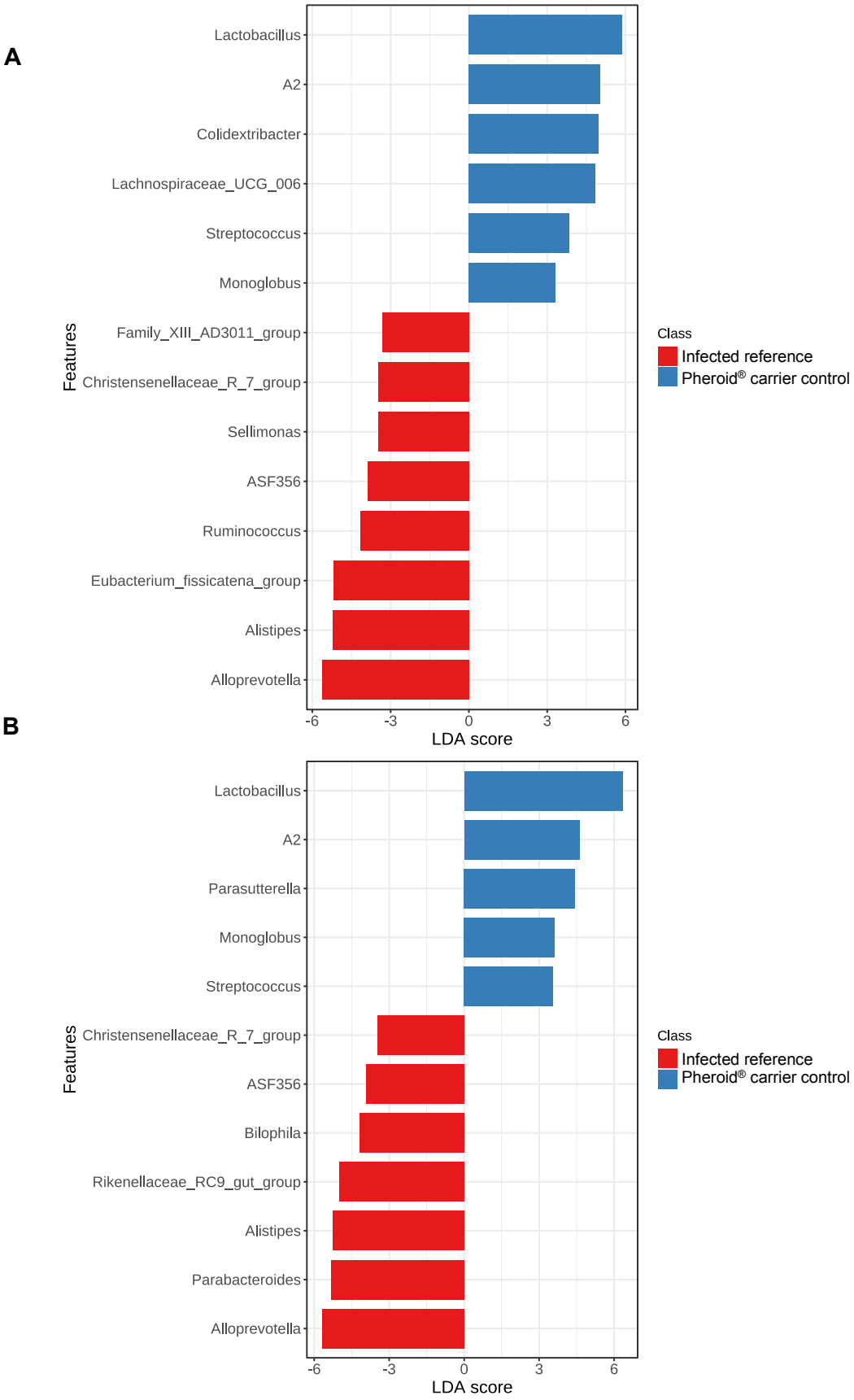


Figure 4-20 LEfSe comparisons illustrating genera that are significantly different between the infected references and Pheroid® carrier controls during (A) treatment with the carrier control (Weeks 1-12) and (B) during the microbiome recovery phases after exposure with the carrier control is ceased (Weeks 16 & 20).

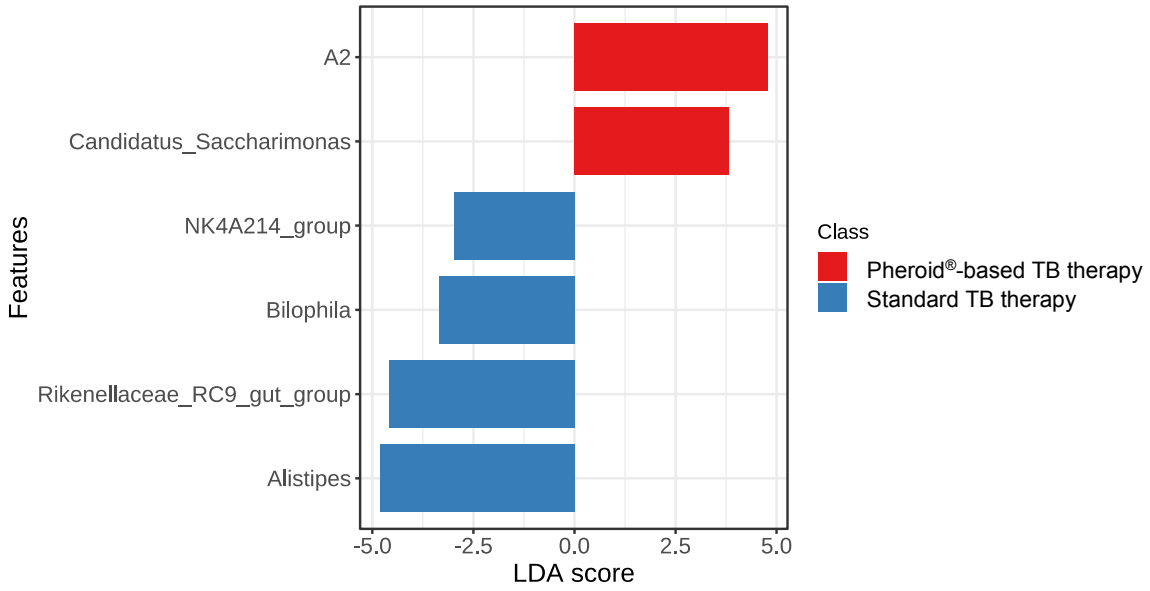


Figure 4-21 Analysis with LEfSe comparing genera that are significantly different between samples recovering from TB therapies. Comparisons were between samples derived from mice treated with standard treatment versus Pheroid®-based treatment (Weeks 1-12).

4.4 Discussion

In the study, distinctive differences in microbial structure was observed between infected reference samples and samples that were treated with the Pheroid® carrier control, and standard and Pheroid®-based TB treatments. Since no healthy controls were available for microbial analysis, composition of the microbiome from infected references was used as a reference point to determine the impact the treatments have on the microbiome structure. Namasivayam *et al*. (2017) and Hu *et al*. (2019) found that infection only caused minor changes in microbiome structure. Additionally, longitudinal changes in the murine mouse model were significantly different only at week 12 of infection (Namasivayam *et al*., 2017). In the present study, similar findings were observed where there were no significant differences in diversity within each sample of the infected references over time.

There are several limitations in determining an appropriate model for TB research. A limiting factor in mice is their inter-individual variations, affecting results in repetitive methods (Zhan *et al*., 2017). We found that there were trends of diversity differences between two samples collected at the same timepoint, in the same group. Inter-individual differences in microbial composition from the same mouse strain is regarded as a normal occurrence (Kostic *et al*., 2013). This was particularly remarkable in the infected reference group, where a drastic difference in OTU counts were

noticed. A much lower diversity was present in one replicate, compared to the other at the same period of infection. A decrease in microbial diversity favours the growth of potential pathogens in the microbiome, mainly represented by members of Enterobacteriaceae (Ribeiro *et al*., 2020). We found that particularly taxa of *Escherichia/Shigella* emerged during this point of treatment within the replicate. The aforementioned taxa are well known enteric pathogens that cause gastro-intestinal infection (Castaño-Rodríguez *et al*., 2018). Tirelle *et al*. (2020) found that exposure to a mixture of potent antibiotics caused a proliferation of specific usually less abundant taxa. However, proliferation due to decreased diversity is suggested to be caused by another external factor, since the infected references did not undergo any sort of treatment or exposure to compounds. Inter-individual variation and different responses to disease progression, including loss of appetite and stress, are expected to influence variance of diversity richness and distribution of the microbiome within each sample (Lanoix *et al*., 2015; Zhan *et al*., 2017; Ribeiro *et al*., 2020). Therefore, this finding may suggest that TB infection does play a role in microbial alterations in the gut in this particular mouse model.

It was previously demonstrated that administration of antibiotics causes dysbiosis of the gastro-intestinal microbiome in humans and in mouse models (Sullivan *et al*., 2001; Jin *et al*., 2016; Liu *et al*., 2020). The effect of TB and subsequently administered TB therapy on the gastro-intestinal microbiome are gaining a growing level of attention, and have been studied in both animal models and in clinical settings (Namasivayam *et al*., 2017; Wipperman *et al*., 2017; Maji *et al*., 2018; Hu *et al*., 2019; Khan *et al*., 2019). At the time of writing, there have been a few similar studies evaluating the impact of TB therapy in an animal model for comparison to previous studies. Furthermore, no study has been conducted in which the effect of first-line TB drugs administered using alternative delivery systems, such as the Pheroid® technology, has been explored. In one previous study, the administration of encapsulated drugs with a nano-drug carrier does seem alter the composition of the microbiome (Song *et al*., 2015). However, similar findings were noted with the free form chemotherapeutic drugs, indicating that the mode of delivery were not particularly the cause of dysbiosis, but the therapy itself. Further, the impact of Pheroid® carriers on the microbiome has not been examined previously. Evaluating the impact of Pheroid® carriers on the microbiome in an animal model is of importance to give an indication of potential effect on the human microbiome structure. Previously, efficacy of both therapies showed no significant difference in reduction of CFU counts in the lungs when comparing standard and Pheroid®-based TB therapies (van der Merwe, 2019; Annexure D) during the initial phase of treatment. Similarly, our results showed no significant difference in diversity abundance of the gastro-intestinal microbiome between mice treated with standard and the novel formulation (Pheroid®-based TB

therapy). Furthermore, the CFUs of *Mtb* determined were not null after either course of treatment (van der Merwe, 2019; Annexure D). In the carrier control, taxa decreased compared to the infected references; however, members from mainly Clostridia were significantly higher in samples during treatment with the carrier control. Additionally, Bacillus taxa were in high abundance as well. High levels of Firmicutes abundance are mainly associated with consumption of a fatty diet that subsequently led to obesity in humans and mice (Sun *et al*.,2020). Prevalence of these taxa remained high during microbiome recovery, though *Parasutterella* emerged during this phase, indicating recolonization of commensal microbiota when the treatment with the alternative approach ceased (Ju *et al*., 2019). It was recently suggested that the gastro-intestinal bacterial composition plays a crucial role in the homeostasis of various metabolisms, including lipid metabolism (Matey-Hernandez *et al*., 2017). The presence of short chain fatty acid (SCFA) and conjugated linoleic acid (CLA) producers, and bile acids in the gastro-intestinal tract aid in the homeostasis of lipid levels. CLA producers include *Lactobacillus,* a significantly proliferated genus amongst mice treated with the Pheroid® carrier control, which act on omega-3 polysaturated fatty acids (PUFAs). Furthermore, CLAs may promote higher levels of SCFA producers and play a beneficial role in lipid metabolism.

In the present study, there were, however, significant differences of microbiome composition between the infected reference and the treatments. Similar to studies conducted by Namasivayam *et al*. (2017) and Khan *et al*. (2019), our results showed a rapid decrease in microbial diversity at onset of treatment, which rebounds, but does not recover, with fluctuations in diversity during weeks following treatment. Furthermore, we found that the effect of TB therapies on the microbiome persists at least three months after treatment was terminated. Similar trends were found by Namasivayam *et al*. (2017) in mice and Wipperman *et al*. (2017) in humans where dysbiosis lasted for three months in mice, but up to over a year in humans. A striking difference between recovery phases from the treatments were the significantly increased abundance of unique taxa in Pheroid®-based treated samples (i.e. members of the phyla Patescibacteria). An opposite occurrence was found by Wang *et al*., (2020) where Patescibacteria were present during treatment of MDR-TB patients and declined after treatment was terminated. The role of the Patescibacteria in the mouse gut is unclear. However, Feng *et al*., (2020) found that co-administration of a digestive supplement, sheng-ling-bai-zhu-san (SLBZS), with pneumonia treatment increased abundancies of Patescibacteria, but decreased after treatment. The authors further concluded that the treatment decreases inflammation caused by *Streptococcus pneumoniae* induced pneumonia. Additionally, increased abundance of Saccharimonadaceae, a significant feature in microbiome abundance recovering from the novel

treatment, was related to elevated immune function in a study conducted by Zhao *et al*. (2020). Our results may thus suggest a possible positive treatment outcome after administration of Pheroid®-based TB therapy, favouring growth of immunomodulators after treatment with *Mtb* still present in the lungs (Annexure D).

By linking results obtained in the companion study by van der Merwe (2019), it was noted that the Pheroid® carrier control did not result in a reduction of *Mtb* CFUs in the lung samples of mice. However, the survival rate of the mice were higher than that of the infected references that did not undergo treatment (please see Sampling in section 4.2). Interestingly, there was no increase in CFU counts of samples from the carrier control, but a relatively stable count throughout treatment and during the microbiome recovery (van der Merwe, 2019; Annexure D). According to Winglee *et al*. (2014) infected Balb/c mice survived for at least 89 days post infection, whereas the Kramnik mice in the companion study survived up until week 8 (day 56) of infection. These observations indicate a lower survival rate of Kramnik mice compared to Balb/c mice. Balb/c mice as model for TB studies are therefore not considered to be ideal, since the mice do not form granulomas as result to infection and haven't endured the disease.

To address the survival of TB infected mice treated with the Pheroid® carrier control, the composition of the formulation should be considered. The oil in the Pheroid® formulation may be seen as a fatty component in diet, especially since treatment was administered daily. With this in mind, Arias *et al*. (2019) found that high fat diets in Kramnik mice provoke an inflammatory response, causing a more rapid progression towards TB disease prior to treatment. A reduced Firmicutes/Bacteroidota ratio within the microbiome was suggested to be the cause of disease progression (Arias *et al*., 2019). According to Liu *et al*. (2012), omega-3 PUFAs reduce the proportion of Bacteriodota present in the microbiome, though not to the extent saturated fatty acids do. Similar to these findings, reductions in Bacteroidota were noticed amongst samples treated with the Pheroid® carrier control, compared to the infected reference. Despite the progression of the TB disease when consuming a fatty diet before treatment is administered, an increase in survival rate was noted in Kramnik mice which developed natural immunity after TB therapy was terminated (Arias *et al*., 2019). Contrarily, mice that were on a normal diet, had a lower survival rate after being infected again and natural immunity was developed post treatment. Our results may suggest that the administration of selective Pheroid® carriers, such as mycolic acid and increased eicosapentaenoic acid, had a positive impact on the survival rate of mice and not necessarily the clearance of *Mtb*, despite its fatty composition. Inhibition of *Mtb* in the lungs are known to be associated with the secretion of tumour necrosis factor alpha (TNF- α), however it was previously shown that the administration of eicosapentaenoic acid (EPA) decreases

secretion of the cytokine, which is known to play a role in defence against intracellular pathogens (Flesch *et al*., 1994; Jordoa *et al*., 2008; Nienaber *et al*., 2020). Nienaber *et al*. (2020) suggest that the supplementation with long chain polyunsaturated fatty acids EPA combined with docosahexaenoic acid (DHA) may have a supporting effect on the resolution of inflammation in the lungs without influencing host immunity. The presence of *Mtb* in the lungs of these mice after exposure to the carrier control may possibly be the cause of morbidity due to disease progression of mice after the second month of recovery, given the persistent dysbiosis of the microbiome after treatment is ceased. Some microbial taxa are positively or negatively associated with immune responses (Zhao *et al*., 2020). Though some significantly featured taxa in the infected reference are positively correlated to immune response, more so were present in the Pheroid® carrier control during treatment and recovery.

4.5 Conclusion

This study was the first to examine the impact of TB therapy on the microbiome using an alternative drug delivery system. By employing a mouse model frequently used in TB research, environmental factors that may influence microbial variation between samples were controlled to best extent. Furthermore, findings suggest that dysbiosis caused by the novel TB therapy formulation does not differ from that of standard TB-treatment in terms of changes in alpha and beta diversity overall and over time. However, the alternative drug delivery approach did result in proliferation of immunomodulating taxa post treatment, compared to standard treatment. Finally, Pheroid®-based treatment does not have any adverse effects on alpha and beta diversity changes in the microbiome, compared to standard therapy. Findings suggest that even though Pheroid® technology does not improve the state of the microbiome during the course of treatment, promising trends in proliferation of immunomodulating bacteria during microbiome recovery arise.

4.6 Data availability

Amplicon sequencing was performed with Illumina MiSeq platform (Illumina, US). Paired reads were combined into single reads and data has been uploaded onto the database of the National Centre for Biotechnology Information (NCBI) Sequence Read Archive (SRA). Data can be found under accession number PRJNA677846.

4.7 Ethics statement

The study involving animal handling and treatment were ethically approved previously. However, the ethics of the use of animal organs in this study were reviewed and approved by NWU-AnimCARE ethic committee according to their guidelines (NWU-00584-19-A5).

4.8 Funding

This work is based on the research supported wholly by the National Research Foundation of South Africa (Grant number: 117255) and the South African Department of Science and Innovation (DSI) in conjunction with the International Mouse Phenotyping Consortium (IMPC). The funders did not contribute to the experimental design, collection of data and interpretation of results.

4.9 Acknowledgements

The authors thank PHENOMIN-ICS (France) for providing 16S PCR, library preparation and bioinformatics analysis in the study.

References

Arias, L., Goig, G.A., Cardona, P., Torres-Puente, M., Díaz, J., Rosales, Y., Garcia Aguilera, E., Tapia, G., Comas, I., Vilaplana, C. & Cardona, P.J. 2019. Influence of gut microbiota on progression to tuberculosis generated by high fat diet-induced obesity in C3HeB/FeJ Mice. *Frontiers in Immunology*, 10:2464. doi:10.3389/fimmu.2019.02464

Beauduy, C.E. & Winston, L.G. 2018. Antimycobacterial drugs. In: Kaztung, B.G. eds. *Basic and clinical Pharmacology, fourteenth edition*. USA: McGraw-Hill Education. pp. 842-852.

Castaño-Rodríguez, N., Underwood, A.P., Merif, J., Riordan, S.M., Rawlinson, W.D., Mitchell, H.M. & Kaakoush, N.O. 2018. Gut microbiome analysis identifies potential etiological factors in acute gastroenteritis. *Infection and Immunity*, 86(7):e00060-18. doi:10.1128/IAI.00060-18

Chong, J., Liu, P., Zhou, G. & Xia, J. 2020. Using MicrobiomeAnalyst for comprehensive statistical, functional, and meta-analysis of microbiome data. *Nature Protocols*, 15(3):799-821. doi:10.1038/s41596-019-0264-1

Clarke, K.R. & Warwick, R.M. 2001. Change in marine communities: an approach to statistical analysis and interpretation. 2nd ed. Plymouth Marine Laboratory, UK: PRIMER-E Ltd.

Ducarmon, Q.R., Hornung, B.V.H., Geelen, A.R., Kuijper, E.J. & Zwittink, R.D. 2020. Toward standards in clinical microbiota studies: comparison of three DNA extraction methods and two bioinformatic pipelines. *Msystems*, 5:e00547. doi:10.1128/mSystems.00547-19

Dumas, A., Corral, D., Colom, A., Levillain, F., Peixoto, A., Hudrisier, D., Poquet, Y. & Neyrolles, O. 2018. The host microbiota contributes to early protection against lung colonization by *Mycobacterium tuberculosis*. *Frontiers in immunology*, *9*:2656. doi:10.3389/fimmu.2018.02656

Escudie, F., Auer, L., Bernard, M., Mariadassou, M., Cauquil, L., Vidal, K., Maman, S., Hernandez-Raquet, G., Combes, S. & Pascal, G. 2018. FROGS: Find, Rapidly, OTUs with Galaxy Solution. *Bioinformatics*, 34(8):1287-1294. doi:10.1093/bioinformatics/btx791

Feng, J., Dai, W., Zhang, C., Chen, H., Chen, Z., Chen, Y., Pan, Q. & Zhou, Y. 2020. Shen-ling-bai-zhu-san ameliorates inflammation and lung injury by increasing the gut microbiota in the murine model of *Streptococcus pneumonia*-induced pneumonia. *BMC Complementary Medicine and Therapies*, 20:1-12. doi:10.1186/s12906-020-02958-9

Flesch, I.E., Hess, J.H., Oswald, I.P. & Kaufmann, S.H. 1994. Growth inhibition of *Mycobacterium bovis* by IFN-γ stimulated macrophages: regulation by endogenous tumor necrosis factor-α and by IL-10. *International Immunology*, 6(5):693-700. doi:0.1093/intimm/6.5.693

Grobler, A.F. 2009. Pharmaceutical applications of Pheroid™ technology. North-West University. (Thesis - PhD).

Grobler, A.F. 2013. Nano & micro-delivery systems: the Pheroid® story. NWU: Potchefstroom Campus (Inaugural lecture).

Harper, J., Skerry, C., Davis, S.L., Tasneen, R., Weir, M., Kramnik, I., Bishai, W.R., Pomper, M.G., Nuermberger, E.L. & Jain, S.K. 2012. Mouse model of necrotic tuberculosis granulomas develops hypoxic lesions. *Journal of Infectious Diseases*, 205(4):595-602. doi:10.1093/infdis/jir786

Hu, Y., Yang, Q., Liu, B., Dong, J., Sun, L., Zhu, Y., Su, H., Yang, J., Yang, F., Chen, X. & Jin, Q. 2019. Gut microbiota associated with pulmonary tuberculosis and dysbiosis caused by anti-tuberculosis drugs. *Journal of Infection*, 78(4):317-322. doi:10.1016/j.jinf.2018.08.006

Jin, Y., Wu, Y., Zeng, Z., Jin, C., Wu, S., Wang, Y. & Fu, Z. 2016. From the cover: exposure to oral antibiotics induces gut microbiota dysbiosis associated with lipid metabolism dysfunction and low-grade inflammation in mice. *Toxicological Sciences*, 154(1):140-152. doi:10.1093/toxsci/kfw150

Johnson, R., Streicher, E.M., Louw, G.E., Warren, R.M., Van Helden, P.D. & Victor, T.C. 2006. Drug resistance in Mycobacterium tuberculosis. *Current issues in Molecular Biology*, 8(2):97-112.

Jordao, L., Lengeling, A., Bordat, Y., Boudou, F., Gicquel, B., Neyrolles, O., Becker, P.D., Guzman, C.A., Griffiths, G. & Anes, E. 2008. Effects of omega-3 and-6 fatty acids on *Mycobacterium tuberculosis* in macrophages and in mice. *Microbes and infection*, 10(12-13):1379-1386. doi:10.1016/j.micinf.2008.08.004

Ju, T., Kong, J.Y., Stothard, P. & Willing, B.P. 2019. Defining the role of *Parasutterella*, a previously uncharacterized member of the core gut microbiota. *The ISME Journal*, 13(6):1520-1534. doi:10.1038/s41396-019-0364-5

Khan, N., Mendonca, L., Dhariwal, A., Fontes, G., Menzies, D., Xia, J., Divangahi, M. & King, I.L. 2019. Intestinal dysbiosis compromises alveolar macrophage immunity to *Mycobacterium tuberculosis*. *Mucosal Immunology*, 12(3):772-783. doi:10.1038/s41385-019-0147-3

Klindworth, A., Pruesse, E., Schweer, T., Peplies, J., Quast, C., Horn, M. & Glöckner, F.O. 2013. Evaluation of general 16S ribosomal RNA gene PCR primers for classical and next-generation sequencing-based diversity studies. *Nucleic acids research*, 41(1):e1. doi:10.1093/nar/gks808

Kolyva, A.S. & Karakousis, P.C. 2012. Old and new TB drugs: mechanisms of action and resistance. In: Cardona, D.P.-J., eds. *Understanding Tuberculosis–New Approaches to Fighting Against Drug Resistance*. Europe: InTech. pp. 209-32.

Kostic, A.D., Howitt, M.R. & Garrett, W.S. 2013. Exploring host–microbiota interactions in animal models and humans. *Genes & Development*, *27*(7):701-718. doi:10.1101/gad.212522.112

Lanoix, J.P., Lenaerts, A.J. & Nuermberger, E.L. 2015. Heterogeneous disease progression and treatment response in a C3HeB/FeJ mouse model of tuberculosis. *Disease Models & Mechanisms*, 8(6):603-610. doi:10.1242/dmm.019513

Lim, M.Y., Song, E.-J., Kim, S.H., Lee, J. & Nam, Y.-D. 2018. Comparison of DNA extraction methods for human gut microbial community profiling. *Systematic and Applied Microbiology*, 41(2):151-157. doi:10.1016/j.syapm.2017.11.008

Liu, L., Wang, Q., Wu, X., Qi, H., Das, R., Lin, H., Shi, J., Wang, S., Yang, J., Xue, Y. & Mao, D. 2020. Vancomycin exposure caused opportunistic pathogens bloom in intestinal microbiome by simulator of the human intestinal microbial ecosystem (SHIME). *Environmental Pollution*, 265(B):114399. doi:10.1016/j.envpol.2020.114399

Liu, T., Hougen, H., Vollmer, A.C. & Hiebert, S.M. 2012. Gut bacteria profiles of *Mus musculus* at the phylum and family levels are influenced by saturation of dietary fatty acids. *Anaerobe*, 18(3):331-337. doi:10.1016/j.anaerobe.2012.02.004

Maji, A., Misra, R., Dhakan, D.B., Gupta, V., Mahato, N.K., Saxena, R., Mittal, P., Thukral, N., Sharma, E., Singh, A., Virmani, R., Gaur, M., Singh, H., Hasija, Y., Arora, G., Agrawal, A., Chaudhry, A., Khurana J.P., Sharma, V.K., Lal, R. & Singh, Y. 2018. Gut microbiome contributes to impairment of immunity in pulmonary tuberculosis patients by alteration of butyrate and propionate producers. *Environmental Microbiology*, 20(1):402-419. doi:10.1111/1462-2920.14015

Matey-Hernandez, M.L., Williams, F.M., Potter, T., Valdes, A.M., Spector, T.D. & Menni, C. 2018. Genetic and microbiome influence on lipid metabolism and dyslipidemia. *Physiological Genomics*, 50(2):117-126. doi:10.1152/physiolgenomics.00053.2017

Matlock, B. 2015. Assessment of nucleic acid purity, technical note 52646. Wilmington, MA, USA: Thermo Fisher Scientific https://assets.thermofisher.com/TFS-Assets/CAD/Product-Bulletins/TN52646-E-0215M-NucleicAcid.pdf Date of access: 26 Nov. 2020.

Namasivayam, S., Maiga, M., Yuan, W., Yuan, V., Costa, D.L., Mittereder, L.R., Wipperman, M.F., Glickman, M.S., Dzutsev, A., Trinchieri, G. & Sher, A. 2017. Longitudinal profiling reveals a persistent intestinal dysbiosis triggered by conventional anti-tuberculosis therapy. *Microbiome*, 5:71. doi:10.1186/s40168-017-0286-2

Nienaber, A., Baumgartner, J., Dolman, R.C., Ozturk, M., Zandberg, L., Hayford, F.E., Brombacher, F., Blaauw, R., Parihar, S.P., Smuts, C.M. & Malan, L. 2020. Omega-3 fatty acid and iron supplementation alone, but not in combination, lower inflammation and anemia of infection in *Mycobacterium tuberculosis*-infected mice. *Nutrients*, 12(9):2897. doi:10.3390/nu12092897

Nieuwoudt, L. 2009. The impact of PheroidTM technology on the bioavailability and efficacy of anti-tuberculosis drugs in an animal model. NWU: Potchefstroom Campus. (Dissertation – MSc).

Ribeiro, C.F.A., Silveira, G.G.D.O.S., Cândido, E.D.S., Cardoso, M.H., Espínola Carvalho, C.M. & Franco, O.L. 2020. effects of antibiotic treatment on gut microbiota and how to overcome its negative impacts on human health. *ACS Infectious Diseases*, 6(10):2544-2559. doi:10.1021/acsinfecdis.0c00036

Singh, A. K., & Gupta, U. D. 2018. Animal models of tuberculosis: Lesson learnt. *The Indian Journal of Medical Research*, 147(5):456–463. doi:10.4103/ijmr.IJMR_554_18

Song, Y., Zhao, R., Hu, Y., Hao, F., Li, N., Nie, G., Tang, H. &Wang, Y. 2015. Assessment of the biological effects of a multifunctional nano-drug-carrier and its encapsulated drugs. *Journal of Proteome Research*, 14(12):5193-5201. doi:10.1021/acs.jproteome.5b00513

Sullivan, Å., Edlund, C. & Nord, C.E. 2001. Effect of antimicrobial agents on the ecological balance of human microflora. *The Lancet infectious diseases*, 1(2):101-114. doi:10.1016/S1473-3099(01)00066-4

Sun, M., Wang, Q., Zhang, M., Zhang, G., Wu, T., Liu, R., Sui, W., Zhang, J., Yin, J. & Zhang, M. 2020. *Leuconostoc pseudomesenteroides* improves microbiota dysbiosis and liver metabolism imbalance and ameliorates the correlation between dihydroceramide and strains of Firmicutes and Proteobacteria in high fat diet obese mice. *Food & Function*, 11(8):6855-6865. doi:10.1039/d0fo01009j

Tirelle, P., Breton, J., Riou, G., Déchelotte, P., Coëffier, M. & Ribet, D. 2020. Comparison of different modes of antibiotic delivery on gut microbiota depletion efficiency and body composition in mouse. *BMC Microbiology*, 20:340. doi:10.1186/s12866-020-02018-9

Van der Merwe. 2019. Determination of the therapeutic efficacy of a novel Pheroid® formulation in a rodent tuberculosis model. NWU: Potchefstroom Campus. (Dissertation – MSc).

Van Zyl, L., Du Preez, J., Gerber, M., Du Plessis, J. & Viljoen, J. 2016. Essential fatty acids as transdermal penetration enhancers. *Journal of Pharmaceutical Sciences*, 105(1):188-193. doi:10.1016/j.xphs.2015.11.032

Wang, J., Xiong, K., Zhao, S., Zhang, C., Zhang, J., Xu, L. & Ma, A. 2020. Long-term effects of multi-drug-resistant tuberculosis treatment on gut microbiota and its health consequences. *Frontiers in Microbiology*, 11:53. doi:10.3389/fmicb.2020.00053

WHO: World Health Organization. 2019. Global tuberculosis report 2019. https://apps.who.int/iris/bitstream/handle/10665/329368/9789241565714-eng.pdf?ua=1 Date of access: 27 Nov. 2020.

Winglee, K., Eloe-Fadrosh, E., Gupta, S., Guo, H., Fraser, C. & Bishai, W. 2014. Aerosol *Mycobacterium tuberculosis* infection causes rapid loss of diversity in gut microbiota. *PLoS One*, 9(5):e97048. doi:10.1371/journal.pone.0097048

Wipperman, M.F., Fitzgerald, D.W., Juste, M.A.J., Taur, Y., Namasivayam, S., Sher, A., Bean, J.M., Bucci, V. & Glickman, M.S. 2017. Antibiotic treatment for tuberculosis induces a profound dysbiosis of the microbiome that persists long after therapy is completed. *Scientific Reports*, 7(1):10767. doi:10.1038/s41598-017-10346-6

Yuan, S., Cohen, D.B., Ravel, J., Abdo, Z. & Forney, L.J. 2012. Evaluation of methods for the extraction and purification of dna from the human microbiome. *PLoS ONE,* 7(3):e33865. doi:10.1371/journal.pone.0033865

Zhan, L., Tang, J., Sun, M., & Qin, C. 2017. Animal models for tuberculosis in translational and precision medicine. *Frontiers in Microbiology*, 8:717. doi:10.3389/fmicb.2017.00717

Zhao, Y., Yan, Y., Zhou, W., Chen, D., Huang, K., Yu, S., Mi, J., Lu, L., Zeng, X. & Cao, Y. 2020. Effects of polysaccharides from bee collected pollen of Chinese wolfberry on immune response and gut microbiota composition in cyclophosphamide-treated mice. *Journal of Functional Foods*, 72:104057. doi:10.1016/j.jff.2020.104057

Chapter 5 Summary and recommendations

5.1 Introduction

In order to end the global tuberculosis (TB) pandemic, cases of active and latent TB have to be treated and cured to prevent further spread of the disease. However, the use of TB therapy has a well-known effect on the gastro-intestinal microbiome. Administration of these drugs cause severe dysbiosis of the gastro-intestinal microbiome. Dysbiosis is proven to proceed in the gastro-intestinal environment long after treatment ceased. An altered gastro-intestinal microbiome paves the way for other diseases and proliferation of potential pathogens that exist in the gastro-intestinal environment. Therefore, the possibility of using an alternative targeted drug delivery system raises the question of whether dysbiosis may occur to a lesser extent than when applying standard drug regimens. In addition to this, new methods to study the effect of TB and TB treatment on the microbiome are needed to successfully characterize the microbiome. New methods for microbiome analysis include the selection of an appropriate DNA extraction method to quantify all bacterial species present within the particular environment.

The general aims of the study were to examine the shifts in the gastro-intestinal microbiome from caecum samples during standard and Pheroid®-based TB therapy in the Kramnik (C3HeB/FeJ) mouse model; and to evaluate the potential role of Pheroid®-based TB therapy for improved treatment outcome.

The objectives of this study were as follows:

i. To evaluate the NWU cell lysis method as preferential tool for downstream gut microbiome analysis;
ii. to evaluate changes in the gastro-intestinal microbiome of C3HeB/FeJ mice infected with the H37Rv *Mycobacterium tuberculosis* (*Mtb*) strain during treatment with courses of both standard and Pheroid®-based TB therapies, using 16S amplicon sequencing;
iii. to compare the changes during treatment with already available colony forming unit (CFU) data; and
iv. to determine whether the microbiome plays a role in improved treatment outcome.

5.2 Summary of study design, execution and results

Even though the study design was not ideal in terms of sample size, some solid conclusions were drawn based on data obtained from available samples. In view of the limited published literature available, the present study was an investigative pilot study only with a limited sample size and suitable for an MSc degree. The extent of the study was also determined by the samples available. Furthermore, samples were selected to best compare timepoints from the previously study (van der Merwe, 2019) from where the samples originated. Additionally, cytokines were not tested to evaluate immunological response, since only caecum samples were available to for present study.

5.2.1 Objective i

The first objective was addressed and is outlined in chapter 3, where different DNA extraction protocols were evaluated with subsequent investigation of the NWU cell lysis method. It was found that extraction methods consisting of a bead beating and chemical lysis step, and a spin column DNA binding step successfully extracted microbial DNA from caecum samples. Furthermore, no significant difference was found between commercial extraction kits and the NWU cell lysis method, indicating that the method is a possible tool for downstream microbial analysis with short-read sequencing techniques, such as 16S amplicon sequencing. However, inter-individual variation between similar samples was present, raising possible limitations for future studies.

5.2.2 Objective ii

To address objective number ii, microbial analysis of mouse caecum samples was performed over time and results are outlined in chapter 4. The study aimed to determine changes in the microbiome during Pheroid®-based TB therapy and whether it had an impact on treatment outcome. Results indicated that there were no statistically significant differences in alpha and beta diversity measurements between standard and Pheroid®-based TB therapies. However, during the microbiome recovery phase, there was a proliferation of the phylum Patescibacteria, which was previously found to be associated with a decrease in inflammation caused by pneumonia. Despite non-significant changes between therapies with active pharmaceutical compounds (APIs), There was an interesting difference between samples from the infected reference group that acted as baseline and the Pheroid® carrier control group (Pheroid® compounds without APIs). These differences were the result of a small, though not significant, decrease in diversity amongst samples treated with the carrier control. Some taxa proliferated during treatment with the carrier control, despite decreased diversity. The Firmicutes: Bacteroidota ratio in the microbiome of mice

treated with the carrier control were significantly increased compared to the infected reference. More particularly a high abundance of *Lactobacillus*, known to play a role in lipid metabolism, was present in the microbiomes of mice treated with the carrier control.

5.2.3 Objective iii

Objective iii was addressed by comparing results obtained by achieving objective ii with already available CFU data (van der Merwe, 2019; Annexure D). Results are also outlined in chapter 4. CFU data of *Mtb* in the lungs between mice that were treated with either standard or Pheroid®-based TB therapy showed no significant differences after treatment (van der Merwe, 2019). This data supports the results obtained where there were no significant differences found in microbiome diversity between the treatment groups. Furthermore, decreased diversity in the microbiome amongst mice treated with the Pheroid® carrier control made way for proliferation of underlying bacteria that was suggested to increase the survival rate of the mice, since there was no decrease in CFUs of *Mtb* in the lungs.

5.2.4 Objective iv

To address the last objective, analysis of significantly abundant taxa between experimental groups indicated that taxa in the microbiome of samples treated with Pheroid®-based TB therapy were positively correlated to immune response and may serve as immunomodulators in the gastro-intestinal environment (please refer to section 4.3.4.3 and 4.4). This may suggest that Pheroid®-based treatments do not necessarily improve the state of the microbiome during treatment, but it may have potential to modulate immune responses to *Mtb* still present in the lungs, since the mice were not cured from TB after treatment was ceased.

In addition, the present study introduced the effect of TB therapy on the microbiome of a specific mouse strain – C3HeB/FeJ (Kramnik). Similar results were obtained in terms of decreases in decreases during treatment compared to studies done in C57BL/6 mouse strains (Namasivayam *et al*., 2017; Kahn *et al*., 2019). Diversity changes between healthy and infected mice were disregarded due to evidence in a previous mouse study, where only minor changes in diversity were caused by TB infection (Namasivayam *et al*., 2017). The inter-individual differences associated with different response during the disease in the present study suggested that *Mtb* infection does have an impact on microbiome composition and structure in the Kramnik mouse model. Therefore, the *Mtb* infected mice served as a reference baseline. Similarly, Winglee *et al.* (2014) found that infection did however cause differences in diversity in another mouse strain –

Balb/c. Given the humanized properties of C3HeB/FeJ, it is suggested that there may be changes in microbial diversity between healthy mice and infected mice. Moreover, evidence of inter-individual differences amongst samples in the mouse model were present. Beta diversity analysis did however indicate that infected mice were clustered closer together, which suggests that the mice have similar responses to infection. The survival rates of infected mice raise a limitation for the use of the model in TB studies, due to the mice becoming *moribund* early on with infection.

5.3 Study limitations and recommendations

During completion of the study, various study limitations and recommendations to rectify the limitations in future studies were identified. Limitations included:

I. Sample size

Sample size is crucial when comparing results statistically. It is recommended that the sample size should include at least five mice per timepoint. By increasing sample size, beta diversity changes between groups at specific timepoints will be made clear. Additionally, inter-individual differences between mice were evident throughout the study, e.g., a difference in the microbial composition from two mice sacrificed from the same groups at the same time. The availability of only one sample of caecum per animal limits confidence due to inter-individual variability of mice. It is therefore recommended that a larger cohort of samples that will allow an averaged outcome should be investigated to overcome variability.

II. Exclusion of an uninfected group

The difference in microbiome structure between healthy and *Mtb* infected C3HeB/FeJ mice remains unknown. The microbiome structure of infected mice has been studied in the present study; however, it could not be compared to healthy mice of the same strain. It is therefore recommended that diversity in the microbiomes of both healthy and infected mice under the same environmental conditions should be determined in future studies, to prove whether infection does indeed affect microbial composition of the specific strain. The inclusion of an uninfected group might also aid in understanding inter-individual variation and whether it is subjected to disease response.

5.4 Future prospects

Results generated from the present study paves the way for future studies. It is therefore recommended that the following should be investigated:

I. Possible immune support function of Pheroid®-based TB therapy in the host and whether it is linked to the gastro-intestinal microbiome.

Though there were no statistically significant differences in microbiome diversity (alpha and beta diversity changes) between standard and Pheroid®-based treatments, animals that were exposed to the Pheroid® carrier control survived longer than the infected mice, despite the presence of *Mtb* CFUs in the lungs (van der Merwe, 2019; Annexure D). The reason for the increased survival rate is unknown, though it is suggested that it is due to the possible immune support function of the Pheroid® compounds. In order to investigate this potential function and the immune response during treatment, it may be of interest to determine whether the formulation has a possible effect. This can be achieved by measuring the production of immune-related cytokines in the blood, as described by Zhao *et al*. (2020), and comparing it to taxa associated with immunity in the gastro-intestinal microbiome.

The use of an alternative animal model to determine efficacy of TB treatment and the effect thereof on the gastro-intestinal microbiome. Similar formulations to that used in the present study should be evaluated in different models. Since the Kramnik mice were not cured after treatment ceased, it would be of interest to examine the efficacy of treatment on another animal model. A frequently used mouse model for TB infection, treatment and the microbiome is C57BL/6 mice (Namasivayam *et al*., 2017; Khan *et al.,* 2019). Mouse models are convenient models, but the use of these models is not the most appropriate since frequently used models such as C57BL/6 mice do not mimic the pathology of the human disease. Animal models such as guinea pigs and non-human primates are particularly useful in TB research, where the disease in non-human primates have most in common with that found in humans, although ethical approval for studies in non-human primates may be difficult to obtain (Dharmadhikari & Nardell, *et al.,* 2008). The efficacy of the TB treatments in these models will therefore give a more accurate representation to that in humans. The animals should be exposed to treatment for a longer period and reflect the drug regimen as in humans (intensive phase for two months and continuation phase for a further four months). Furthermore, the follow up phase after treatment is ceased should continue for at least six months. In addition to efficacy studies in alternative animal models, the examination of changes in the microbiome in these models raises questions. This includes whether it has the same effect on microbiome diversity, whether the variability between individual mice is lesser in extent than in Kramnik mice, whether the microbiome rebounds after treatment is stopped and whether microbiome recovery is complete and how long does it take for complete recovery. There was a significant increase in diversity from animals over the period of treatment, and from animals in the recovery phase. Apart from alternative animal models, it is recommended that monitoring

of the Kramnik mice after three months in recovery should be included to determine whether the microbiome recovers fully.

II. Clinical trial with increased treatment period of the various TB treatments.

Aside from animal models that portray the human response to TB therapy, a clinical trial in humans, by employing similar formulations of TB therapy used in the present study, can be considered as a future prospective for microbiome research. Although mice in the present study were not cured of the disease, the CFU counts did decrease during the course of therapy (van der Merwe; Annexure D). Currently, standard first-line TB treatment does require a course of drugs over a long period of time, where treatment of the prospective study only consisted of treatment for 12 weeks (three months). However, all four of the first-line drugs were administered for the entire period in a fixed dose combination in the animal model. In humans, the standard TB treatment regimen consists of an intensive and continuation phase. The initial intensive phase is the administration of all four drugs for two months where rifampin and isoniazid are administered for a following four months in the continuation phase. With an extended treatment period and incorporating the standard regimen in humans, a clinical trial would benefit in understanding the effects of TB and these treatments on the human gastro-intestinal microbiome, together with the immunological response of the human gut.

References

Dharmadhikari, A.S. & Nardell, E.A. 2008. What animal models teach humans about tuberculosis. *American journal of respiratory cell and molecular biology*, 39(5):503-508. doi:10.1165/rcmb.2008-0154TR

Khan, N., Mendonca, L., Dhariwal, A., Fontes, G., Menzies, D., Xia, J., Divangahi, M. & King, I.L. 2019. Intestinal dysbiosis compromises alveolar macrophage immunity to *Mycobacterium tuberculosis*. *Mucosal Immunology*, 12(3):772-783. doi:10.1038/s41385-019-0147-3

Namasivayam, S., Maiga, M., Yuan, W., Yuan, V., Costa, D.L., Mittereder, L.R., Wipperman, M.F., Glickman, M.S., Dzutsev, A., Trinchieri, G. & Sher, A. 2017. Longitudinal profiling reveals a persistent intestinal dysbiosis triggered by conventional anti-tuberculosis therapy. *Microbiom**e***, 5:71. doi:10.1186/s40168-017-0286-2

Van der Merwe. 2019. Determination of the therapeutic efficacy of a novel Pheroid® formulation in a rodent tuberculosis model. NWU: Potchefstroom Campus. (Dissertation – MSc).

Winglee, K., Eloe-Fadrosh, E., Gupta, S., Guo, H., Fraser, C. & Bishai, W. 2014. Aerosol *Mycobacterium tuberculosis* infection causes rapid loss of diversity in gut microbiota. *PLoS One*, 9(5):e97048. doi:10.1371/journal.pone.0097048

Zhao, Y., Yan, Y., Zhou, W., Chen, D., Huang, K., Yu, S., Mi, J., Lu, L., Zeng, X. & Cao, Y. 2020. Effects of polysaccharides from bee collected pollen of Chinese wolfberry on immune response and gut microbiota composition in cyclophosphamide-treated mice. *Journal of Functional Foods*, 72:104057. doi:10.1016/j.jff.2020.104057

Annexure A Ethics approval

Private Bag X1290, Potchefstroom
South Africa 2520

Tel: 086 016 9698
Web: http://www.nwu.ac.za/

North-West University Animal Care, Health and Safety Research Ethics Committee (NWU-AnimCareREC)

Tel: 018 299-1208
Email: Ethics-AnimCare@nwu.ac.za (for animal studies)

6 October 2019

ETHICS APPROVAL LETTER OF STUDY

Based on approval by the North-West University Animal Care, Health and Safety Research Ethics Committee (NWU-AnimCareREC) on 06/10/2019, the NWU-AnimCareREC hereby approves your study as indicated below. This implies that the NWU-AnimCareREC grants its permission that, provided the general conditions specified below are met and pending any other authorisation that may be necessary, the study may be initiated, using the ethics number below.

Study title: Shifts in the microbiome during anti-tuberculosis therapy in an animal model
Principal Investigator/Study Supervisor/Researcher: Prof AF Grobler
Student: Ms C Wepener - 26124823

Ethics number:

N	W	U	-	0	0	5	8	4	-	1	9	-	A	5
Institution				Study Number						Year			Status	

Status: S = Submission; R = Re-Submission; P = Provisional Authorisation; A = Authorisation

Application Type: Category 0 study
Commencement date: 06/10/2019
Expiry date: 31/10/2020

Risk: **Category 0**

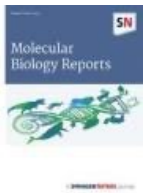
Approval of the study is provided for a year, after which continuation of the study is dependent on receipt and review of an annual monitoring report and the concomitant issuing of a letter of continuation. A monitoring report is due at the end of October annually until completion.

General conditions:

While this ethics approval is subject to all declarations, undertakings and agreements incorporated and signed in the application form, the following general terms and conditions will apply:

- *The principal investigator/study supervisor/researcher must report in the prescribed format to the NWU-AnimCareREC:*
  - *Annually on the monitoring of the study, whereby a letter of continuation will be provided annually, and upon completion of the study; and*
  - *without any delay in case of any adverse event or incident (or any matter that interrupts sound ethical principles) during the course of the study.*
- *The approval applies strictly to the proposal as stipulated in the application form. Should any amendments to the proposal be deemed necessary during the course of the study, the principal investigator/study supervisor/researcher must apply for approval of these amendments at the NWU-AnimCareREC, prior to implementation. Should there be any deviations from the study proposal*

Annexure B Submission guidelines: Molecular Biology Reports



Molecular Biology Reports
An International Journal on Molecular and Cellular Biology

- Journal home
- Submission guidelines

Submission guidelines

Contents

- Instructions for Authors
  - General
  - Original Research Article Guidelines
  - Guidelines for Short Communication Articles
  - (Mini-) Review Article Guidelines
  - Abstract Format
  - Manuscript Submission
  - Title page
  - Text
  - References
  - Tables
  - Artwork and Illustrations Guidelines
  - Supplementary Information (SI)
  - English Language Editing
  - Additional Information
  - Ethical Responsibilities of Authors
  - Authorship principles
  - Compliance with Ethical Standards
  - Conflicts of Interest / Competing Interests
  - After acceptance
  - Open Choice

- Open access publishing

Instructions for Authors

General

The cover letter must include a valid institutional email address for each author. If this is not

possible, the cover letter must include a means of verifying each author – such as an ORCID ID (that contains information on publications, do not include empty IDs) or Scopus ID or a link to their publication record(s).

Authors are encouraged to suggest suitable reviewers and/or request the exclusion of certain individuals when they submit their manuscripts. When suggesting reviewers, authors should make sure they are totally independent and not connected to the work in any way. It is strongly recommended to have a mix of reviewers from different countries and different institutions. When suggesting reviewers, the Corresponding Author must provide an institutional email address for each suggested reviewer, or, if this is not possible to include other means of verifying the identity such as a link to a personal homepage, a link to the publication record or a researcher or author ID in the submission letter. Please note that the Journal may not use the suggestions, but suggestions are appreciated and may help facilitate the peer review process.

Please be sure to check the Compliance with Ethical Standards section. Conflict of Interest statement, ethical approval for animal studies and ethical approval together with informed consent for human studies are mandatory.

Back to top

Original Research Article Guidelines

1. Maximum Word Count: 5,000 words

2. References: 50 or less

3. Results and Discussion: sections should be separate, not combined,

4. Figures and/or Tables: maximum 5 separate figures/tables. A figure should have a maximum of 4 panels.

Back to top

Guidelines for Short Communication Articles

1. Maximum Word Count: 2,500 words

2. References: 25 or less

3. Results and Discussion: sections may be combined

4. Figures and/or Tables: 3 or less (4 panels maximum per figure)

Back to top

(Mini-) Review Article Guidelines

1. Maximum Word Count: 10,000 words (5,000 words for mini-review)

2. References: 100 or less (60 or less for mini-review)

3. Figures and/or Tables: 4 or less

4. Content/Format suggestion: A review article should focus on a single topic of a field and should discuss the most recent findings. They should not be focused on the author's own work but should try to incorporate the work of several different researchers. Language should be simple, new concepts should be defined and specialized terminology must be explained.

The main text of the review article should be divided into sections.

Back to top

Abstract Format

Max Word Count: 250 words

Format: The abstract should be presented divided into subheadings as follows (unless it is a mini or full review article):

I. Background: Brief summary of basic, relevant background info (2-3 sentences). Rationale and

purpose of the study.

II. Methods and Results: Brief explanation of experimental procedure and presentation of

significant results. Include sample sizes as well as animal species if applicable.

III. Conclusions: Succinct interpretation of results as well as significance of findings. Statement

of the main conclusion of the study. Emphasis should be on new information found during the study.

Back to top

Manuscript Submission

Manuscript Submission

Submission of a manuscript implies: that the work described has not been published before; that it is not under consideration for publication anywhere else; that its publication has been approved by all co-authors, if any, as well as by the responsible authorities – tacitly or explicitly – at the institute where the work has been carried out. The publisher will not be held legally responsible should there be any claims for compensation.

Permissions

Authors wishing to include figures, tables, or text passages that have already been published elsewhere are required to obtain permission from the copyright owner(s) for both the print and online format and to include evidence that such permission has been granted when submitting their

papers. Any material received without such evidence will be assumed to originate from the authors.

Online Submission

Please follow the hyperlink "Submit manuscript" on the right and upload all of your manuscript files following the instructions given on the screen.

Please ensure you provide all relevant editable source files. Failing to submit these source files might cause unnecessary delays in the review and production process.

Back to top

Title page

Title Page

Please make sure your title page contains the following information.

Title

The title should be concise and informative.

Author information

- The name(s) of the author(s)
- The affiliation(s) of the author(s), i.e. institution, (department), city, (state), country
- A clear indication and an active e-mail address of the corresponding author
- If available, the 16-digit ORCID of the author(s)

If address information is provided with the affiliation(s) it will also be published.

For authors that are (temporarily) unaffiliated we will only capture their city and country of residence, not their e-mail address unless specifically requested.

Abstract

Please provide an abstract of 150 to 250 words. The abstract should not contain any undefined abbreviations or unspecified references.

For life science journals only (when applicable)

Trial registration number and date of registration

Trial registration number, date of registration followed by "retrospectively registered"

Keywords

Please provide 4 to 6 keywords which can be used for indexing purposes.

Declarations

All manuscripts must contain the following sections under the heading 'Declarations'.

If any of the sections are not relevant to your manuscript, please include the heading and write 'Not applicable' for that section.

To be used for all articles, including articles with biological applications

Funding (information that explains whether and by whom the research was supported)

Conflicts of interest/Competing interests (include appropriate disclosures)

Availability of data and material (data transparency)

Code availability (software application or custom code)

Authors' contributions (optional: please review the submission guidelines from the journal whether statements are mandatory)

Additional declarations for articles in life science journals that report the results of studies involving humans and/or animals

Ethics approval (include appropriate approvals or waivers)

Consent to participate (include appropriate statements)

Consent for publication (include appropriate statements)

Please see the relevant sections in the submission guidelines for further information as well as various examples of wording. Please revise/customize the sample statements according to your own needs.

Back to top

Text

Text Formatting

Manuscripts should be submitted in Word.

- Use a normal, plain font (e.g., 10-point Times Roman) for text.
- Use italics for emphasis.
- Use the automatic page numbering function to number the pages.
- Do not use field functions.
- Use tab stops or other commands for indents, not the space bar.
- Use the table function, not spreadsheets, to make tables.
- Use the equation editor or MathType for equations.
- Save your file in docx format (Word 2007 or higher) or doc format (older Word versions).

Manuscripts with mathematical content can also be submitted in LaTeX.

LaTeX macro package (Download zip, 188 kB)

Headings

Please use no more than three levels of displayed headings.

Abbreviations

Abbreviations should be defined at first mention and used consistently thereafter.

Footnotes

Footnotes can be used to give additional information, which may include the citation of a reference included in the reference list. They should not consist solely of a reference citation, and they should never include the bibliographic details of a reference. They should also not contain any figures or tables.

Footnotes to the text are numbered consecutively; those to tables should be indicated by superscript lower-case letters (or asterisks for significance values and other statistical data). Footnotes to the title or the authors of the article are not given reference symbols.

Always use footnotes instead of endnotes.

Acknowledgments

Acknowledgments of people, grants, funds, etc. should be placed in a separate section on the title page. The names of funding organizations should be written in full.

Back to top

References

Citation

Reference citations in the text should be identified by numbers in square brackets. Some examples:

1. Negotiation research spans many disciplines [3].

2. This result was later contradicted by Becker and Seligman [5].

3. This effect has been widely studied [1-3, 7].

Reference list

The list of references should only include works that are cited in the text and that have been published or accepted for publication. Personal communications and unpublished works should only be mentioned in the text. Do not use footnotes or endnotes as a substitute for a reference list.

The entries in the list should be numbered consecutively.

If available, please always include DOIs as full DOI links in your reference list (e.g. “https://doi.org/abc”).

- Journal article

  Gamelin FX, Baquet G, Berthoin S, Thevenet D, Nourry C, Nottin S, Bosquet L (2009) Effect of high intensity intermittent training on heart rate variability in prepubescent children. Eur J Appl Physiol 105:731-738. https://doi.org/10.1007/s00421-008-0955-8

  Ideally, the names of all authors should be provided, but the usage of “et al” in long author lists will also be accepted:

  Smith J, Jones M Jr, Houghton L et al (1999) Future of health insurance. N Engl J Med 965:325–329

- Article by DOI

  Slifka MK, Whitton JL (2000) Clinical implications of dysregulated cytokine production. J Mol Med. https://doi.org/10.1007/s001090000086

- Book

  South J, Blass B (2001) The future of modern genomics. Blackwell, London

- Book chapter

  Brown B, Aaron M (2001) The politics of nature. In: Smith J (ed) The rise of modern genomics, 3rd edn. Wiley, New York, pp 230-257

- Online document

  Cartwright J (2007) Big stars have weather too. IOP Publishing PhysicsWeb. http://physicsweb.org/articles/news/11/6/16/1. Accessed 26 June 2007

- Dissertation

  Trent JW (1975) Experimental acute renal failure. Dissertation, University of California

Always use the standard abbreviation of a journal's name according to the ISSN List of Title Word Abbreviations, see

ISSN.org LTWA

If you are unsure, please use the full journal title.

Authors preparing their manuscript in LaTeX can use the bibtex file spbasic.bst which is included in Springer's LaTeX macro package.

Back to top

Tables

- All tables are to be numbered using Arabic numerals.
- Tables should always be cited in text in consecutive numerical order.
- For each table, please supply a table caption (title) explaining the components of the table.
- Identify any previously published material by giving the original source in the form of a reference at the end of the table caption.
- Footnotes to tables should be indicated by superscript lower-case letters (or asterisks for significance values and other statistical data) and included beneath the table body.

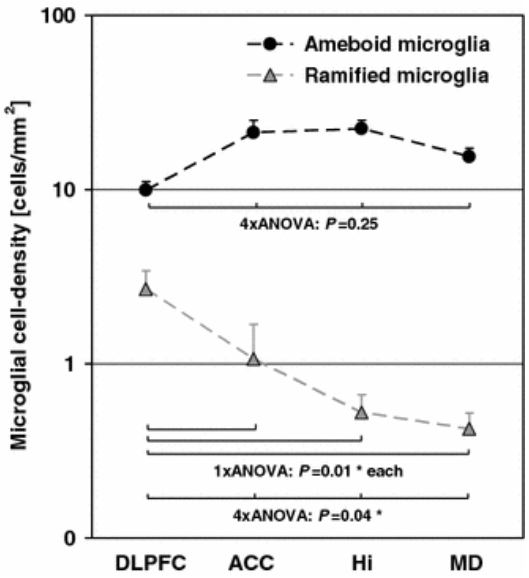
Back to top

Artwork and Illustrations Guidelines

Electronic Figure Submission

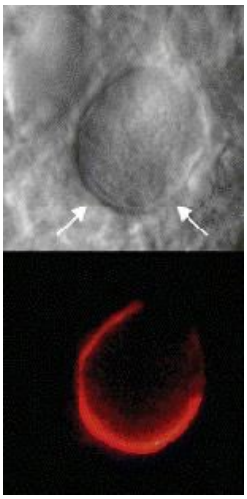
- Supply all figures electronically.
- Indicate what graphics program was used to create the artwork.
- For vector graphics, the preferred format is EPS; for halftones, please use TIFF format. MSOffice files are also acceptable.
- Vector graphics containing fonts must have the fonts embedded in the files.
- Name your figure files with "Fig" and the figure number, e.g., Fig1.eps.

Line Art



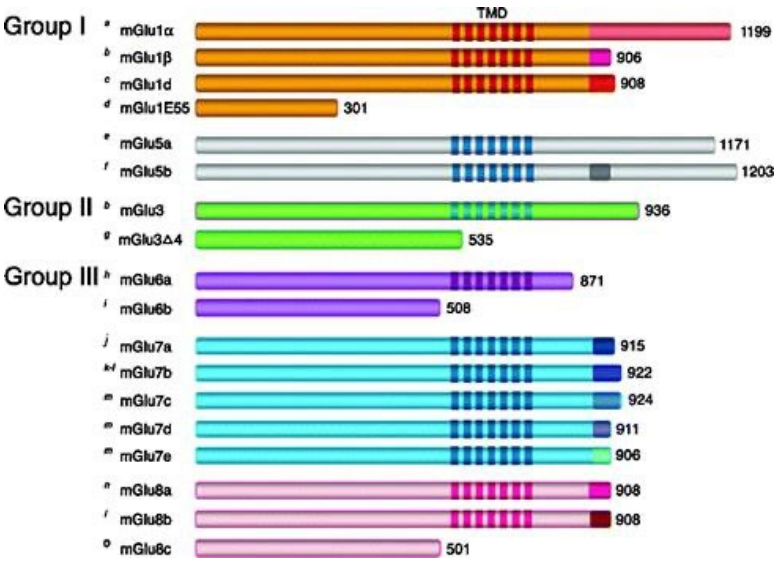
- Definition: Black and white graphic with no shading.
- Do not use faint lines and/or lettering and check that all lines and lettering within the figures are legible at final size.
- All lines should be at least 0.1 mm (0.3 pt) wide.
- Scanned line drawings and line drawings in bitmap format should have a minimum resolution of 1200 dpi.
- Vector graphics containing fonts must have the fonts embedded in the files.

Halftone Art



- Definition: Photographs, drawings, or paintings with fine shading, etc.
- If any magnification is used in the photographs, indicate this by using scale bars within the figures themselves.
- Halftones should have a minimum resolution of 300 dpi.

Combination Art



- Definition: a combination of halftone and line art, e.g., halftones containing line drawing, extensive lettering, color diagrams, etc.
- Combination artwork should have a minimum resolution of 600 dpi.

Color Art

- Color art is free of charge for online publication.
- If black and white will be shown in the print version, make sure that the main information will still be visible. Many colors are not distinguishable from one another when converted to black and white. A simple way to check this is to make a xerographic copy to see if the necessary distinctions between the different colors are still apparent.
- If the figures will be printed in black and white, do not refer to color in the captions.
- Color illustrations should be submitted as RGB (8 bits per channel).

Figure Lettering

- To add lettering, it is best to use Helvetica or Arial (sans serif fonts).
- Keep lettering consistently sized throughout your final-sized artwork, usually about 2–3 mm (8–12 pt).
- Variance of type size within an illustration should be minimal, e.g., do not use 8-pt type on an axis and 20-pt type for the axis label.
- Avoid effects such as shading, outline letters, etc.
- Do not include titles or captions within your illustrations.

Figure Numbering

- All figures are to be numbered using Arabic numerals.
- Figures should always be cited in text in consecutive numerical order.
- Figure parts should be denoted by lowercase letters (a, b, c, etc.).
- If an appendix appears in your article and it contains one or more figures, continue the consecutive numbering of the main text. Do not number the appendix figures,"A1, A2, A3, etc." Figures in online appendices [Supplementary Information (SI)] should, however, be numbered separately.

Figure Captions

- Each figure should have a concise caption describing accurately what the figure depicts. Include the captions in the text file of the manuscript, not in the figure file.
- Figure captions begin with the term Fig. in bold type, followed by the figure number, also in bold type.

- No punctuation is to be included after the number, nor is any punctuation to be placed at the end of the caption.
- Identify all elements found in the figure in the figure caption; and use boxes, circles, etc., as coordinate points in graphs.
- Identify previously published material by giving the original source in the form of a reference citation at the end of the figure caption.

Figure Placement and Size

- Figures should be submitted separately from the text, if possible.
- When preparing your figures, size figures to fit in the column width.
- For large-sized journals the figures should be 84 mm (for double-column text areas), or 174 mm (for single-column text areas) wide and not higher than 234 mm.
- For small-sized journals, the figures should be 119 mm wide and not higher than 195 mm.

Permissions

If you include figures that have already been published elsewhere, you must obtain permission from the copyright owner(s) for both the print and online format. Please be aware that some publishers do not grant electronic rights for free and that Springer will not be able to refund any costs that may have occurred to receive these permissions. In such cases, material from other sources should be used.

Accessibility

In order to give people of all abilities and disabilities access to the content of your figures, please make sure that

- All figures have descriptive captions (blind users could then use a text-to-speech software or a text-to-Braille hardware)
- Patterns are used instead of or in addition to colors for conveying information (colorblind users would then be able to distinguish the visual elements)
- Any figure lettering has a contrast ratio of at least 4.5:1

Back to top

Supplementary Information (SI)

Springer accepts electronic multimedia files (animations, movies, audio, etc.) and other supplementary files to be published online along with an article or a book chapter. This feature can add dimension to the author's article, as certain information cannot be printed or is more convenient in electronic form.

Before submitting research datasets as Supplementary Information, authors should read the journal's Research data policy. We encourage research data to be archived in data repositories wherever possible.

Submission

- Supply all supplementary material in standard file formats.
- Please include in each file the following information: article title, journal name, author names; affiliation and e-mail address of the corresponding author.
- To accommodate user downloads, please keep in mind that larger-sized files may require very long download times and that some users may experience other problems during downloading.

Audio, Video, and Animations

- Aspect ratio: 16:9 or 4:3
- Maximum file size: 25 GB
- Minimum video duration: 1 sec
- Supported file formats: avi, wmv, mp4, mov, m2p, mp2, mpg, mpeg, flv, mxf, mts, m4v, 3gp

Text and Presentations

- Submit your material in PDF format; .doc or .ppt files are not suitable for long-term viability.
- A collection of figures may also be combined in a PDF file.

Spreadsheets

- Spreadsheets should be submitted as .csv or .xlsx files (MS Excel).

Specialized Formats

- Specialized format such as .pdb (chemical), .wrl (VRML), .nb (Mathematica notebook), and .tex can also be supplied.

Collecting Multiple Files

- It is possible to collect multiple files in a .zip or .gz file.

Numbering

- If supplying any supplementary material, the text must make specific mention of the material as a citation, similar to that of figures and tables.
- Refer to the supplementary files as “Online Resource”, e.g., "... as shown in the animation (Online Resource 3)", “... additional data are given in Online Resource 4”.
- Name the files consecutively, e.g. “ESM_3.mpg”, “ESM_4.pdf”.

Captions

- For each supplementary material, please supply a concise caption describing the content of the file.

Processing of supplementary files

- Supplementary Information (SI) will be published as received from the author without any conversion, editing, or reformatting.

Accessibility

In order to give people of all abilities and disabilities access to the content of your supplementary files, please make sure that

- The manuscript contains a descriptive caption for each supplementary material
- Video files do not contain anything that flashes more than three times per second (so that users prone to seizures caused by such effects are not put at risk)

Back to top

English Language Editing

For editors and reviewers to accurately assess the work presented in your manuscript you need to ensure the English language is of sufficient quality to be understood. If you need help with writing in English you should consider:

- Asking a colleague who is a native English speaker to review your manuscript for clarity.
- Visiting the English language tutorial which covers the common mistakes when writing in English.
- Using a professional language editing service where editors will improve the English to ensure that your meaning is clear and identify problems that require your review. Two such services are provided by our affiliates Nature Research Editing Service and American Journal Experts. Springer authors are entitled to a 10% discount on their first submission to either of these services, simply follow the links below.

English language tutorial

Nature Research Editing Service

American Journal Experts

Please note that the use of a language editing service is not a requirement for publication in this journal and does not imply or guarantee that the article will be selected for peer review or accepted.

If your manuscript is accepted it will be checked by our copyeditors for spelling and formal style before publication.

.

为便于编辑和评审专家准确评估您稿件中陈述的研究工作，您需要确保您的英语语言质量足以令人理解。如果您需要英文写作方面的帮助，您可以考虑：

● 请一位以英语为母语的同事审核您**的稿件是否表意清晰**。

● 查看一些有关英语写作中常见语言错误的教程。

● 使用专业语言编辑服务，编辑人员会对英语进行润色，以确保您的意思表达清晰，并识别需要您复核的问题。我们的附属机构 Nature Research Editing Service 和合作伙伴 American Journal Experts 即可提供此类服务。

教程

Nature Research Editing Service

American Journal Experts

请注意，使用语言编辑服务并非在期刊上发表文章的必要条件，同时也并不意味或保证文章将被选中进行同行评议或被接受。

如果您的稿件被接受，在发表之前，我们的文字编辑会检查您的文稿拼写是否规范以及文体是否正式。

.

エディターと査読者があなたの論文を正しく評価するには、使用されている英語の質が十分に高いことが必要とされます。英語での論文執筆に際してサポートが必要な場合には、次のオプションがあります：

・英語を母国語とする同僚に、原稿で使用されている英語が明確であるかをチェックしてもらう。

・英語で執筆する際のよくある間違いに関する英語のチュートリアルを参照する。

・プロの英文校正サービスを利用する。校正者が原稿の意味を明確にしたり、問題点を指摘し、英語の質を向上させます。Nature Research Editing Service とAmerican Journal Experts の2つは弊社と提携しているサービスです。Springer の著者は、いずれのサービスも初めて利用する際には10%の割引を受けることができます。以下のリンクを参照ください。

英語のチュートリアル

Nature Research Editing Service

American Journal Experts

英文校正サービスの利用は、投稿先のジャーナルに掲載されるための条件ではないこと、また論文審査や受理を保証するものではないことに留意してください。

原稿が受理されると、出版前に弊社のコピーエディターがスペルと体裁のチェックを行います。

.

영어 원고의 경우, 에디터 및 리뷰어들이 귀하의 원고에 실린 결과물을 정확하게 평가할 수 있도록, 그들이 충분히 이해할 수 있을 만한 수준으로 작성되어야 합니다. 만약 영작문과 관련하여 도움을 받기를 원하신다면 다음의 사항들을 고려하여 주십시오:

• 귀하의 원고의 표현을 명확히 해줄 영어 원어민 동료를 찾아서 리뷰를 의뢰합니다.

• 영어 튜토리얼 페이지에 방문하여 영어로 글을 쓸 때 자주하는 실수들을 확인합니다.

• 리뷰에 대비하여, 원고의 의미를 명확하게 해주고 리뷰에서 요구하는 문제점들을 식별해서 영문 수준을 향상시켜주는 전문 영문 교정 서비스를 이용합니다. Nature Research Editing Service와 American Journal Experts에서 저희와 협약을 통해 서비스를 제공하고 있습니다. Springer 저자들이 본 교정 서비스를 첫 논문 투고를 위해 사용하시는 경우 10%의 할인이 적용되며, 아래의 링크를 통하여 확인이 가능합니다.

영어 튜토리얼 페이지

Nature Research Editing Service

American Journal Experts

영문 교정 서비스는 게재를 위한 요구사항은 아니며, 해당 서비스의 이용이 피어 리뷰에 논문이 선택되거나 게재가 수락되는 것을 의미하거나 보장하지 않습니다.

원고가 수락될 경우, 출판 전 저희측 편집자에 의해 원고의 철자 및 문체를 검수하는 과정을 거치게 됩니다.

Back to top

Additional Information

Authors should suggest six to eight individuals with position, affiliation, country, email address and expertise. To avoid possible bias and conflicts of interest, authors are not allowed to suggest reviewers from the same institute. Non-American authors must list at least four reviewers from outside their country of origin. Papers may be returned without review if authors do not adhere to the above rules.

Back to top

Ethical Responsibilities of Authors

This journal is committed to upholding the integrity of the scientific record. As a member of the Committee on Publication Ethics (COPE) the journal will follow the COPE guidelines on how to deal with potential acts of misconduct.

Authors should refrain from misrepresenting research results which could damage the trust in the journal, the professionalism of scientific authorship, and ultimately the entire scientific endeavour. Maintaining integrity of the research and its presentation is helped by following the rules of good scientific practice, which include*:

- The manuscript should not be submitted to more than one journal for simultaneous consideration.
- The submitted work should be original and should not have been published elsewhere in any form or language (partially or in full), unless the new work concerns an expansion of previous work. (Please

provide transparency on the re-use of material to avoid the concerns about text-recycling ('self-plagiarism').

- A single study should not be split up into several parts to increase the quantity of submissions and submitted to various journals or to one journal over time (i.e. 'salami-slicing/publishing').
- Concurrent or secondary publication is sometimes justifiable, provided certain conditions are met. Examples include: translations or a manuscript that is intended for a different group of readers.
- Results should be presented clearly, honestly, and without fabrication, falsification or inappropriate data manipulation (including image based manipulation). Authors should adhere to discipline-specific rules for acquiring, selecting and processing data.
- No data, text, or theories by others are presented as if they were the author's own ('plagiarism'). Proper acknowledgements to other works must be given (this includes material that is closely copied (near verbatim), summarized and/or paraphrased), quotation marks (to indicate words taken from another source) are used for verbatim copying of material, and permissions secured for material that is copyrighted.

Important note: the journal may use software to screen for plagiarism.

- Authors should make sure they have permissions for the use of software, questionnaires/(web) surveys and scales in their studies (if appropriate).
- Research articles and non-research articles (e.g. Opinion, Review, and Commentary articles) must cite appropriate and relevant literature in support of the claims made. Excessive and inappropriate self-citation or coordinated efforts among several authors to collectively self-cite is strongly discouraged.
- Authors should avoid untrue statements about an entity (who can be an individual person or a company) or descriptions of their behavior or actions that could potentially be seen as personal attacks or allegations about that person.
- Research that may be misapplied to pose a threat to public health or national security should be clearly identified in the manuscript (e.g. dual use of research). Examples include creation of harmful consequences of biological agents or toxins, disruption of immunity

of vaccines, unusual hazards in the use of chemicals, weaponization of research/technology (amongst others).

- Authors are strongly advised to ensure the author group, the Corresponding Author, and the order of authors are all correct at submission. Adding and/or deleting authors during the revision stages is generally not permitted, but in some cases may be warranted. Reasons for changes in authorship should be explained in detail. Please note that changes to authorship cannot be made after acceptance of a manuscript.

*All of the above are guidelines and authors need to make sure to respect third parties rights such as copyright and/or moral rights.

Upon request authors should be prepared to send relevant documentation or data in order to verify the validity of the results presented. This could be in the form of raw data, samples, records, etc. Sensitive information in the form of confidential or proprietary data is excluded.

If there is suspicion of misbehavior or alleged fraud the Journal and/or Publisher will carry out an investigation following COPE guidelines. If, after investigation, there are valid concerns, the author(s) concerned will be contacted under their given e-mail address and given an opportunity to address the issue. Depending on the situation, this may result in the Journal's and/or Publisher's implementation of the following measures, including, but not limited to:

- If the manuscript is still under consideration, it may be rejected and returned to the author.
- If the article has already been published online, depending on the nature and severity of the infraction:

  - an erratum/correction may be placed with the article

  - an expression of concern may be placed with the article

  - or in severe cases retraction of the article may occur.

The reason will be given in the published erratum/correction, expression of concern or retraction note. Please note that retraction means that the

article is **maintained on the platform**, watermarked "retracted" and the explanation for the retraction is provided in a note linked to the watermarked article.

- The author's institution may be informed
- A notice of suspected transgression of ethical standards in the peer review system may be included as part of the author's and article's bibliographic record.

Fundamental errors

Authors have an obligation to correct mistakes once they discover a significant error or inaccuracy in their published article. The author(s) is/are requested to contact the journal and explain in what sense the error is impacting the article. A decision on how to correct the literature will depend on the nature of the error. This may be a correction or retraction. The retraction note should provide transparency which parts of the article are impacted by the error.

Suggesting / excluding reviewers

Authors are welcome to suggest suitable reviewers and/or request the exclusion of certain individuals when they submit their manuscripts. When suggesting reviewers, authors should make sure they are totally independent and not connected to the work in any way. It is strongly recommended to suggest a mix of reviewers from different countries and different institutions. When suggesting reviewers, the Corresponding Author must provide an institutional email address for each suggested reviewer, or, if this is not possible to include other means of verifying the identity such as a link to a personal homepage, a link to the publication record or a researcher or author ID in the submission letter. Please note that the Journal may not use the suggestions, but suggestions are appreciated and may help facilitate the peer review process.

Back to top

Authorship principles

These guidelines describe authorship principles and good authorship practices to which prospective authors should adhere to.

Authorship clarified

The Journal and Publisher assume all authors agreed with the content and that all gave explicit consent to submit and that they obtained consent from the responsible authorities at the institute/organization where the work has been carried out, **before** the work is submitted.

The Publisher does not prescribe the kinds of contributions that warrant authorship. It is recommended that authors adhere to the guidelines for authorship that are applicable in their specific research field. In absence of specific guidelines it is recommended to adhere to the following guidelines*:

All authors whose names appear on the submission

1) made substantial contributions to the conception or design of the work; or the acquisition, analysis, or interpretation of data; or the creation of new software used in the work;

2) drafted the work or revised it critically for important intellectual content;

3) approved the version to be published; and

4) agree to be accountable for all aspects of the work in ensuring that questions related to the accuracy or integrity of any part of the work are appropriately investigated and resolved.

* Based on/adapted from:

ICMJE, Defining the Role of Authors and Contributors,

Transparency in authors' contributions and responsibilities to promote integrity in scientific publication, McNutt at all, PNAS February 27, 2018

Disclosures and declarations

All authors are requested to include information regarding sources of funding, financial or non-financial interests, study-specific approval by the appropriate ethics committee for research involving humans and/or

animals, informed consent if the research involved human participants, and a statement on welfare of animals if the research involved animals (as appropriate).

The decision whether such information should be included is not only dependent on the scope of the journal, but also the scope of the article. Work submitted for publication may have implications for public health or general welfare and in those cases it is the responsibility of all authors to include the appropriate disclosures and declarations.

Data transparency

All authors are requested to make sure that all data and materials as well as software application or custom code support their published claims and comply with field standards. Please note that journals may have individual policies on (sharing) research data in concordance with disciplinary norms and expectations.

Role of the Corresponding Author

One author is assigned as Corresponding Author and acts on behalf of all co-authors and ensures that questions related to the accuracy or integrity of any part of the work are appropriately addressed.

The Corresponding Author is responsible for the following requirements:

- ensuring that all listed authors have approved the manuscript before submission, including the names and order of authors;
- managing all communication between the Journal and all co-authors, before and after publication;*
- providing transparency on re-use of material and mention any unpublished material (for example manuscripts in press) included in the manuscript in a cover letter to the Editor;
- making sure disclosures, declarations and transparency on data statements from all authors are included in the manuscript as appropriate (see above).

* The requirement of managing all communication between the journal and all co-authors during submission and proofing may be delegated to a

Contact or Submitting Author. In this case please make sure the Corresponding Author is clearly indicated in the manuscript.

Author contributions

In absence of specific instructions and in research fields where it is possible to describe discrete efforts, the Publisher recommends authors to include contribution statements in the work that specifies the contribution of every author in order to promote transparency. These contributions should be listed at the separate title page.

Examples of such statement(s) are shown below:

• Free text:

All authors contributed to the study conception and design. Material preparation, data collection and analysis were performed by [full name], [full name] and [full name]. The first draft of the manuscript was written by [full name] and all authors commented on previous versions of the manuscript. All authors read and approved the final manuscript.

Example: CRediT taxonomy:

• Conceptualization: [full name], ...; Methodology: [full name], ...; Formal analysis and investigation: [full name], ...; Writing - original draft preparation: [full name, ...]; Writing - review and editing: [full name], ...; Funding acquisition: [full name], ...; Resources: [full name], ...; Supervision: [full name],....

For **review articles** where discrete statements are less applicable a statement should be included who had the idea for the article, who performed the literature search and data analysis, and who drafted and/or critically revised the work.

For articles that are based primarily on the **student's dissertation or thesis**, it is recommended that the student is usually listed as principal author:

A Graduate Student's Guide to Determining Authorship Credit and Authorship Order, APA Science Student Council 2006

Affiliation

The primary affiliation for each author should be the institution where the majority of their work was done. If an author has subsequently moved, the current address may additionally be stated. Addresses will not be updated or changed after publication of the article.

Changes to authorship

Authors are strongly advised to ensure the correct author group, the Corresponding Author, and the order of authors at submission. Changes of authorship by adding or deleting authors, and/or changes in Corresponding Author, and/or changes in the sequence of authors are **not** accepted **after acceptance** of a manuscript.

- **Please note that author names will be published exactly as they appear on the accepted submission!**

Please make sure that the names of all authors are present and correctly spelled, and that addresses and affiliations are current.

Adding and/or deleting authors at revision stage are generally not permitted, but in some cases it may be warranted. Reasons for these changes in authorship should be explained. Approval of the change during revision is at the discretion of the Editor-in-Chief. Please note that journals may have individual policies on adding and/or deleting authors during revision stage.

Author identification

Authors are recommended to use their ORCID ID when submitting an article for consideration or acquire an ORCID ID via the submission process.

Deceased or incapacitated authors

For cases in which a co-author dies or is incapacitated during the writing, submission, or peer-review process, and the co-authors feel it is

appropriate to include the author, co-authors should obtain approval from a (legal) representative which could be a direct relative.

Authorship issues or disputes

In the case of an authorship dispute during peer review or after acceptance and publication, the Journal will not be in a position to investigate or adjudicate. Authors will be asked to resolve the dispute themselves. If they are unable the Journal reserves the right to withdraw a manuscript from the editorial process or in case of a published paper raise the issue with the authors' institution(s) and abide by its guidelines.

Confidentiality

Authors should treat all communication with the Journal as confidential which includes correspondence with direct representatives from the Journal such as Editors-in-Chief and/or Handling Editors and reviewers' reports unless explicit consent has been received to share information.

Back to top

Compliance with Ethical Standards

To ensure objectivity and transparency in research and to ensure that accepted principles of ethical and professional conduct have been followed, authors should include information regarding sources of funding, potential conflicts of interest (financial or non-financial), informed consent if the research involved human participants, and a statement on welfare of animals if the research involved animals.

Authors should include the following statements (if applicable) in a separate section entitled "Compliance with Ethical Standards" when submitting a paper:

- Disclosure of potential conflicts of interest
- Research involving Human Participants and/or Animals
- Informed consent

Please note that standards could vary slightly per journal dependent on their peer review policies (i.e. single or double blind peer review) as well as

per journal subject discipline. Before submitting your article check the instructions following this section carefully.

The corresponding author should be prepared to collect documentation of compliance with ethical standards and send if requested during peer review or after publication.

The Editors reserve the right to reject manuscripts that do not comply with the above-mentioned guidelines. The author will be held responsible for false statements or failure to fulfill the above-mentioned guidelines.

Back to top

Conflicts of Interest / Competing Interests

Authors are requested to disclose interests *that are directly or indirectly related to the work submitted for publication*. Interests within the last 3 years of beginning the work (conducting the research and preparing the work for submission) should be reported. Interests outside the 3-year time frame must be disclosed if they could reasonably be perceived as influencing the submitted work. Disclosure of interests provides a complete and transparent process and helps readers form their own judgments of potential bias. This is not meant to imply that a financial relationship with an organization that sponsored the research or compensation received for consultancy work is inappropriate.

Interests that should be considered and disclosed but are not limited to the following:

Funding: Research grants from funding agencies (please give the research funder and the grant number) and/or research support (including salaries, equipment, supplies, reimbursement for attending symposia, and other expenses) by organizations that may gain or lose financially through publication of this manuscript.

Employment: Recent (while engaged in the research project), present or anticipated employment by any organization that may gain or lose financially through publication of this manuscript. This includes multiple affiliations (if applicable).

Financial interests: Stocks or shares in companies (including holdings of spouse and/or children) that may gain or lose financially through publication of this manuscript; consultation fees or other forms of remuneration from organizations that may gain or lose financially; patents or patent applications whose value may be affected by publication of this manuscript.

It is difficult to specify a threshold at which a financial interest becomes significant, any such figure is necessarily arbitrary, so one possible practical guideline is the following: "Any undeclared financial interest that could embarrass the author were it to become publicly known after the work was published."

Non-financial interests: In addition, authors are requested to disclose interests that go beyond financial interests that could impart bias on the work submitted for publication such as professional interests, personal relationships or personal beliefs (amongst others). Examples include, but are not limited to: position on editorial board, advisory board or board of directors or other type of management relationships; writing and/or consulting for educational purposes; expert witness; mentoring relations; and so forth.

Primary research articles require a disclosure statement. Review articles present an expert synthesis of evidence and may be treated as an authoritative work on a subject. Review articles therefore require a disclosure statement.Other article types such as editorials, book reviews, comments (amongst others) may, dependent on their content, require a disclosure statement. If you are unclear whether your article type requires a disclosure statement, please contact the Editor-in-Chief.

Please note that, in addition to the above requirements, funding information (given that funding is a potential conflict of interest (as mentioned above)) needs to be disclosed upon submission of the manuscript in the peer review system. This information will automatically be added to the Record of CrossMark, however it is **not added** to the manuscript itself. Under 'summary of requirements' (see below) funding information should be included in the '**Declarations**' section.

Summary of requirements

The above should be summarized in a statement and placed in a 'Declarations' section before the reference list under a heading of 'Funding' and/or 'Conflicts of interests'/'Competing interests'. Other declarations include Ethics approval, Consent, Data, Material and/or Code availability and Authors' contribution statements.

Please see the various examples of wording below and revise/customize the sample statements according to your own needs.

When all authors have the same (or no) conflicts and/or funding it is sufficient to use one blanket statement.

Examples of statements to be used when funding has been received:

- Partial financial support was received from [...]
- The research leading to these results received funding from [...] under Grant Agreement No[...].
- This study was funded by [...]
- This work was supported by [...] (Grant numbers [...] and [...]

Examples of statements to be used when there is no funding:

- The authors did not receive support from any organization for the submitted work.
- No funding was received to assist with the preparation of this manuscript.
- No funding was received for conducting this study.
- No funds, grants, or other support was received.

Examples of statements to be used when there are interests to declare:

- **Financial interests:** Author A has received research support from Company A. Author B has received a speaker honorarium from Company Wand owns stock in Company X. Author C is consultant to company Y.

Non-financial interests: Author C is an unpaid member of committee Z.

- **Financial interests:** The authors declare they have no financial interests.

  Non-financial interests: Author A is on the board of directors of Y and receives no compensation as member of the board of directors.

- **Financial interests:** Author A received a speaking fee from Y for Z. Author B receives a salary from association X. X where s/he is the Executive Director.

  Non-financial interests: none.

- **Financial interests:** Author A and B declare they have no financial interests. Author C has received speaker and consultant honoraria from Company M and Company N. Dr. C has received speaker honorarium and research funding from Company M and Company O. Author D has received travel support from Company O.

  Non-financial interests: Author D has served on advisory boards for Company M, Company N and Company O.

Examples of statements to be used when authors have nothing to declare:

- The authors have no relevant financial or non-financial interests to disclose.
- The authors have no conflicts of interest to declare that are relevant to the content of this article.
- All authors certify that they have no affiliations with or involvement in any organization or entity with any financial interest or non-financial interest in the subject matter or materials discussed in this manuscript.
- The authors have no financial or proprietary interests in any material discussed in this article.

Authors are responsible for correctness of the statements provided in the manuscript. See also Authorship Principles. The Editor-in-Chief reserves the right to reject submissions that do not meet the guidelines described in this section.

Back to top

After acceptance

Upon acceptance, your article will be exported to Production to undergo typesetting. Once typesetting is complete, you will receive a link asking you to confirm your affiliation, choose the publishing model for your article as well as arrange rights and payment of any associated publication cost.

Once you have completed this, your article will be processed and you will receive the proofs.

Article publishing agreement

Depending on the ownership of the journal and its policies, you will either grant the Publisher an exclusive licence to publish the article or will be asked to transfer copyright of the article to the Publisher.

Offprints

Offprints can be ordered by the corresponding author.

Color illustrations

Online publication of color illustrations is free of charge. For color in the print version, authors will be expected to make a contribution towards the extra costs.

Proof reading

The purpose of the proof is to check for typesetting or conversion errors and the completeness and accuracy of the text, tables and figures. Substantial changes in content, e.g., new results, corrected values, title and authorship, are not allowed without the approval of the Editor.

After online publication, further changes can only be made in the form of an Erratum, which will be hyperlinked to the article.

Online First

The article will be published online after receipt of the corrected proofs. This is the official first publication citable with the DOI. After release of the printed version, the paper can also be cited by issue and page numbers.

Back to top

Open Choice

Open Choice allows you to publish open access in more than 1850 Springer Nature journals, making your research more visible and accessible immediately on publication.

Article processing charges (APCs) vary by journal – view the full list

Benefits:

- Increased researcher engagement: Open Choice enables access by anyone with an internet connection, immediately on publication.
- Higher visibility and impact: In Springer hybrid journals, OA articles are accessed 4 times more often on average, and cited 1.7 more times on average*.
- Easy compliance with funder and institutional mandates: Many funders require open access publishing, and some take compliance into account when assessing future grant applications.

It is easy to find funding to support open access – please see our funding and support pages for more information.

*) Within the first three years of publication. Springer Nature hybrid journal OA impact analysis, 2018.

Open Choice

Funding and Support pages

Copyright and license term – CC BY

Open Choice articles do not require transfer of copyright as the copyright remains with the author. In opting for open access, the author(s) agree to publish the article under the Creative Commons Attribution License.

Find more about the license agreement

Back to top

Open access publishing

Molecular Biology Reports publishes open access articles. Authors of open access articles published in this journal retain the copyright of their articles and are free to reproduce and disseminate their work.

Visit our Open access publishing page to learn more.

Back to top

For authors

Submission guidelinesEthics & disclosuresFees and fundingContact the journalSubmit manuscript

Explore

Online first articlesVolumes and issues Sign up for alerts

Publish with us

Authors & Editors
Journal authors
Publishing ethics
Open Access & Springer

Discover content

SpringerLink
Books A-Z
Journals A-Z
Video

Other services

Instructors
Librarians (Springer Nature)
Societies and Publishing Partners
Advertisers
Shop on Springer.com

About Springer

About us
Help & Support
Contact us
Press releases
Impressum

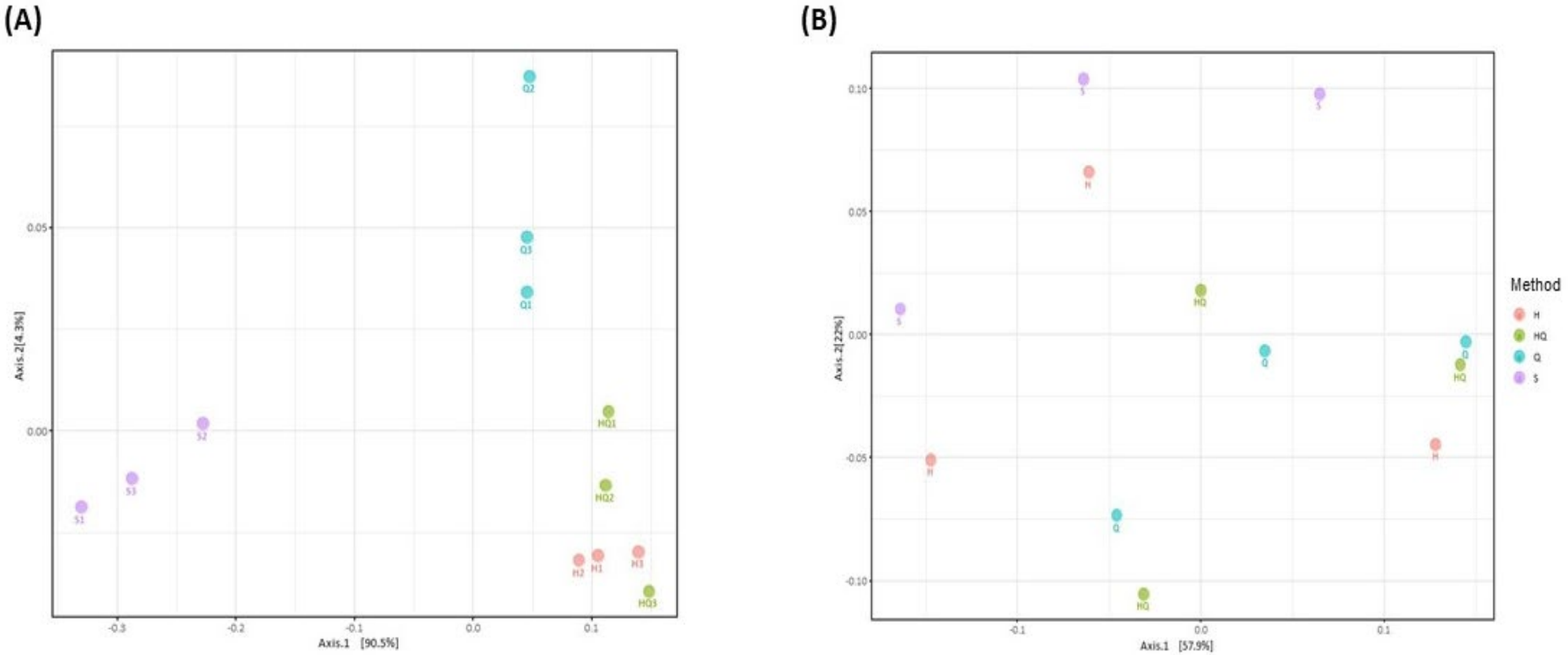
Legal

General term & conditions
California Privacy Statement
Rights & permissions
Privacy
How we use cookies
Manage cookies/Do not sell my data
Accessibility

Not logged in - 217.29.214.21
Not affiliated

© 2021 Springer Nature Switzerland AG. Part of Springer Nature.

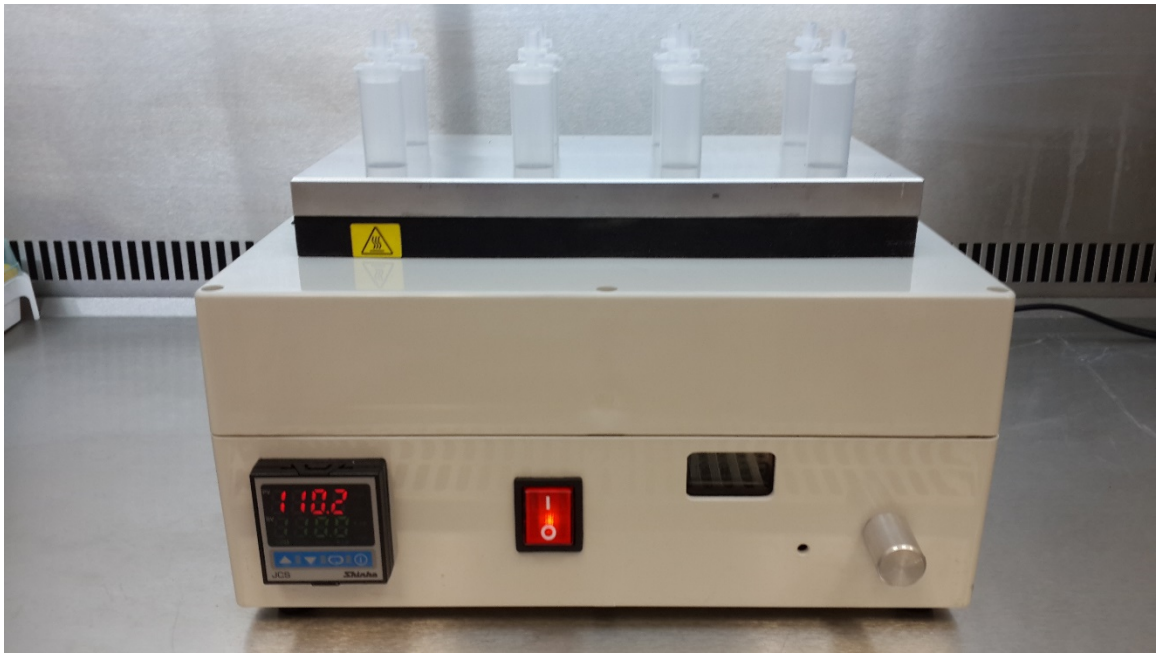
Annexure C Supplementary figures associated with manuscript (Chapter 3)



Supplementary figure 1: Principal coordinates analysis based on Bray–Curtis distances of samples extracted by various methods for selected clinical sputum sample (A) and representative gut sample (B). Samples that are more similar to one another are ordinated closer together.



Supplementary figure 2: Lyses micro tube (LMT).



Supplementary figure 3: NWU automated lyser device.

Annexure D Colony forming units (CFUs) of *Mycobacterium tuberculosis* (*Mtb*) in the lungs of C3HeB/FeJ mice during and after TB therapies (van der Merwe, 2019)

Table 7-2: Lung CFU during the treatment phase

Study group	Week 1	Week 2	Week 3	Week 4	Week 8	Week 12
Positive control	6.23 ± 0.15^{aD}	4.99 ± 0.64^{aC}	4.28 ± 0.57^{aAC}	3.74 ± 0.45^{aAB}	3.94 ± 0.87^{aA}	2.56 ± 0.40^{aB}
Carrier control	6.84 ± 0.30^{bB}	7.54 ± 0.26^{bAB}	7.60 ± 0.35^{bAB}	7.84 ± 0.39^{bA}	8.15 ± 0.52^{bA}	7.60 ± 0.82^{bAB}
Test formulation	6.03 ± 0.36^{aC}	5.62 ± 0.42^{aBC}	4.53 ± 0.80^{aABC}	4.25 ± 1.00^{aAB}	4.01 ± 1.23^{aA}	2.36 ± 0.51^{aD}
Negative control	6.40±0.08*	-	-	5.19±1.94*	7.07±0.28*	-

$^{a/A}$ A value belonging to group A according to the Tukey HSD variability test. This value will differ statistically significant compared to a value belonging to group B. Small letter should be interpreted vertically and capital letters horizontally.
$^{b/B}$ A value belonging to group B according to the Tukey HSD variability test. This value will differ statistically significant compared to a value belonging to group A. Small letter should be interpreted vertically and capital letters horizontally.
$^{c/C}$ A value belonging to group C according to the Tukey HSD variability test. This value will differ statistically significant compared to a value belonging to group A or B. Small letter should be interpreted vertically and capital letters horizontally
$^{ab/AB}$ A value belonging to both group A and B. This value does not differ statistically significant from either a value in group A or B according to the Tukey HSD variability test. Small letter should be interpreted vertically and capital letters horizontally.
***No statistically significant conclusions could be made with regards to the negative control**

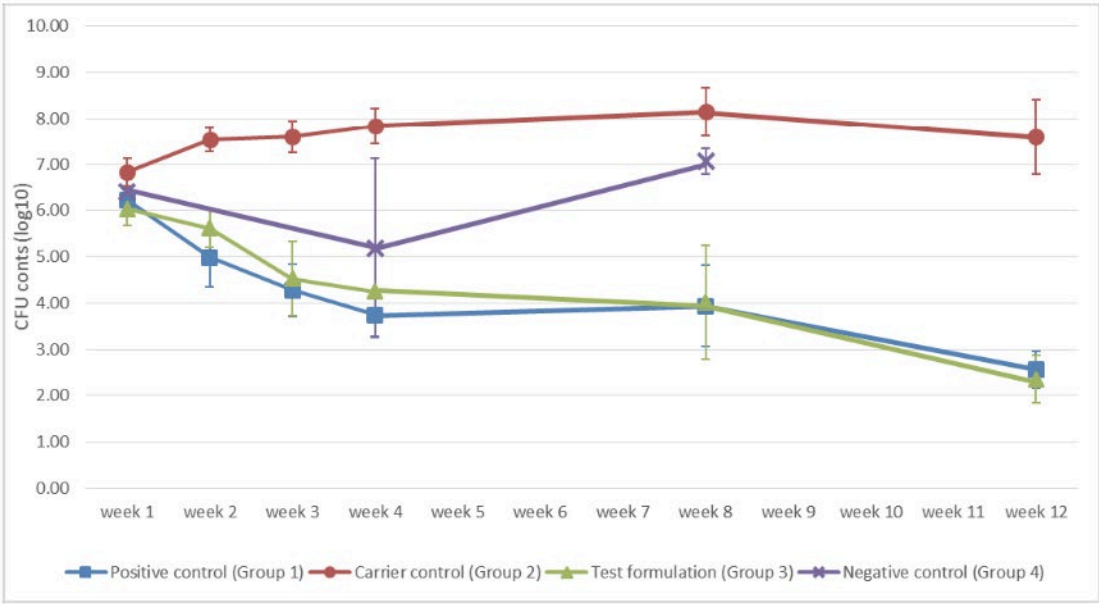


Figure 7-12: The average lung CFU /gram sample (log10) at different time points during the treatment phase.

Figure 1 Extracted from van der Merwe (2019), the average lung CFU/gram sample (log10) at different timepoints during the treatment phase. The positive control (blue) was renamed to standard TB therapy; carrier control (red) was renamed to Pheroid® carrier control; test formulation (green) was renamed to Pheroid® based TB therapy; and the negative control (purple) was renamed to infected reference. Images were extracted with permission from the author.

Table 7-3: Lung CFU during the follow-up phase

Study group	*Month 1*	*Month 2*	*Month 3*
Positive control	3.55 ± 0.55^{aA}	5.22 ± 1.51^{aB}	3.32 ± 0.61^{aA}
Carrier control	7.24 ± 0.54^{bA}	7.58 ± 0.54^{bA}	-
Test formulation	3.54 ± 0.57^{aA}	3.83 ± 0.53^{aA}	3.88 ± 0.46^{aA}
Negative control*	-*	-*	-*

a/A A value belonging to group A according to the Tukey HSD variability test. This value will differ statistically significant compared to a value belonging to group B or C. Small letter should be interpreted vertically and capital letters horizontally.
b/B A value belonging to group B according to the Tukey HSD variability test. This value will differ statistically significant compared to a value belonging to group A or C. Small letter should be interpreted vertically and capital letters horizontally.
c/C A value belonging to group C according to the Tukey HSD variability test. This value will differ statistically significant compared to a value belonging to group A or B. Small letter should be interpreted vertically and capital letters horizontally
ab/AB A value belonging to both group A and B. This value does not differ statistically significant from either a value in group A or B according to the Tukey HSD variability test. Small letter should be interpreted vertically and capital letters horizontally.
*** The negative control was not included in the follow-up phase.**

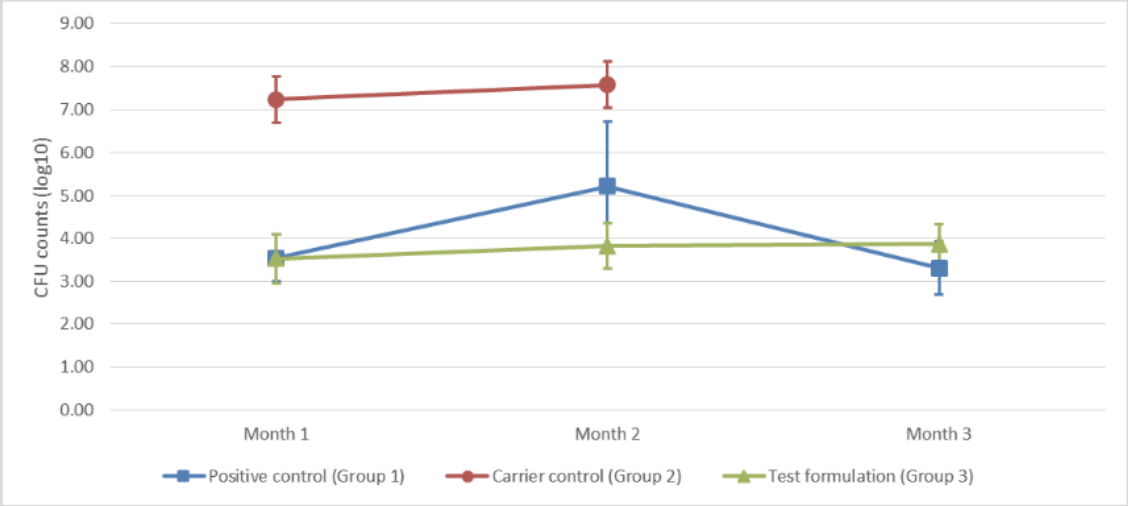


Figure 7-13: The average lung CFU /gram sample (log10) at different time points during the follow up phase.

Figure 2 Extracted from van der Merwe (2019), the average lung CFU/gram sample (log10) at different timepoints during the follow up phase, renamed to microbiome recovery phase. The positive control (blue) was renamed to standard TB therapy; carrier control (red) was renamed to Pheroid® carrier control; test formulation (green) was renamed to Pheroid® based TB therapy; and the negative control (purple) was renamed to infected reference. Images were extracted with permission from the author